Department of
Industry and Resources

REPORT
101

ARCHEAN VOLCANIC AND SEDIMENTARY ROCKS OF THE WHIM CREEK GREENSTONE BELT PILBARA CRATON, WESTERN AUSTRALIA

by G. Pike, R. A. F. Cas, and A. H. Hickman

Geological Survey of Western Australia

GEOLOGICAL SURVEY OF WESTERN AUSTRALIA

REPORT 101

ARCHEAN VOLCANIC AND SEDIMENTARY ROCKS OF THE WHIM CREEK GREENSTONE BELT, PILBARA CRATON, WESTERN AUSTRALIA

by
G. Pike[1], R. A. F. Cas[2], and A. H. Hickman[3]

[1] Shell Deepwater Services, P. O. Box 576, Houston, Texas 77001-0576, U.S.A.
[2] School of Geosciences, Monash University, P. O. Box 28E, Victoria 3800, Australia
[3] Geological Survey of Western Australia, 100 Plain Street, East Perth, W.A. 6004, Australia

Perth 2006

MINISTER FOR RESOURCES
Hon. John Bowler MLA

DIRECTOR GENERAL, DEPARTMENT OF INDUSTRY AND RESOURCES
Jim Limerick

EXECUTIVE DIRECTOR, GEOLOGICAL SURVEY OF WESTERN AUSTRALIA
Tim Griffin

REFERENCE
The recommended reference for this publication is:
PIKE, G., CAS, R. A. F., and HICKMAN, A. H., 2006, Archean volcanic and sedimentary rocks of the Whim Creek greenstone belt, Pilbara Craton, Western Australia: Western Australia Geological Survey, Report 101, 104p.

National Library of Australia
Cataloguing-in-publication entry

Pike, Geoff (Geoffrey John James Edward), 1976–
Archean volcanic and sedimentary rocks of the Whim Creek greenstone belt, Pilbara Craton, Western Australia

Bibliography.
ISBN 1 74168 024 7

1. Geology — Western Australia — Whim Creek Region.
2. Geology, Stratigraphic — Archaean.
3. Sedimentology.
4. Whim Creek Region (W.A.).
I. Cas, Ray.
II. Hickman, A. H. (Arthur Hugh), 1947– .
III. Geological Survey of Western Australia.
IV. Title. (Series : Report (Geological Survey of Western Australia); 101).

559.9413

ISSN 0508–4741

Grid references in this publication refer to the Geocentric Datum of Australia 1994 (GDA94). Locations mentioned in the text are referenced using Map Grid Australia (MGA) coordinates, Zone 50. All locations are quoted to at least the nearest 100 m.

Copy editor: D. P. Reddy
Cartography: A. Blake, S. Dowsett, M. Prause
Desktop publishing: K. S. Noonan

Published 2006 by Geological Survey of Western Australia
This Report is published in digital format (PDF) and is available online at www.doir.wa.gov.au/gswa/onlinepublications.
Laser-printed copies can be ordered from the Information Centre for the cost of printing and binding.

Further details of geological publications and maps produced by the Geological Survey of Western Australia are available from:
Information Centre
Department of Industry and Resources
100 Plain Street
EAST PERTH, WESTERN AUSTRALIA 6004
Telephone: +61 8 9222 3459 Facsimile: +61 8 9222 3444
www.doir.wa.gov.au/gswa/onlinepublications

Cover photograph:
Outcrop of volcaniclastic conglomerate in the Red Hill Volcanics on the northern slopes of Red Hill (MGA 55 5500E 76 81800N)

Contents

Appendices

Plates

1. Geology of areas within the Whim Creek greenstone belt, Pilbara Craton, Western Australia: Mons Cupri (scale 1:10 000)
2. Geology of areas within the Whim Creek greenstone belt, Pilbara Craton, Western Australia: Good Luck Well, Red Hill, and Salt Creek (scale 1:10 000)

Figures

Tables

Archean volcanic and sedimentary rocks of the Whim Creek greenstone belt, Pilbara Craton, Western Australia

by

G. Pike[1], R. A. F. Cas[2], and A. H. Hickman[3]

Abstract

The Whim Creek greenstone belt comprises two volcano-sedimentary basin fragments from the Archean Pilbara Craton. The older rocks of the c. 3010 Ma Whim Creek Group are basalt and dacite with lesser andesitic volcaniclastic rocks. The unconformably overlying Bookingarra Group contains a c. 2950 Ma succession of conglomerate, quartzite, shale, and basalt.

The Whim Creek Group includes tholeiitic basalt and high-level intrusive sills, autobreccia, and hyaloclastite of the Warambie Basalt that underlies and is partly interbedded with the Red Hill Volcanics. The Red Hill Volcanics includes mass-flow reworked hyaloclastite, epiclastic volcanic breccia, and sandstone, and proximal to distal products of subaqueous pyroclastic flows. It is dominated by the calc-alkaline Mons Cupri Dacite Member that includes high-level intrusions and a single, large-volume sill or lava flow. The Whim Creek Group was probably deposited within an intra-arc basin at c. 3009 ± 4 Ma.

The Bookingarra Group contains an upward-fining succession of subaqueous fanglomerate, breccia, sandstone (Cistern Formation), and shale (Rushall Slate) that was deposited within isolated half-graben sub-basins. The Rushall Slate is conformably overlain by the Mount Negri Volcanics. The Louden Volcanics overlie the Mount Negri Volcanics, and the two units contain plume-related siliceous komatiitic basalt. The Bookingarra Group is a remnant of the regionally extensive Mallina Basin.

The association of c. 3000 Ma calc-alkaline volcanic rocks unconformably overlain by chemically mature sedimentary rocks and thick basalt is a global phenomenon with examples from cratonic blocks in Australia, Africa, Asia, Europe, and North and South America. A package of overlying rocks may include basal polymictic conglomerate, wacke, quartz-rich sandstone, quartz arenite, shale, iron formation, and lesser carbonate. The igneous component typically comprises basalt, komatiitic basalt, and lesser komatiite lavas and subvolcanic intrusions. This characteristic association is referred to here as the sandstone–shale–basalt association. The common occurrence of this association at c. 3000 Ma implies a particular global set of climatic and tectonic conditions. A model for crustal evolution at c. 3000 Ma incorporates accretion of crustal fragments, uplift–regression, and the generation of thick sedimentary basins associated with abundant mantle-derived magma.

KEYWORDS: Archean, Bookingarra Group, continental crust, Pilbara Craton, volcanic rocks, Whim Creek Group.

Introduction

Present study

The Whim Creek greenstone belt was mapped between 1998 and 2001 to complement detailed mapping of the granite–greenstones of the northern Pilbara Craton, and to assist in the geological understanding of small polymetallic sulfide deposits (e.g. the Whim Creek and Mons Cupri deposits). This work formed the basis of an unpublished PhD thesis accepted by Monash University, Melbourne, in 2001 (Pike, 2001). Much of the information in Pike (2001) was used in this Report to provide a detailed description of the stratigraphic succession of the 3010–2940 Ma Whim Creek greenstone belt. There is a focus on the petrogenesis of the wide range of lithofacies in this greenstone belt, but (unlike Pike, 2001) no discussion on mineralization.

Four accompanying 1:10 000-scale geological maps (Plates 1 and 2) show the distribution of most of the sedimentary and volcanic facies described in this Report. However, some of the facies described form units too small to be mapped at 1:10 000 scale, and others are restricted to areas of the greenstone belt outside Plates 1 and 2.

The study included geochemical and geochronological work carried out in association with the Australian

[1] Shell Deepwater Services, P. O. Box 576, Houston, Texas 77001-0576, U.S.A.

[2] School of Geosciences, Monash University, P. O. Box 28E, Victoria 3800, Australia.

[3] Geological Survey of Western Australia, 100 Plain Street, East Perth, W.A. 6004, Australia.

Geological Survey Organisation (AGSO, now Geoscience Australia) and the Geological Survey of Western Australia (GSWA), and results are presented. An introductory structural interpretation of the Whim Creek greenstone belt is also provided.

This Report concludes with summaries of c. 3000 Ma successions in other continents, and discusses possible implications of the similarities in terms of global Archean tectonic processes and environments.

Previous work

Previous geoscientific investigations of the Whim Creek area are summarized in regional reviews by Hickman (1983), Barley (1987), Hickman and Smithies (2001), and Van Kranendonk et al. (2002). Mineralization in the area was reviewed and discussed by Ruddock (1999), Huston et al. (2000), and Pike et al. (2002).

Terminology

Throughout this Report igneous and sedimentary nomenclature is used because metamorphism is weak, and primary depositional characteristics are well preserved. Orientations of both planar and linear structures are expressed as dip/dip-direction.

Regional setting

The Pilbara Craton comprises Archean and Paleoproterozoic rocks that outcrop in the Pilbara region of northwestern Western Australia (Fig. 1). Van Kranendonk et al. (2002, 2004) subdivided the Archean granite–greenstones of the northern Pilbara Craton into five components (Fig. 2):

- East Pilbara Granite–Greenstone Terrane (EPGGT, 3720–2830 Ma);
- West Pilbara Granite–Greenstone Terrane (WPGGT, 3270–2930 Ma);
- Mallina Basin (MB, 2970–2930 Ma);
- Kurrana Terrane (3300–2830 Ma);
- Mosquito Creek Basin (MCB, 2950–2920 Ma).

The EPGGT is the oldest component of the northern Pilbara Craton and is a 'dome-and-basin' granite–greenstone terrane in which ovoid granites are flanked by arcuate, volcano-sedimentary packages. The WPGGT is structurally very different from the EPGGT, and has an almost entirely different greenstone stratigraphy and evolutionary history (Van Kranendonk et al., 2002; Hickman, 2004). A suture separating the two terranes is inferred to be buried beneath the younger sedimentary and volcanic rocks of the Whim Creek greenstone belt and the Mallina Basin, parts of which are the subject of the present study. The Whim Creek greenstone belt and the Mallina Basin were formed during post-3020 Ma tectonic events between rifted segments of a pre-3240 Ma proto-continent (Hickman, 2001, 2004; Van Kranendonk et al., 2002, 2004). Components of this old continent are largely restricted to the EPGGT, although remnants are also interpreted in the Roebourne area of the WPGGT (Hickman, 2004; Van Kranendonk et al., 2004).

Whim Creek greenstone belt

The Whim Creek greenstone belt (Fig. 3) is a tectonic unit bound by crustal-scale faults to the north, east, and south, and unconformably overlain by the basal part of the Hamersley Basin succession to the west (Fig. 2). The 250 to 300 km-long Sholl Shear Zone (SSZ) north of the belt (Fig. 3) has been interpreted as a major terrane boundary (Smith et al., 1998), and was studied in detail by Beintema (2003), who described four main deformations:

- c. 3150 Ma initiation (pre-Whim Creek Group);
- 3020 Ma sinistral movement (pre-Whim Creek Group);
- 2930 Ma reverse to dextral movement (?syn-Bookingarra Group);
- younger than 2930 Ma 40 km dextral displacement (?post-Bookingarra Group).

On the eastern margin of the Whim Creek greenstone belt the largely concealed, subvertical Loudens Fault offsets the Mallina Shear Zone by about 1 km (Fig. 3a), with sinistral displacement (Smithies, 1998). West of this structure the great thickness of the Constantine Sandstone and Mallina Formation (correlated with the Bookingarra Group, e.g. Smithies et al., 2001) suggests that the Loudens Fault was a basin-controlling fault at c. 2970 Ma, although there is no evidence that it is a terrane boundary fault (cf. Krapez and Eisenlohr, 1998). The Mallina Shear Zone is a steeply south-dipping zone of intense shear, and comprises east–west and east-northeast–west-southwest fault zones that approximately parallel the Sholl Shear Zone to the north.

The Whim Creek greenstone belt is arcuate due to deformation by a granite-cored fold termed the Sherlock Anticline (Fig. 3b), which plunges to the northeast. Much of the northwestern limb has been offset and buried by the Sholl Shear Zone. The fold pre-dates the c. 2770 Ma Fortescue Group mafic volcanic rocks that unconformably overlie its southeastern limb.

Stratigraphy

The Whim Creek greenstone belt comprises rocks of the Whim Creek and the Bookingarra Groups (Fig. 4). The Whim Creek Group, deposited in the Whim Creek Basin, comprises the Warambie Basalt and the Red Hill Volcanics (including the Mons Cupri Dacite Member). The Bookingarra Group, deposited in the northwestern part of the Mallina Basin, disconformably and unconformably overlies the Whim Creek Group, and comprises the Cistern Formation, Rushall Slate, Mount Negri Volcanics, Louden Volcanics, and Kialrah Rhyolite. The sedimentary rocks of the Cistern Formation (coarse-grained sandstone–conglomerate) and Rushall Slate (fine-grained shale) are overlain by two basaltic formations — the Louden Volcanics and Mount Negri Volcanics. The Kialrah Rhyolite is interpreted to be a slightly younger formation,

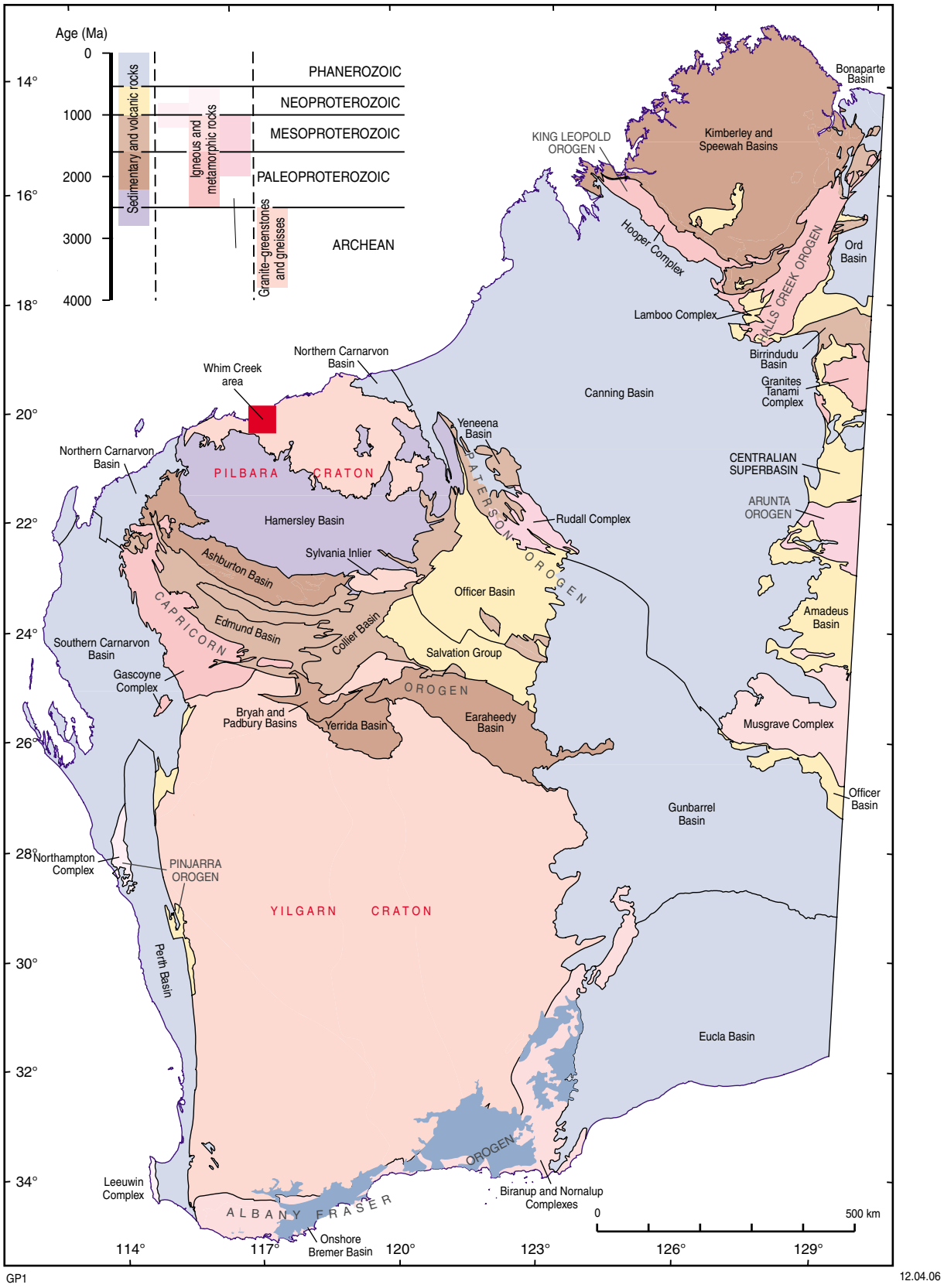

Figure 1. Major geological units of Western Australia (after Tyler and Hocking, 2001). The exposed area of the Pilbara Craton is about 10% of that of the Yilgarn Craton, although more Archean crust is expected below the Capricorn Orogen

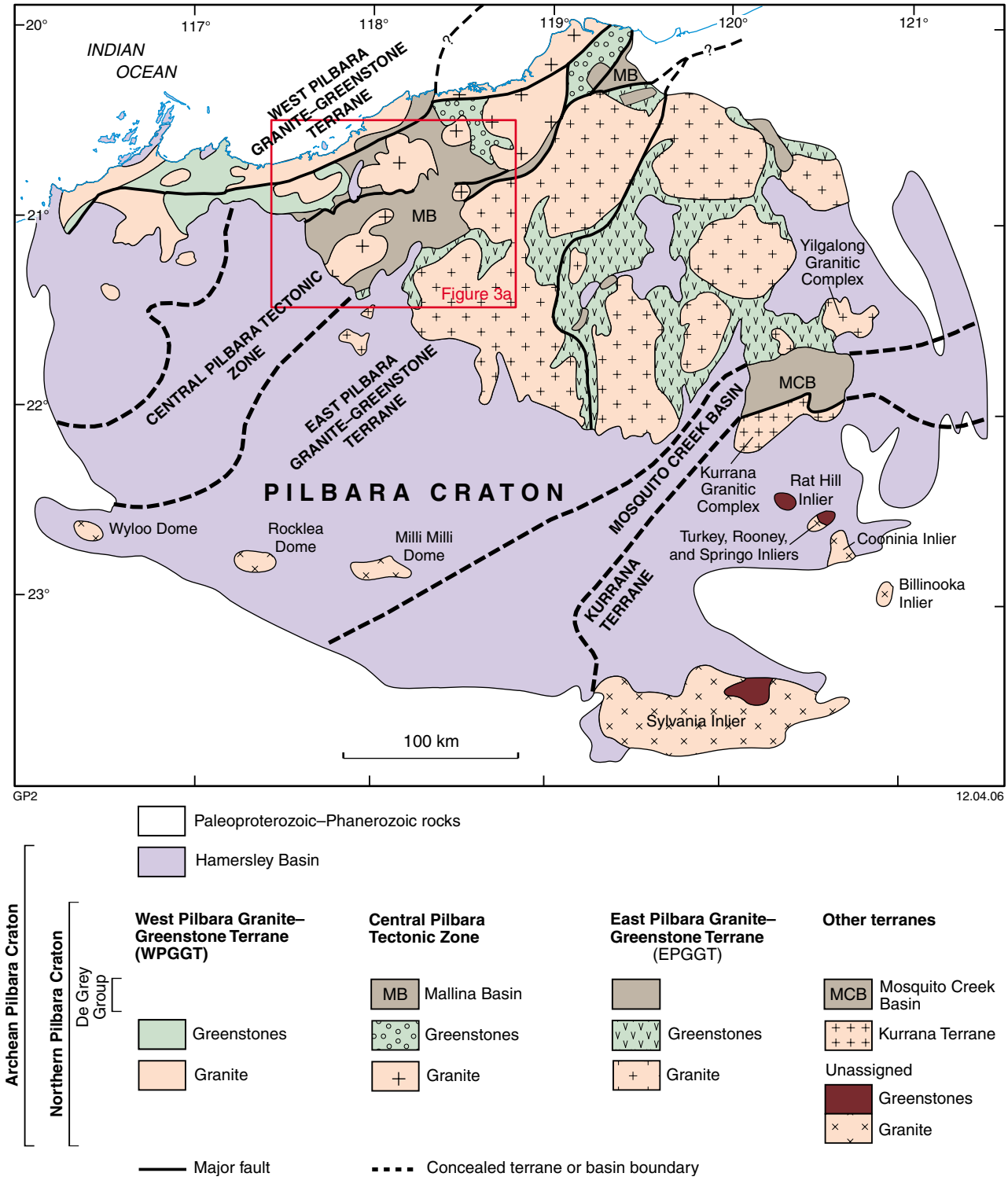

Figure 2. Terrane and basin subdivision of the northern Pilbara Craton (modified from Van Kranendonk et al., 2002)

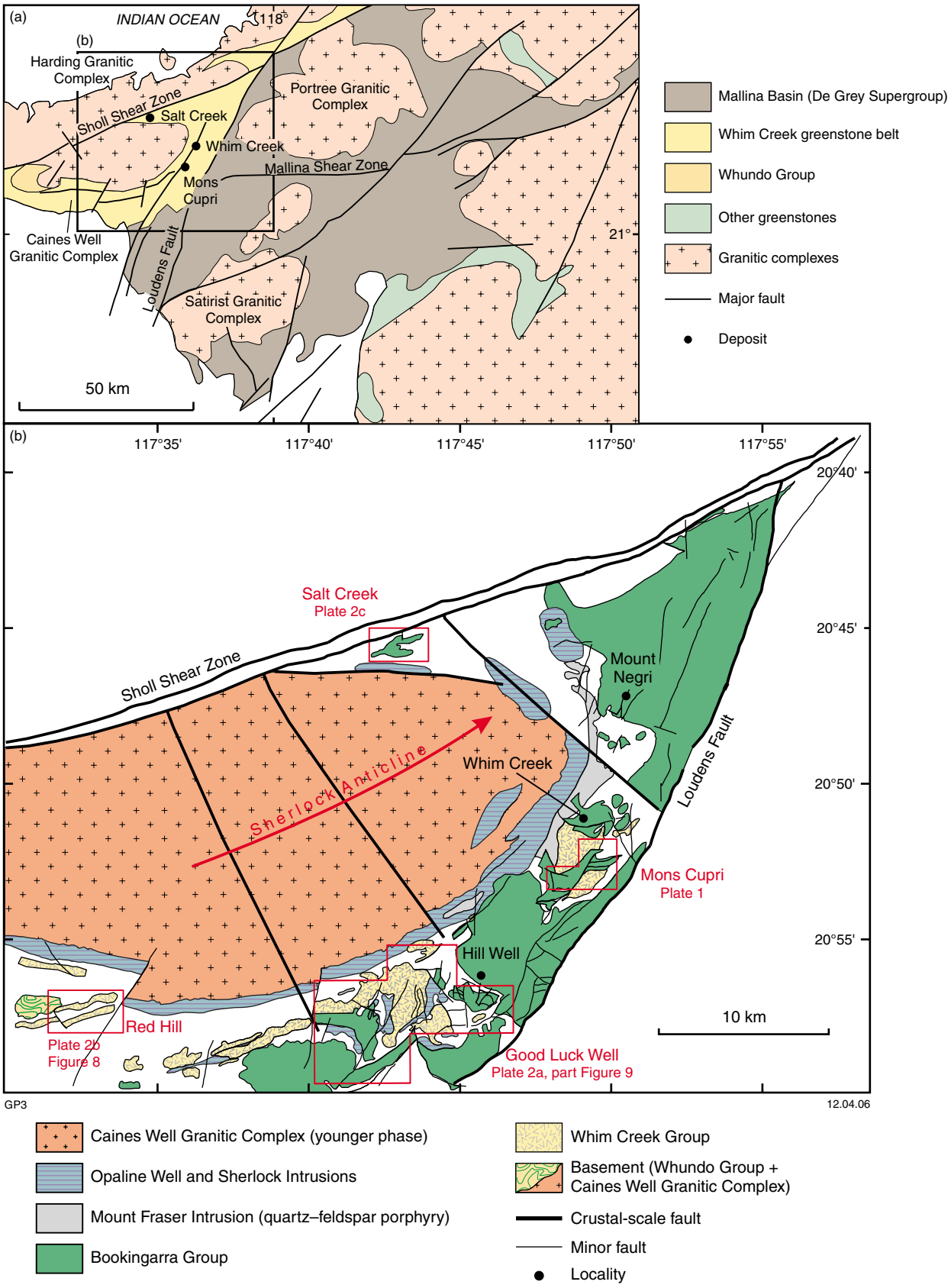

Figure 3. Simplified geological maps of the Whim Creek greenstone belt, showing: a) regional location in the West Pilbara Granite–Greenstone Terrane; b) areas mapped at 1:10 000 scale (Plates 1 and 2; after Smithies, 1998)

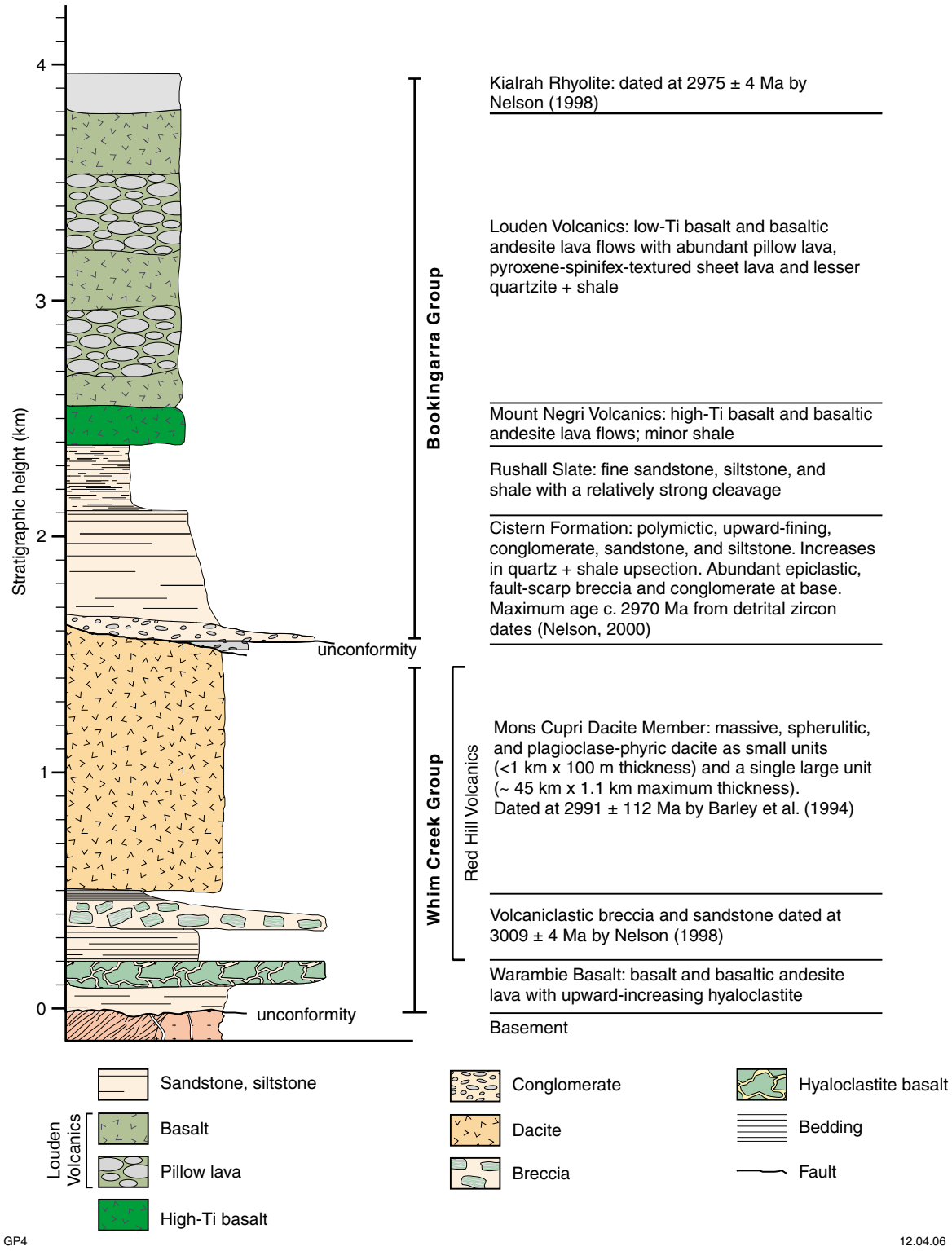

Figure 4. Schematic stratigraphic log illustrating the composition, age, and maximum thickness of lithostratigraphic units outcropping in the Whim Creek greenstone belt. The unconformably overlying Mount Roe Basalt lavas are not shown

although no contacts with other components of the Bookingarra Group are exposed in the areas mapped. Basement rocks of the WPGGT unconformably underlying the Whim Creek Group are rarely exposed in the areas mapped during this study, but include amphibolite-facies metavolcanic rocks of the c. 3120 Ma Whundo Group (Figs 3, 4, and 5). The Whim Creek Group unconformably overlies the oldest phase (c. 3090 Ma) of the Caines Well Granitic Complex. The base of the Whim Creek Group locally contains conglomerate, with clasts of basalt and granite, that is intruded by younger granite, most probably along the basal unconformity (Fig. 6).

Felsic intrusions

The Caines Well Granitic Complex lies in the core of the Sherlock Anticline, and is very poorly exposed. The oldest phase intruded the Whundo Group at 3093 ± 4 Ma (Nelson, 1997). A syn- to post-Whim Creek Group phase was emplaced at around 2990 Ma, before deposition of the Bookingarra Group, and a third phase was intruded after deposition of the Bookingarra Group (Pike, 2001). A fourth phase is represented by a granophyric quartz–feldspar porphyry — the Mount Fraser Intrusion. This intrusion is intensely altered to sericite–quartz or sericite–chlorite–quartz. The porphyry intrudes the Whim Creek Group near Red Hill, and was probably emplaced after the Bookingarra Group. Pike et al. (2002) suggested that the Mount Fraser Intrusion was a possible source for the Whim Creek and Mons Cupri mineralization.

Mafic intrusions

Smithies (1998) described three main mafic intrusions. The Millindinna Intrusion is composed of coarse-grained gabbro and intrudes the Mallina Formation. The Sherlock Intrusion separates the Caines Well Granitic Complex and the overlying Whim Creek and Bookingarra Groups

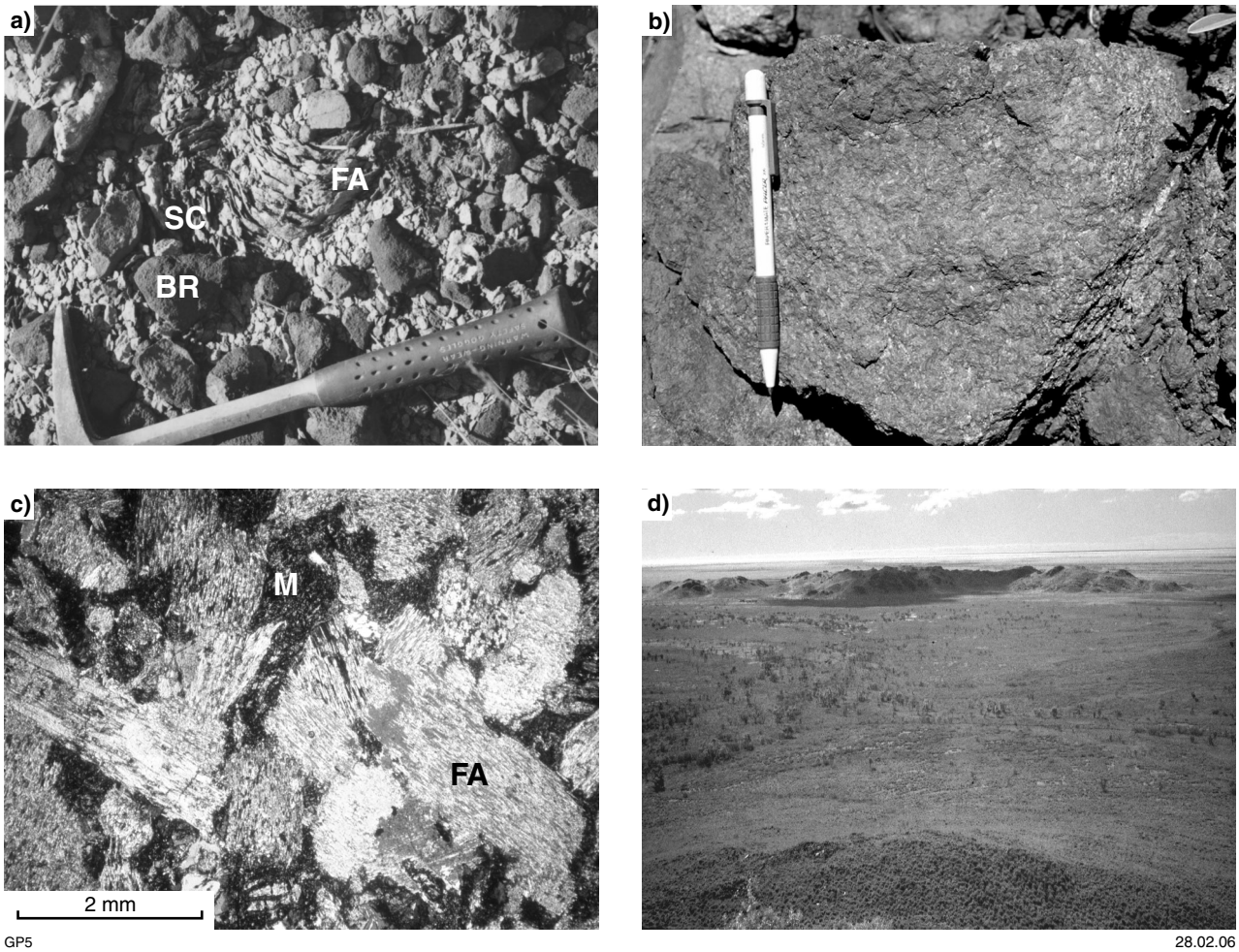

Figure 5. The Whundo Group 'basement' near Red Hill: a) showing typical poor exposures near Red Hill, mainly as rubbly outcrops (BR) and subcrop (SC) between alluvial deposits. The fabric of the amphibolite-facies metabasalt is deformed by tight folds (FA) that are absent from the overlying, and much lower grade, Whim Creek Group; b) equigranular amphibolite-facies metabasalt (MGA 5569989E 7682688N); c) thin section of amphibolite, showing abundant fibrous amphibole (FA) with quartz–K-feldspar-rich, fine-grained crystalline matrix (M); d) view of poorly outcropping Whundo Group north of Red Hill

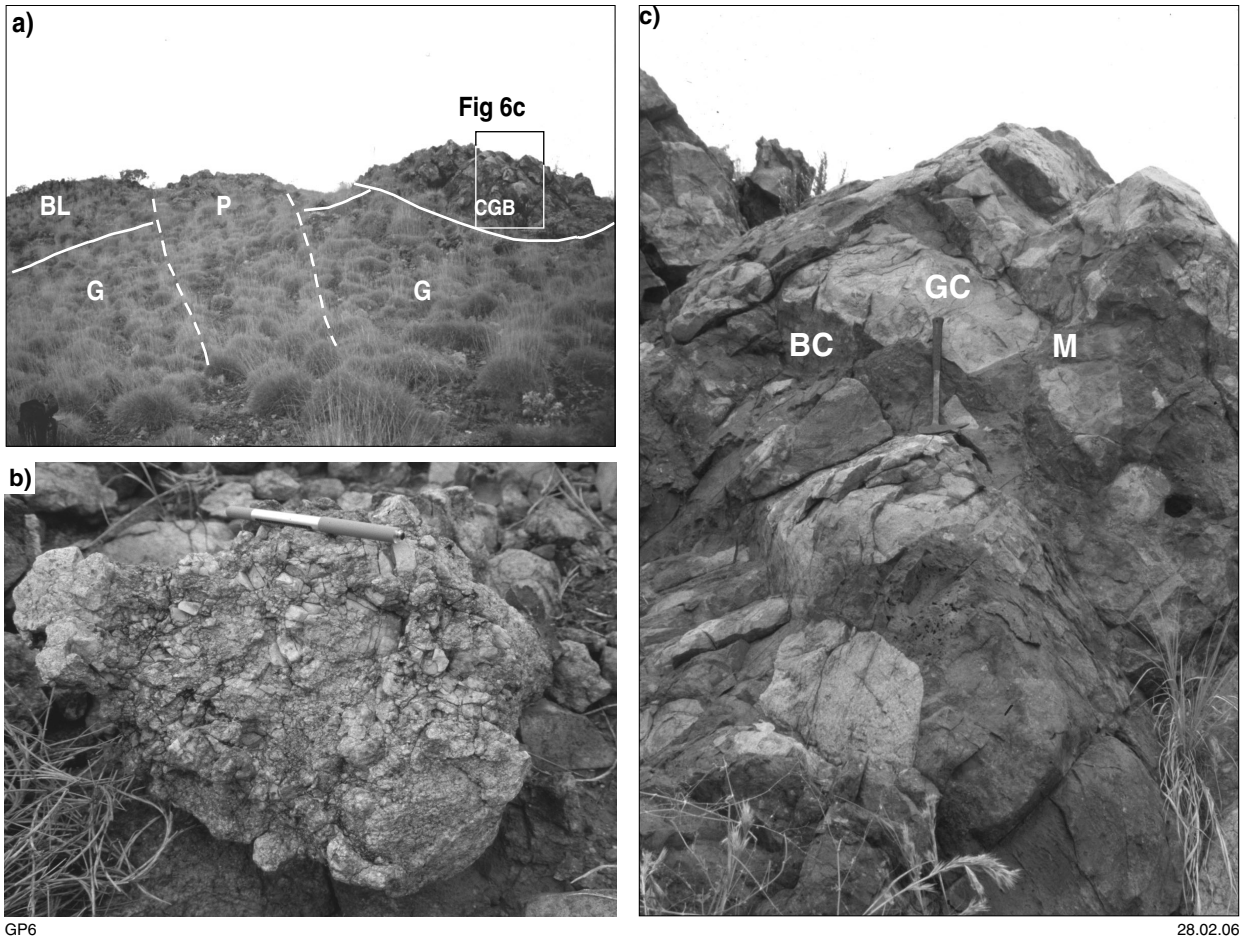

Figure 6. The coarse-grained granite breccia facies of the Warambie Basalt at Red Hill (area around MGA 55249E 7683006N): a) the only outcrop of the facies (CGB) separated from basalt (BL) by a pegmatite (P). The basement is likely to be granite (G) based on abundant granite debris, but to the west is amphibolite-bearing metamorphic rock of the Whundo Group; b) pegmatite, showing a coarse-grained, blocky, K-feldspar-dominated texture; c) angular granite clasts (GC) and a subrounded–subangular basalt clast (BC) in a coarse-grained sandstone–granulestone matrix (M)

(Fig. 3), and must have intruded syn-to post-Bookingarra Group deposition. The Opaline Well Intrusion comprises basalt, dolerite, and gabbro, and forms thick (~100 m) sills into the Bookingarra Group and dykes into the Whim Creek Group. The Opaline Well Intrusion is probably an intrusive phase of the Louden Volcanics (see **Mount Negri Volcanics and Louden Volcanics**) and therefore part of the Bookingarra Group.

Geochronology

Key magmatic and detrital U–Pb sensitive high-resolution ion microprobe (SHRIMP) dates constrain depositional, intrusive, and deformational events. The majority of samples were collected and analysed by GSWA to support 1:100 000-scale mapping since 1996, and the collection, sampling, and analysis of detrital zircon ages are discussed in detail by Nelson (2001). Table 1 lists the key analyses from the Whim Creek greenstone belt.

Structural geology

Structural interpretations from the four areas mapped in this study are summarized into a single deformation history for the Whim Creek greenstone belt in Table 2. This history is separated into a phase of basin opening ('extension') and a compressional folding–faulting ('deformation') event. Approximate ages are from Pike (2001), Van Kranendonk et al. (2002), and Beintema (2003). Folds and fabrics are consecutively numbered F_1/S_1, S_2, F_3/S_3 and so on. Block diagrams in Figure 7 illustrate the formation of the main structural features of the Whim Creek greenstone belt.

Whim Creek extension (E_1), c. 3010 Ma

The 'autochthonous' component of the Whim Creek Group is essentially bimodal basalt–dacite and requires an extensional setting. This is discussed in detail later (in

Table 1. Geochronology of the Whim Creek greenstone belt

Stratigraphic unit	*Rock type*	*Age (Ma)*	*Source*	*Interpretation*
Opaline Well Granite	Porphyritic biotite monzogranite	2765 ± 5	Nelson (1997)	Magmatic
Caines Well Granitic Complex	Foliated granite	2925 ± 4	Nelson (1997)	Magmatic
Kialrah Rhyolite	Plagioclase-phyric rhyolite	2975 ± 4	Nelson (1998)	Magmatic
Cistern Formation[a]	Quartz arenite sandstone	2980–2960	Nelson (2000)	Deposition
Caines Well Granitic Complex	Granite	2990 ± 5	Nelson (2000)	Magmatic
Mons Cupri Dacite Member	Plagioclase-phyric rhyolite lava	2991 ± 12	Barley et al. (1994)	Volcanism
Red Hill Volcanics[b]	Welded tuff	3009 ± 4	Nelson (1998)	Volcanism
Caines Well Granitic Complex	Biotite monzogranite gneiss	3093 ± 4	Nelson (1997)	Magmatic

NOTES: (a) Quartz-rich sandstone facies (*ABc2*) maximum age of deposition
(b) Rhyodacite pumice breccia facies (*ACh11*) age of volcanism and sedimentation

Basin evolution, The tectonic setting of the Bookingarra Group), but there is too little evidence recorded to define a most probable orientation for the extension that formed the Whim Creek greenstone belt.

Bookingarra extension (E_2), c. 2970 Ma

The second extension relates to the opening of the Mallina Basin (and the deposition of the Bookingarra Group in the Whim Creek greenstone belt and the Constantine Sandstone – Mallina Formation succession in the Mallina Basin). Beintema (2003) suggested east–west extension and sinistral movement on the Sholl Shear Zone. However, Pike (2001) described east–west-trending extensional faults with associated condensed sections (i.e. maximum extension oriented north–south). Hence the Bookingarra Group was deposited either within a component of the Mallina Basin with a different stress regime or was perhaps an early rift basin component perpendicular to the later, more extensive, transitional or sag phase of the Mallina Basin. Another complexity is the abundance of basaltic rocks in the Bookingarra Group (and boninite in the central part of the Mallina Basin) that show a mantle influence. This is discussed in more detail later (in **Basin evolution, The tectonic setting of the Bookingarra Group**).

Deformation D_1, c. 2970 Ma

The first deformation is subdivided into D_{1A} (early folds) and D_{1B}, during which the main cleavage in the Whim Creek greenstone belt was formed. D_{1A} resulted in minor folds in the Rushall Slate near the Whim Creek mine site, and has been studied in detail by Black (1998). The main fabric S_2 is a cleavage in metamorphosed shale, and is defined by clast flattening or spherulite–amygdale flattening in coarse-grained sedimentary and volcanic rocks. It is pervasive throughout every part of the Whim Creek greenstone belt. S_2 is typically parallel to bedding of the Bookingarra Group, but not to bedding of the Whim Creek Group, and there is no associated folding.

Deformation D_2, c. 2955–2930 Ma

All major folding (and associated fabric development) is assigned to a compressional event at c. 2955–2930 Ma. Smithies (1998) assigned this event to D_3, suggesting a

Table 2. Deformations recorded in the west Pilbara (modified from Van Kranendonk et al., 2002)

Extension and deformation events		*Structure(s)*	*Age (Ma)*
Regional	*Whim Creek greenstone belt*		
D_{10}	?D_3	East–west fabric (Sholl Shear Zone)	–
D_9		–	–
D_8		Dextral strike-slip fault movement on the Sholl Shear Zone	2920
D_7		North-northwest Maitland Shear Zone developed with parallel tectonic fabric	
D_6	D_{2b}	Northeast-trending tight to open folds due to northwest–southeast compression	2955–2930
D_5		North-trending folds in the Mallina Basin	–
D_4	D_{2a}	East-trending folds and thrusts in the Warambie Basalt	–
E_2	E_2/D_1	Bookingarra Group	2970
~ ~ ~ ~ ~ ~ ~ ~ ~ ~ ~ ~		Erosional unconformity or disconformity	–
E_1	E_1	Whim Creek Group	3010–3000
~ ~ ~ ~ ~ ~ ~ ~ ~ ~ ~ ~		Erosional unconformity	–

NOTES: E: Extension
D General deformation

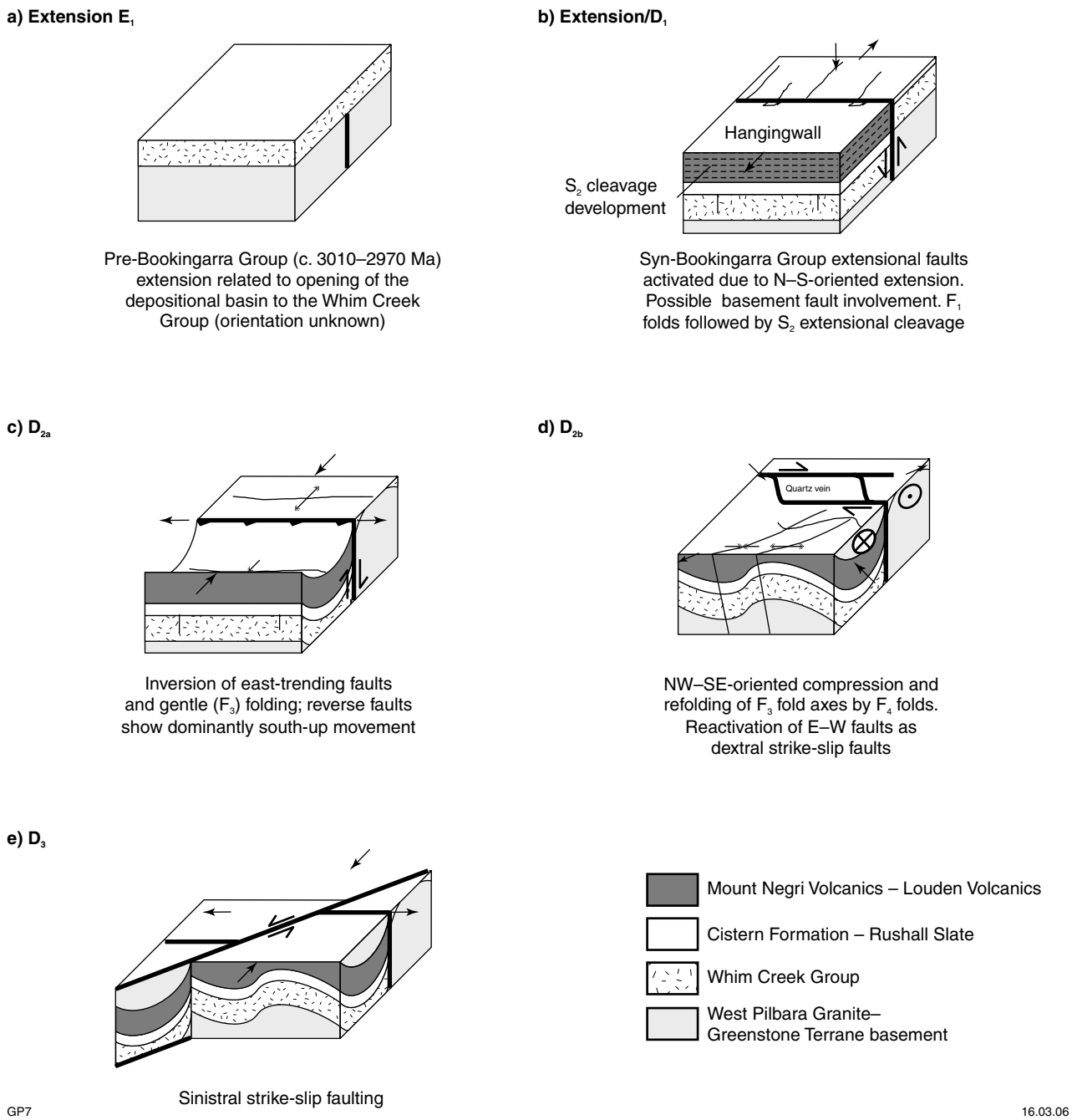

Figure 7. Block models illustrating the formation of the main structural features of the Whim Creek greenstone belt (see Table 2 for more details)

2950–2930 Ma age. Beintema (2003) suggested that it occurred at c. 2930 Ma. F_3 folds and weak S_3 fabric trend easterly and are associated with east-trending reverse faults. These are all folded around broad (kilometre-scale or larger), northeast-plunging, angular, open folds that include the Sherlock Anticline. These later F_4 folds (and weak S_4 fabric) correlate with major northeast-trending folds in the WPGGT (D_4) that Van Kranendonk et al. (2002) suggested were aged between 2950 and 2940 Ma, based on data from that terrane. The F_4 folds of the Whim Creek area pre-date mineralization that Krapez and Eisenlohr (1998) suggested is hosted within (and is younger than) the fold hinges.

Deformation D_3, age poorly constrained

Northeast–southwest sinistral strike-slip faults dissect much or all of the Whim Creek greenstone belt with offsets of more than 1 km in many places. The faults are older than the c. 2770 Ma volcanic rocks of the basal Mount Bruce Supergroup, but otherwise their age is poorly constrained.

Whim Creek Group

Warambie Basalt

Basaltic volcanic, volcaniclastic, and rare siliciclastic sedimentary rocks of the Warambie Basalt outcrop immediately north of Red Hill (Fig. 8, Plate 2b) and throughout the Good Luck Well area (Fig. 9, Plate 2a). An inlier south of Whim Creek was mapped in the Mons Cupri area (Plate 1). A lot of work has been done on the Warambie Basalt (e.g. Fitton et al., 1975; Barley, 1987; Hickman, 1983; Horwitz, 1990; Smithies, 1998; Krapez and Eisenlohr, 1998), and most studies show a general agreement on the broad facies architecture and geochemistry of the component units. Table 3 lists the facies associations and facies of the Warambie Basalt, and notes the areas in which each facies is best developed. Many of these facies (note (a) in Table 3) form units too small to be mapped at 1:10 000 scale, and are consequently not listed in the Reference for Plates 1 and 2. The facies associations and facies are described in detail below.

Basalt lava and breccia association

Dark, charcoal-grey, coherent and fragmental rocks comprising aphanitic to plagioclase-phyric, amygdaloidal types are characteristic of the basalt lava and breccia association. Basalt ranges from aphyric to 30% plagioclase-phyric–glomeroporphyritic and is variably amygdaloidal (up to 40%). Logged sections from the Red Hill area (Fig. 8) are presented in Figure 10 (schematic Warambie Basalt log), and in Figures 11–15 (Warambie Basalt and lower Red Hill Volcanics logs).

Coarse-grained granite breccia facies

The coarse-grained granite breccia facies outcrops near Red Hill and contains boulder-sized, angular clasts of granite

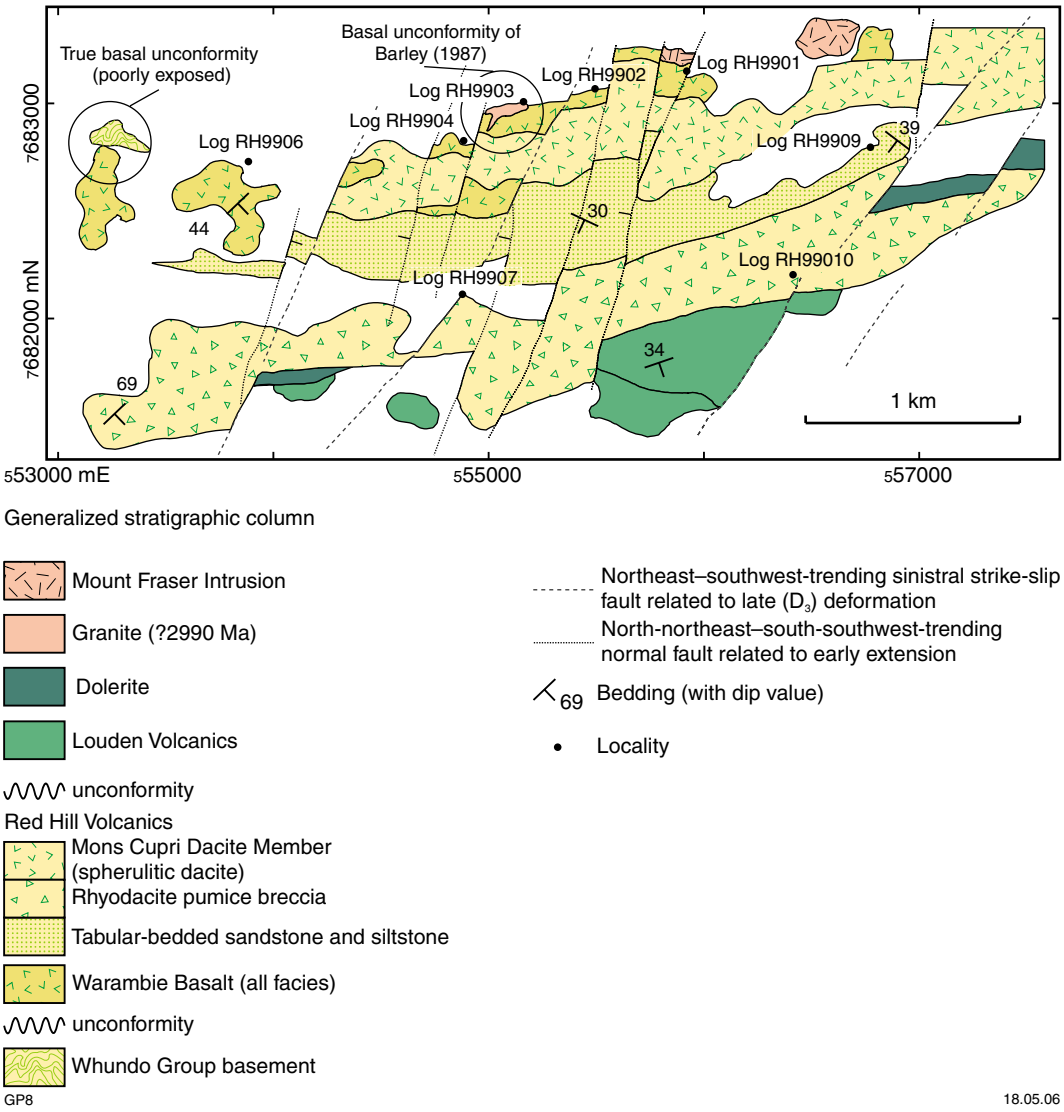

Figure 8. Simplified geological map of the Red Hill area, showing locations of logged sections mentioned in the text (see Fig. 3 for regional location)

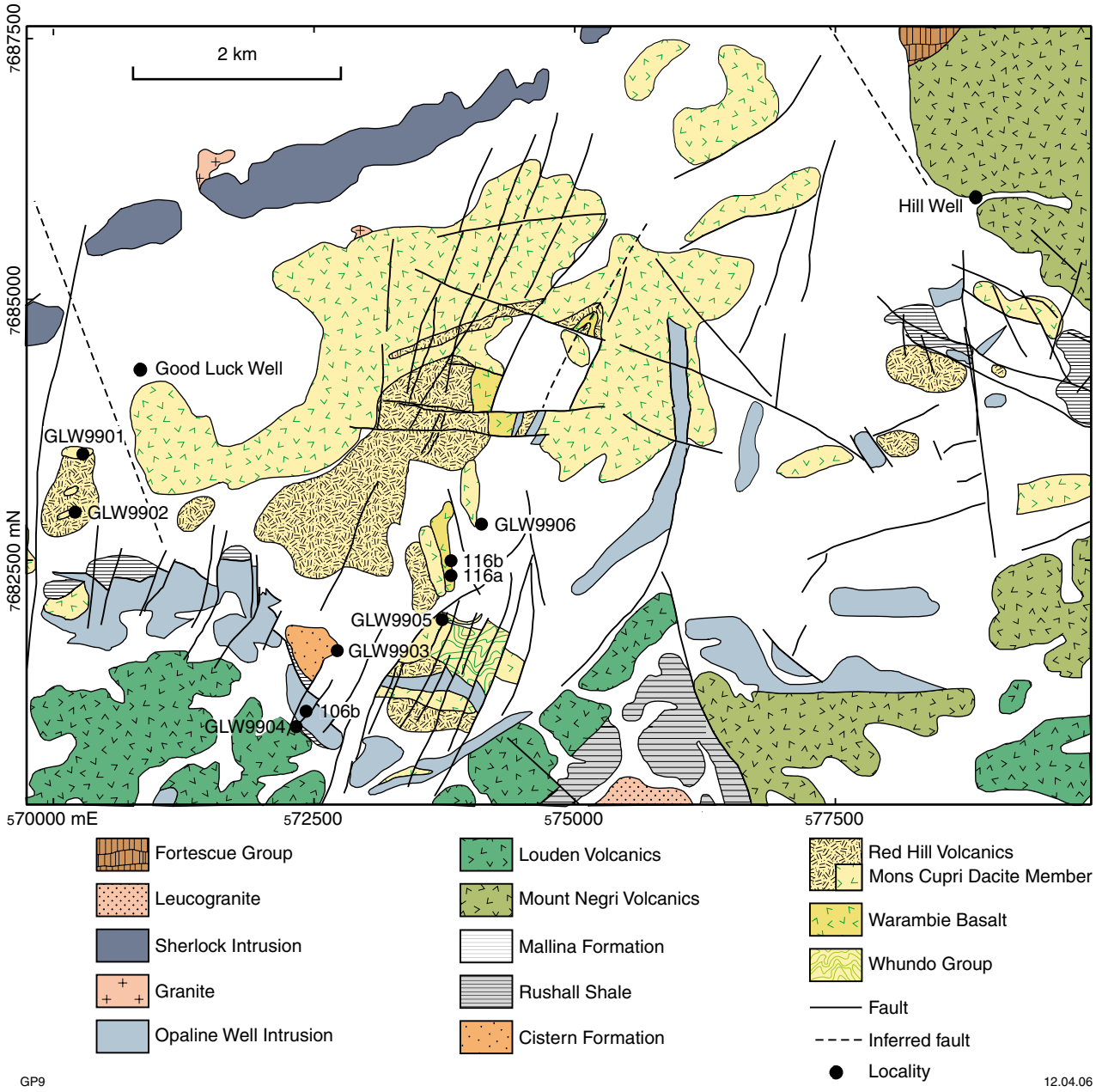

Figure 9. Simplified geological map of the Good Luck Well area, showing locations of logged sections mentioned in the text (see Fig. 3 for regional location)

(60%) and basalt (40%), and is locally the stratigraphically lowest unit of the Warambie Basalt (Fig. 6). The facies is restricted to a single, massive outcrop (MGA 555039E 7682955N) of about 5 m thickness and about 10 m^2 lateral extent, but the exposure is too small to show on the 1:10 000-scale Plate 2b. The breccia is clast supported and dominated by subangular to angular clasts. However, many of the smaller (pebble-sized) granite and basalt clasts show good rounding, indicating a more distal source or greater net transport or both. Unstrained granitic clasts are up to a metre in length and weakly elongate. Individual granitic clasts vary in composition and grain size and an average (field-estimated) composition is quartz (30%), feldspar (65%), and mafic (biotite, amphibole, and later chlorite) crystals (5%). Thin section examination highlights two main clast components: a chlorite-altered granite and a carbonate–chlorite-altered basalt. In thin section the matrix of the breccia is an unsorted mixture of angular clasts (0.1–4 mm) of monocrystalline plutonic quartz (25%), monocrystalline etched alkali feldspar (including microcline) and plagioclase (20%), fine-grained chloritic lithic fragments (40%), chlorite (5%), and anhedral carbonate (10%).

Interpretation

The angular and subangular granitic boulders in the facies indicate proximity to source. Some pebble-sized granitic clasts and most of the basaltic clasts are weakly rounded, indicating limited transportation, and may be

Table 3. Facies and facies associations of the Warambie Basalt

Facies association	*Facies*	*Area*	*Code*
..... *Conformably overlying Red Hill Volcanics*			
Grey dolerite and basalt	Schistose basalt	Mons Cupri	ACw1
	Grey basalt intrusive breccia[a]	Good Luck Well	–
	Grey dolerite and basalt	Good Luck Well	ACw2
Arkosic sandstone and conglomerate	Arkosic sandstone[a]	Red Hill	ACw6
	Matrix-supported conglomerate[a]	Red Hill	ACw7
Basalt lava and breccia	Scoriaceous basalt breccia[a]	Red Hill	–
	Aphanitic basalt breccia	Red Hill	ACw3
	Basaltic pebble breccia and conglomerate[a]	Red Hill	ACw5
	Thick- and thin-sheet basalt	Red Hill	ACw4
	Coarse-grained granite breccia[a]	Red Hill	–
~ ~ ~ ~ ~ ~ ~ ~ ~ ~ ~ ~ ~ *Basal unconformity over Whundo Group or Cleaverville Formation of the Gorge Creek Group* ~ ~ ~ ~ ~ ~ ~ ~ ~ ~ ~ ~ ~			

NOTE: (a) Facies too restricted to be shown on Plates 1 and 2

more distal in origin than the granite boulders. Transport of the larger clasts was probably by gravitational sliding or rolling rather than suspension within a flow. The facies is of limited lateral extent, and may be localized within a paleochannel or structurally controlled topographic low. Patches of relatively well sorted and rounded matrix material indicate tractional transport and deposition from a moderate-energy current, with periodic high-energy pulses that deposited pebble- to boulder-sized material. The rounded nature of the smaller clasts suggests that they were either derived from a different source than the larger fragments or retained in the transport cycle for a longer period. Basalt clasts are typically smaller than granite clasts, suggesting that the two types were derived from different areas and mixed before or during deposition. Hence, there is evidence for moderate- to high-energy transportation with the addition of large blocks from adjacent topographic highs. Modern analogues of the coarse-grained granite breccia facies may include exposed beaches (in which large fragments in angular rockfall debris are intercalated with subrounded and rounded pebble- to cobble-sized material), shallow-water fans fed by high-energy currents or by high-energy, braided fluvial systems. The lack of Whundo Group clasts suggests that the source region was restricted to isolated granite highs (rather than a regional topographic high), possibly related to initial rifting of the basin system. Small horst blocks of granite are the probable source of the large angular granite blocks. These may have fallen, slid, or rolled onto a paleobeach or shallow-water fan, consisting of variably reworked (and possibly fluvially transported) debris. Basaltic debris appears proximal and shows variable reworking. The favoured paleoenvironmental interpretation is a beach or shallow-water fan subject to wave and storm reworking, although there is no definitive evidence to preclude a fluvial origin.

Thick- and thin-sheet basalt facies, and basaltic pebble breccia and conglomerate facies

Coherent basalt overlying the coarse-grained granite breccia facies is assigned to the thick- and thin-sheet basalt facies (*ACw4* on Plates 1 and 2), based primarily on variability in the size and geometries of component flows. Thick flows (up to 24 m thick) typically underlie thin flows (0.5 – 5 m thick) within the facies, but there is also considerable interlayering of thick and thin flows (Fig. 10). Thick flows are tabular, extend for more than 100 m along strike, and can be correlated between logged sections. Individual bodies are aphanitic and show little associated breccia. Amygdales are largely confined to centimetre-thick zones within the flow and are less abundant (<5%) than in the thin flows.

Most thin flows cannot be traced for more than a few metres, partly due to relatively poor exposure, but also as a result of lateral variation. Amygdales, 5–8 mm across, are generally absent or form less than 5% of the rock (maximum 30%), and are partly or wholly filled with calcite or chlorite or both. However, well-developed narrow (~5 cm thick) horizons containing about 40% spherical amygdales extend for several metres along strike (Fig. 16a) locally. Coherent basalt forms around 40% of exposure, and is intercalated with large volumes of angular basaltic debris (Fig. 16b). This breccia contains elongate, monomictic cobble- to boulder-sized basalt clasts with a finer grained matrix component and forms irregular units a few metres thick that overlie sheet lava. The granule- to pebble-sized matrix clasts are angular basalt with planar margins. Clasts typically display jigsaw-fit texture (Fig. 17a,c), although clast-rotated subfacies are also recognized. The large clasts may be amygdaloidal, with both rounded and angular margins, and form blocks up to about 1 m in diameter (Fig. 16b). These clasts have planar to rounded margins and also show a transition to finer grained clasts within the matrix. In some examples coherent basaltic apophyses intrude the breccia and show transition from coherent to fractured to clastic textures.

The thick- and thin-sheet basalt facies contains subfacies of aphanitic basalt (*ACw4(a)*) and plagioclase-glomeroporphyritic basalt *(ACw4(b)*), with the former dominating; both are mapped on Plate 2. The aphanitic basalt subfacies is composed of irregular, 0.5 to 2.0 m-thick, basalt units, with either reworked conglomerate tops (low in the stratigraphy) or hyaloclastite caps

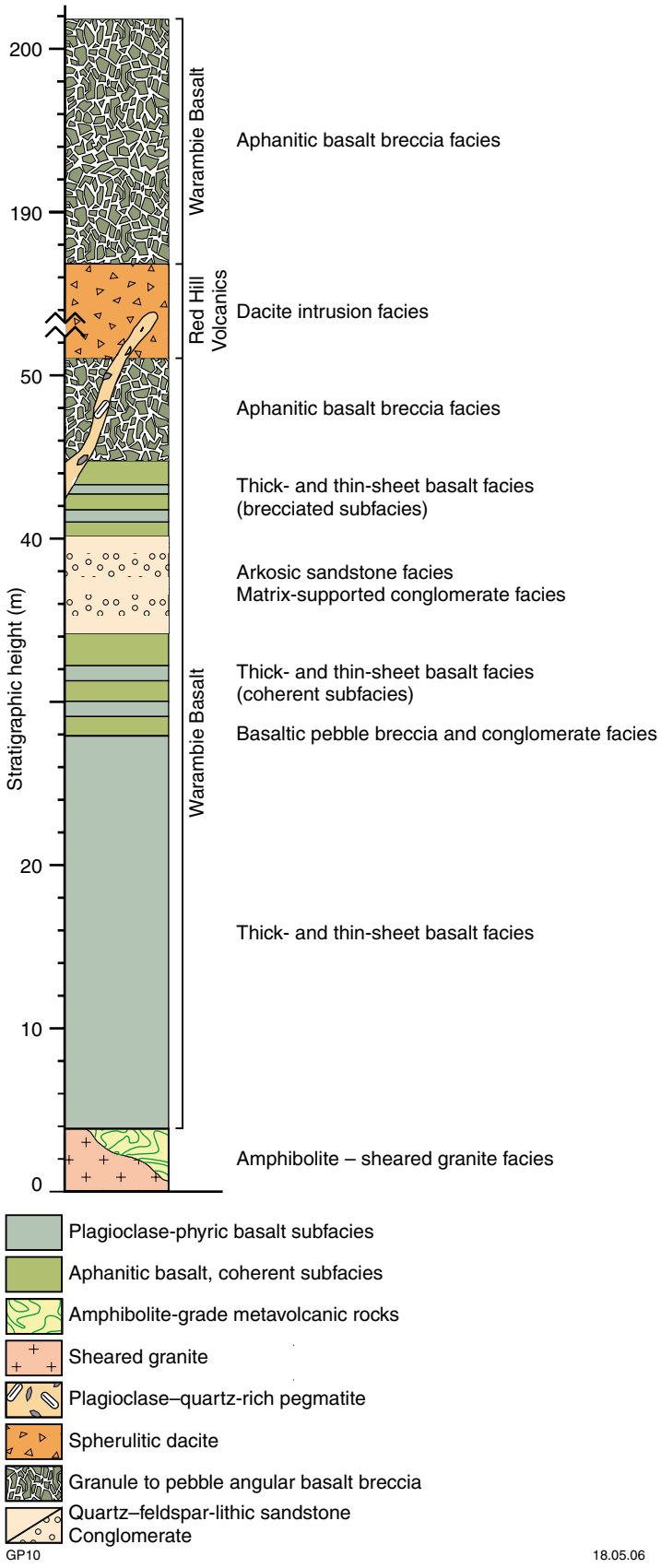

Figure 10. Representative stratigraphic log for the Warambie Basalt succession in the Red Hill area (see Table 3). The Red Hill area preserves the most complete, least deformed, and best exposed Warambie Basalt

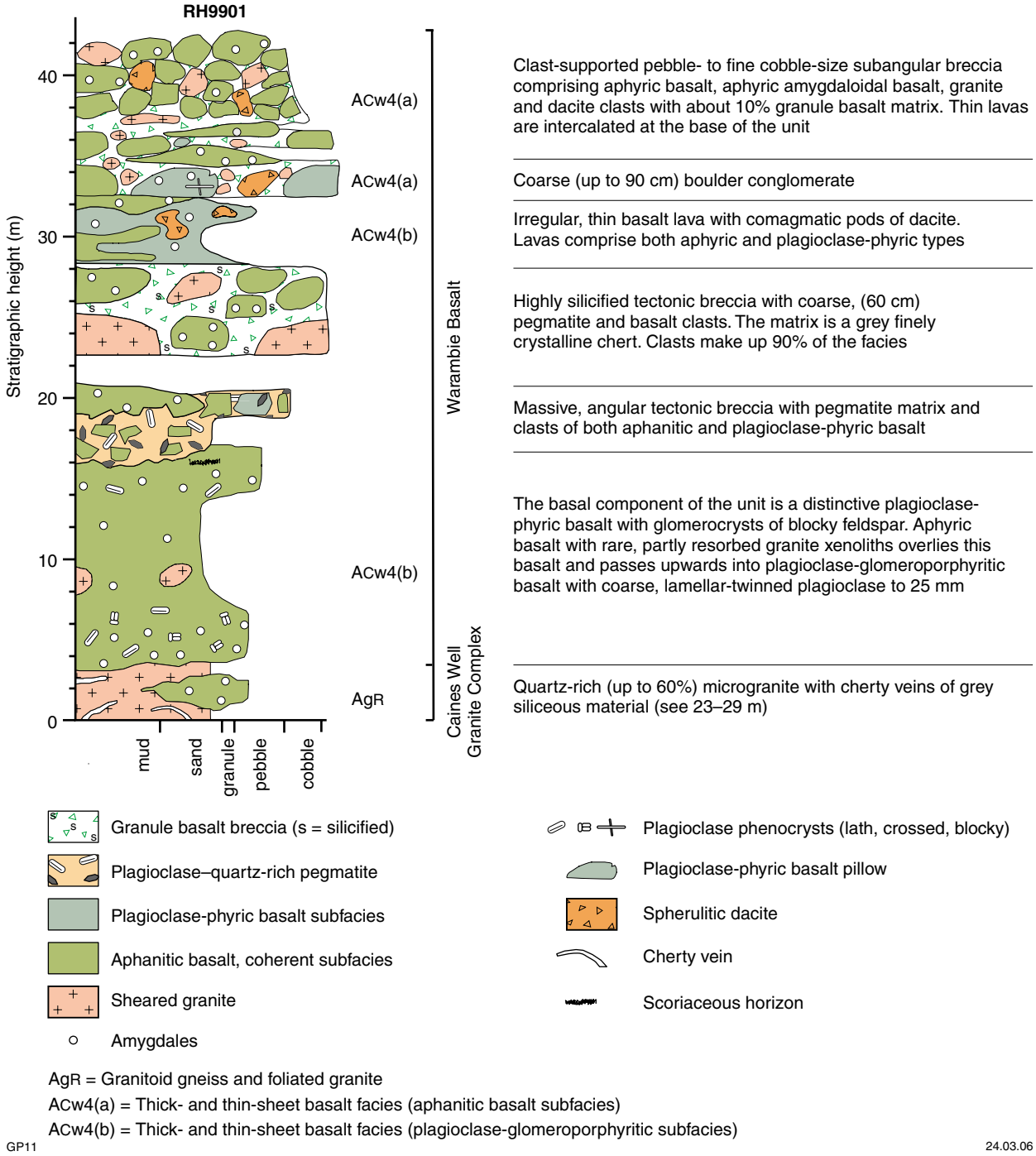

Figure 11. Stratigraphic log RH9901 (base at MGA 555950E 7683175N), illustrating the thin, dominantly clastic, facies of the Warambie Basalt, from the easternmost section of the Red Hill area (see Fig. 8 for regional location)

(high in the stratigraphy), and with common separation layers; plagioclase phenocrysts are rare or absent. The plagioclase-glomeroporphyritic basalt subfacies consists of irregular, 0.5 to 2.0 m-thick, basalt units containing blocky and lath-shaped plagioclase phenocrysts that are typically in clusters.

Angular breccia and rare conglomerate of the basaltic pebble breccia and conglomerate facies (*ACw5*) near the base of the succession is too thin to be shown on the 1:10 000-scale Plate 2. This clastic facies comprises breccia and conglomerate, with clast-supported to subrounded–subangular clasts (Fig. 16c). The facies is preserved only up to 50 m above the base of the Warambie Basalt, and forms thin (<1 m), massive, and poorly exposed units (Fig. 13). The matrix comprises granule-sized grains of basalt with no apparent (nonbasaltic) siliciclastic material or sand-sized component. Clasts are randomly oriented and vary considerably in amygdale content, phenocryst morphology, and abundance. They

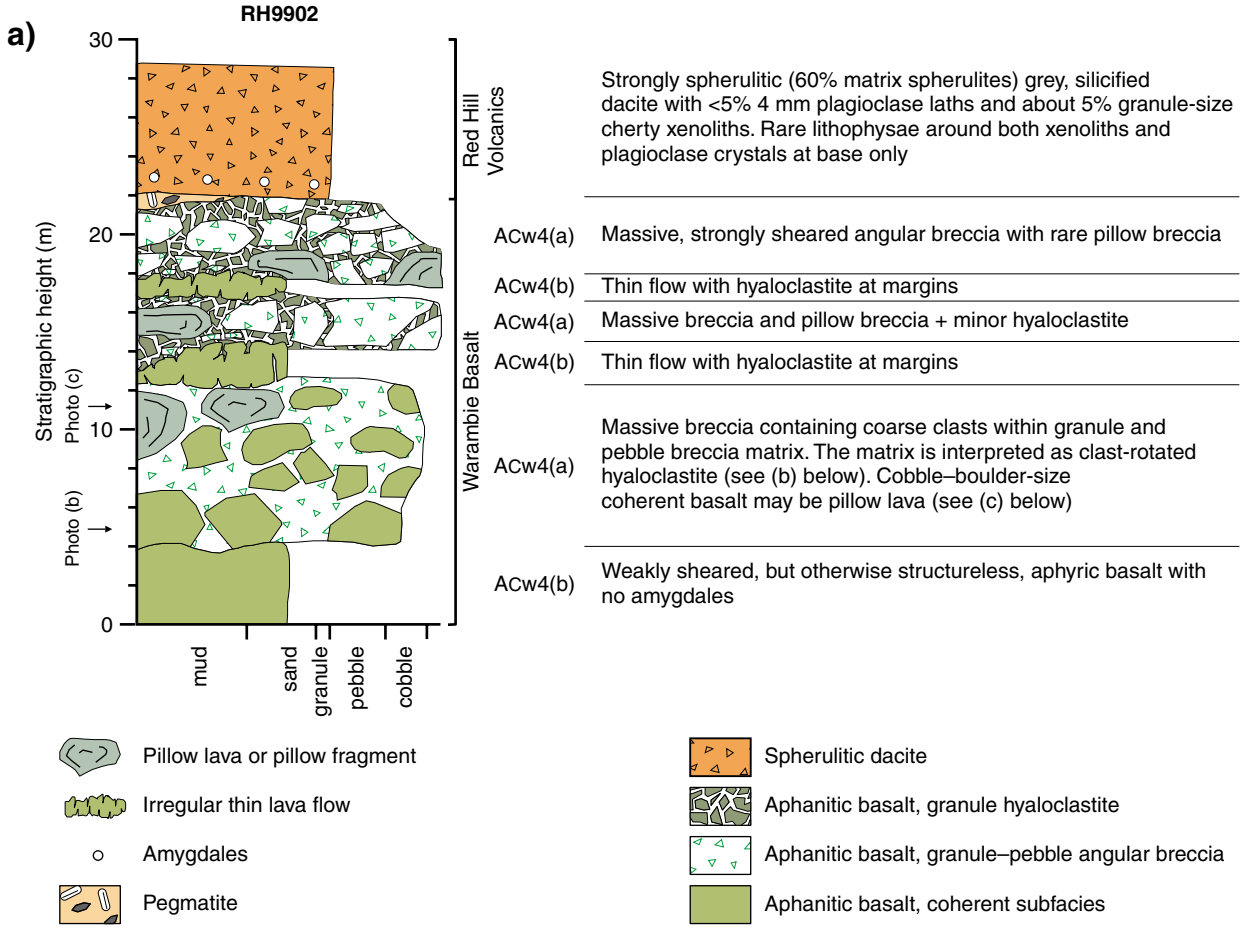

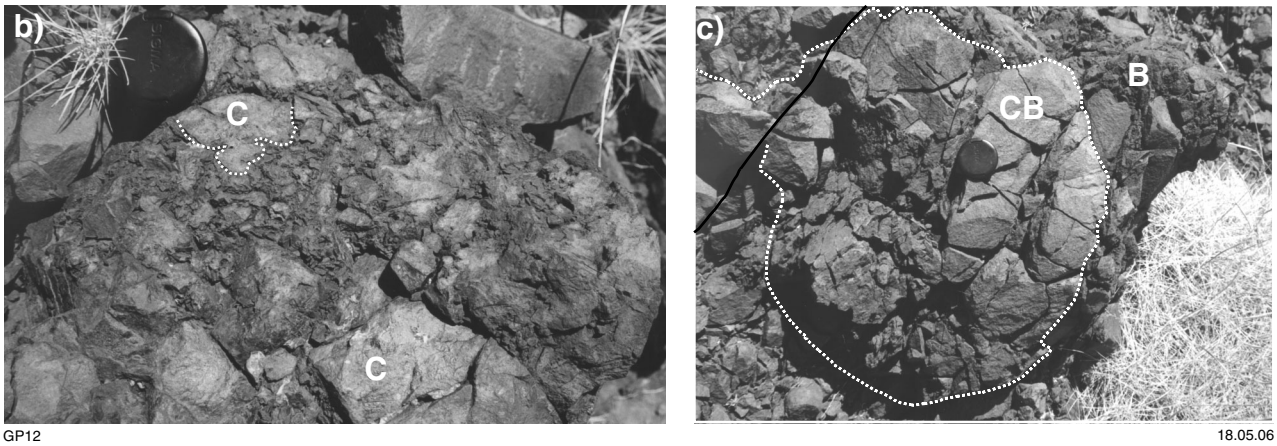

Figure 12. a) Stratigraphic log RH9902 (base at MGA 55552E 7683045N), Warambie Basalt, Red Hill area (see Fig. 8 for regional location): b) coarse, irregular breccia containing pebble–cobble clasts (C) with irregular margins (dashed line). Note extremely poor sorting and angular shape of clasts; c) subrounded coherent basalt (CB) unit (white dashed line) within granule–pebble breccia (B). The coherent basalt is possibly a pillow and offset by a minor fracture

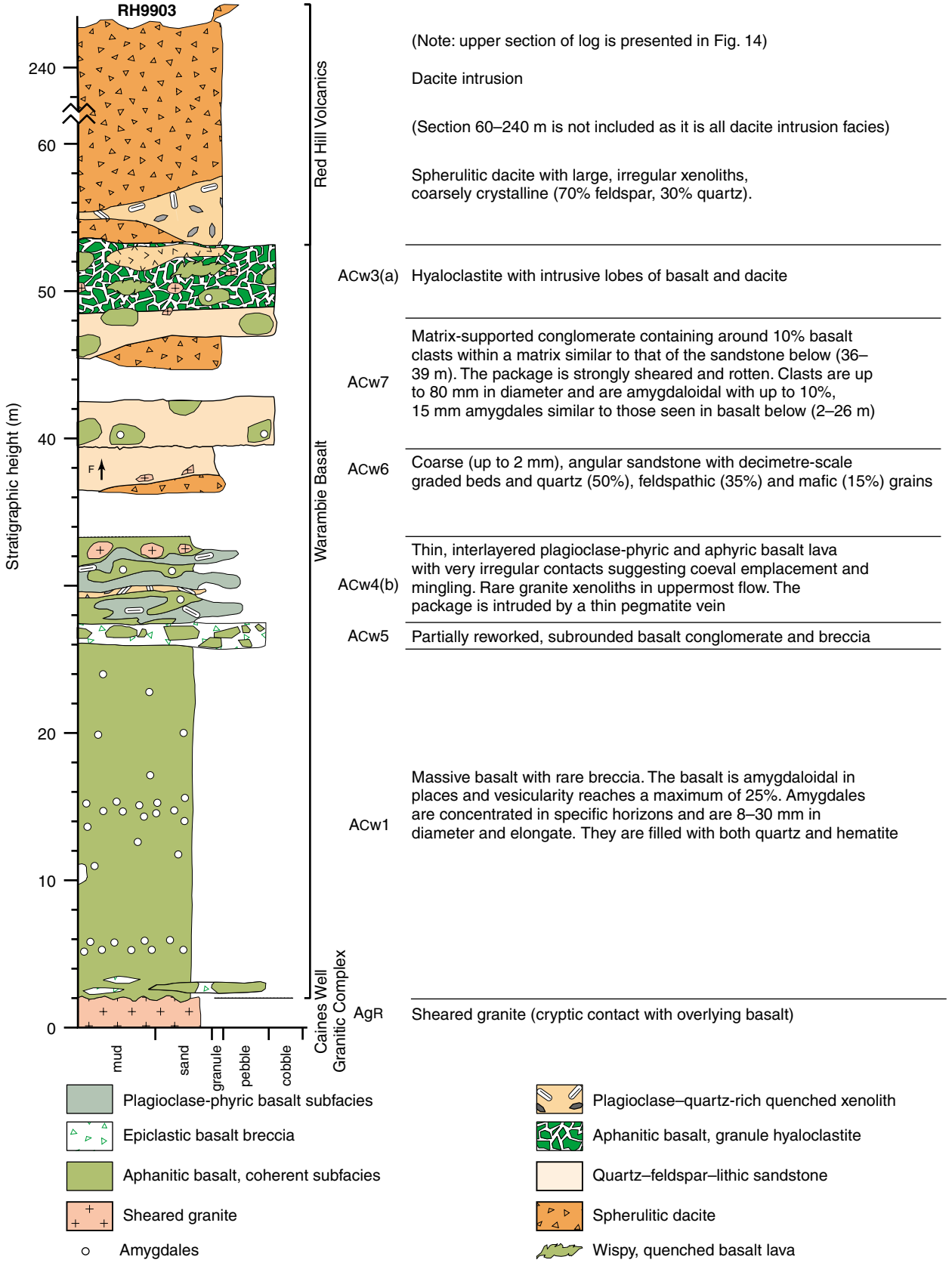

Figure 13. Lower section of stratigraphic log RH9903 (base at MGA 55260E 7682960N), Warambie Basalt, Red Hill area (see Fig. 8 for regional location). Note the thick sheet basalt facies that forms a marker horizon across the succession

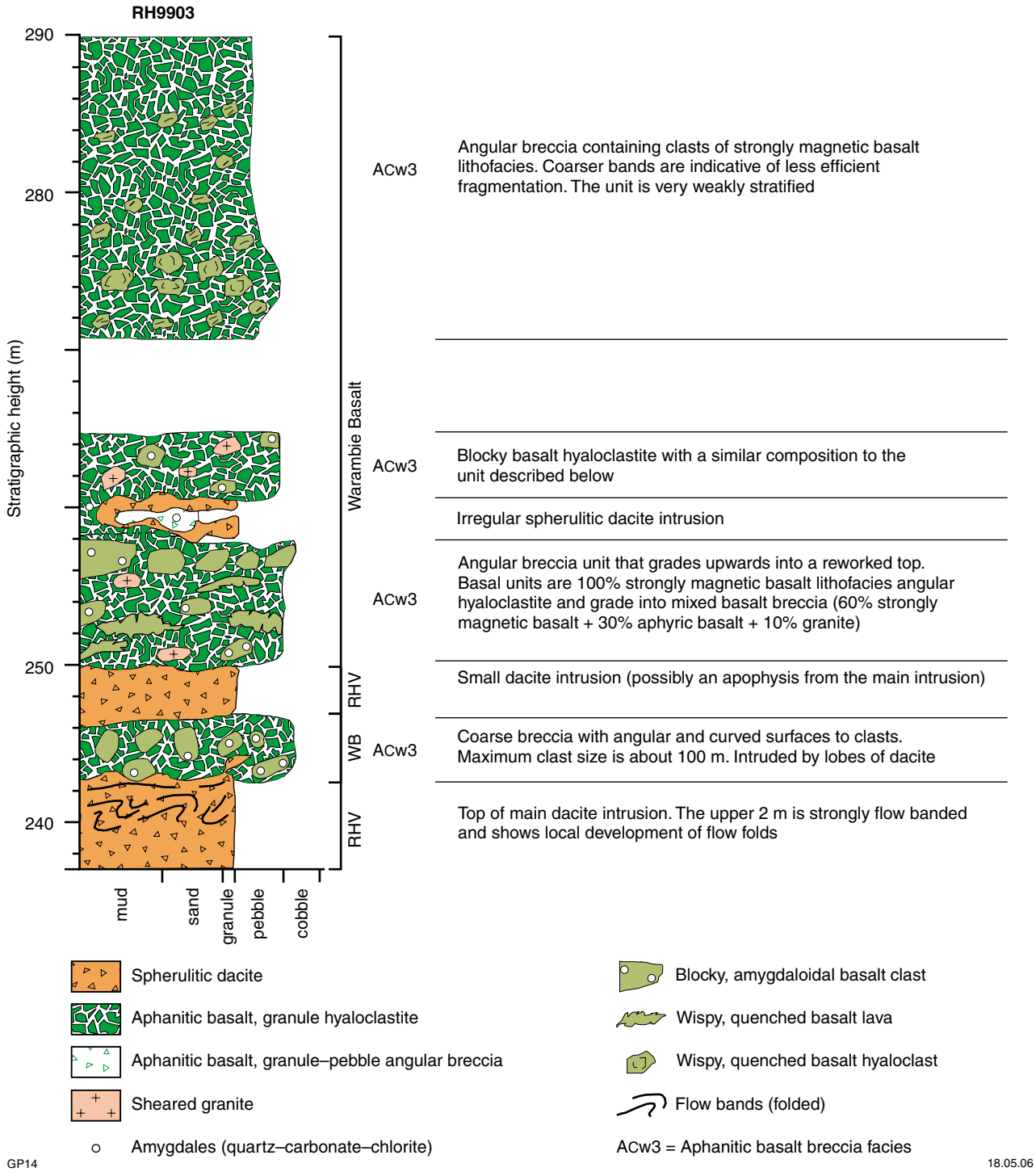

Figure 14. Upper section of stratigraphic log RH9903 (base at MGA 55260E 7682960N), Warambie Basalt, Red Hill area (see Fig. 8 for regional location); RHV = Red Hill Volcanics, WB = Warambie Basalt

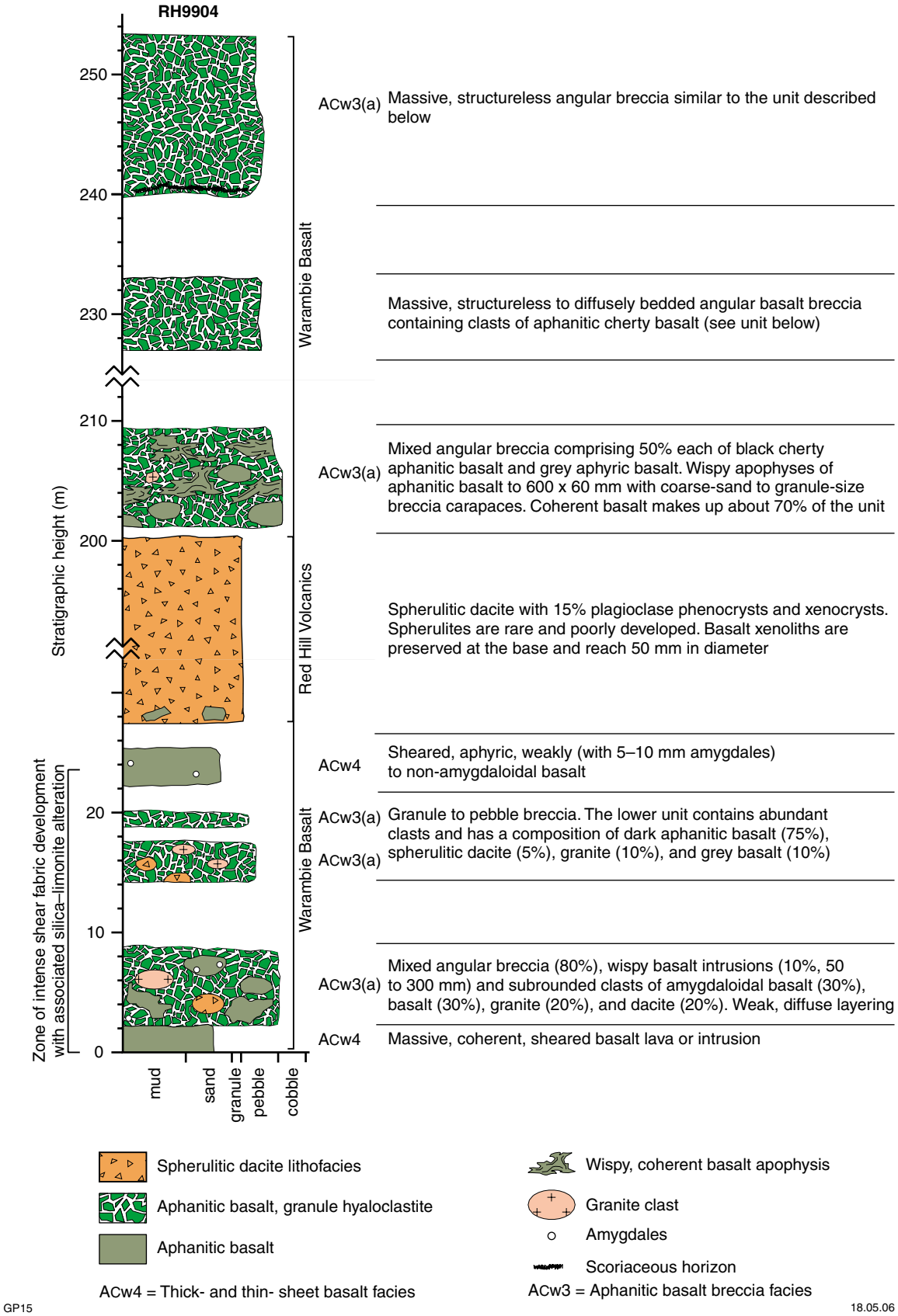

Figure 15. Stratigraphic log RH9904 (base at MGA 554860E 7682775N), from the Red Hill area, which is dominated by basalt brecia with subordinate lava (see Fig. 8 for regional location)

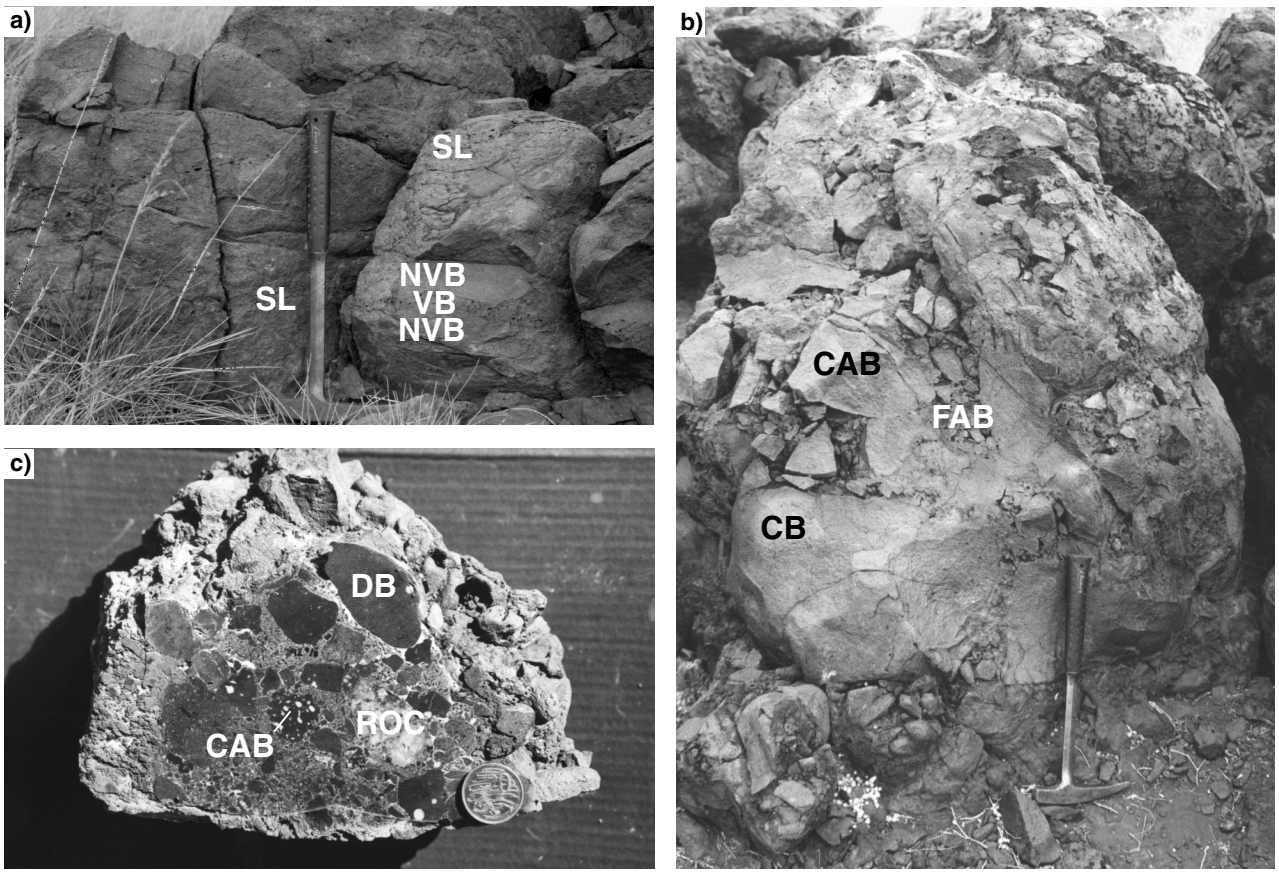

Figure 16. Facies of the Warambie Basalt near Red Hill: a) thin sheet basalt facies (SL), comprising nonvesicular basalt (NVB) and thin (~5 cm) vesicular horizons (VB); b) thin sheet basalt facies, showing the transition between coherent basalt (CB) and a range of coarse- (CAB) and fine-grained (FAB) breccia. Coarse breccia includes angular pebble and cobble clasts and may include both autobreccia and hyaloclastite. Fine breccia is composed of granule- and pebble-sized clasts and is dominantly hyaloclastite; c) slab of the basaltic pebble breccia and conglomerate facies, showing a range of basalt clast types, including dense (nonvesicular) basalt (DB), calcite amygdaloidal basalt (CAB), and a single, red, oxidized clast (ROC; MGA 55138E 7682856N)

typically include aphanitic basalt (commonly weathered light blue-grey), plagioclase-phyric basalt, and coarse-grained basalt–dolerite. The sedimentary matrix is poorly sorted, angular, basaltic volcaniclastic sandstone.

Interpretation

The weathered tops of flows in the thick- and thin-sheet basalt facies are strongly suggestive of a lava flow origin. Vesicle layers in basalt are interpreted as segregation horizons that formed due to late vesiculation (probably induced by crystallization). The vesicles accumulated beneath the upper crust of the cooling flow. Although typical of basalt lava successions, such structures could also form in cooling shallow intrusions where vapour pressures exceeded lithostatic pressure. Angular breccia transitional into coherent basalt is mixed autobreccia (larger clasts) with matrix hyaloclastite.

The basaltic pebble breccia and conglomerate facies shows evidence of moderate, but variable, clast rounding and preserves a range of subrounded to subangular clasts. The subrounded clasts indicate high-energy reworking of coherent basalt or juvenile basaltic breccia. There is no evidence for prolonged transport by tractional currents (sorting or clast imbrication), and very little or no allochthonous nonbasaltic material is preserved (e.g. granitic clasts). Basalt clasts similar in composition to the remainder of the Warambie Basalt suggest that the basaltic pebble breccia and conglomerate facies was reworked in situ or transported only a short distance. A subaerial or shallow subaqueous origin is envisaged in which the clasts were subject to erosion by wave or storm activity.

Aphanitic basalt breccia facies and scoriaceous basalt breccia facies

Granule- to pebble-sized (and rare cobble-sized) breccia of the aphanitic basalt breccia facies (*ACw3*) at the top of the Warambie Basalt in the Red Hill area contains angular clasts of aphanitic, charcoal-grey, cherty, strongly magnetic basalt (a distinctive characteristic of the lithofacies is a strong magnetic signature that prevents the use of a compass close to the outcrop). The typically jigsaw-fit breccia has angular irregular clasts of even grain size. Clasts display millimetre-scale flow-band laminae defined by subtle colour variations. Complex, elongate, wispy apophyses of similar composition have transitional

texture indicating margin fragmentation (Fig. 18a). The apophyses are also millimetre banded with bands parallel to the margins. A coherent unit illustrated in Figure 19 is a beautifully preserved lava lobe with pillow character. Massive units of poorly exposed aphanitic basalt breccia facies (locally up to 80 m in thickness) are commonly associated with very small volumes of the scoriaceous basalt breccia facies. Mapping in the Red Hill area distinguished two subfacies of the aphanitic basalt breccia facies: the main subfacies contains grey aphanitic basalt clasts (*ACw3(a)*), and the glomeroporphyritic basalt subfacies (*ACw3(b)*) is composed of angular, granule- to pebble-sized plagioclase-glomeroporphyritic basaltic breccia.

The scoriaceous basalt breccia facies (not sufficiently extensive to be shown on the 1:10 000-scale Plates 1 and 2) is similar to the aphanitic basalt breccia facies, but is dominated by weakly scoriaceous basaltic breccia (Fig. 20). Importantly, a clast-rotated subfacies is preserved. The margins of clasts are commonly nonvesicular or are less vesicular than the centre.

Interpretation

Both facies are interpreted as largely in situ hyaloclastite based on the quenched (cherty) aphanitic appearance, demonstrable intrusive contacts with coherent intrusive material of the same composition, and recognition of angular jigsaw-fit breccia texture. The recognition of a strong aligned magnetic effect on a compass may also indicate that the clasts were not rotated after cooling. Wispy apophyses may be connected in three dimensions or form isolated bodies frozen before complete quench fragmentation. A subaqueous setting is thus indicated. Volumetrically, the aphanitic, scoriaceous basalt breccia facies is insignificant, and suggests that much of the parent magma was degassed before or during eruption. Clasts with amygdale-rich centres and dense margins indicate that cooling prevented degassing of the freezing magma and is consistent with the interpretation of rapid quench fragmentation. These clasts also suggest that the magma was emplaced before vesiculation that occurred during cooling, and before formation of the glassy matrix.

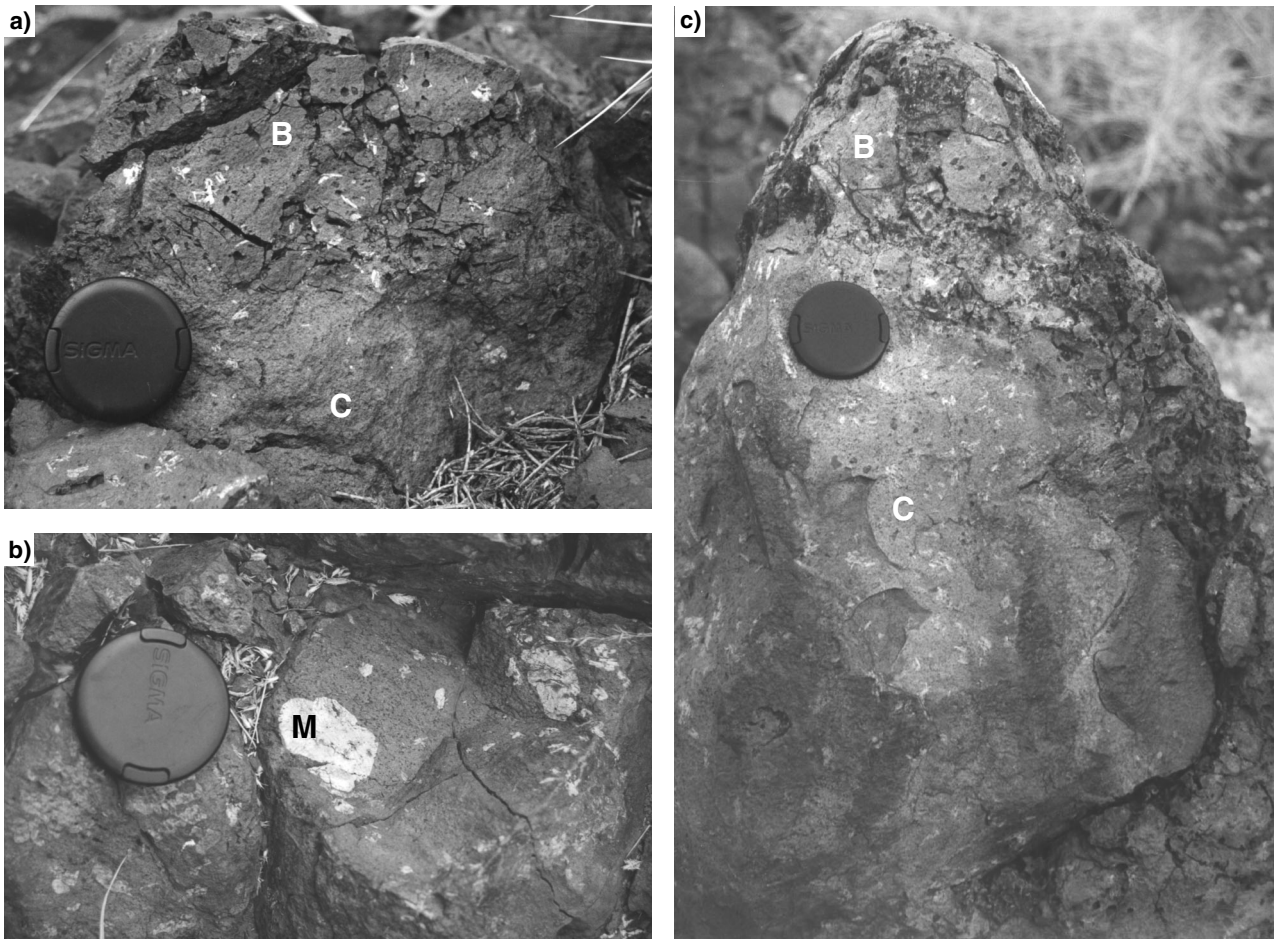

Figure 17. Photographs from stratigraphic log RH9906 (MGA 53960E 7682680N; see Fig. 8 for regional location): a) transitional basalt outcrop from coherent basalt at the base (C) to (jigsaw-fit) brecciated basalt at the top (B); b) plagioclase megacrysts (M) showing rounded resorbed margins. The largest megacrysts are about 40 × 30 mm and some have small satellite laths of plagioclase; c) transitional coherent (C) to (jigsaw-fit) brecciated (B) basalt

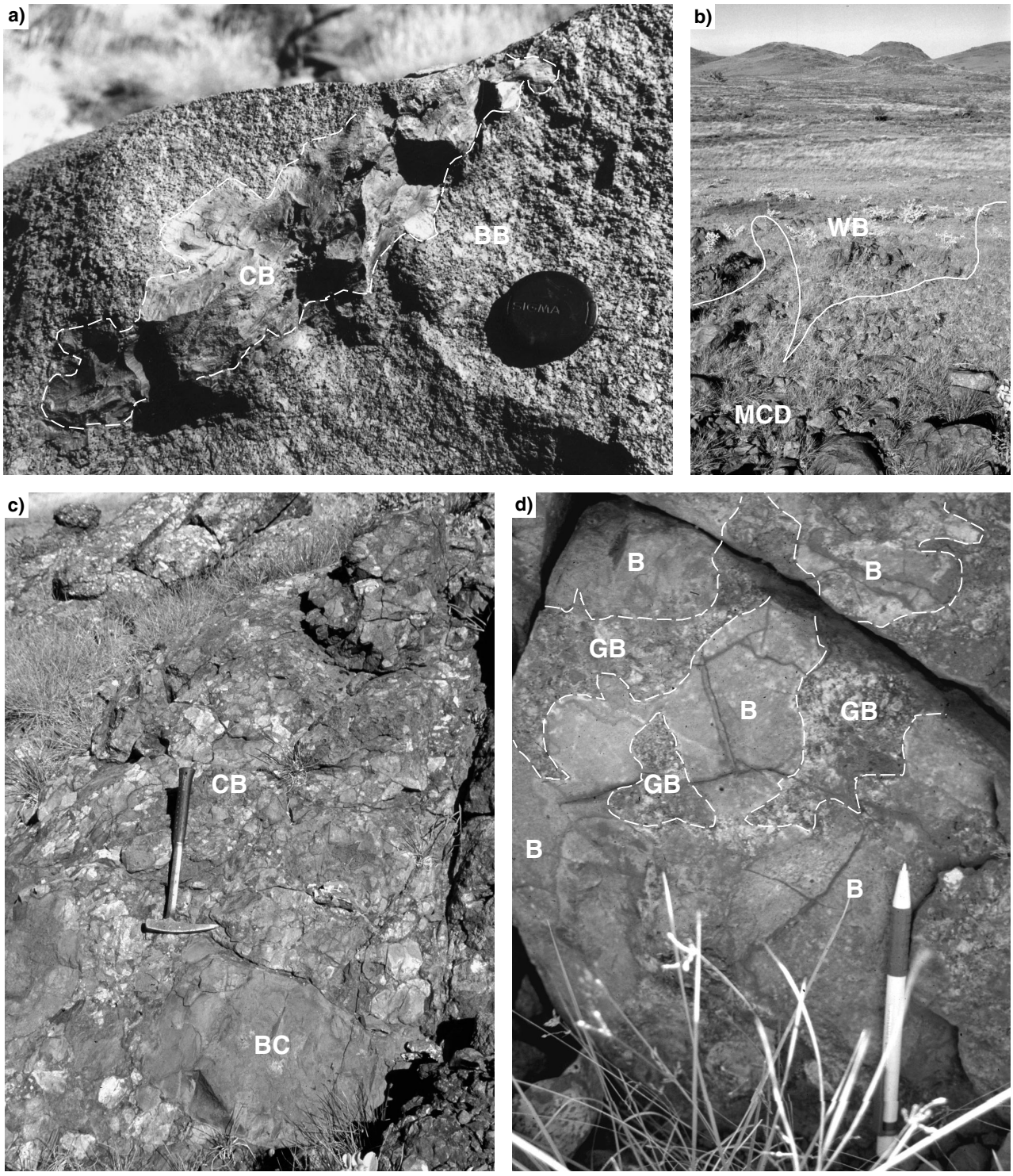

Figure 18. Facies of the Warambie Basalt: a) typical exposure of aphanitic basalt breccia facies (*ACw3*) dominated by granule basalt breccia (BB). A wispy, coherent basalt unit (CB) preserved within the centre of the unit may represent the core of a strongly brecciated unit or may have intruded the breccia immediately after brecciation. The latter interpretation is favoured here because the contact with the breccia is dominantly planar (MGA 554939E 7682456N); b) irregular boundary between the grey dolerite and basalt facies (*ACw2*) of the Warambie Basalt and the Mons Cupri Dacite Member (MCD; MGA 573962E 7682198N; c) volcaniclastic breccia, containing an upward-fining succession including a single, aphyric boulder clast of basalt (BC) at the base of an upward-fining cobble breccia (CB). The outcrop is part of the massive volcaniclastic breccia facies (*ACh8*) of the Red Hill Volcanics, whereas the boulder clast is part of the grey dolerite and basalt facies of the Warambie Basalt; d) irregular contact between basalt (B; grey dolerite and basalt facies, Warambie Basalt) and granule breccia (GB; massive volcaniclastic breccia facies, Red Hill Volcanics; MGA 573925E 7682237N). The basalt clearly intruded the granule breccia and the recognition of an isolated clast of the sedimentary rock within the basalt suggests dynamic mixing of unconsolidated sediment and basalt magma, resulting in the formation of a peperite

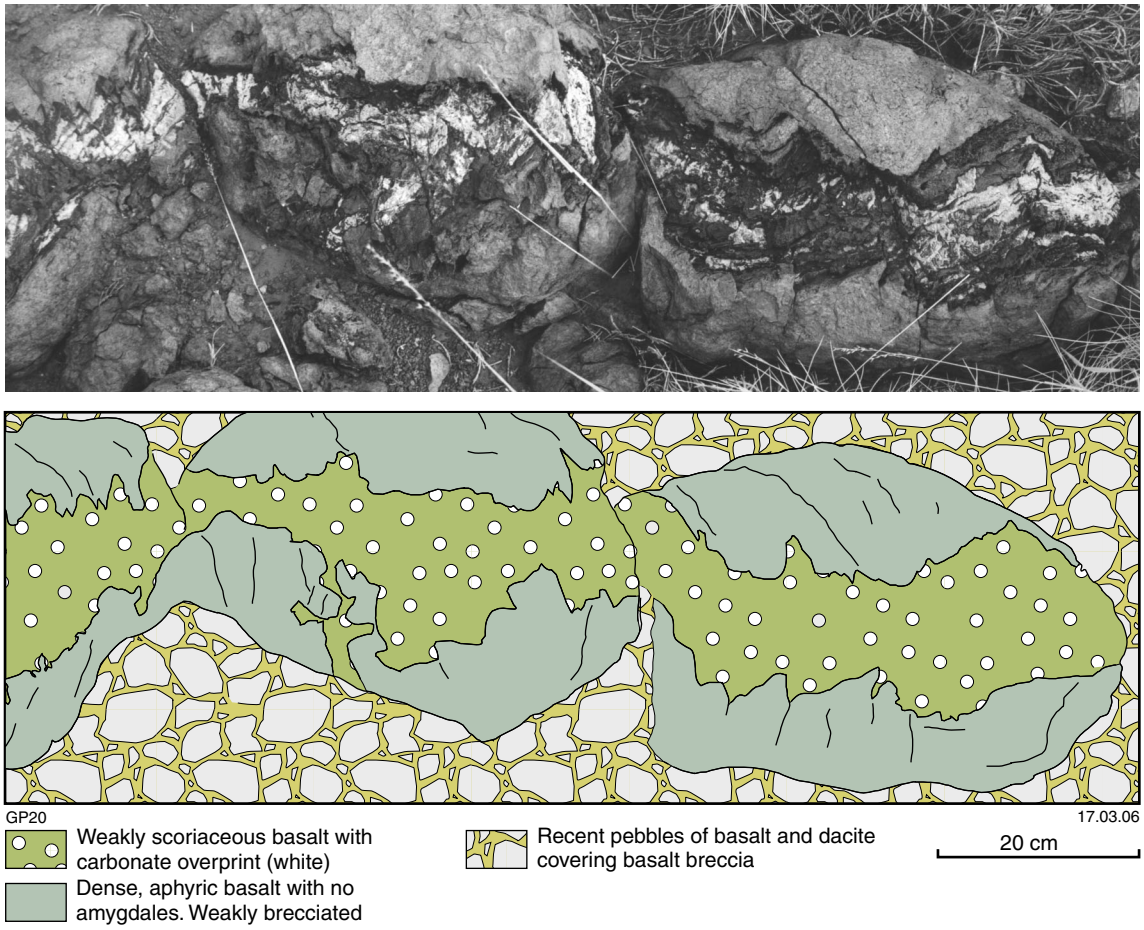

Figure 19. Lava 'toe' in Warambie Basalt, showing three pillow-like structures separated by narrow 'necks'. Propagation of the lava toe break-out from the front of each pillow structure was due to inflation from the magma channelled through the centre of the structure

Arkosic sandstone and conglomerate association

Medium- to coarse-grained, polymictic rocks recognized from a single stratigraphic section (*ACw6* and *ACw7*, Fig. 13) have limited outcrop. The facies association is locally up to 6 m in stratigraphic thickness, but has little lateral extent (<50 m) and is not shown on the 1:10 000-scale Plates 1 and 2. However, the association is important because of the dominance of siliciclastic material (quartz and granitic lithics). Arkosic sandstone and conglomerate outcrop with the thick- and thin-sheet basalt facies of the basalt lava and breccia association.

Arkosic sandstone facies and matrix-supported conglomerate facies

Coarse-grained sandstone and granulestone of the arkosic sandstone facies (*ACw6*, Fig. 13) contain angular grains of plutonic quartz (50%), feldspar (35%), and mafic (amphibole and secondary chlorite) grains (15%). Individual beds are decimetre-scale, massive, upward fining, and contain basal, monomictic, granitic microbreccia zones. The basal contacts of beds are planar and appear to be non-erosive. The granite clasts are of granule to fine-pebble size and only at the base of each fining-upward package. The composition of sand-sized grains is similar to that of granule- to pebble-sized granitic lithics and suggests a similar (granitic) source for both components. The sandstones have no interbedded fine-grained layers, are laterally discontinuous (?lensoidal), and commonly only a few metres thick.

Coarser grained sedimentary rocks of the matrix-supported conglomerate facies (*ACw7*, Fig. 13) contain up to 10% basaltic cobbles, up to 80 mm in diameter. The matrix is identical in composition to the framework grains of the arkosic sandstone facies. Basalt clasts are typically subrounded and amygdaloidal (10% 15 mm spherical vesicles), and are randomly dispersed in, and surrounded and supported by, the sandstone matrix. The matrix preserves a strong tectonic fabric and appears otherwise massive. Floating basalt clasts are clearly derived from a separate source to the sandstone matrix.

Interpretation

The basalt clasts of the matrix-supported conglomerate facies are subrounded, indicative of high-energy reworking. Hence, these clasts have been transported some distance or have remained in the transport cycle

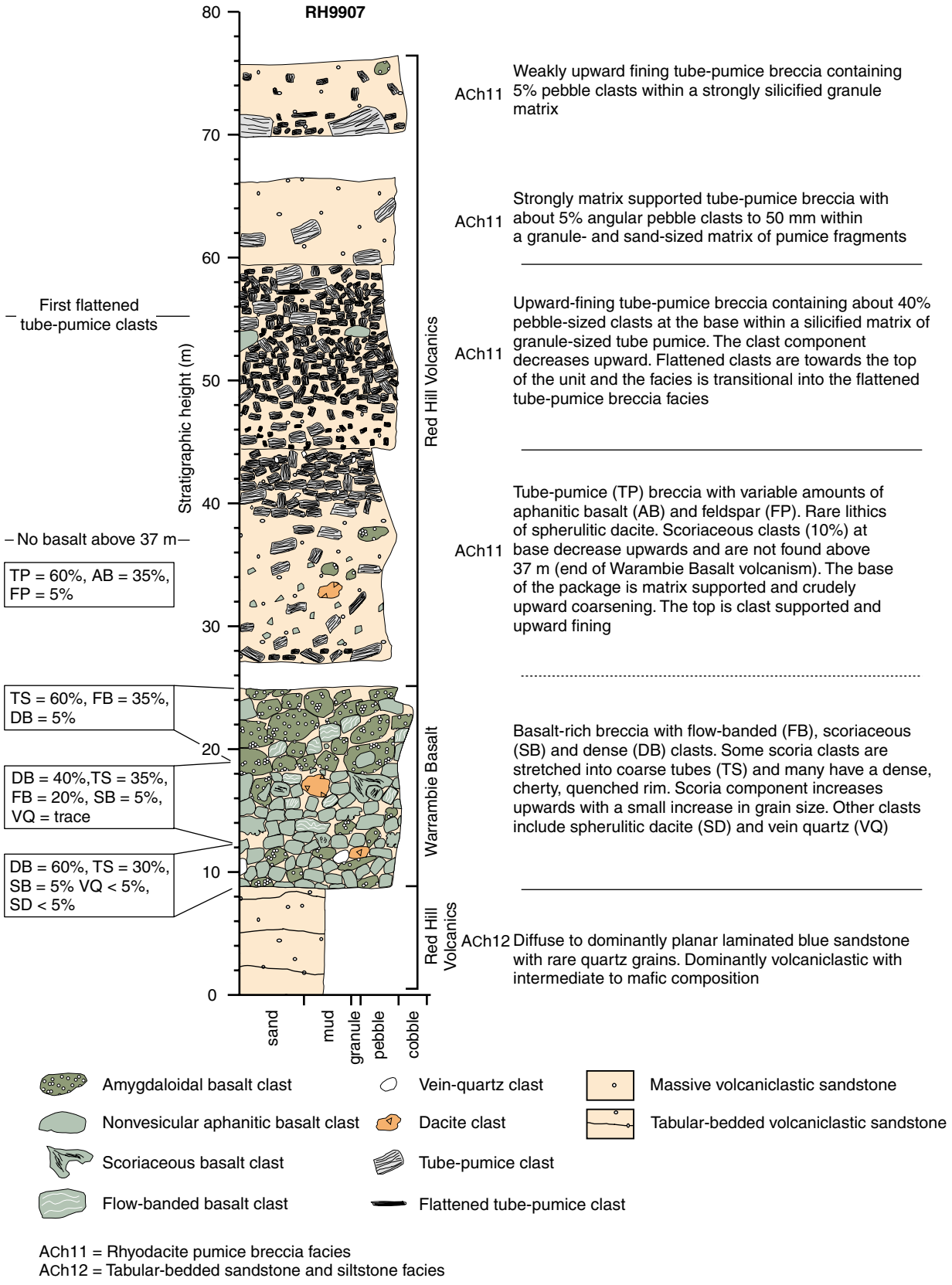

Figure 20. Stratigraphic log RH9907 (base at MGA $_{5}$54860E $_{76}$82040N), from the Red Hill area, illustrating the maximum preserved thickness of the scoriaceous basalt breccia facies of the Warambie Basalt (see Fig. 8 for regional location)

for some time. The association of large basaltic clasts and quartz-rich sandstone indicates rapid deposition with little physical or chemical erosion. Basalt clasts are clearly reworked (subrounded margins) and were probably mixed with siliciclastic matrix before deposition. Possible transport mechanisms include debris flows, grain flows, and high-concentration turbidity currents. Upward-fining beds of the arkosic sandstone facies are consistent with deposition from turbidity currents or sandy debris flows (e.g. Shanmugam, 1997). Within the matrix-supported conglomerate facies the large basalt clasts are much coarser grained than the matrix material. The entire arkosic sandstone and conglomerate association may be interpreted as debris flows (matrix-supported conglomerate facies) and pseudolaminar to turbulent, high-density turbidity currents (arkosic sandstone facies). The favoured environmental setting is a subaqueous fan adjacent to a beach or shallow shelf.

Grey dolerite and basalt association

The grey dolerite and basalt association is developed close to the basal unconformity with the Whundo Group in the Good Luck area, and is therefore at a similar stratigraphic level to the Warambie Basalt at Red Hill. Basalts are typically dark grey and weakly pyroxene-phyric.

Grey dolerite and basalt facies, and grey basalt intrusive breccia facies

The grey dolerite and basalt facies (*ACw2*) comprises mainly crystalline, dark charcoal-grey dolerite and basalt that contain both plagioclase and altered pyroxene crystals. Dolerite is interlayered with basaltic rocks of identical colour, but finer grain size. Packages of dolerite and basalt are typically tens of metres thick and have a tabular geometry. The facies may be intrusive or extrusive, but a basaltic volcaniclastic sandstone subfacies suggests that it was exposed for some period and eroded and redeposited.

The upper margin of the grey dolerite and basalt facies may be irregular, with large blocks of fine-grained basaltic material intermixed with clastic rocks of the Red Hill Volcanics. This is termed the grey basalt intrusive breccia facies (not shown on the 1:10 000-scale Plates 1 and 2), and the basalt differs slightly from the grey dolerite and basalt facies. It has a dark-grey to blue colour and contains abundant (~30%), elongate, 10–15 mm vesicles at the contact with overlying sedimentary facies. Typically, large cobble- and boulder-sized clasts are angular, and an order of magnitude larger than the framework clasts of overlying facies in the Red Hill Volcanics (Fig. 18c). The irregular margins of quenched basaltic clasts suggest that they are extremely juvenile. In a single outcrop (Fig. 18d), angular irregular apophyses of the basalt intrude the base of sandstone and breccia facies in the overlying Red Hill Volcanics. This basalt displays a transition from coherent basalt through to mixed angular basalt breccia within a structureless sand- and granule-rich matrix.

Interpretation

The grey basalt intrusive breccia facies contains peperite and is interpreted to have formed through the synvolcanic mixing of quench breccia and sedimentary material. The peperite indicates that the grey dolerite and basalt association was approximately contemporaneous with sedimentation of the Red Hill Volcanics. Large basalt clasts within the Red Hill Volcanics, immediately above the peperite contact, indicate that the emplacement of the Warambie Basalt caused doming and slumping of coarse-grained sedimentary rocks.

Schistose basalt facies

The schistose basalt facies (*ACw1*) is exposed in one location between Whim Creek and Mons Cupri, and consists of quartz amygdaloidal basalt, of uncertain stratigraphic position, that displays limonite–chlorite–silica alteration. No direct correlation can be made with any other facies or lithofacies. Fitton et al. (1975) and Huston (D. L., 1999, written comm.) mapped this outcrop as Warambie Basalt, and this interpretation is supported by a similar cleavage (S_2) as in the Warambie Basalt in other areas.

Red Hill Volcanics

The Red Hill Volcanics, defined by Pike and Cas (2002) and Pike et al. (2002), conformably overlie the Warambie Basalt, although some components of the Warambie Basalt were emplaced during early sedimentation of the Red Hill Volcanics. The Red Hill Volcanics are volumetrically dominated by the intrusive to extrusive Mons Cupri Dacite Member (Fig. 8), but the formation also contains medium- to coarse-grained volcaniclastic rocks, here assigned to a number of allochthonous sedimentary facies. The facies and facies associations for the Red Hill Volcanics are shown in Table 4. During previous investigations of the Whim Creek greenstone belt, most of these volcaniclastic rocks were misidentified as 'tuffs', and included within the 'Mons Cupri Volcanics' (old formation name; Fitton et al., 1975).

Allochthonous sedimentary facies

Juvenile volcaniclastic association

The Red Hill Volcanics in the Red Hill area contain three facies assigned to the juvenile volcaniclastic association (Table 4); all three facies conformably overlie the Warambie Basalt. In stratigraphic order they are the tabular-bedded sandstone and siltstone facies, the rhyodacite pumice breccia facies, and the flattened tube-pumice breccia facies. Stratigraphic logs of the facies associations of the Red Hill Volcanics are presented in Figures 20 to 22.

Tabular-bedded sandstone and siltstone facies

The tabular-bedded sandstone and siltstone facies (*ACh12*; Fig. 23a) outcrops in small creek beds over an area of 4 km × 500 m (maximum thickness 140 m). The facies conformably overlies subaqueous hyaloclastite and minor lava of the Warambie Basalt. Tabular, centimetre- to decimetre-scale beds with no internal grading, but excellent sharp bedding, and diffuse planar lamination

Table 4. Facies and facies associations of the Red Hill Volcanics

Facies association	*Facies*	*Area*	*Code*
Dacite-associated coarse-grained sedimentary	Coarse-grained dacite-rich breccia	Good Luck Well	ACh6
	Polymictic conglomerate and breccia	Good Luck Well	ACh1
	Imbricate conglomerate	Good Luck Well	ACh2
Large volume dacite (Mons Cupri Dacite Member)	Large volume dacite	Good Luck Well	AChm1
Small volume dacite (Mons Cupri Dacite Member)	Mixed dacite breccia–sandstone[(a)]	Good Luck Well	–
	Crystalline inclusions[(a)]	Good Luck Well / Red Hill	–
	Small volume dacite	Good Luck Well / Red Hill	AChm2
	Dacite pods	Red Hill	AChm3
Grey breccia and sandstone	Siltstone	Good Luck Well	ACh3
	Pumice and crystal-rich breccia	Good Luck Well	ACh4
	Massive sandstone	Good Luck Well	ACh5
	Coarse-grained dacite-rich breccia	Good Luck Well	ACh6
	Sandstone and breccia	Good Luck Well	ACh7
	Massive volcaniclastic breccia	Good Luck Well	ACh8
	Tabular-bedded sandstone	Good Luck Well	ACh9
Juvenile volcaniclastic	Flattened tube-pumice breccia	Red Hill	ACh10
	Rhyodacite pumice breccia	Red Hill	ACh11
	Tabular-bedded sandstone and siltstone	Red Hill	ACh12

NOTE: (a) Facies too restricted to be shown on Plates 1 and 2

are characteristic. Microbreccia, sandstone, and siltstone are noted, and bed thickness is greatest for units with the coarsest grain size. Typically, coarser grained (sandstone) beds are overlain by a siltstone layer of similar thickness or thinner, and the two may define individual bed sets. Thin section analysis reveals aphanitic chlorite-altered clasts with shard-like textures (Fig. 23b) of pumice, tube pumice, and weakly vesicular to nonvesicular rocks. Grains include plagioclase-phyric volcanic rocks (65%), subrounded polycrystalline quartz (15%), and 5% each of devitrified glass shards, pumice, perlite-fractured volcanic rocks, and plagioclase. There are small amounts (<5%) of subrounded aphanitic andesite (containing abundant matrix plagioclase laths) as well as monocrystalline and polycrystalline, silt- to sand-sized quartz grains. The quartz grains are irregular in shape, show no evidence of rounding, and may be volcanic in origin. Polycrystalline quartz grains are mostly angular and could be either detrital or xenolithic in origin, and were derived from a plutonic source.

Many of the flow-banded angular clasts have a scoriaceous centre surrounded by a thin (millimetre-scale) cherty rim. Some clasts have moulded plastically around other clasts and brecciated clast margins are relatively common. Dacite and vein quartz lithic fragments are also noted. No obvious fine-grained matrix is noted in the field, but this may be due to poor exposure and preferential weathering between clasts.

Rhyodacite pumice breccia facies

The rhyodacite pumice breccia facies (*ACh11*) contains beds up to 20 m thick of clast-supported pumiceous material (Fig. 24) within a sandy, shard-rich matrix. The facies forms a tabular, up to 145 m-thick, unit over about 4.5 km strike length. A basal vesicle-poor subfacies (*ACh11(a)*) is interbedded with the tabular-bedded sandstone and siltstone facies (*Ach12*) where the latter forms 1–4 m-thick massive beds (Fig. 22, 10–43 m). The subfacies is typically 10 m in total stratigraphic thickness, and comprises angular volcanic lithic clasts of amygdale-poor andesite or dacite with rare spherulitic dacite. The remainder of the rhyodacite pumice breccia facies comprises upward-fining, dominantly matrix supported, monomictic pumice breccia (pebble subfacies, *ACh11(c)*), sandstone (sandstone subfacies, (*ACh11(d)*), and granule-sized monomictic tube-pumice breccia with a fine-grained, recrystallized ash matrix (granule subfacies, (*ACh11(b)*). Beds are typically massive at the base (~10 m thick) and fine upward into millimetre-scale laminated chert at the highest stratigraphic level (Fig. 25a). Some of the laminated chert shows evidence of laminae truncation and onlap (Fig. 25b), suggesting that the lamina were deposited from a moving current.

The largest clasts within the facies are typically pebble- to (rare) cobble-sized tube pumice with elongate, quartz-filled amygdales. Most are angular, although cobble-sized clasts may show some rounding. Thin section examination (Fig. 26) shows rocks dominated by angular chloritic shards and tube pumice. Shards are typically 0.2 – 1 mm long and unflattened pumice clasts are typically 5 mm or longer. Lithic clasts include polycrystalline (probably plutonic) material (Fig. 26a) rich in sieve-textured plagioclase and secondary chlorite and calcite. These lithic clasts may be xenoliths derived from country rock or cognate xenoliths from the magma chamber.

Flattened tube-pumice breccia facies

The flattened tube-pumice breccia facies (*ACh10*) is very similar to the rhyodacite pumice breccia facies. Clasts are monomictic, variably squashed tube pumice. In extreme cases the pumice forms sheets about 1 mm thick and several centimetres long. Flattening is unaligned, bears no obvious relation to the weak cleavage observed in the area,

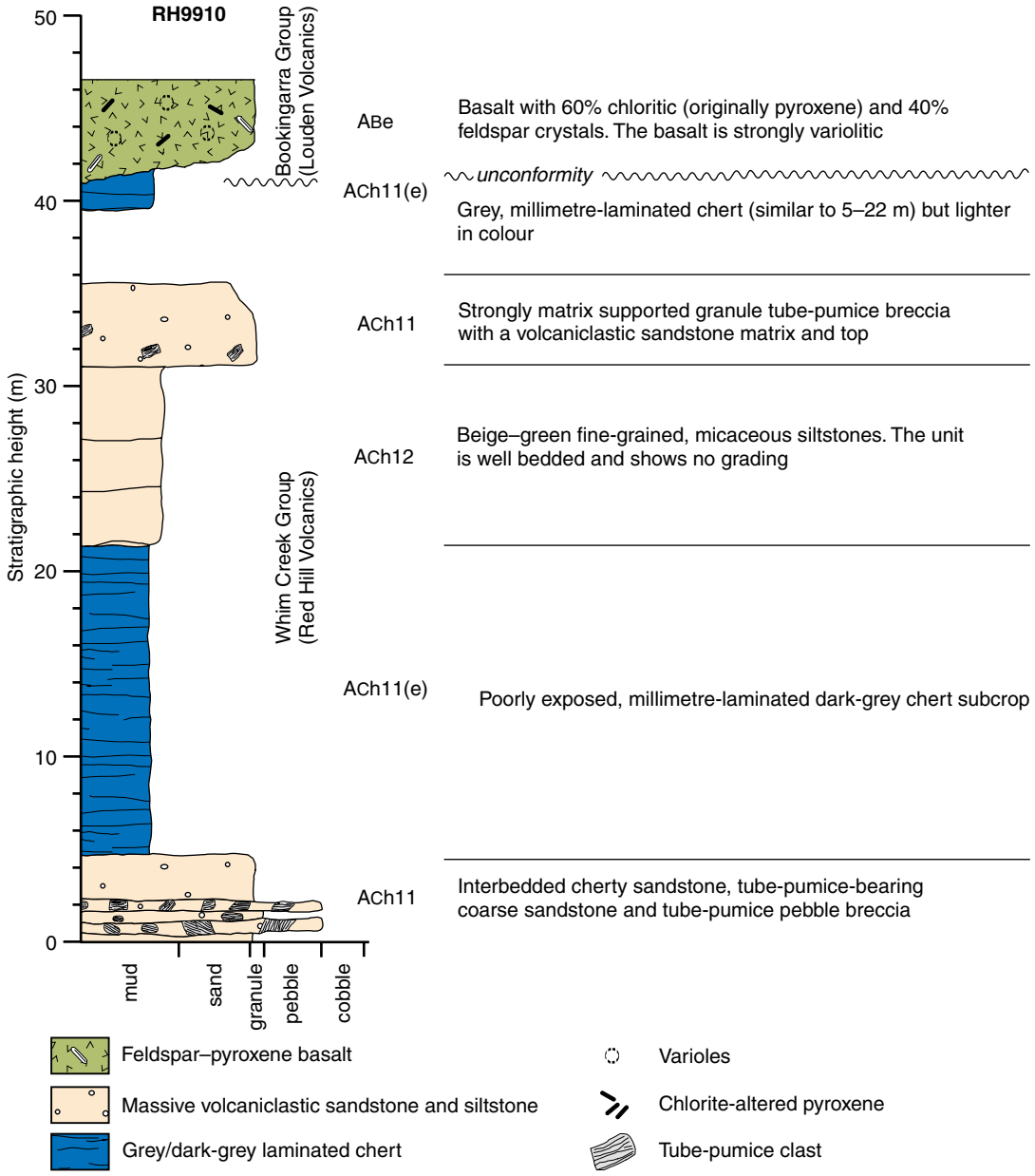

ACh11 = Rhyodacite pumice breccia facies
ACh11(e) = Rhyodacite pumice breccia facies (laminated siltstone subfacies; not mapped on Plates 1 and 2)
ACh12 = Tabular-bedded sandstone and siltstone facies
ABe = Louden Volcanics

Figure 21. Stratigraphic log RH9910 (MGA 556439E 7682202N), Red Hill Volcanics, Red Hill area, illustrating the interbedded nature of fine- and coarse-grained volcanic debris of the Red Hill Volcanics. Fine laminated chert of the rhyodacite pumice breccia facies (*ACh11*) represents either the preserved top of a large flow unit or a period of low-energy hemipelagic fallout with very fine sediment derived from distal flows. This section includes a very low angle unconformity and is overlain by massive, pyroxene–plagioclase-phyric lava and intrusions of the Louden Volcanics (see Fig. 8 for regional location)

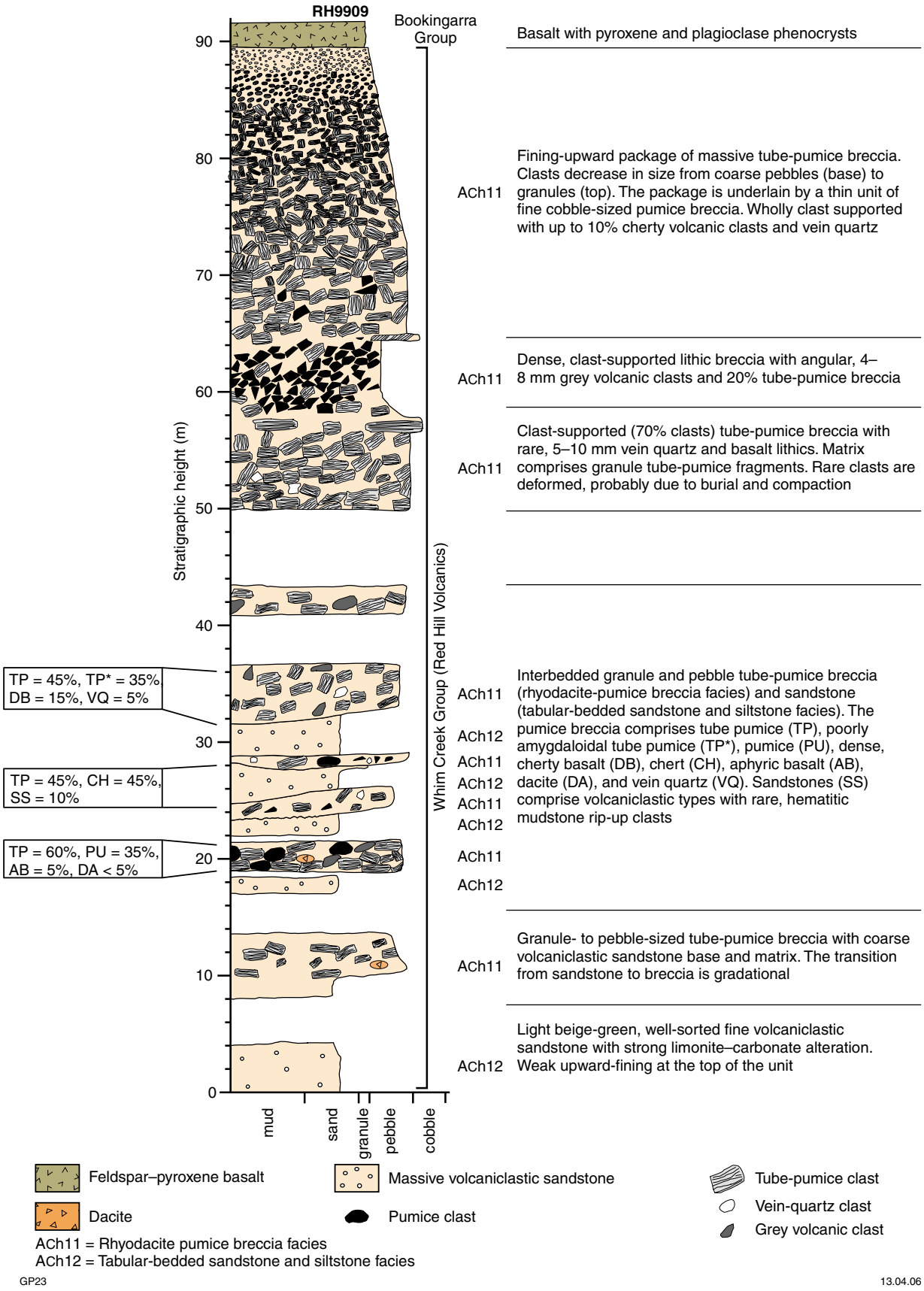

Figure 22. Stratigraphic log RH9909 (base at MGA $_{55}$6797E $_{76}$82794N), from the Red Hill area, illustrating thick massive units of the rhyodacite pumice breccia facies (*ACh11*) of the Red Hill Volcanics. The upper flow unit is of particular importance because it appears to show excellent hydraulic sorting of lighter (pumiceous) and denser (poorly to nonvesicular) debris (see Fig. 8 for regional location)

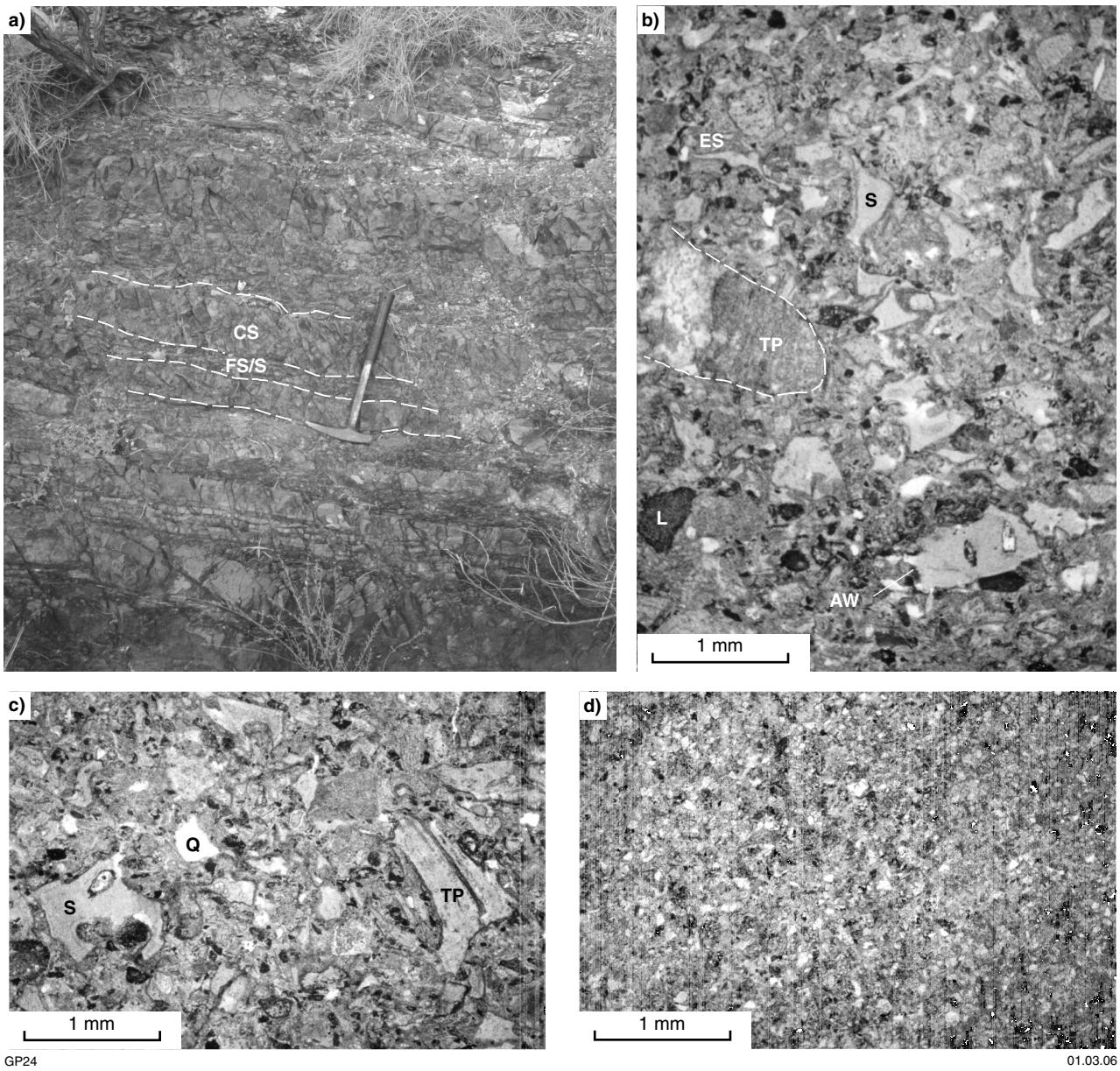

Figure 23. Tabular-bedded sandstone and siltstone facies (*ACh12*), Red Hill Volcanics: a) outcrop (MGA 555439E 7682456N), showing beds cut by closely spaced fractures. Beds dip gently south-southeast (CS = coarse sandstone, FS/S = fine sandstone/siltstone); b and c) photomicrographs of coarse-grained, shard-rich sandstone and granulestone comprising chlorite-altered, originally glassy, shards (S) and rare tube-pumice clasts (TP). Elongate shards (ES) are very well preserved, and show that there was little reworking before deposition. Some shards display cuspate margins due to fragmentation of amygdale walls (AW). Minor quartz (Q) is associated with all samples; d) photomicrograph of a reworked volcaniclastic sandstone typically interbedded with juvenile debris

and shows no associated welding textures. It is interpreted as a diagenetic compaction feature.

Interpretation

No in situ volcanic equivalent facies of the juvenile volcanic association were mapped, and very few paleocurrent data are available. Consequently, the location of the source region remains entirely cryptic. The association is dominated by tube pumice and angular chloritic shards that may have formed as a result of explosive fragmentation (e.g. Cas, 1992; Fisher and Schminke, 1984), quench fragmentation (Pichler, 1965), autobrecciation or reworking of coherent and brecciated volcanic material. Shards may also have been derived from attrition of glassy clasts during transportation (McPhie et al., 1993). The considerable thickness, large aerial extent, and inferred large original volume of the package points to a dominantly explosive system. Elongate clasts with cuspate margins (Fig. 26b,c) are similar to glass shards produced by explosive volcanism. Allen and McPhie (2000) suggested that angular pumice clasts (e.g. Fig. 26b,c) are commonly formed by magmatic volatile-driven explosive eruptions. The dominance of tube pumice

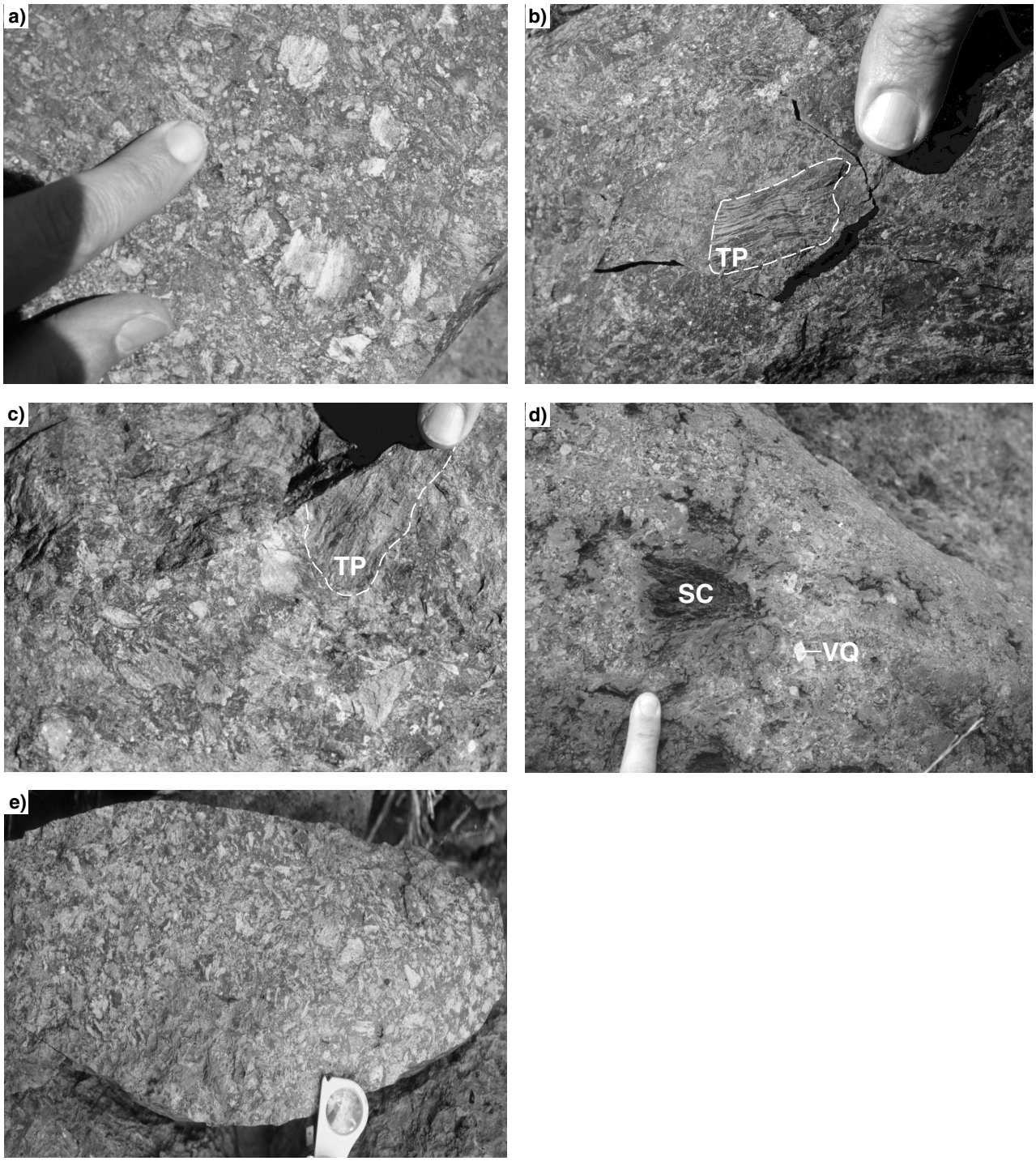

Figure 24. The rhyodacite pumice breccia facies (*ACh11*), Red Hill Volcanics, Red Hill area: a) dense, equant, angular breccia containing very weakly amygdaloidal tube-pumice clasts; b and c) poorly sorted subfacies, composed of blocky, pebble-sized, strongly amygdaloidal tube-pumice clasts (TP) within a sand, granule, and fine-grained pebble matrix; d) tube-pumice breccia with rare clasts of scoriaceous basaltic breccia (SC), and vein quartz (VQ). The basaltic clasts may have been derived from the scoriaceous basalt breccia facies of the Warambie Basalt or from a related volcanic episode; e) clast-supported, highly angular, well-sorted breccia with clasts similar to the dense clasts in (a)

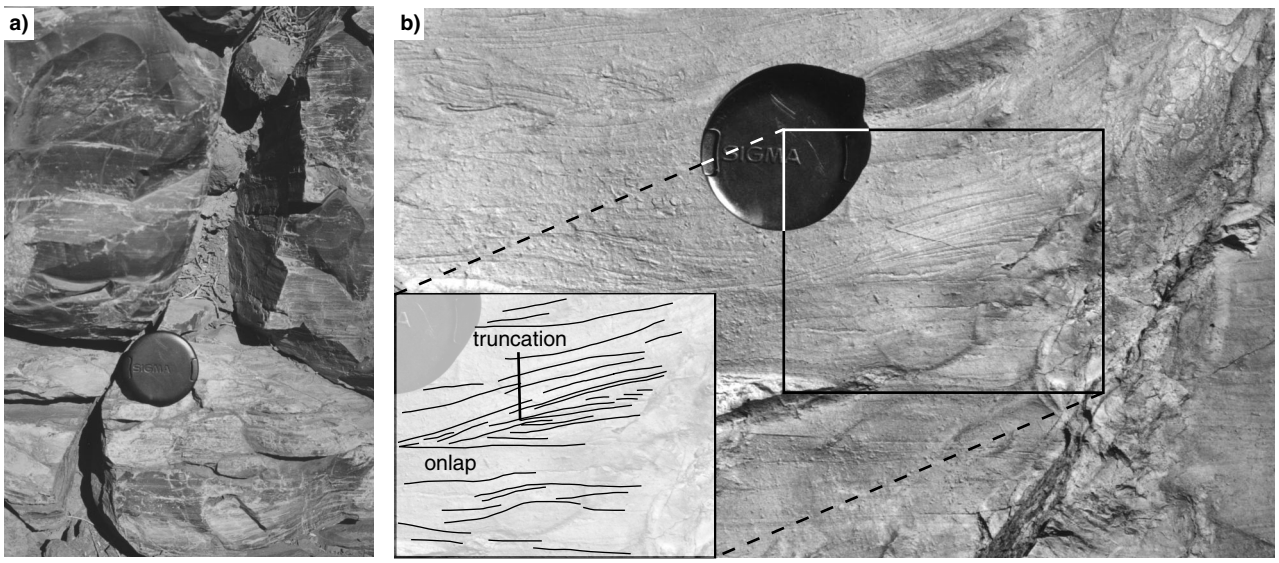

Figure 25. Laminated chert subfacies of the rhyodacite pumice breccia facies (*ACh11*), Red Hill Volcanics (MGA 555839E 7681856N): a) laminated blue chert; b) laminated chert showing onlap and truncation features. This outcrop suggests that at least some of the subfacies was deposited from the distal ends of currents, rather than as fallout from a water column

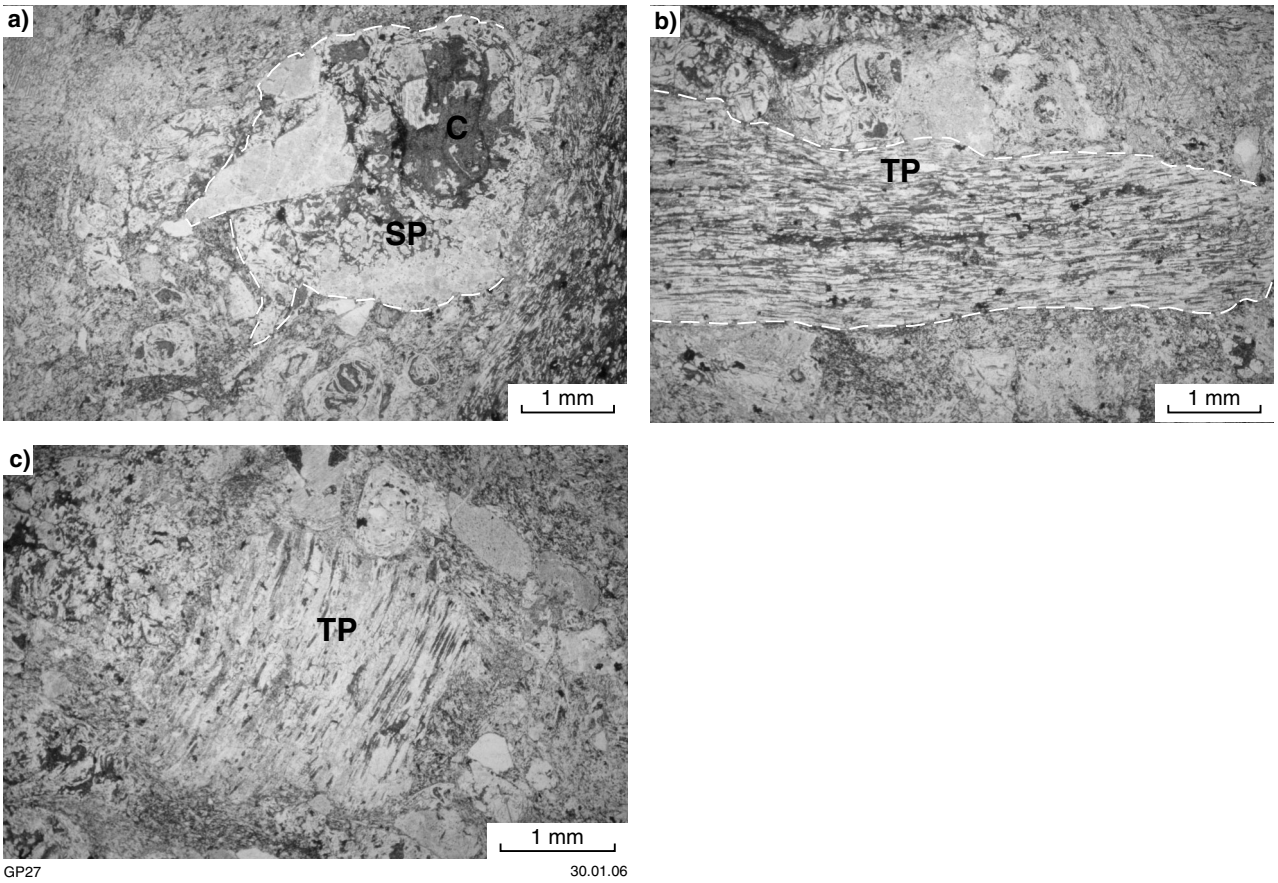

Figure 26. Photomicrographs of rhyodacite pumice breccia facies (*ACh11*), Red Hill Volcanics (MGA 572638E 7682753N): a) coarse-grained lithic mass derived from a plagioclase-rich plutonic rock or xenolith. Abundant chlorite (C) may replace a mafic phase. Sieve-textured plagioclase (SP) is relatively common. The clast has a rounded shape, suggesting reworking or dissolution within a magma chamber; b) elongate tube-pumice clast (TP); c) equant blocky tube-pumice clast (TP)

in rocks from the Red Hill area shows that vesiculation occurred during eruption and suggests high eruption rates or shear stress (or both). Hence, explosive expansion of magmatic volatiles is the most reasonable mechanism of fragmentation for much of the pumice breccia and shard-rich sandstone.

The tabular-bedded sandstone and siltstone facies comprises well-sorted, tabular-bedded, and weakly planar laminated sandstone with thinner siltstone or shale caps that are similar to Bouma T_aT_e turbidite (e.g. Walker, 1975). In this interpretation T_a units are the products of basal sandy debris flows (massive sandstone) and turbidity currents (diffuse planar-laminated sandstone) with a cap of siltstone derived from low-energy flows of the Bouma T_d. The lack of fine-grained ash or clay suggests one or both of upstream elutriation of fine-grained particles or deposition of clay-sized material downstream, or, alternatively, that clay-sized ash was not produced.

The rhyodacite pumice breccia facies contains massive beds of relatively deep subaqueous origin based on the recognition of a thick upward-fining succession capped by laminated chert, and shows no evidence of subsequent erosion. Sorting increases towards the top of the succession, and is accompanied by a decrease in grain size, suggesting that turbulent flow became more important as the depositional system evolved. Coarse-grained breccias are thick, massive, and have sandy matrices. Dominantly angular clasts suggest little clast interaction, and a probable debris-flow origin. Weakly vesicular clasts are largely restricted to basal sections, and may have been efficiently sorted during earlier flow. The rhyodacite pumice breccia facies appears to be the result of a debris flow of pumice and ash with associated development of turbidity currents containing finer ash-sized material.

All three facies are of explosive origin and were derived from pyroclastic flows, their resedimented equivalents, or from later reworking of large volumes of loose pyroclastic debris.

Grey breccia and sandstone association

The grey breccia and sandstone association outcrops in the Good Luck Well area, and to a lesser extent in the Mons Cupri area. The association contains seven facies (Table 4) characterized by thick tabular beds of grey volcanic sandstone and breccia. Locations of logged sections are shown on Figure 9 and key stratigraphic logs and photos are presented in Figures 27 to 32. Many of the clastic rocks exposed in the Good Luck Well area are poorly exposed or strongly calcretized and, consequently, little is known about their sedimentology.

Tabular-bedded sandstone facies

The tabular-bedded sandstone facies (*ACh9*) comprises dominantly coarse-grained sandstone with lesser granulestone and thin (centimetre-scale) tabular fine-grained sandstone–siltstone. The facies contains decimetre- and metre-scale tabular beds that may be traced for tens to hundreds of metres along strike, and the facies is interbedded with the coarse-grained dacite-rich breccia facies (*ACh6*, units too small to be shown on Plates 1 and 2) and the massive volcaniclastic breccia facies (*ACh8*, Figs 28–32). Bed sets commonly include a lower, ungraded coarse-grained sandstone–granulestone (~50 cm thick) capped by a chert-like laminated fine-grained sandstone (<10 cm thick) with a sharp lower contact. Typical sedimentary structures include coarse- to fine-grained sandstone beds with sharp planar contacts, normally graded coarse-grained sandstone, and diffuse planar-laminated coarse-grained sandstone (Fig. 33a–c). Figure 33 illustrates other structures such as mudstone rip-up clasts, flame structures, thin sandstone dykes, asymmetric ripple marks, breccia-filled microchannels, isolated large boulders, and low-angle dune cross-beds. Thin sections show reworked shard-rich and quartz-rich volcanic sandstone. Elongate shards are less common than in the juvenile volcaniclastic association. Quartz grains are commonly subspherical, highly angular, and dominated by plutonic quartz (some with undulose extinction) and lesser vein quartz. Andesite lithics contain microlaths of plagioclase within a strongly iron-altered groundmass.

Interpretation

The tabular-bedded sandstone facies was deposited under moderate- to high-energy flow conditions. Massive, graded, and diffuse planar-laminated beds contain large cobbles. Attenuated small rip-up clasts of sandstone and mudstone appear to have moved only a few centimetres relative to each other during flow, suggesting transport by debris flow. Rare, graded, diffuse, planar-laminated and dune cross-bedded examples are interpreted as the products of turbidity currents. Flame structures and sandstone dykes indicate dewatering, caused by the rapid loading of water-saturated sediments. The tops of individual flame structures are truncated suggesting that the overlying laminae or beds were eroded, most probably by a turbulent flow. Ripple marks are rarely preserved suggesting that low-energy currents reworked the surface of beds. Volcanic shards are poorly vesicular, with a weak chlorite overprint, and were originally glassy fragments derived from explosion, quench fragmentation, or mechanical abrasion of pumiceous material.

Massive volcaniclastic breccia facies

The massive volcaniclastic breccia facies (*ACh8*) is interbedded with the tabular-bedded sandstone facies (*ACh9*, Figs 28–32) and has a similar composition, dominated by light-grey aphanitic volcanic debris of intermediate to felsic composition. Figure 34 illustrates the range of clast types and general appearance of the facies. Numerous subfacies may be recognized, including clast-supported (dominant) and matrix-supported types, but all are related by a coarse grain size (granule to cobble), volcanic clasts, and massive structureless beds. Aphanitic light-grey (?andesitic) clasts with up to 30% amygdales and millimetre-scale flow bands are the most abundant (~75%). Lesser clast types include aphanitic dark charcoal-grey angular irregular basalt, light-grey angular felsic–intermediate volcanic rocks, granite pebbles, subrounded dacite (Mons Cupri Dacite Member), and

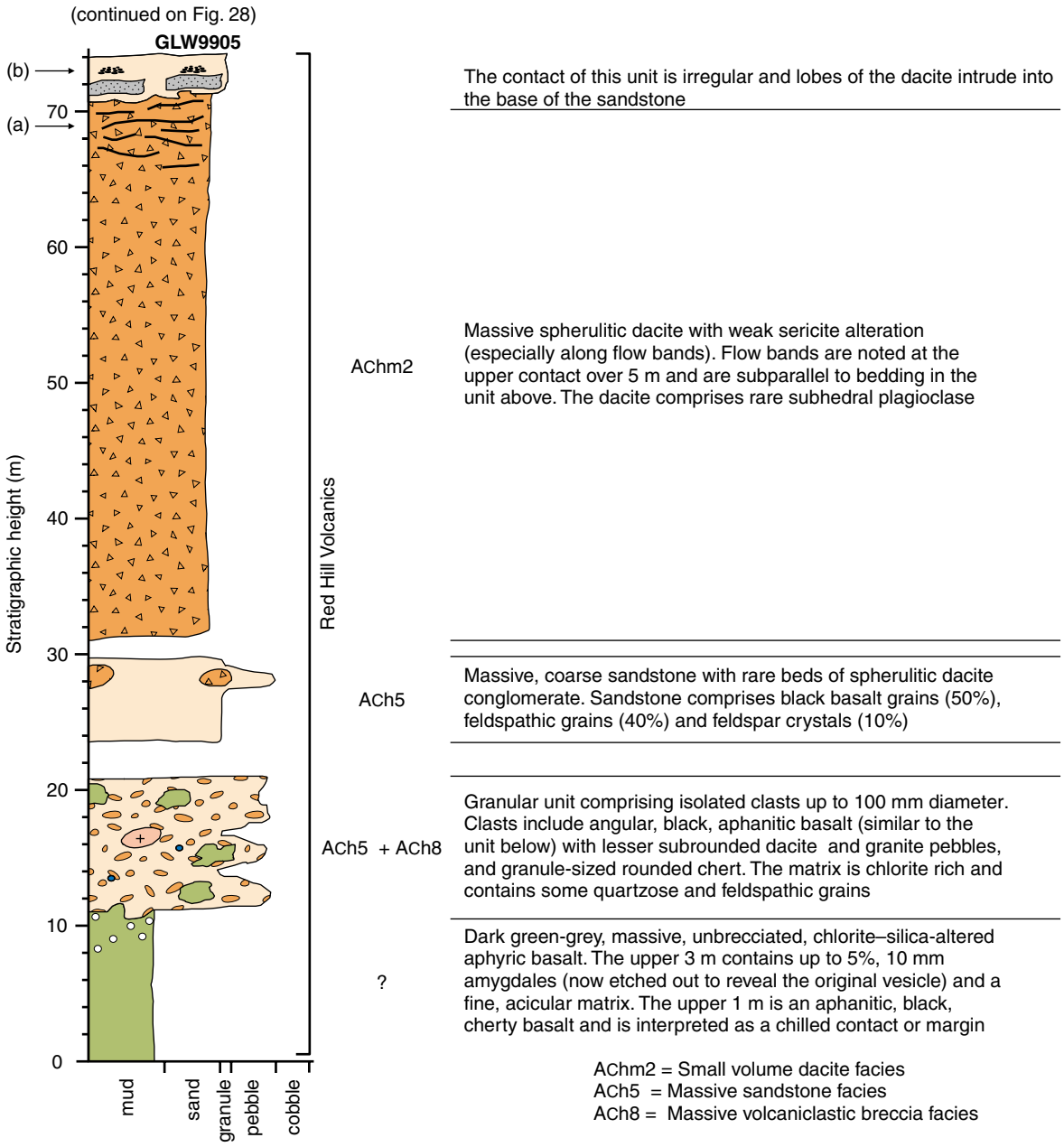

Figure 27. Lower section of stratigraphic log GLW9905 (base at MGA 573587E 7681696N), Red Hill Volcanics, Good Luck Well area. The log is dominated by products of the grey breccia and sandstone association: a) flow bands within the Mons Cupri Dacite Member; b) diffuse planar bedding within coarse-grained sandstone (see Fig. 9 for regional location and Fig. 28 for legend)

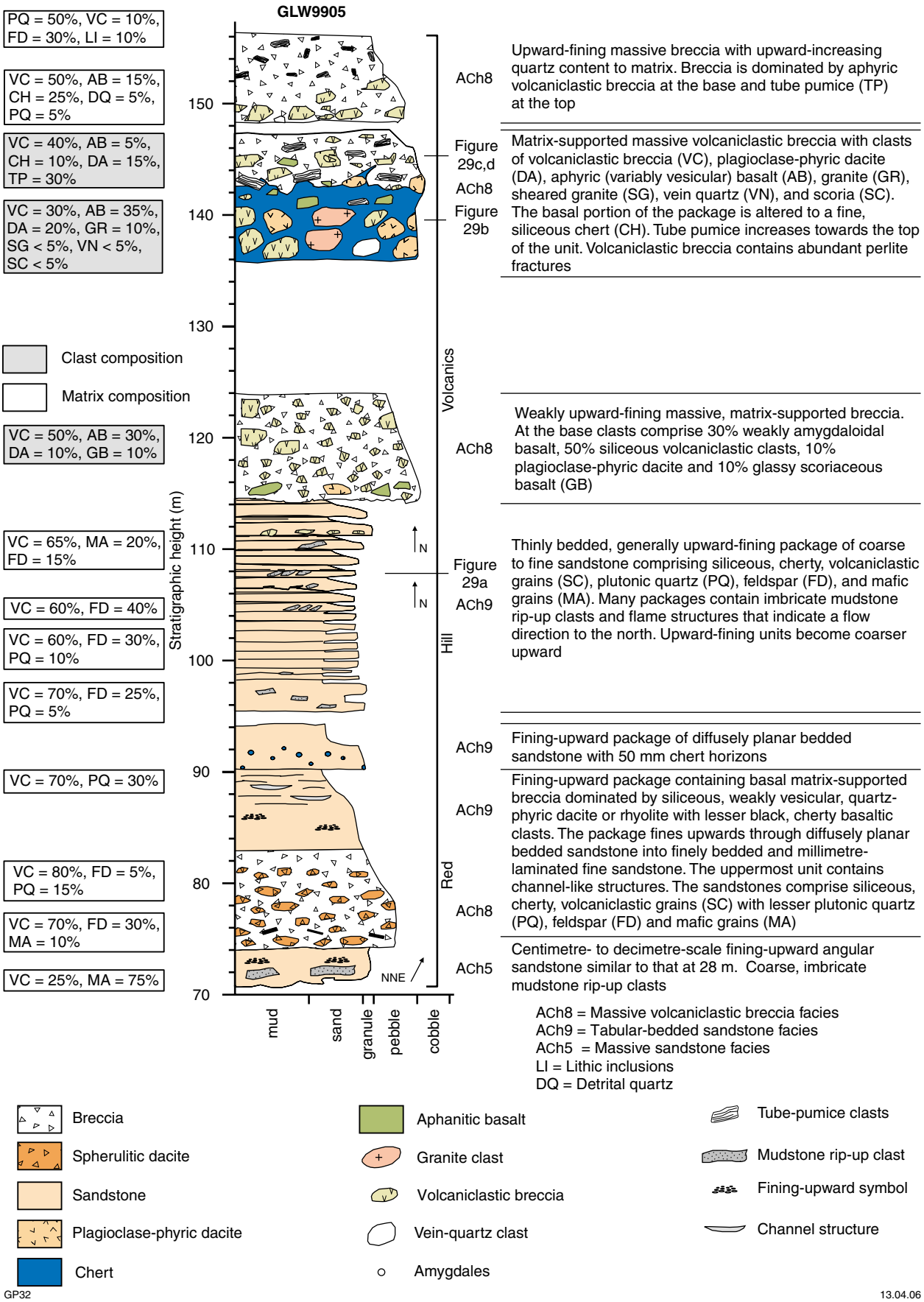

Figure 28. Upper section of stratigraphic log GLW9905 (base at MGA 573587E 7681696N), Red Hill Volcanics, Good Luck Well area

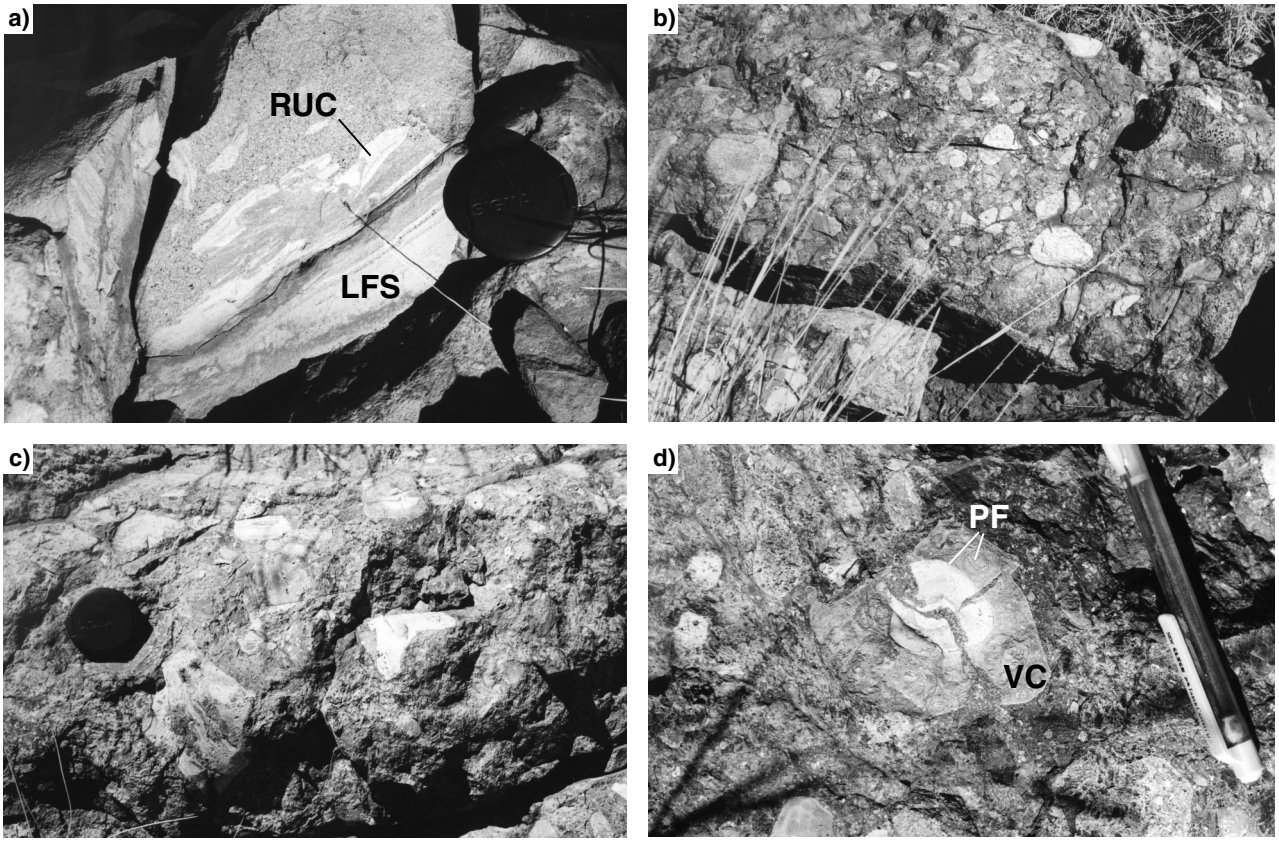

Figure 29. Outcrops of the Red Hill Volcanics in stratigraphic log GLW9905: a) disturbed bed of laminated fine-grained sandstone (LFS) overlain by a coarser grained sandstone hosting rip-up clasts (RUC). The rip-up clasts indicate both upstream erosion and transport within a flow that has significant matrix strength; b) conglomerate from the base of the massive 12 m-thick unit, comprising basalt, dacite, granite, sheared granite, vein quartz, scoria, and chert in a silicified matrix; c) angular breccia at the top of the massive 12 m-thick unit. Clasts are dominantly of light-grey volcanic rocks; d) light-grey (?andesitic) aphanitic clast (VC) with centimetre-scale perlite fractures (PF)

granular intraclasts of matrix material. Numerous clasts with centimetre-scale subcircular fractures and colour zonation are interpreted as perlite fractures that form due to quench fragmentation and volume reduction in volcanic glass (e.g. McPhie et al., 1993). Relatively common flow bands defined by subtle colour variations form due to shear stress during movement of cooling magma. Rare examples show evidence of synvolcanic fractures that cut an alteration rim and suggest a quench origin (e.g. Fig. 34a). A clast in Figure 34b shows a sediment inclusion (SI) that probably resulted from injection of matrix material into a fracture.

Interpretation

The inclusions within this facies indicate some form of interaction between clasts and sediment, and the facies may include a significant component of reworked hyaloclastite or peperite or both. Nearly all clasts in Figure 34 are angular or subangular, and some have narrow apophyses that would be easily removed under tractional transportation. Transport required a mechanically strong matrix to prevent fragmentation of angular irregular clast apophyses, and a cohesive sandy debris-flow or grain-flow origin is preferred.

Massive sandstone facies

Sandstone containing abundant chloritic debris is termed the massive sandstone facies (*ACh5*; Figs 27, 28, and 30), and is otherwise very similar to the tabular-bedded sandstone facies. Sandstones are characteristically massive, but may contain diffuse planar bedding that is defined on weathered surfaces. A dominantly volcaniclastic composition includes 50% chlorite–quartz-altered, perlite-fractured volcanic debris with 30% quartz-rich cherty grains, 10% polycrystalline lithic components (consisting of lamellar-twinned and sieve-textured plagioclase, alkali-feldspar, and quartz), less than 5% monocrystalline sieve-textured feldspar, and less than 5% sericite–carbonate clasts (probably after basalt lithics). The matrix forms around 5% of the rock and is composed of recrystallized quartz–alkali-feldspar and chlorite.

Interpretation

The facies was deposited under a relatively high-energy flow regime. Abundant plagioclase crystals, chlorite–carbonate clasts, and chloritic volcanic debris suggest an intermediate or mafic precursor. Transport and deposition were most probably from turbidity currents in the case of stratified deposits, and possibly from grain flow or

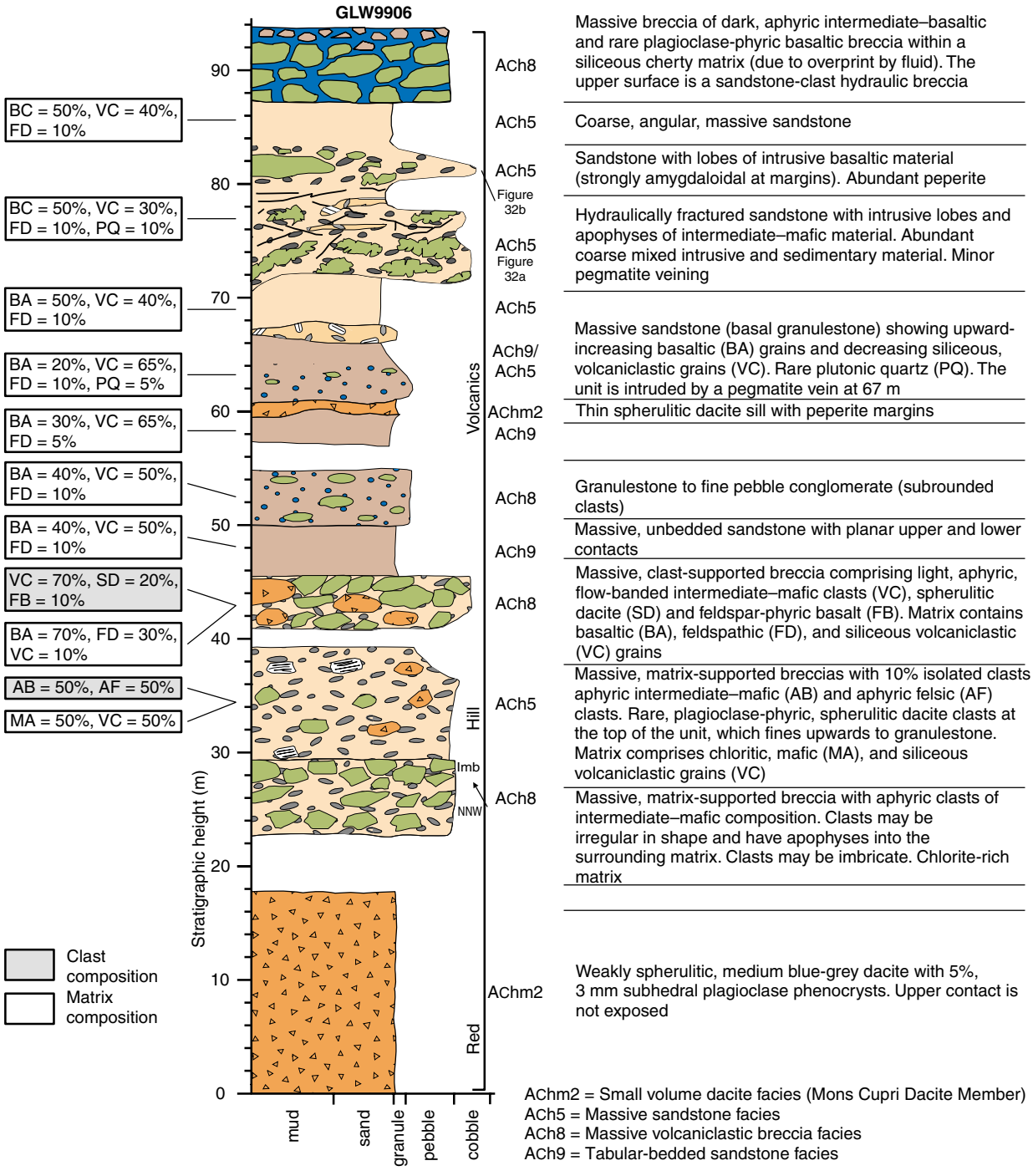

Figure 30. Lower section of stratigraphic log GLW9906 (base at MGA $_{5}$73997E $_{76}$82438N), Red Hill Volcanics, Good Luck Well area (see Fig. 9 for regional location and Fig. 31 for legend)

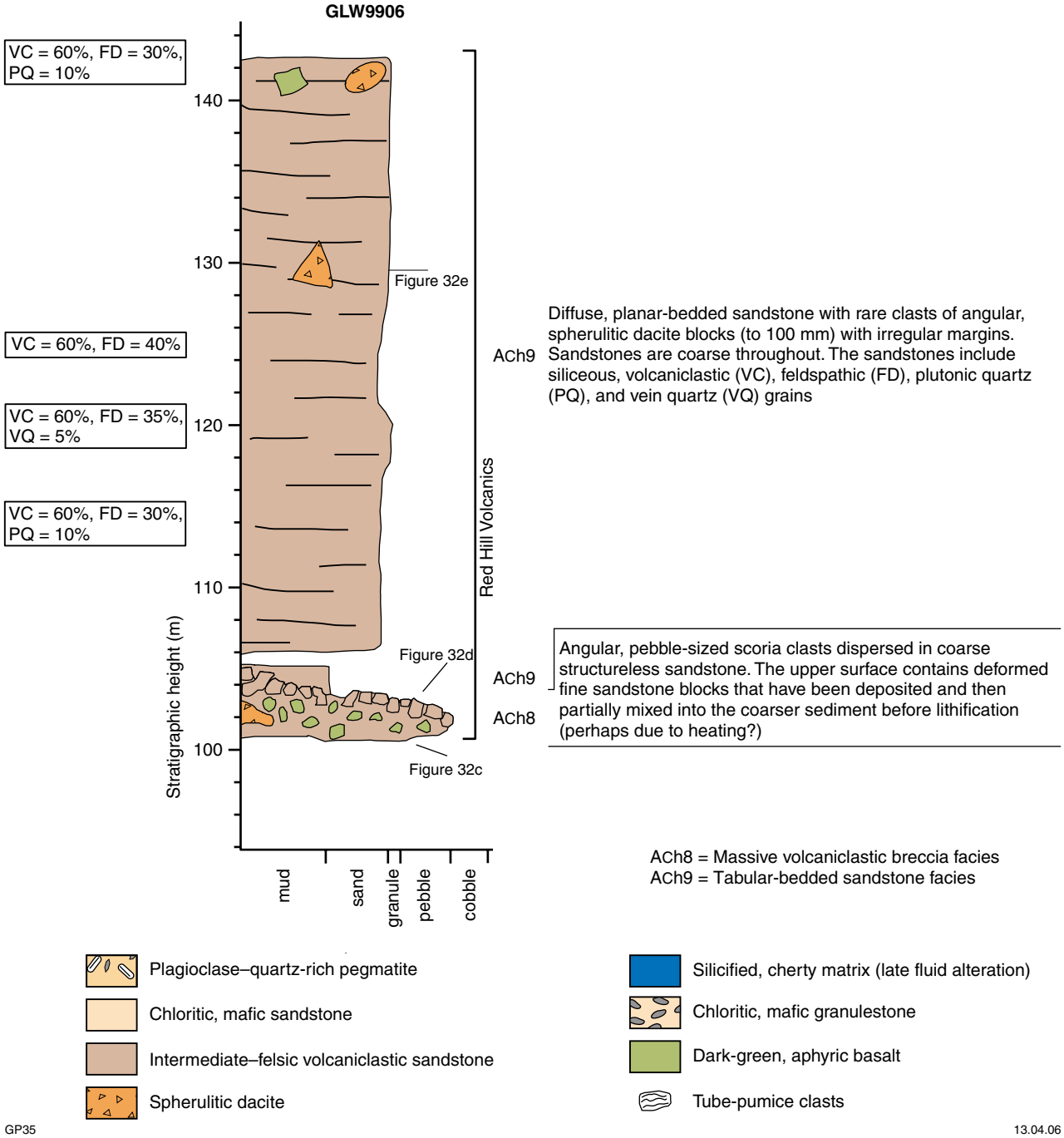

Figure 31. Upper section of stratigraphic log GLW9906, Red Hill Volcanics, Good Luck Well area

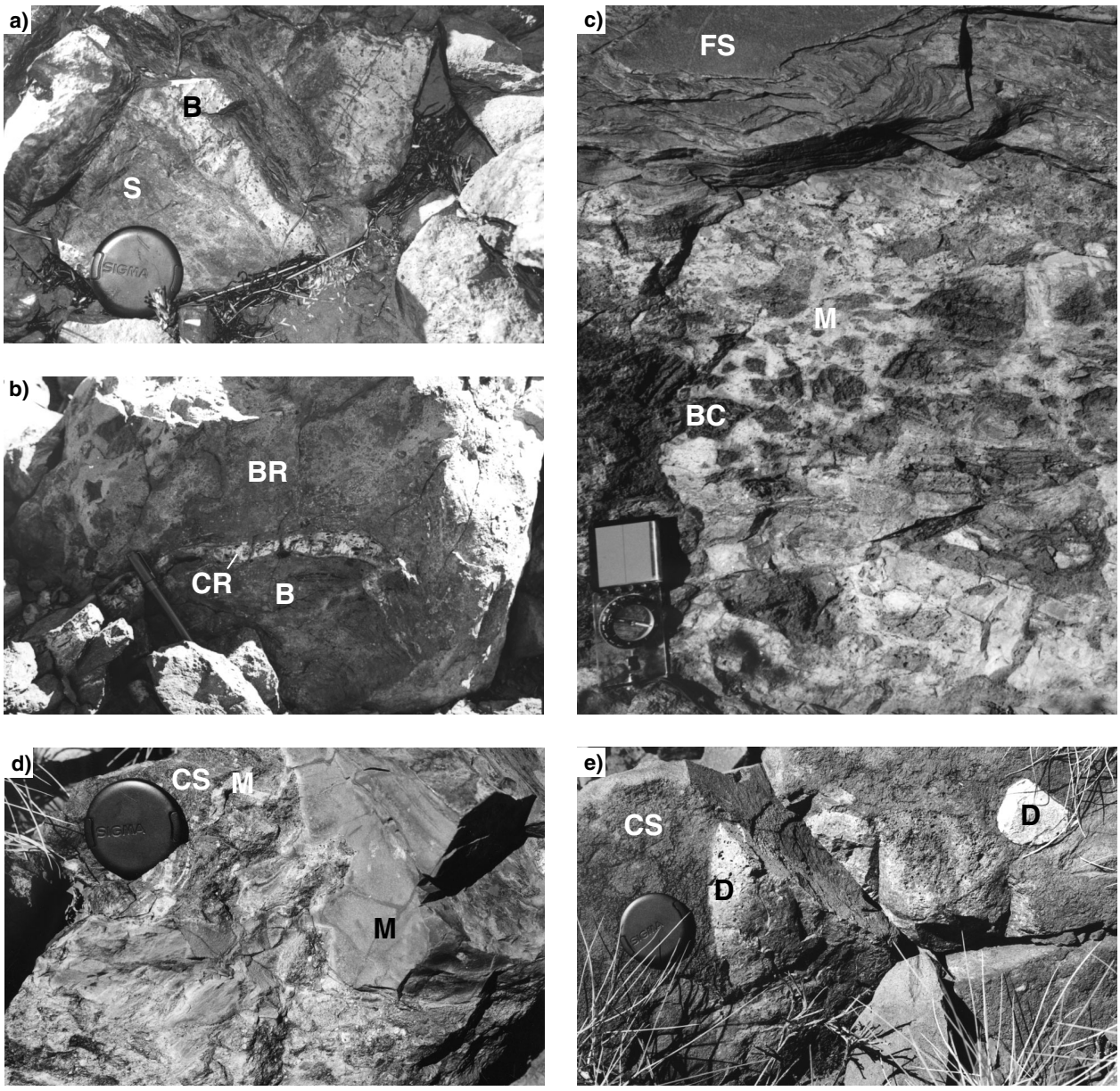

Figure 32. Outcrops of Red Hill Volcanics in stratigraphic log GLW9906: a) thin apophysis of light-grey, intermediate to mafic (?basalt; B) within chloritic sandstone (S); b) intrusive lobe of basalt (B) with a cherty vesicular rim (CR), hosted within a massive volcanic breccia (BR); c) coarse-grained angular basaltic clasts (BC) dispersed within a lighter volcanic matrix (M), overlain by a fine-grained sandstone unit (FS); d) angular deformed clasts of mudstone (M) within a coarse-grained sandstone matrix (CS). The origin of this unit is uncertain. There is disruption of a fine-grained bed and mixing of semicoherent clasts of mudstone with the underlying sandstone, but there is no apparent movement (e.g. slumping) indicated by the brecciation, nor is there any associated folding; e) coarse-grained dacite breccia clasts (D) 'floating' in a coarse-grained sandstone matrix (CS)

debris flow in the coarser grained more massive deposits. Large polycrystalline plagioclase-dominant lithic grains suggest that the volcanic source region contained exposed plutonic (granodiorite or quartz diorite) rocks or abundant xenolithic material within magma chambers.

Pumice and crystal-rich breccia facies

The pumice and crystal-rich breccia facies (*ACh4*) contains granule- to cobble-sized pumice breccia. The facies is poorly sorted and dominated by tube pumice. Amygdales are large (up to 2 mm in diameter) in clasts that are typically 10–100 mm in diameter. Plagioclase crystals, 1–2 mm across, are in the quartz–chlorite-altered matrix, but not within clasts. Component clasts include 60% aphanitic tube-pumice breccia, 15% dense aphanitic grains, 10% carbonate-replaced grains, 5% perlite-fractured volcanic grains, 5% lamellar-twinned plagioclase, and 5% monocrystalline quartz. The tube pumice is wholly aphanitic, but dense volcanic clasts

contain plagioclase phenocrysts, suggesting that this was the source for the feldspar grains. Quartz is angular, embayed, and monocrystalline, and may be of volcanic origin. The facies has a thickness of up to 20 m, and is massive.

Interpretation

Deposition occurred during or immediately after volcanism. Dense volcanic grains including aphanitic, feldspar-phyric, and carbonate-altered types are noted. Many clasts display subrounded margins indicative of reworking before deposition. Consequently, the facies contains approximately equal proportions of juvenile and reworked volcaniclastic material, and significant mixing must have occurred before or during flow. Material was almost certainly transported by mass flow because the facies is massive and structureless; a debris flow is favoured because much of the pumice has been little affected by clast interaction.

Siltstone facies

The siltstone facies (*ACh3*), mapped in a single locality, is characterized by a low abundance of quartz grains in the sandstone component, and has a conformable contact with underlying coarser grained facies. The facies shows little internal structure, and preserves a relatively strong cleavage.

Interpretation

Conformable, upward-fining contacts with sandstone of the tabular-bedded sandstone facies suggests that the siltstone facies was deposited from low-energy turbidity currents.

Sandstone and breccia facies

The sandstone and breccia facies (*ACh7*) comprises dominantly massive and diffuse planar-bedded sandstone with lesser volcanic breccia and is considered to represent altered versions of the tabular-bedded sandstone facies and massive volcaniclastic breccia facies.

Summary

The source area of the grey breccia and sandstone association was volcanically active and probably included exposed granitic crust. High-grade metamorphic rocks were not observed and this, coupled with the abundance of volcanic rocks, suggests a dominantly extensional or transtensional setting that would allow magma access to the surface. A number of felsic, intermediate, and mafic lithologies are represented, with intermediate material dominant. The abundance of perlite-fractured breccia suggests that much of the material was glassy and underwent hydration. Circular perlite fractures suggest that the original glass was relatively isotropic with little flow banding or layering. Shard-rich sandstone of the tabular-bedded sandstone, massive sandstone, and massive volcaniclastic breccia facies is analogous to that of the tabular-bedded sandstone and siltstone facies of the juvenile volcaniclastic association, and likewise suggests an explosive origin with variable sediment storage or reworking before final deposition.

Dacite-associated coarse-grained sedimentary association

Coarse-grained clastic rocks of the dacite-associated coarse-grained sedimentary association outcrop in the west of the Good Luck Well area. Clasts are dominantly epiclastic, and derived from eroded volcanic rocks.

Coarse-grained dacite-rich breccia facies

The coarse-grained dacite-rich breccia facies (*ACh6*) is poorly exposed, and outcrops large enough to be mapped at 1:10 000 scale are restricted to the Good Luck Well area (Plate 2a), where the facies is intimately associated with the small volume dacite facies of the Mons Cupri Dacite Member. The coarse-grained dacite-rich breccia facies consists of coarse-grained pebble breccia and contains a single clast population that is similar to quenched material of the small volume dacite facies. Clasts typically form around 35% of the facies, and the breccia is matrix supported. Individual clasts have a very angular or irregular morphology, and clast margins are straight or cuspate-lobate. Rarely, clasts show apophyses into the matrix material, and may completely enclose small amounts of matrix. The matrix itself is a moderately well sorted, structureless, medium-grained sandstone. It is dominated by light, chert-like, volcanic grains, lesser feldspar grains, and dark (?basaltic) lithic grains. Quartz grains are rare. Overall, the matrix material is identical to that of the coarse-grained sandstone component of the tabular-bedded sandstone facies (grey breccia and sandstone association).

Interpretation

Clasts within the coarse-grained dacite-rich breccia facies were probably derived from the Mons Cupri Dacite Member, and little transport has occurred. Some dacite clasts contain sediment inclusions, suggesting that there was some interaction of the clasts with sediment before cooling. Hence, many of the clasts may be hyaloclasts derived from quench fragmentation against wet sediment. Resedimentation may have occurred due to inflation and oversteepening as the associated dacite body was emplaced. This facies provides evidence that at least part of the Mons Cupri Dacite Member was emplaced before the end of clastic deposition of the Red Hill Volcanics.

Polymictic conglomerate and breccia facies

Coarse-grained clastic rocks of the polymictic conglomerate and breccia facies (*ACh1*) include both matrix- and clast-supported types, and form massive units with no obvious bedding or internal structure (Fig. 35). Clasts range from pebble to cobble size (maximum ~100 mm), and include rounded, pebble- to cobble-sized feldspar-phyric dacite with 5–20% blocky feldspar (~60%); irregular, angular, pebble- to small cobble-sized aphanitic dacite with 10–20%, 2 mm amygdales; basalt; dark-brown, hematite-altered, aphanitic, scoriaceous basalt (<5%); spherulitic dacite; grey chert; and black

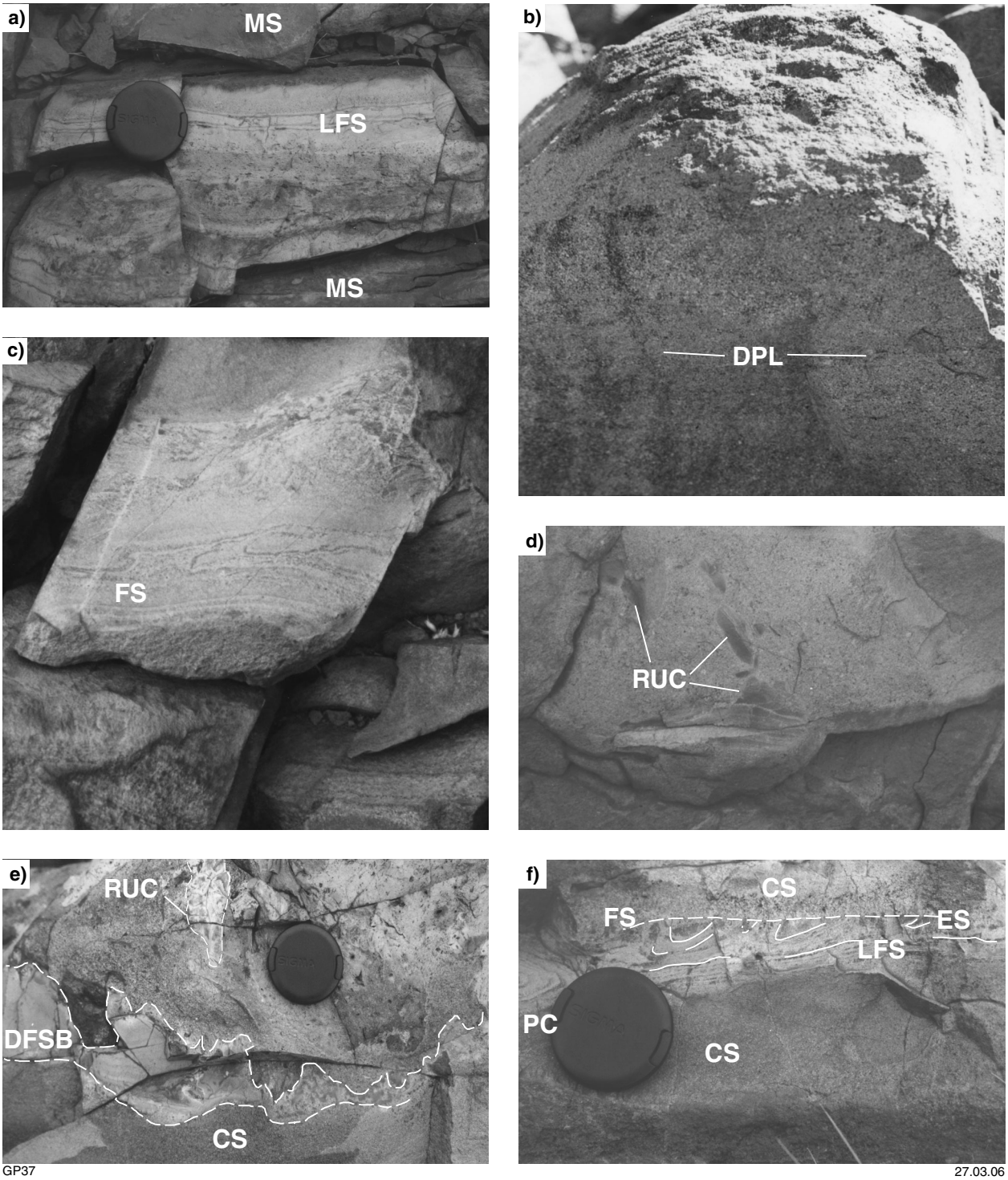

Figure 33. Sedimentary structures in the tabular-bedded sandstone facies (*ACh9*), Red Hill Volcanics: a) interlayered laminated fine-grained sandstone (LFS) and coarse-grained, massive sandstone (MS). The boundaries between the coarse and fine sandstone units are typically planar, non-erosive and nongradational, suggesting two distinct components to the flow — a (laminar) debris-flow sandstone and a hemipelagic fallout (Bouma T_e) or fine-grained turbidite (Bouma T_d; MGA 573435E 7681780N); b) diffuse planar layering (DPL) in coarse-grained sandstone demonstrates the effects of a waning current. The planar laminae represent minor depositional breaks within a single flow and indicate deposition from turbidity currents; c) flame structures (FS) within fine-grained sandstone, with the flames showing a sense of shear from left to right (MGA 573723E 7682935N); d) fine-grained, weakly laminated sandstone with mudstone rip-up clasts (RUC). The sandstone shows weak lamination similar to that in (a). The clasts are entrained in the flow fabric and are identical in composition, suggesting only centimetres of relative movement (MGA 573435E 7681780N); e) deformed fine-grained sandstone (DFSB) and underlying coarse-grained sandstone (CS). The fine-grained sandstone has a relatively planar (weakly folded) contact with the coarse-grained sandstone, but its upper surface is highly irregular, and appears to have been eroded and thinned by the overlying sandstone. The upper sandstone contains rip-up clasts (RUC) of similar composition to the fine sandstone, providing evidence of erosive flows (MGA 573798E 7682595N)

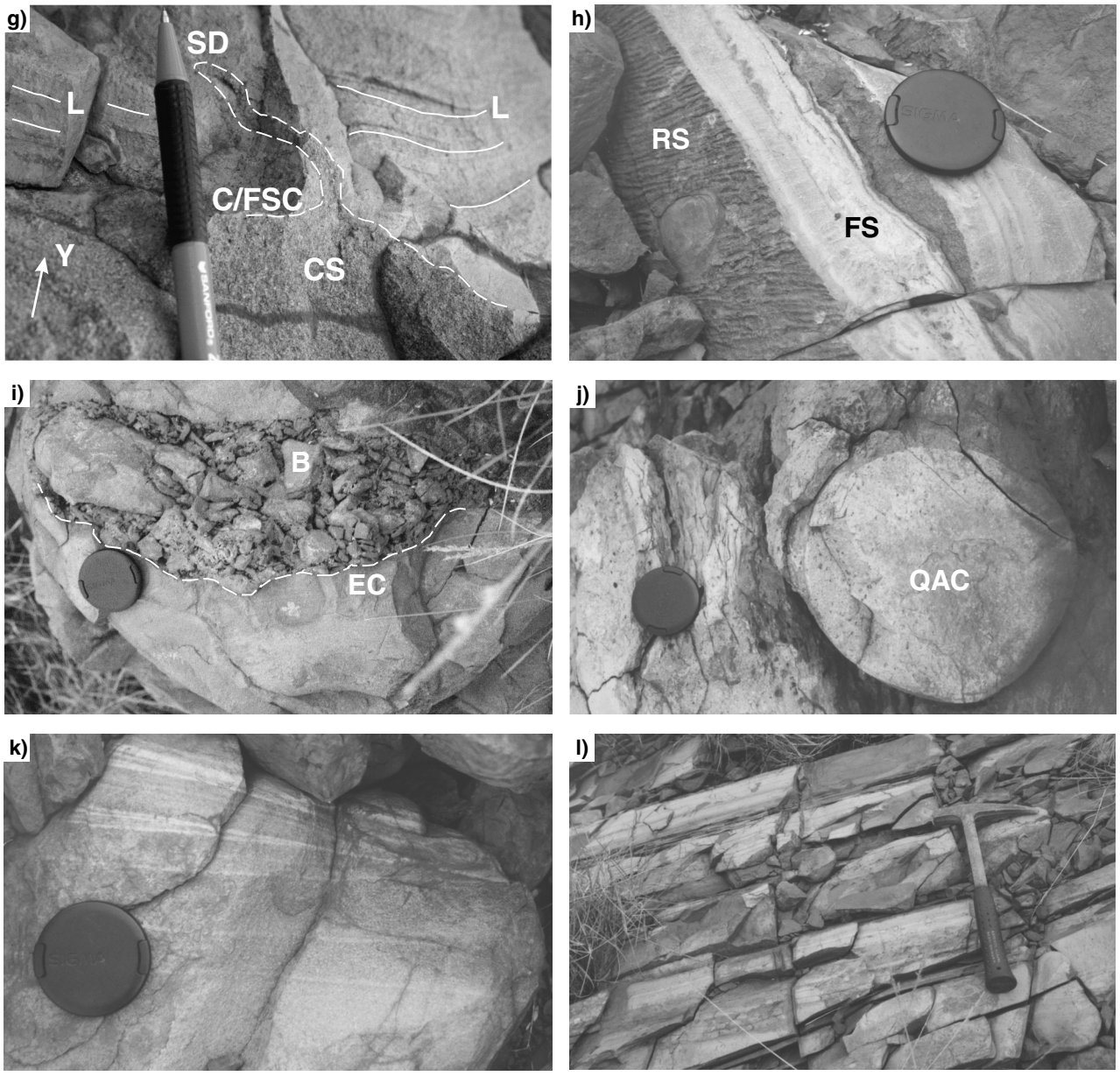

Figure 33. (continued) f) coarse-grained (CS) and fine-grained laminated sandstone (LFS) bedset, as in (a), but the fine-grained sandstone shows post-depositional movement of grains that form poorly developed flame structures (FS, with shear left to right). The upper surface has been eroded (ES) by the following flow before deposition of the overlying sandstone. In this example, erosion is approximately parallel to bedding (MGA 572326E 7682494N); g) subvertical beds with coarse-grained sandstone (CS) to the right and fine-grained laminated sandstone (L) to the left. The contact (C/FSC) is normally planar, but an apophysis of the coarse-grained sandstone intrudes left (originally upward) into the fine-grained sandstone, forming a sandstone dyke (SD), which shows that the succession youngs (Y) to the left (MGA 573435E 7681780N); h) rippled surface (RS) of a fine-grained sandstone bed (FS). Ripples are asymmetric and show current flow from bottom to top. The sandstone bed contains no internal cross-beds, and the ripples are interpreted to be the result of the interaction of a low-energy, nondepositional flow over an already deposited bed (MGA 573435E 7681780N); i) breccia-filled channel with monomictic subangular breccia (B) intraclasts of sandstone. The basal contact is an erosional surface (EC), and the sandstone intraclasts have a similar composition to the host sedimentary rock (MGA 572326E 7682494N); j) outsized quartz-amygdaloidal clast (QAC). The degree of rounding of the clast indicates that the source region contained shallow-water or subaerial environments in which debris was stored and reworked (MGA 573307E 7681107N);k) low-angle dune foresets, indicating upper flow-regime conditions, which are very rare in the tabular-bedded sandstone facies (MGA 573417E 7681145N); l) well-bedded, fine-grained sandstone units (MGA 573435E 7681780N), which are interpreted as products of turbidity currents, but more distal than the units shown in (a)–(g)

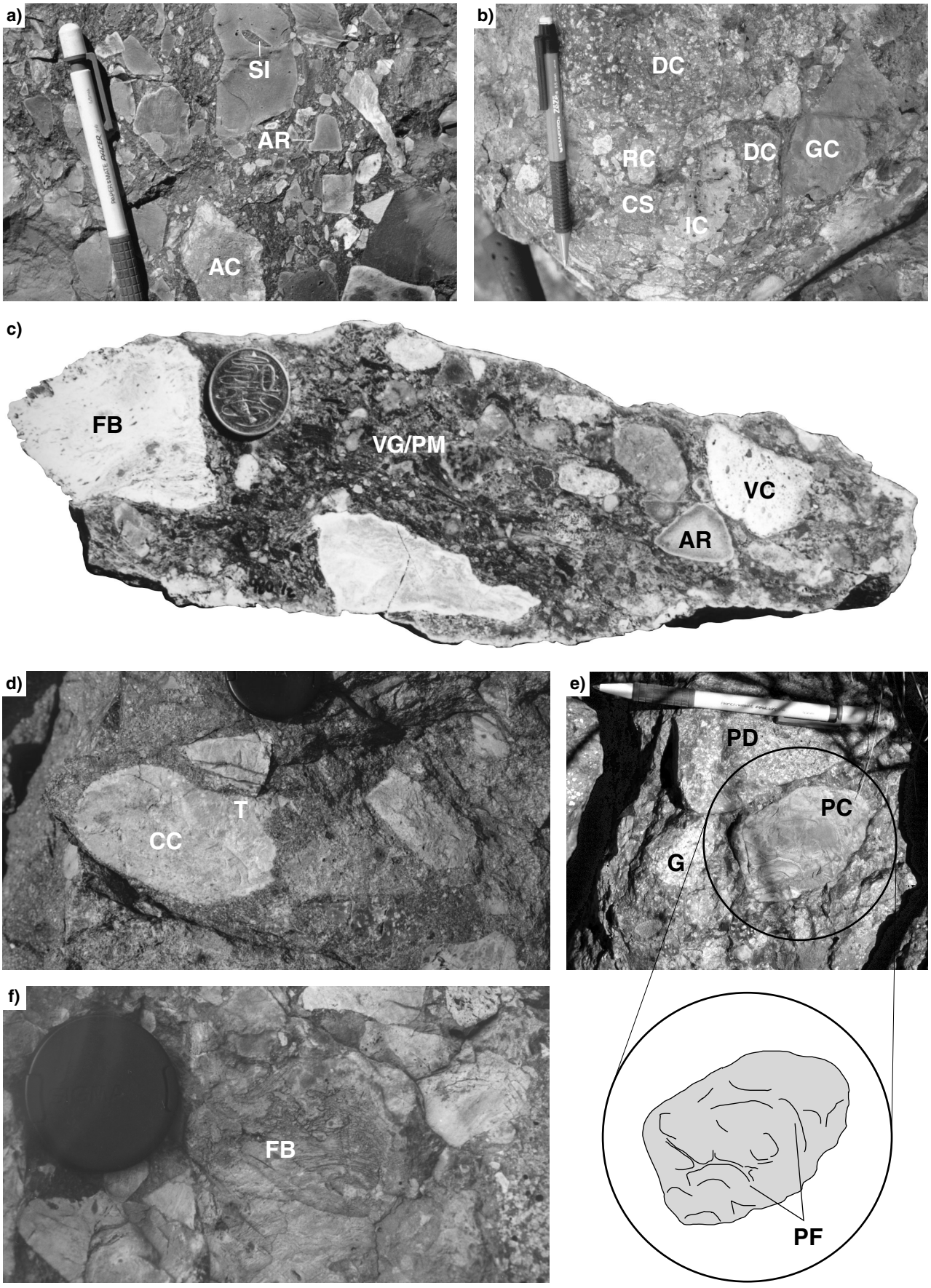

GP39

01.03.06

quartz-rich sandstone with angular, large quartz grains and subrounded, pebble-sized microgranite. The matrix is rich in light-grey, sand-sized grains that are dominated by volcanic lithic grains with lesser quartz and feldspar. The matrix forms around 15% of the rock overall, but locally reaches 80%. In some sections the facies displays dominantly normal grading with lesser reverse grading. Bedding is very poorly defined by layers with a distinct dominant clast population that are typically a few metres thick.

Interpretation

Outcrop patterns and stratigraphic logging from the Good Luck Well area indicate that the polymictic conglomerate and breccia facies is up to 74 m thick, but it shows limited lateral extent of up to 2 km, indicating a fan-like geometry. Much of the coarse-grained component was derived from the Mons Cupri Dacite Member. Rare chert and sandstone clasts were probably transported into the basin from surrounding topographic highs. The presence of thick horizons of massive, poorly sorted, matrix-supported subfacies suggests transport by debris flow supported by a mechanically strong sandstone matrix. There is little evidence preserved of depositional environment. A subaqueous environment is favoured by interpretation of other facies associations. The dacite-associated coarse-grained sedimentary association is intimately associated with the Mons Cupri Dacite Member (Figs 35, 36, and 37), and is probably a proximal deposit. In places the large volume dacite facies (Mons Cupri Dacite Member) has intruded the coarse-grained clastic rocks, again supporting a proximal interpretation. The depositional environment was most probably a subaqueous fan, fed by debris flow from shallow-water or subaerial erosion, or possibly a fluvial system.

Imbricate conglomerate facies

The imbricate conglomerate facies (*ACh2)* is restricted to a single locality (MGA 573330E 7680549N), and comprises centimetre- to decimetre-scale interbedded pebble breccia and conglomerate with coarse-grained sandstone. The entire package is around 10 m in thickness. Beds do not show sharp boundaries, but are clearly defined by distinctive clast-sized populations. The sandstone component typically displays diffuse bedding with dune cross-bedding and rare, high-angle ripple cross-bedding. Clasts are monomictic, light-grey, silicified volcanic pebbles of variably angular material. The clasts have remnant plagioclase phenocrysts and are petrographically similar to the Mons Cupri Dacite Member.

Interpretation

The imbricate conglomerate facies is a product of high, but variable, energy deposition of medium- and coarse-grained detritus. The variable angularity of clasts implies very different amounts of reworking. Well-developed clast imbrication, combined with low-angle dune and ripple cross-beds, is a common characteristic of high-energy braided river systems, although there is no definitive evidence for a fluvial setting.

Mons Cupri Dacite Member

The Mons Cupri Dacite Member (*AChm*) of the Red Hill Volcanics is a major component of the Whim Creek greenstone belt, and outcrops over larger areas than either the Warambie Basalt or other components of the Red Hill Volcanics. It has been interpreted as an intrusive unit (e.g. Fitton et al., 1975, Smithies, 1998), a lava (e.g. Fitton et al., 1975), an extrusive rheomorphic ignimbrite (e.g. Fitton et al., 1975, Barley, 1987), or a combination of these styles. The Mons Cupri Dacite Member comprises two facies associations (*AChm1* and *AChm2*) that include a number of facies and subfacies, most of which are mapped on Plates 1 and 2; the associations and facies are summarized in Table 4.

Subfacies

Subfacies of the Mons Cupri Dacite Member are defined on the basis of colour, phenocryst content, and groundmass appearance. Detailed petrography is given in Pike et al. (2002). The three main lithofacies types are:

- spherulitic dacite: light-grey silicified dacite with 5% plagioclase (lesser alkali-feldspar) phenocrysts with abundant 'cauliflower-shaped' matrix spherulites (20–70%);
- feldspar-phyric dacite: dark-grey to steel-blue with 1–15% plagioclase (lesser alkali-feldspar) phenocrysts and no matrix spherulites;

Figure 34. Clast types and sedimentary structures of the massive volcaniclastic breccia facies (*ACh8*), Red Hill Volcanics: a) matrix-supported volcanic breccia containing aphanitic clasts (AC) with alteration rims (AR). A single clast shows a small sediment inclusion (SI) that may be connected to the matrix material in three dimensions. Such textures indicate dynamic mixing of coarse clasts and volcanic sediment before deposition. (MGA 573872E 7682299N); b) clast-supported polymictic breccia comprising coarse sandstone (CS; ?intra)clasts, nonvesicular, subangular to subrounded dacite clasts (DC), and aphanitic, light-grey, amygdaloidal (10%, 2 mm amygdales) irregular basalt (IC). Rounded clasts (RC) indicate reworking before emplacement. The clast marked GC is dark grey and probably andesitic to basaltic in composition. The breccia is interbedded with the unit illustrated in Figure 36; c) slab of volcanic breccia showing well-preserved alteration rims (AR) around clasts. Some well-preserved flow-banded (FB), white, felsic aphyric clasts (VC) are weakly quartz amygdaloidal and were originally either vesicular clasts or epiclastic amygdaloidal clasts (VG/PM = volcanic granule/pebble matrix). The breccia is interbedded with rocks of the outcrop illustrated in Figure 38; d) cherty volcaniclastic clast (CC) with a thin 'tail' (T) that can only have been preserved by very low degrees of transport or transport within a dense plug of debris with little internal clast movement; e) polymictic breccia displaying a light-grey, perlite-fractured clast (PC). The inset shows the distribution of perlite fractures (PF) within the clast. Other clasts include silicified, plagioclase-phyric dacite (PD) and granite (G; MGA 572202E 7682814N); f) aphanitic, volcaniclastic-dominated breccia with a strongly flow-banded clast (FB; MGA 573739E 7682130N)

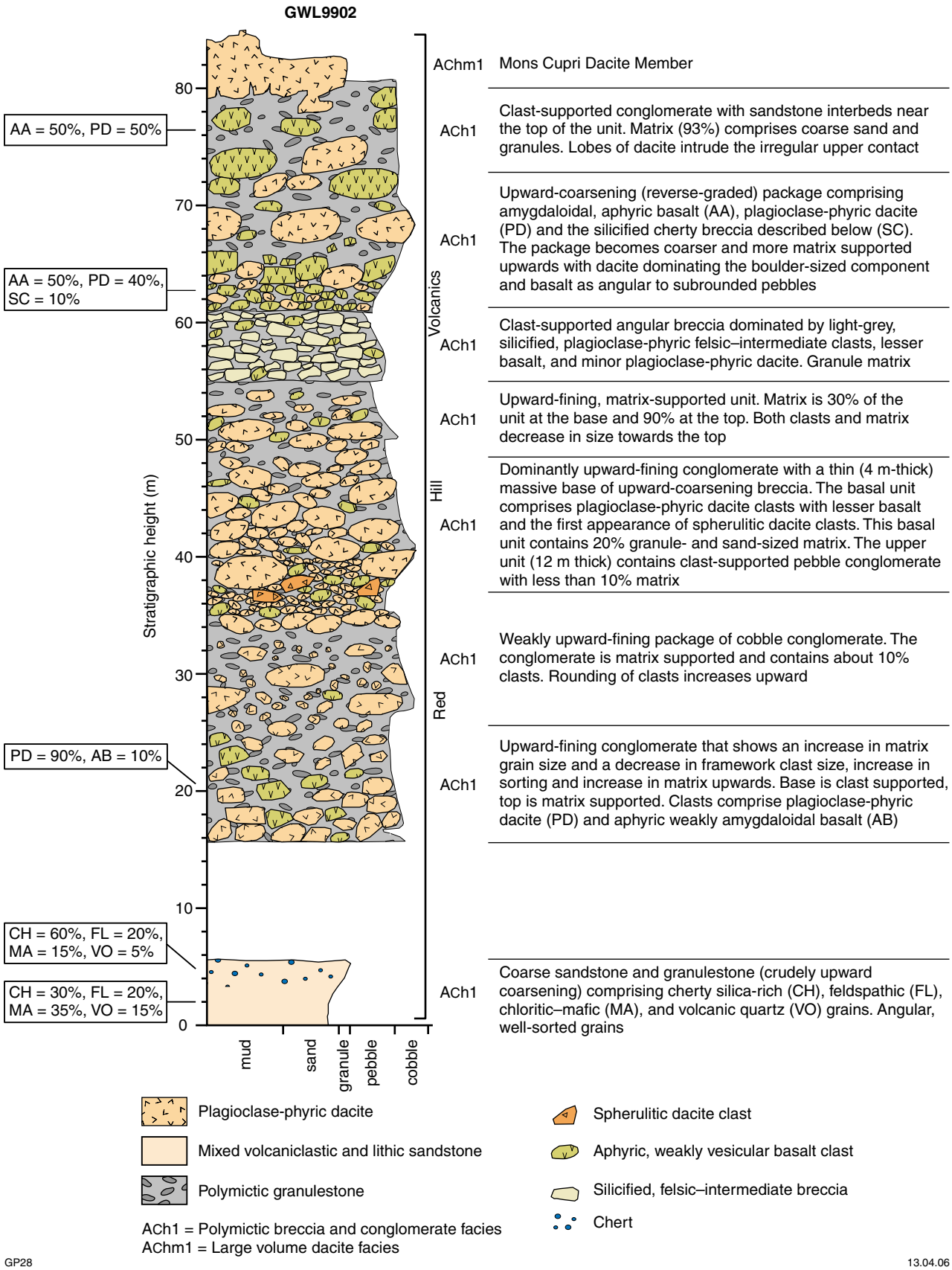

Figure 35. Lower section of stratigraphic log GLW9902 (base at MGA $_{5}$70080E $_{76}$82494N), Red Hill Volcanics, Good Luck Well area. The log contains abundant facies from the dacite-associated coarse-grained sedimentary association (see Fig. 9 for regional location)

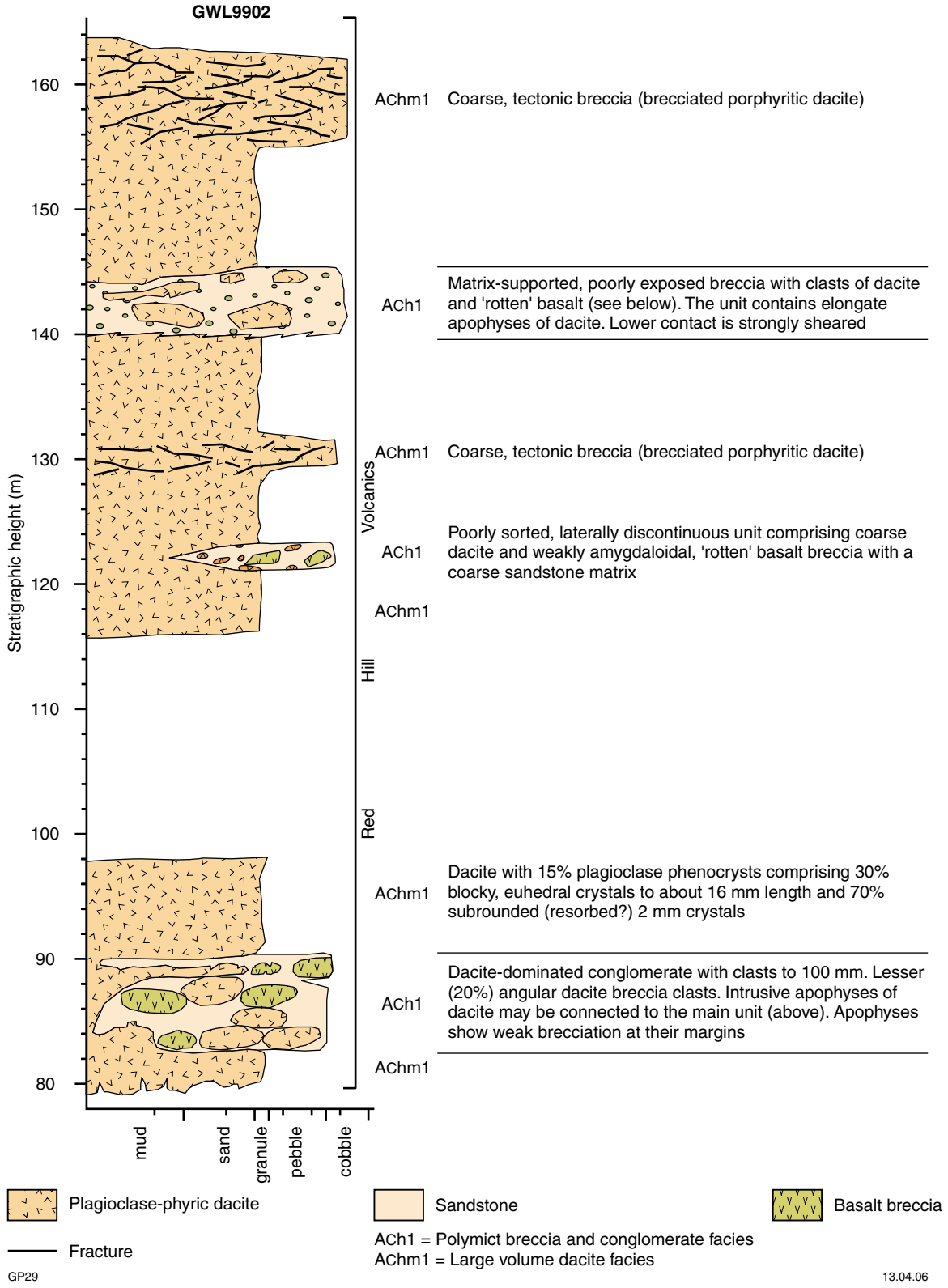

Figure 36. Upper section of stratigraphic log GLW9902, Mons Cupri Dacite Member (*AChm1*), Red Hill Volcanics, Good Luck Well area (see Fig. 9 for regional location)

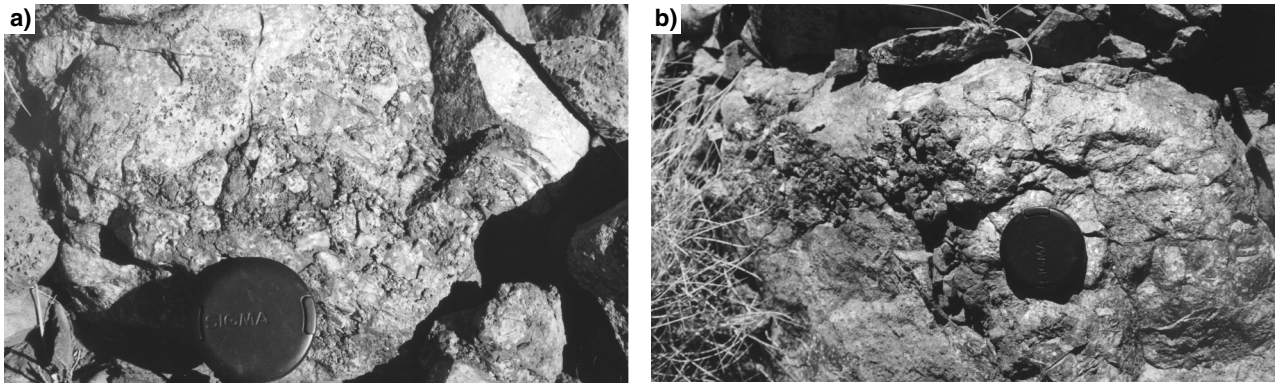

Figure 37. Outcrops of Mons Cupri Dacite Member, at 80 m level on log GLW9902 (Fig. 36), Good Luck Well area: a) angular brecciated dacite; b) apophysis of angular brecciated dacite within a coarse-grained sedimentary matrix. These are locally jigsaw-fit breccias at the transition between the Mons Cupri Dacite Member and the dacite-associated coarse-grained sedimentary association of the Red Hill Volcanics. The breccias are interpreted as hyaloclastite that formed due to quench fragmentation of the Mons Cupri Dacite Member either during or immediately after deposition of the Red Hill Volcanics

- grey dacite: dark-grey (weakly chlorite altered) dacite with minor 1 – 1.2 mm blocky, etched plagioclase (not visible in hand specimen) phenocrysts.

Small volume dacite association

Dacite pods facies

The dacite pods facies (*AChm3*) is restricted to the Red Hill area (Plate 2b). The facies contains individual units (pods) that are typically between 0.5 and 40 m in diameter, and are elongate along bedding of the surrounding lava and breccia. Small pods typically display round smooth margins, whereas larger pods are sufficiently extensive to be mapped, and contain a dark-grey or purple, plagioclase-phyric groundmass, with local quartz–sericite alteration along margins. A feldspar-phyric dacite subfacies (*AChm3(a)*) is locally mapped within the dacite pods facies of the Red Hill area.

Interpretation

Contacts of the dacite pods facies are nonplanar and highly irregular, taking the form of wedge-shaped apophyses into surrounding clastic material. The irregular dacite margins are also associated with thin apophyses of sedimentary rock into the dacite pod facies. Hence, primary contacts suggest intrusion of the dacite magma into a pile of lava and coarse-grained breccia. The intrusive interpretation is unusual because dacite magmas are expected to have very high viscosities, thus hindering the formation of very small intrusions. Possible causes of lower viscosity may have included one or more of superheating by basalt magma immediately before emplacement, high initial volatile contents, and retention of volatiles during emplacement.

Small volume dacite facies

Units of the small volume dacite facies (*AChm2*) are about 100 m thick, with strike lengths of less 1 km. They are composed of either the spherulitic dacite (*AChm2(b)*) or feldspar-phyric dacite (*AChm2(a)*) lithofacies (mapped as subfacies). Primary, unaltered margins of individual units are of three types: planar, flow banded, and brecciated. The small volume dacite facies is vesicle poor, except at the margins where vesicles may account for up to 30% of the rock. Flow bands are very common along the outer 10 m of the facies, and are defined by alternating light and dark groundmass, abundance of spherulites, or vesicular and nonvesicular bands.

Interpretation

Flow banding within the small volume dacite facies is interpreted to represent shear-induced laminar flow at the margins of the bodies as the dacite magma cooled and became more viscous. One well-exposed contact between the small volume dacite facies and the grey dolerite and basalt facies (Warambie Basalt) shows a highly irregular trace illustrated in Figure 38. At this contact, dacite passes southward (along strike) into basalt, indicating a lateral facies change. The irregularity of the contact could be explained by late intrusion of one of the facies, but an alternative interpretation is coeval emplacement; both facies are fine grained, and are either high-level intrusions or lava flows.

Crystalline inclusions facies

Units of the crystalline inclusions facies may be many metres to decimetres in strike length and 2–3 m in thickness, but are too restricted to be shown on the 1:10 000-scale maps. The facies is within both the small volume dacite and large volume dacite associations. Flow-banded crystalline inclusions are associated with the outer margin of the small volume dacite association.

The two main types of crystalline inclusions are termed rounded and flow-banded crystalline inclusions based on their characteristic morphology. These two types are included in the logs shown in Figures 39 and

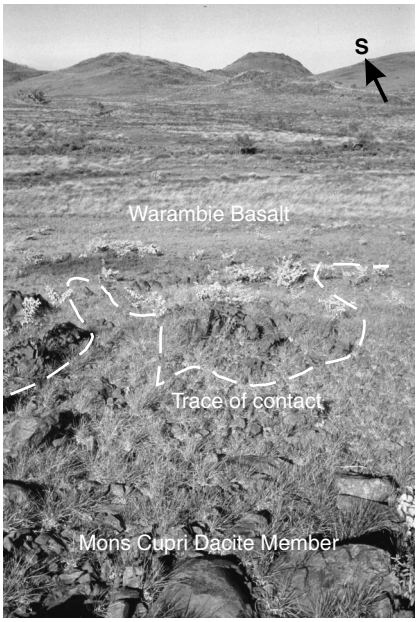

Figure 38. An irregular contact between the Warambie Basalt and the Mons Cupri Dacite Member (MGA 573962E 7682198N). The photograph was taken looking south-southwest, and the rocks locally dip west (to the right). The contact is not well preserved, but is visibly irregular, and does not appear to be disrupted by any minor folding or faulting. The contact is suggestive of coeval Warambie Basalt – Mons Cupri Dacite Member magmatism

40 respectively within the small volume dacite facies section, and rounded crystalline inclusions are illustrated in detail in Figure 41. The coarse-grained, crystalline inclusions are dominated by feldspar and quartz. A typical unit contains 30–90% large crystals with a very fine grained, crystalline, quartz–feldspar-rich groundmass similar to that of the host dacite. Plagioclase dominates the crystal component. Rounded crystalline inclusions are spherical to ovoid in shape and vary in size from a few centimetres to 1.5 m. The well-preserved example in Figure 41a is about 1.5 m in diameter, and is surrounded by flow-banded dacite in which the flow bands wrap and fold around the inclusion. This suggests that the inclusions were solid or semisolid when the main dacite body was emplaced. They were able to flow and deform with the main dacite body and are considered to have behaved plastically or as viscous fluids during emplacement. The margins of both types are gradational into the host dacite. Abundant polycrystalline feldspar and minor quartz aggregates in the large volume dacite facies and the small volume dacite facies may be related to mixing of crystalline inclusion-like material before or during emplacement.

Interpretation

The coarse-grained crystalline component suggests that the crystalline inclusions had considerable time to form from the primary felsic melt. The facies is found at both the top and bottom of the small volume dacite facies. The lack of the facies within the centre of dacite bodies suggests that they were preferentially incorporated into zones of relatively high shear between cooling magma and the intruded sediment. Large crystals are polycrystalline, and may have originated from a dominantly crystalline material with a smaller amount of melt ('crystal mush'). Hence, there is evidence for prolonged crystallization followed by reworking of early crystals into the melt. The crystallizing rock was probably a granodiorite or quartz diorite in composition, based on the dominance of plagioclase with lesser quartz and rare alkali-feldspar.

Mixed dacite breccia–sandstone facies

The upper contact between the small volume dacite facies and volcaniclastic rocks of the grey breccia and sandstone association is typically planar, and shows no evidence for either synsedimentary or late intrusion. However, one excellent exposure shows a transition between coherent unaltered dacite and the grey breccia and sandstone association over a distance of 20 m. This exposure (too small to be mapped at 1:10 000 scale) is within a small valley (MGA 573639E 7681955N), and only a single face shows a well-preserved contact (Fig. 42).

Two types of breccia are recognized within the mixed dacite breccia–sandstone facies: 'Type 1 breccia' is characterized by approximately equal volumes of deformed fine-grained volcanic sandstone and fine-grained dacite clasts, whereas 'Type 2 breccia' consists of coherent to fragmented dacite with thin (millimetre-scale to 2 cm-thick) apophyses of fine-grained sandstone. Both breccia types are dominated by blocky dacite clasts, but rare fluidal dacite clasts are also noted. The sand-sized component of all mixed breccias is essentially the same material as described for the tabular-bedded sandstone facies, and comprises variable amounts of subangular volcanic grains, angular chloritic shards, and lesser quartz. Most of this material is massive.

Type 1 breccia (Fig. 42a,b) comprises elongate, structureless, irregular sedimentary units that surround entire clasts of angular dacite. The dacite is typically blocky, equant to elongate, and has irregular margins that show millimetre-scale apophyses into the sedimentary material. Rare clasts have curved margins and a rounded appearance and the clast margins are commonly planar to slightly curved. The clasts are aphanitic and light brown in colour. Many contain abundant vesicles (up to 20%) from 1 to 4 mm in diameter. Larger clasts show well-developed flow banding as centimetre-scale, layered, dark-brown, feldspar-phyric dacite and light-brown aphanitic dacite. The flow banding may contain thin flow-band-parallel apophyses of sedimentary material interpreted to have formed by ingestion of slabs of sediment before or during formation of flow bands or soft-sediment intrusion into the dacite (Fig. 42a). The majority of dacite clasts are between 2 and 100 mm in length. The sedimentary matrix material was originally of fine-grained sand size,

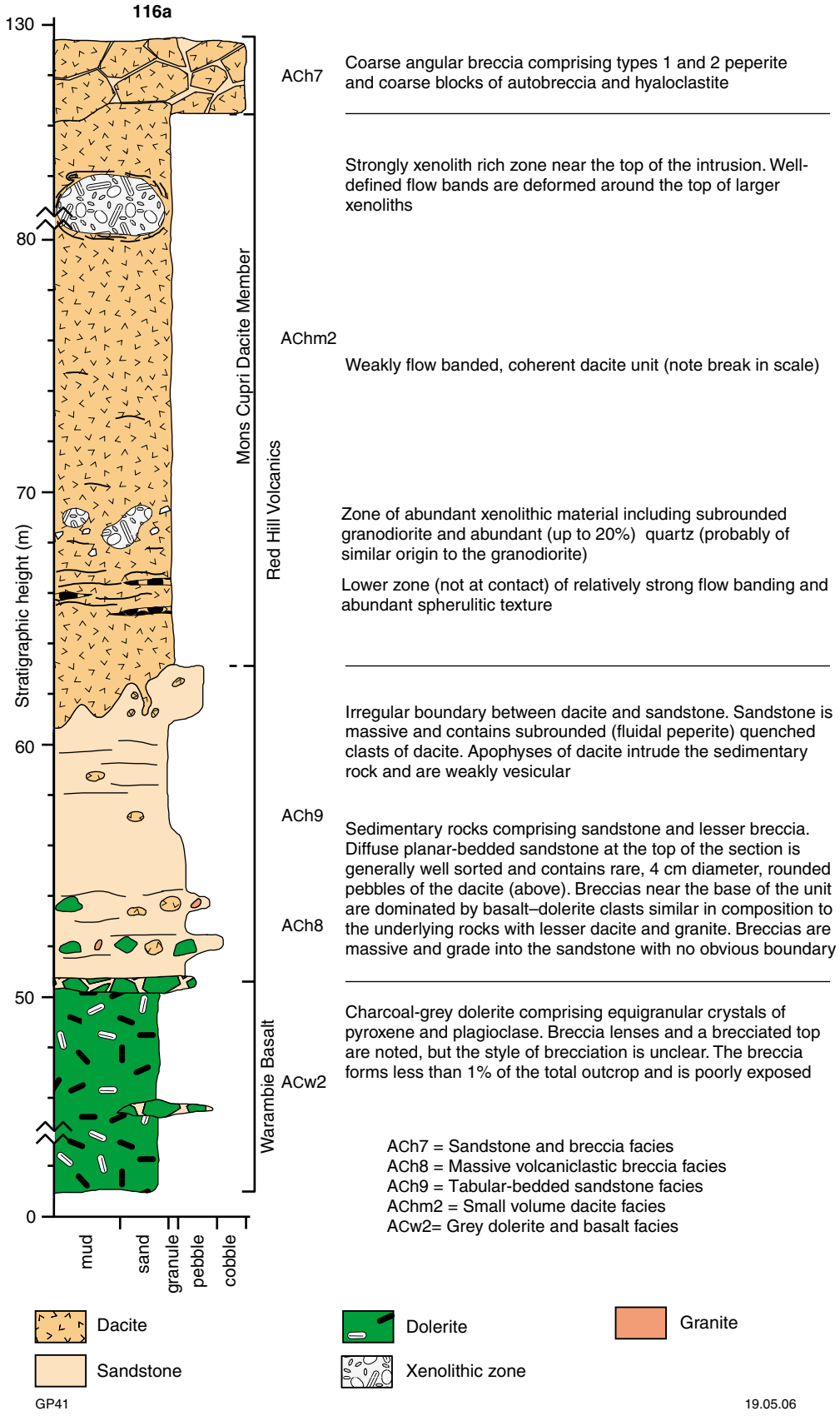

Figure 39. Stratigraphic log 116a, Warambie Basalt through Red Hill Volcanics into the Mons Cupri Dacite Member (MGA 573678E 7681878N; see Fig. 9 for regional location)

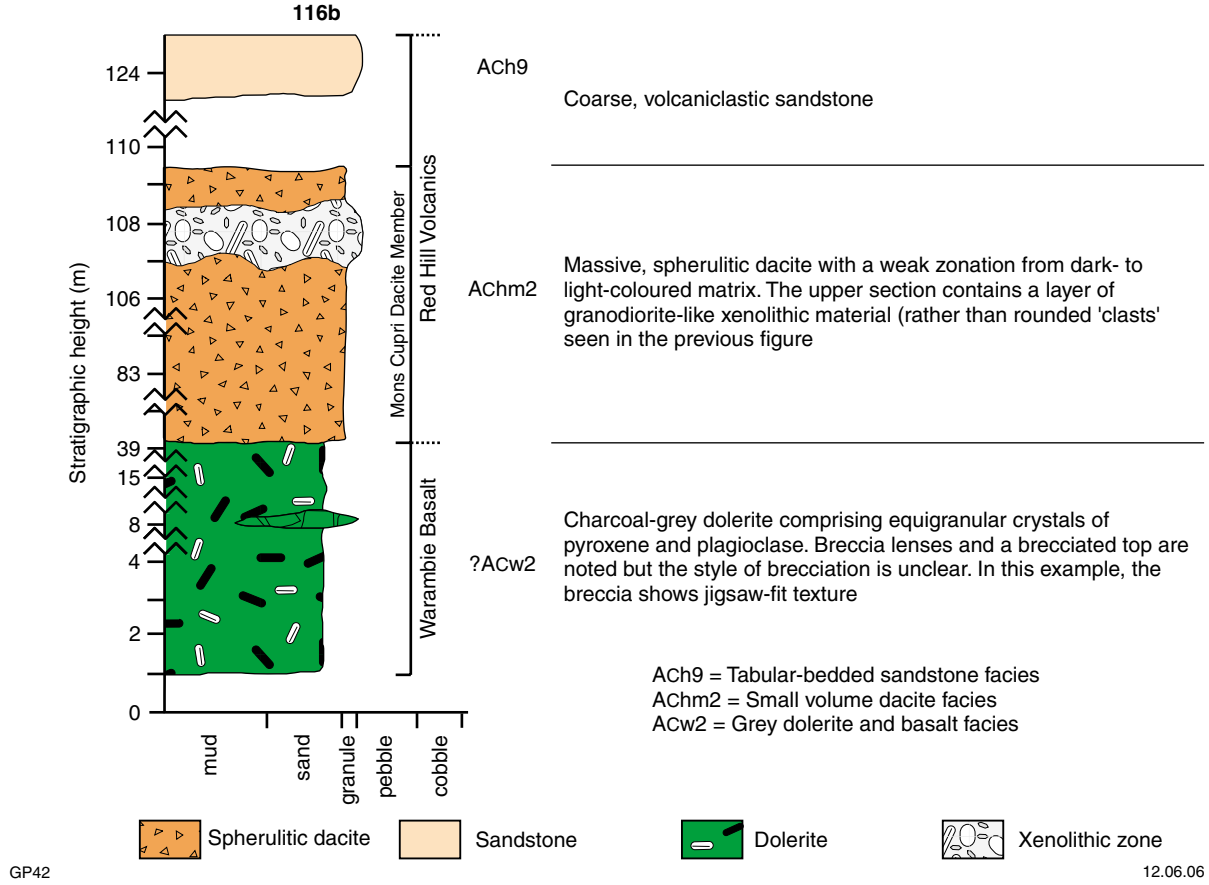

Figure 40. Stratigraphic log 116b (base at MGA 573673E 7681031N), Warambie Basalt through Red Hill Volcanics into the Mons Cupri Dacite Member (150 m east of section in log 116a; see Fig. 9 for regional location)

and now has a chert-like appearance. Type 1 breccia is found only at the top of the dacite units. Thin section petrography (Fig. 43a,d) shows angular clasts of aphanitic, carbonate–quartz-amygdaloidal and sieve feldspar-phyric, flow-banded dacite. Both blocky (Fig. 43a) and fluidal (Fig. 43d) textures are noted. The matrix material was originally bedded, and contains quartz–lithic sandstone and monomictic, glass-shard sandstone beds.

Type 2 breccia (Fig. 43c) is dominated by weakly to moderately brecciated, flow-banded dacite with smaller volumes (<25%) of sedimentary material. The dacite clasts are large, angular, and blocky, and may contain (up to 10%) elongate vesicles up to 25 mm long, with an average length of around 10 mm. The margins of the clasts form a characteristic cuspate-lobate morphology with lobate margins to dacite apophyses and cuspate margins to sedimentary apophyses at the top of the unit. Sedimentary apophyses are typically centimetre to decimetre scale, but local narrow (~1 mm) apophyses appear to cut the dacite as sedimentary dykes.

Flow banding associated with peperite formation (Figs 43 and 44) is defined by alternating vesicular aphanitic and nonvesicular feldspar-phyric bands. The upper margin of the coherent dacite body contains a single, boulder-sized, subrounded clast of dacite similar in composition to the main body (Fig. 44a).

Large volume dacite association

Large volume dacite facies

The large volume dacite facies (*AChm1*) forms a regionally extensive unit outcropping discontinuously between Red Hill and the area northwest of Mount Negri. The thickness of the large volume dacite facies varies from about 160 m at Red Hill to 1.1 km in the Good Luck Well area. Volume estimates, based on it being an approximately circular body with strike length equal to the diameter, indicate a volume between 250 and 900 km^3. However, the original volume of the unit may have been greater, partly because of insufficient mapping data, but also because part of the unit may have been eroded.

The large volume dacite facies locally contains one or more of the spherulitic dacite (*AChm1(b)*), feldspar-phyric dacite (*AChm1(a)*), and grey dacite (*AChm1(c)*) subfacies. Silicified plagioclase-phyric dacite (*AChm1(d)*) is mapped as a fourth facies in the Good Luck Well area (Plate 2a). Where all subfacies are present, the composite unit is horizontally layered, with spherulitic dacite forming the lower portion overlain by feldspar-phyric dacite. Grey dacite forms an upper layer, but no contact relationships have been recognized in the field. North of Mons Cupri, the proximal reworked conglomerate facies of the Cistern Formation of the Bookingarra Group contains a clast assemblage derived from both spherulitic and feldspar-

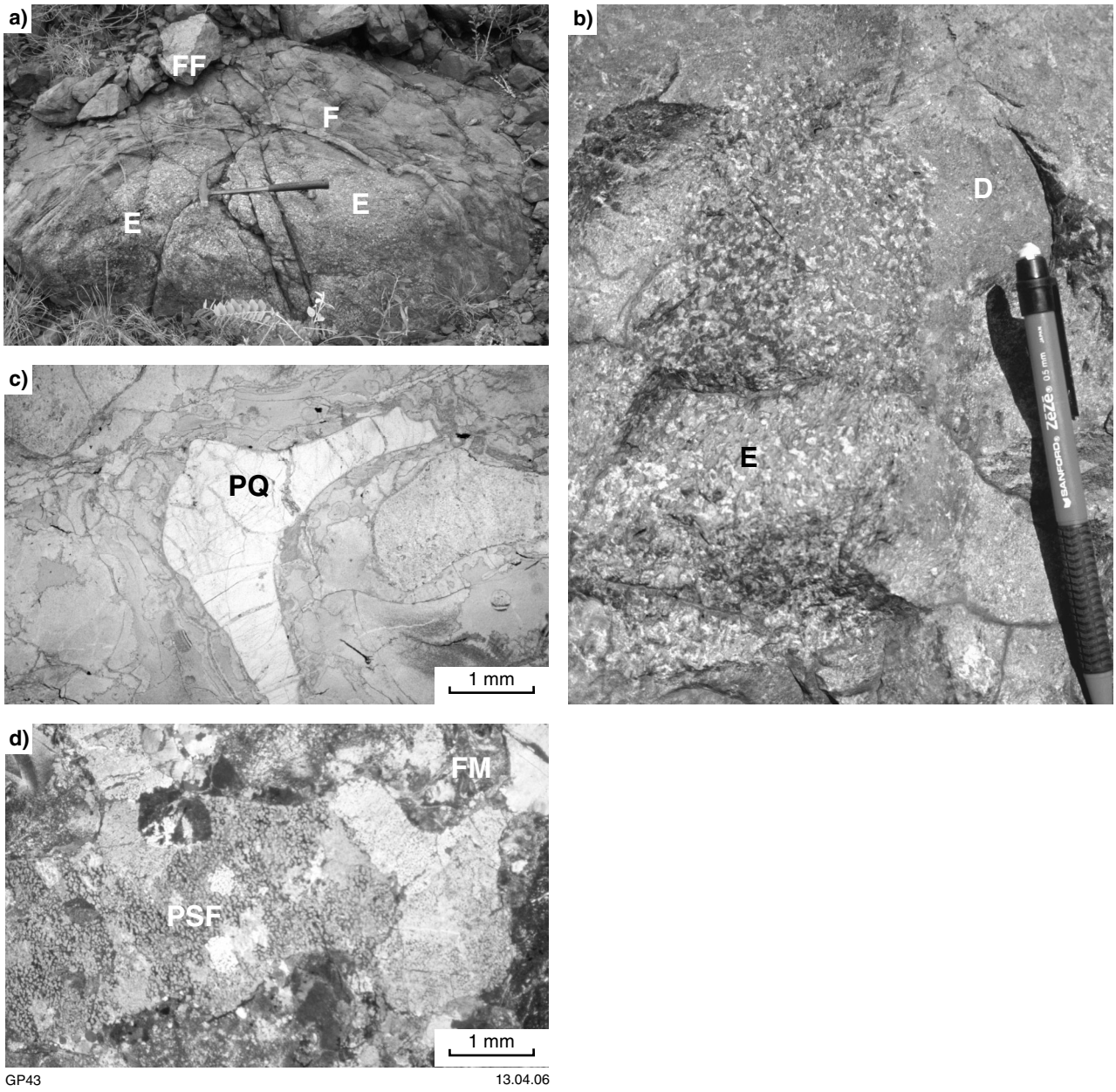

Figure 41. The crystalline inclusions facies, Mons Cupri Dacite Member, Red Hill Volcanics, showing outcrop geology and petrography from photographs from stratigraphic log 116a (Fig. 39). Photographs (a), (c), and (d) are from 122 m and (b) is from 68.5 m: a) a subrounded body (1.5 m exposed diameter) of the crystalline inclusions facies (E) within the upper part of the small volume dacite facies. Flow bands (F) wrap around the body and are locally folded (FF), suggesting that it behaved as a rigid body relative to the cooling magma host; b) coarsely crystalline inclusions (subrounded body) within dacite (D); c) photomicrograph showing polycrystalline, anhedral quartz crystals within the coarser grained component of the crystalline inclusions facies (outcrop in (a) above); d) photomicrograph, from the sample as (c), showing coarse-grained, polycrystalline, sieve-textured plagioclase (PSF) in a finer grained matrix (CFM) of quartz and feldspar, and lesser chlorite

phyric dacite, indicating that the feldspar-phyric dacite was removed during erosion and deposition of the Cistern Formation. Hence, the composite portion of the large volume dacite body may have extended from the Good Luck Well area to the Mons Cupri area, a distance of about 17 km.

Interpretation

The spherulites within the spherulitic dacite indicate high-temperature devitrification of volcanic glass (Lofgren, 1971; McArthur et al., 1998). Spherulites at the centre of the 160 m-thick section of the dacite body at Red Hill indicate that it must have cooled relatively quickly. This observation constrains the emplacement model for the large volume dacite facies, and suggests that it must be either a lava flow or high-level intrusion. The upper contact of the spherulitic dacite in the Red Hill area shows large lobes of dacite penetrating the overlying aphanitic basalt breccia facies of the Warambie Basalt. Although these upper-surface lobes could be interpreted as erosional paleotopographic features, the thin (<10 m) outer zones of strong flow banding parallel to the margins of the bodies indicate that the entire body is preserved. In this interpretation the flow-banded zones are thought to represent shear-induced laminar flow zones at the margins of the body, implying that this material was at the upper surface during emplacement. Hence, there is evidence from the Red Hill area that the large volume dacite facies was emplaced at high level, within subaqueous volcanic breccia as a subaqueous intrusion.

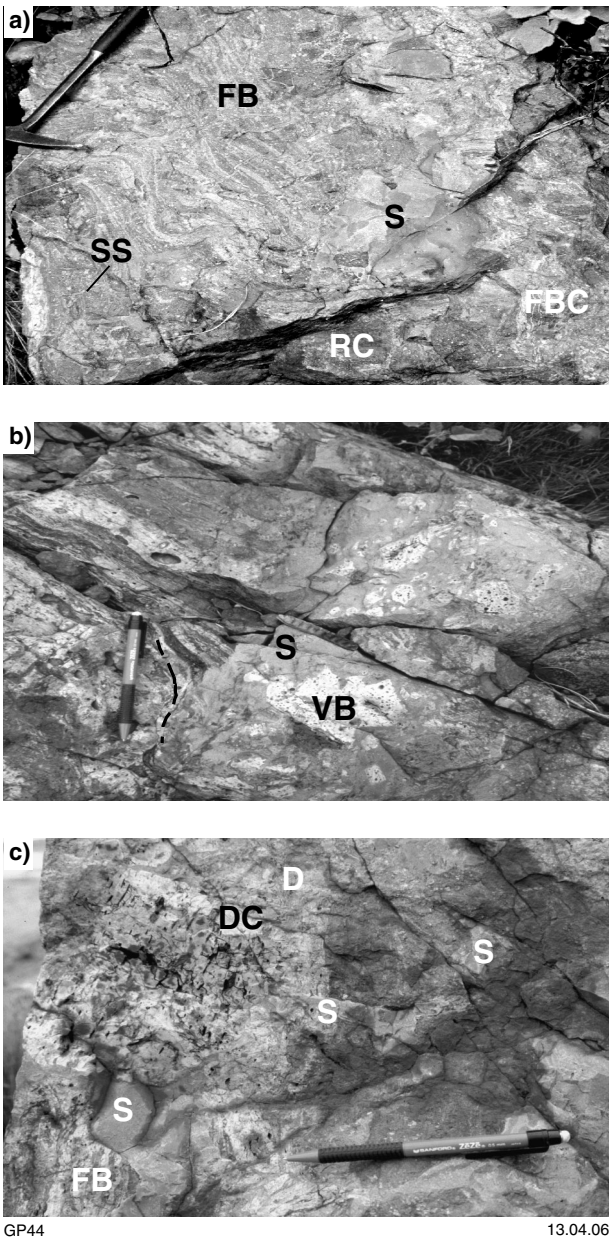

GP44 13.04.06

Figure 42. The mixed dacite breccia–sandstone facies, Mons Cupri Dacite Member, Red Hill Volcanics: a) mixed coherent, strongly flow-banded (FB) dacite, clastic flow-banded dacite breccia (FBC), and structureless fine-grained volcanic sandstone (S). The flow-banded dacite breccia has an unusual texture and the appearance of rounded clasts (RC) in the bottom of the photograph. Rare sedimentary slices (inclusions, SS) are preserved within the flow-banded dacite and the illustrated example is bent into a boomerang shape along with the flow bands. This inclusion shows that sediment was incorporated into the dacite before quenching and formation of the flow bands; b) flow-banded dacite (FB), fine-grained, structureless volcanic sandstone (S), and highly angular clasts of vesicular breccia (VB). In this example the angular dacite is hosted by the sedimentary material. The irregular folding in the dacite is flow folding and suggests plastic deformation during mixing with the sediment while the dacite was still relatively hot and plastic; c) a large dacite clast (DC) detached from the main body of dacite, and surrounded by relatively coherent dacite (D), flow-banded dacite (FB), and thin apophyses of volcanic sandstone (S). The dacite clast has stretched large vesicles

Bookingarra Group

Until recently, siliciclastic sedimentary rocks and voluminous basalt lava from the upper stratigraphic levels of the Whim Creek greenstone belt were stratigraphically assigned to either the upper part of the Whim Creek Group or to two overlying formations — the Louden Volcanics and Mount Negri Volcanics (Hickman, 1983; Smithies, 1998). New mapping, facies analyses, and geochronology have resulted in the definition of the Bookingarra Group (e.g. Pike and Cas, 2002; Van Kranendonk et al., 2002). This group combines two former formations of the Whim Creek Group — the Cistern Formation (*ABc*; conglomerate and sandstone) and the Rushall Slate (*ABr*; mudstone) — with the Mount Negri Volcanics (*ABt*) and Louden Volcanics (*ABe*; both composed of basalt). A previously described unconformity between the Rushall Slate and the Mount Negri Volcanics (Fitton et al., 1975; Hickman, 1983) is no longer regarded as a significant stratigraphic break because contacts between these formations in other areas are conformable. West of the area mapped in the

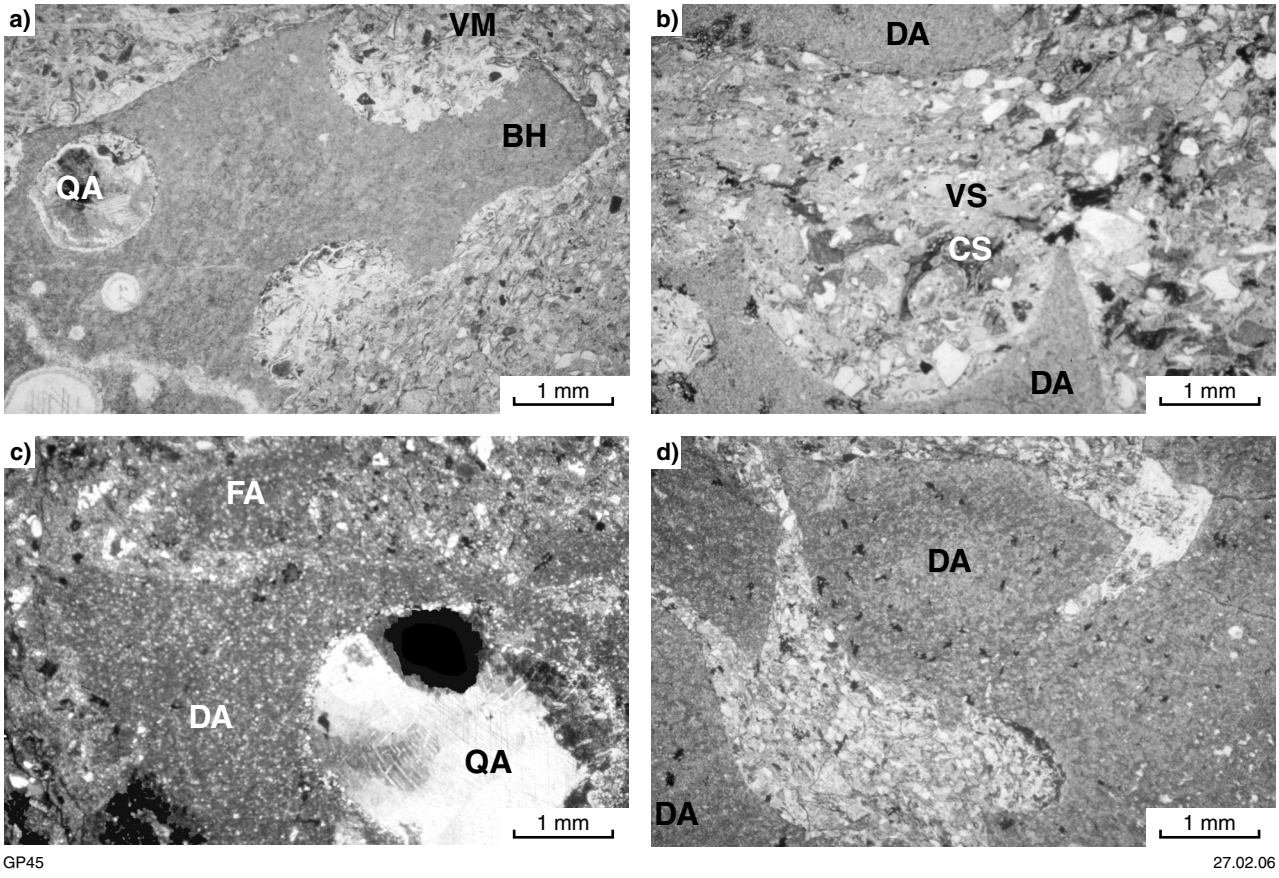

Figure 43. Textures from the margin of the mixed dacite breccia–sandstone facies, Red Hill Volcanics (MGA 570239E 7682056N): a) blocky, angular dacite hyaloclast (BH) within a matrix of chloritic volcaniclastic sandstone (VM). The margins are concave suggesting that the clast has fractured through vesicle walls. A single quartz amygdale (QA) suggests that some vesicles remained isolated and unbroken. The walls of fractured vesicles may show irregular outlines where individual grains of matrix material have pushed into the clast, perhaps while it was a hot plastic glass; b) blocky peperite with well-developed dacite (DA) vesicle margin, and associated fill of volcaniclastic sandstone (VS) and chloritic shard debris (CS); c) fluidal peperite comprising a clast of dacite (DA) with large quartz amygdale, and a fluidal apophysis (FA) frozen in the process of becoming detached from the larger clast; d) fluidal peperite with apophysis (similar to (c) above)

present study, the Kialrah Rhyolite (Hickman, 1997) forms a fifth formation of the group, and intrudes or overlies the Louden Volcanics (Smithies et al., 2001). Highly deformed rocks in the Salt Creek area are also now assigned to the Bookingarra Group.

Cistern Formation and Rushall Slate

The Cistern Formation (*ABc*) is the basal unit of the Bookingarra Group, and is conformably overlain by the Rushall Slate. The Cistern Formation is characterized by upward-fining sedimentary rocks with an upward-increasing siliciclastic content. The maximum thickness of 600 m is preserved in the Good Luck well area. The Cistern Formation is subdivided into three facies associations based on the relative proportions of epiclastic volcanic clasts (mostly derived from the Whim Creek Group) and siliciclastic clasts. These are the volcaniclastic-dominated sedimentary rock, mixed sedimentary rock, and siliciclastic-dominated sedimentary rock associations (Table 5). The Rushall Slate is up to 300 m thick, and dominated by metamorphosed shale containing minor siltstone, sandstone, and chert. It contains only two facies — the shale facies and the blue chert facies.

Volcaniclastic-dominated sedimentary rock association

Conglomerate facies

The conglomerate facies (*ABc6*) is exposed in the area between Whim Creek and Mons Cupri. The facies grades upward into the volcanic breccia, graded sandstone, or quartz-rich sandstone facies. A minimum thickness of 50 m is preserved northeast of Mons Cupri. The facies is restricted to the area around Mons Cupri, suggesting limited lateral continuity, and individual depositional packages are not recognized. The facies covers a range of rock types including both conglomerate and

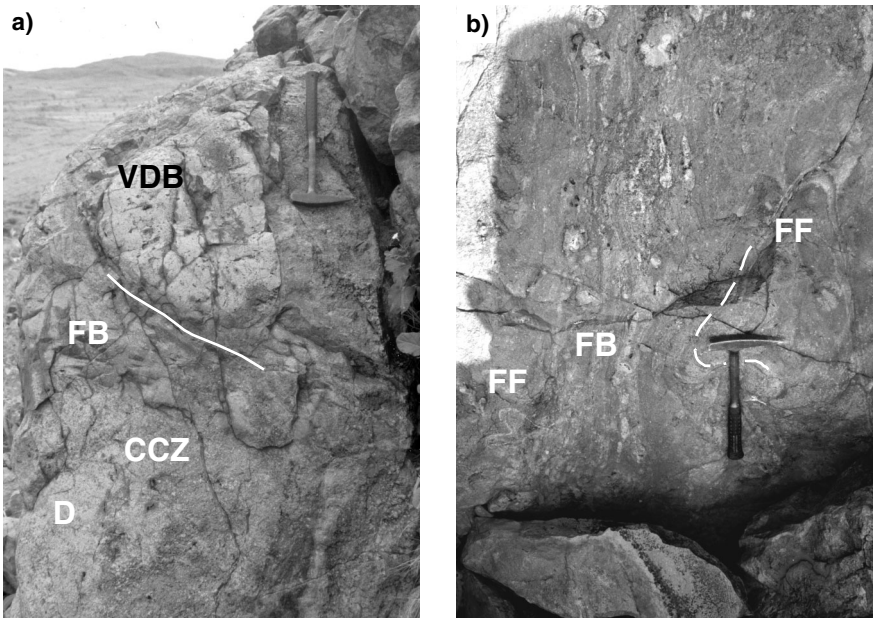

Figure 44. The upper section of the small volume dacite facies, Mons Cupri Dacite Member, Red Hill Volcanics (MGA 570239E 7682056N): a) vesicular dacite boulder (VDB) entrained in coherent dacite. The boulder is rounded and contains large, open, stretched vesicles that are elongate at a high angle to the elongation of the clast. The dacite (D) contains coarsely crystalline zones (CCZ) that give a rubbly texture, and is part of the flow-banded crystalline inclusions facies. The white line highlights weak flow bands (FB) that wrap around the boulder; b) strong flow banding (FB) and flow folding (FF) in the upper (coherent) part of the facies

breccia (e.g. Fig. 45a), with the former dominant. The characteristic features of the facies are the prevalence of large felsic volcanic clasts within a mixed quartz and lithic sand- or granule-sized matrix. The entire facies shows an upward-fining trend, and sandstone interbeds are at the highest stratigraphic level. Typically, the facies is strongly deformed by a widely spaced S_2 cleavage or clast flattening, and consists of massive, matrix- to clast-supported boulder and cobble conglomerate, and has a matrix of smaller cobbles and sand-sized material. Clasts are of three main types: feldspar-phyric dacite (Mons Cupri Dacite Member), lesser spherulitic dacite (Mons Cupri Dacite Member), and less than 10% amphibole-bearing granite and microgranite clasts.

Interpretation

The coarse grain size strongly suggests transport as single clasts (rolling, sliding), or by debris flow. There is little direct evidence for subaqueous deposition, and the setting may have been a fan in alluvial or subaqueous setting. However, the conformable relationship between conglomerate facies and the graded sandstone facies suggests that a subaqueous setting is more probable. Conglomerate was deposited synchronously with a volcanic event (based on the recognition of pumice clasts), but there is no requirement for this event to have been within or local to the depositional basin.

Sheared conglomerate facies

Coarse-grained clastic rocks of the sheared conglomerate facies are exposed along the western margin of the Croydon–Mallina road (outside areas of Plates 1 and 2), where they form a prominent ridge. The facies is up to 128 m thick, but poor preservation suggests a maximum thickness of 200 m. Individual depositional units are not recognized and the facies is of limited lateral extent (<5 km). The sheared conglomerate facies contains clast- and matrix-supported subtypes, and differs from the conglomerate facies by containing a strong tectonic fabric, having an abundance of granule-sized quartz grains in the matrix, and containing fewer clasts. The facies is dominantly matrix supported, although clast-supported examples are also relatively common. Clasts are dominated by spherulitic dacite (Mons Cupri Dacite Member) with lesser amounts of granite and fuchsitic (altered mafic–ultramafic) material. Clasts vary from pebble to cobble size (4–250 mm), and are rounded. The facies is strongly sheared along its entire outcrop, and many of the clasts are elongate along the tectonic fabric. The matrix material is coarse-grained sandstone and contains coarser grained quartz (to 3 mm) and aphyric tube pumice.

Interpretation

The facies was derived from the erosion of uplifted Mons Cupri Dacite Member rocks and granite. It is

Table 5. Facies and facies associations of the Bookingarra Group (sedimentary component)

Facies association	*Facies*	*Area*	*Code*
..... *Conformably overlying Mount Negri Volcanics*			
Siliciclastic-dominated sedimentary rock	Shale (Rushall Slate)	Mons Cupri	ABr1
	Cleaved mudstone facies[a]	Salt Creek	–
	Blue chert[a] (Rushall Slate)	Mons Cupri	–
	Sandstone turbidite (Cistern Fm)	Mons Cupri	ABc1
	Quartz-rich sandstone (Cistern Fm)	Mons Cupri, Salt Creek	ABc2
	Lithic sandstone (Cistern Fm)	Mons Cupri, Salt Creek	ABc3
Mixed sedimentary rock (Cistern Fm)	Rippled sandstone	Good Luck Well	ABc4
	Black chert breccia	Good Luck Well	ABc5
Volcaniclastic-dominated sedimentary rock (Cistern Fm)	Volcanic breccia[a]	Mons Cupri	ABc7
	Sheared conglomerate[a]	Outside area of Plates 1 & 2	–
	Conglomerate	Mons Cupri	ABc6
---------- *Unconformably/disconformably underlying Whim Creek Group* ----------			

NOTES: (a) Facies too restricted to be shown on Plates 1 and 2

likely that the facies is similar to subaqueous fanglomerate of the conglomerate facies, and may simply represent a compositionally different facies equivalent.

Volcanic breccia facies

The volcanic breccia facies is related to the conglomerate facies, and is dominated by pebble-sized clasts of basalt, dacite, volcaniclastic sandstone, and granite. It is rarely more than a few metres in thickness (too small to be mapped at 1:10 000 scale), and is interbedded with finer grained clastic rock types. The bases of individual units are typically planar. The matrix is poorly to moderately sorted sandstone with about 25% each of plutonic quartz and feldspar and 50% lithic clasts that are similar to the framework clasts. Although the clasts dominate the rock (~80%), many appear to 'float' due to a thin film of matrix separating the fragments. The facies tends to be better sorted upwards as the matrix becomes coarser grained, and clasts fine to a granule breccia.

Interpretation

The volcanic breccia facies shows similar clast content as the conglomerate and sheared conglomerate facies. Upward increase in sorting precludes a true debris-flow origin and suggests that larger clasts were deposited from the flow, whereas smaller clasts were removed. The planar bases to most units indicate laminar flows. These features may be explained by a high-concentration turbidity current with basal laminar shear.

Mixed sedimentary rock association

Black chert breccia facies

Coarse-grained lithic arenite and granulestone of the black chert breccia facies (*ABc5*) are locally interbedded with the volcanic breccia facies with erosional or transitional, upward-fining or upward-coarsening boundaries. The facies comprises metre-scale depositional units with diffuse planar bedding and a tabular geometry. The facies (Fig. 46) has a maximum thickness of 230 m in the Good Luck Well area. The characteristic features of the facies are coarse sand- to granule-sized grains with larger clasts dominated by chert fragments. Two main types of chert are recognized. The dominant type is black chert (Fig. 47a,b) that is typically structureless, but may contain millimetre-scale laminae indicating a sedimentary origin. Clasts are commonly elongate and rectangular with very angular margins, suggesting that they were lithified before erosion and deposition. The second main type of clast is a light-brown chert, commonly containing very fine grained, submillimetre-scale lamination. These clasts are typically elongate and rounded. Large clasts make up to 30% of the facies (light chert 50%, black chert 30%, felsic volcanic clasts 10%, and basalt 10%). The matrix material varies throughout the facies. At the base it consists of a mixture of feldspar, grey siliceous lithic clasts, dull-grey (?plutonic) quartz, and dark-grey vitreous (volcanic) quartz (Fig. 47e,f). In general, the amount of feldspathic and grey siliceous grains decreases upwards, and is consistent with the decrease in volcaniclastic material. The dark-grey quartz also decreases in abundance upward. Some of the quartz is polycrystalline or associated with plagioclase (Fig. 47d), or both, and is clearly derived from a granitic source. Straight extinction of the quartz implies only weak deformation of the source rocks before erosion. In the highest stratigraphic levels the facies is dominated by coarse-grained sandstone with rare, and generally smaller, chert clasts. This level has the first large sedimentary intraclasts, which may be up to 20 cm in diameter (Fig. 47c), and are much larger than the largest chert clasts (typically 0.5–2 cm). These intraclasts include both sandstone and mudstone, are weakly elongate or equant, and have well-rounded margins. A characteristic feature of this facies is the similarity between chert and matrix composition, and the irregular clast margins into which some of the matrix is embedded. These features suggest that the clasts were coherent, but unlithified, and probably represent finer grained material that was initially deposited

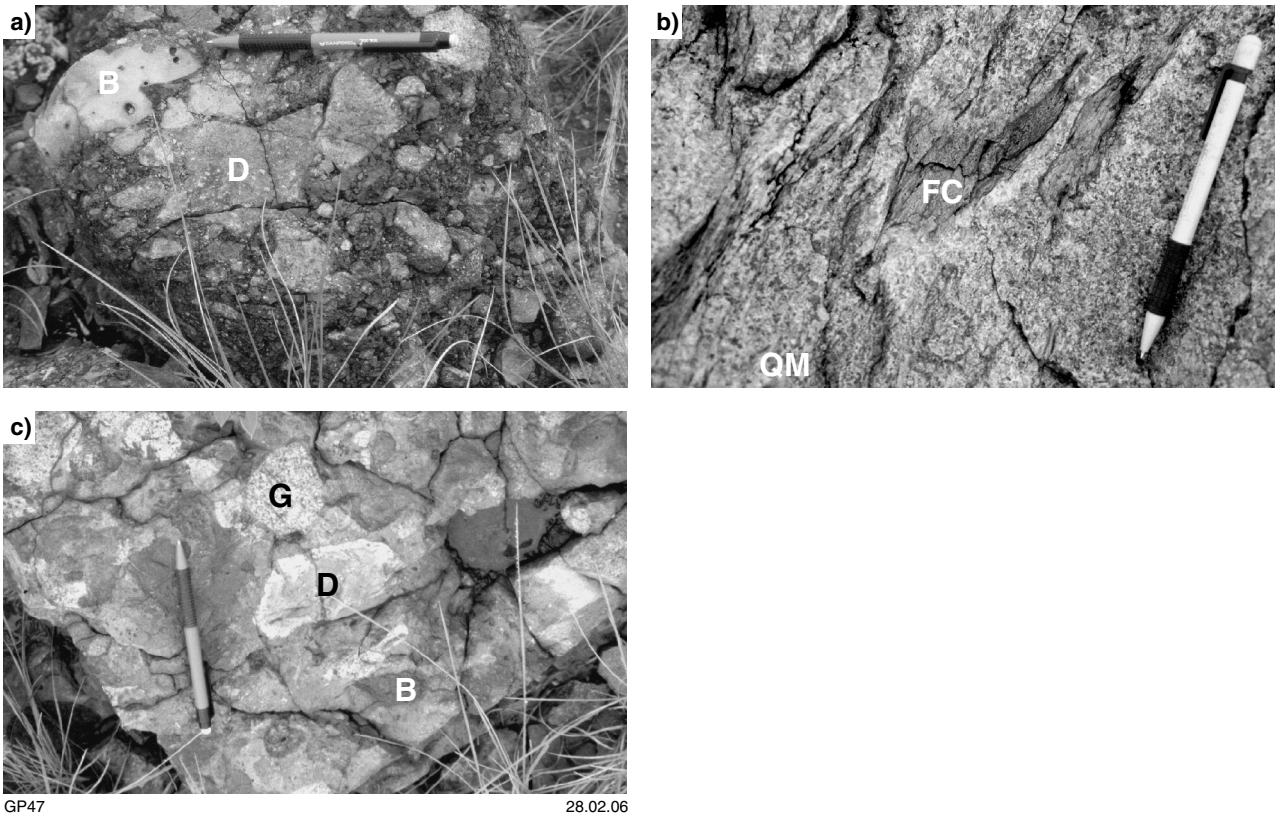

Figure 45. The volcaniclastic-dominated sedimentary rock association, Cistern Formation, Bookingarra Group: a) breccia that is similar to the volcanic breccia facies, but contains clasts identical to those of the conglomerate facies. This particular unit is placed within the latter facies where it is locally abundant immediately below granulestone and sandstone units (MGA 585839E 7691155N). This breccia is near the stratigraphic top of the facies and comprises angular vesicular basalt (B) and abundant dacite (D) that is petrographically the same lithofacies as the feldspar-phyric dacite (Mons Cupri Dacite Member); b) the sheared conglomerate facies 1 m north of the locality sampled by Nelson (2000). The dark clast in the centre is fuchsitic (FC, originally mafic–ultramafic), and is hosted by a coarse-grained, quartz-rich matrix (QM); c) the volcaniclastic breccia facies, including clasts of basalt (B), granite (G), and dacite (D). The matrix is poorly sorted, medium- to coarse-grained sandstone with quartz, feldspar, and abundant lithic grains (MGA 572439E 7681355N)

upstream and then eroded by later flows. This suggests that the flows were erosive and turbulent.

Interpretation

Mudstone rip-up clasts indicate turbulent erosive upstream conditions, and deposition of finer grained sediment upstream from the site of deposition during inter-flow periods or lower energy flows. These observations are consistent with a turbidite origin in which the finer grained, muddy components were ripped up and reworked downstream. Imbricate chert clasts are consistent with this interpretation. The change in composition from volcaniclastic and feldspar-rich to quartz-rich material within depositional packages indicates aggradation from a flow rather than plug-flow of material. Both Whim Creek Group and granitic sources are recognized, but the abundant black and grey sedimentary chert suggests a more widespread source, including exposed chert (?Cleaverville Formation).

Rippled sandstone facies

The stratigraphically highest sections of the mixed sedimentary rock association form thick, poorly preserved sandstone units of the rippled sandstone facies (*ABc4*; Figs 46 and 48a). The facies has a maximum thickness of 100 m in the Good Luck Well area, and is a fine-grained equivalent (lithic arenite) of the volcanic breccia facies and black chert breccia facies. The rippled sandstone facies is interbedded with the black chert breccia facies. The facies is characterized by light-blue sandstone composed predominantly of siliceous (quartz–chert) grains (70%) with lesser feldspar (20%) and dull-grey quartz (10%). Most samples are well sorted, with planar lamination or bedding (commonly 5–15 mm beds), and local ripples, where the entire ripple form is preserved. Ripples have wavelengths of 5–10 cm and amplitudes of less than 1 cm, and are at very low angles. Rare flame structures are noted, as are rip-up clasts up to about 15 cm length.

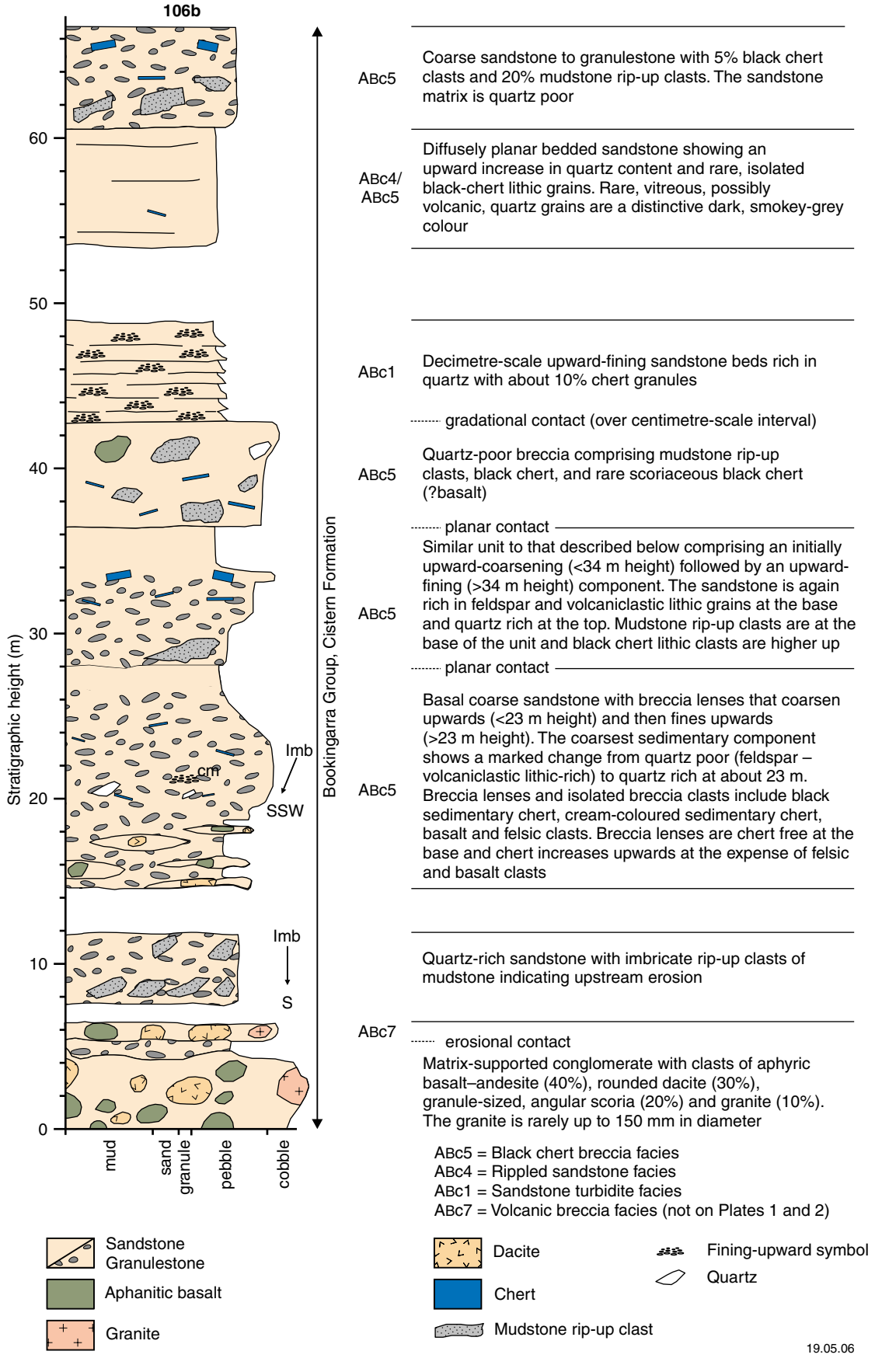

Figure 46. Stratigraphic log 106b (base at MGA 572599E 7681157N), Cistern Formation, Bookingarra Group, Good Luck Well area, showing various facies (see Fig. 9 for regional location)

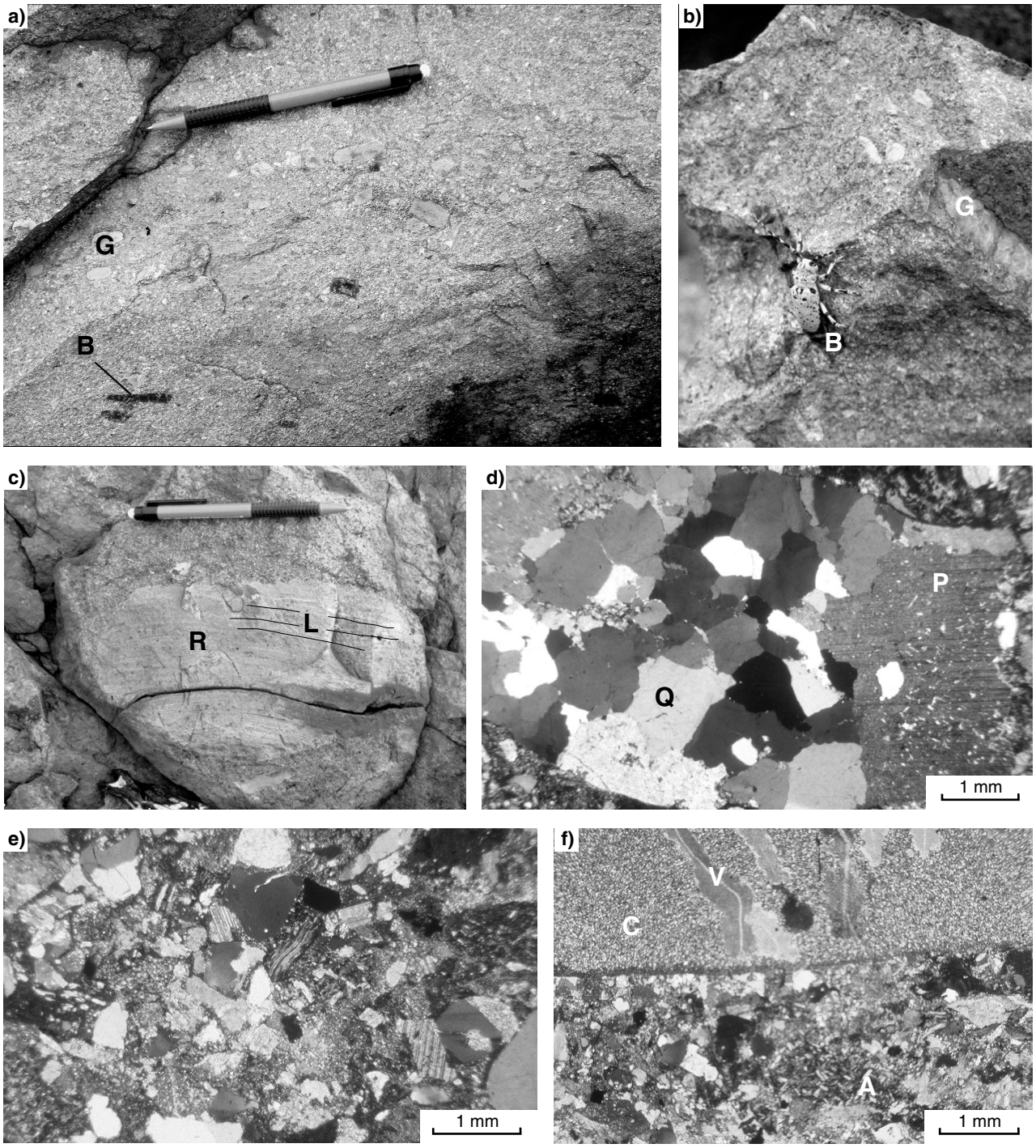

Figure 47. Features of the black chert breccia facies (*ABc5*), Cistern Formation, Bookingarra Group, Good Luck Well area. Outcrops (a)–(c) immediately overlie the volcanic breccia facies illustrated in Figure 46 (from near MGA 572439E 7681355N). Thin section photographs (d)–(f) are from the outcrop illustrated in (b): a) outcrop showing an equal proportion of black (B) and grey (G) chert clasts. The elongate clasts are typically imbricate; b) outcrop showing large chert clasts (beetle is about 2 cm long); c) outcrop showing a large rip-up clast (bottom, centre) within a coarse-grained sandstone matrix. Note the original lamination (L) within the clast (R); d) photomicrograph of a quartz-dominated (Q) large granitic clast, with lesser plagioclase (P); e) photomicrograph of arkose or wacke, comprising abundant quartz with lesser feldspar and lithic clasts; f) photomicrograph illustrating the margin of a large chert clast (C). Carbonate veins (V) show that the chert was lithified and weakly brecciated before uplift and erosion. The matrix contains andesitic clasts (A) as well as quartz, feldspar, and other lithics

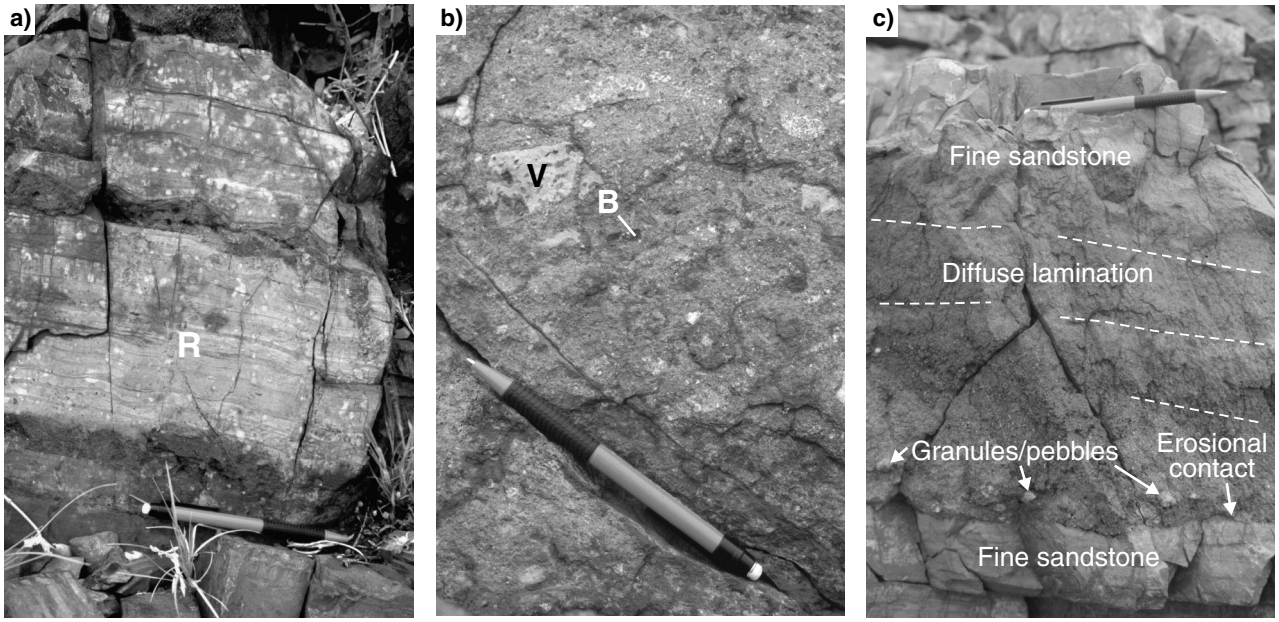

Figure 48. The rippled sandstone (*ABc4*) and sandstone turbidite (*ABc1*) facies, Cistern Formation, Bookingarra Group: a) wavy bedding and asymmetric ripples (R) in the rippled sandstone facies. The ripples appear similar to tectonic folds, but internal asymmetry shows that they are sedimentary; b) poorly sorted granulestone–pebble breccia of the sandstone turbidite facies, Mons Cupri area. This rock type forms part of the upward transition from conglomerate to graded sandstone and contains felsic volcaniclastic (F) and basaltic (B) clasts; c) graded sandstone turbidite facies with erosional base and upward fining (MGA 5985939E 7691855N)

Interpretation

Rip-up clasts suggest turbulent erosive conditions upstream. The ripples suggest that the upper surfaces of beds were reworked by the passage of currents, and may explain the lack of mudstone caps. Flame structures are also consistent with a turbidity current origin, and suggest rapid deposition of water-rich sediment.

Siliciclastic-dominated sedimentary rock association

The siliciclastic-dominated sedimentary rock association comprises five facies, two of which are confined to the Rushall Slate (Table 5).

Lithic sandstone facies

The lithic sandstone facies (*ABc3*; Figs 49 and 50a) underlies and is interbedded with the Rushall Slate, and forms centimetre-thick beds of limited lateral extent. Around 20 m of this facies recognized above the basal unconformity of the Bookingarra Group probably represents the maximum development of the facies. The facies contains well-sorted lithic sandstone with a strong chlorite overprint. The grains include relatively abundant volcaniclastic, basaltic or andesitic clasts, and more quartz than in previously described facies.

Interpretation

The facies contains a range of coarse- to fine-grained sandstones, and many examples show weak upward fining, suggestive of a turbidity current origin. The facies is important in that it indicates either a source of mafic volcanism or uplifted mafic material immediately before, and during, deposition of the Rushall Slate.

Quartz-rich sandstone facies

Coarse-grained sandstone of the quartz-rich sandstone facies (*ABc2*) is of limited thickness (≤10 m) and outcrops at the transition between the conglomerate facies (Cistern Formation) and shale facies (Rushall Slate), east of the Mons Cupri area. Nelson (2000), using the SHRIMP U–Pb method, dated zircons from a sample (GSWA 142949) of the quartz-rich sandstone facies. The largest, and youngest, zircon population was dated at 2978 ± 5 Ma, which was interpreted as the maximum depositional age of the sandstone.

Metre-scale depositional units with very diffuse planar lamination typify the facies. Grains are dominantly quartz and altered feldspar and rare, fine-grained, sand-sized, black, cubic or rectangular clast material, similar to that in the black chert breccia facies. Grains are poorly to well rounded, but display excellent sorting. Some quartz grains are lithics with a polycrystalline texture, suggesting that they have been sourced from granitic rocks. Unstable grains have commonly broken down to a kaolin-rich white clay, preserving a porous open rock that has been stained by chlorite (purple) and malachite (green). Five subfacies of the quartz-rich sandstone facies are mapped in the Salt Creek area.

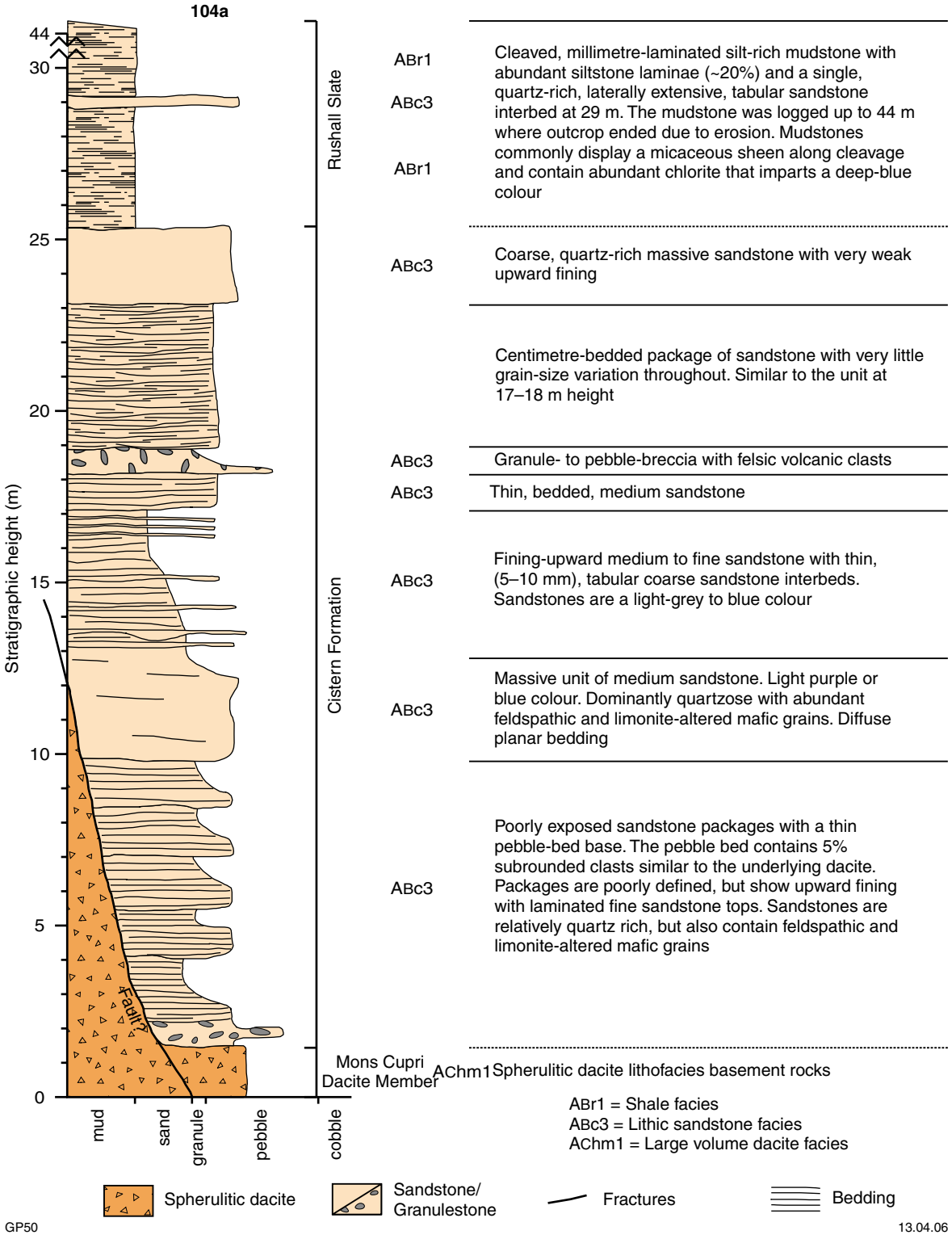

Figure 49. Stratigraphic log 104a (base at MGA 586799E 7693525N), Cistern Formation and Rushall Slate, Bookingarra Group, south of the Whim Creek mine site (MGA 586465E 7694565N)

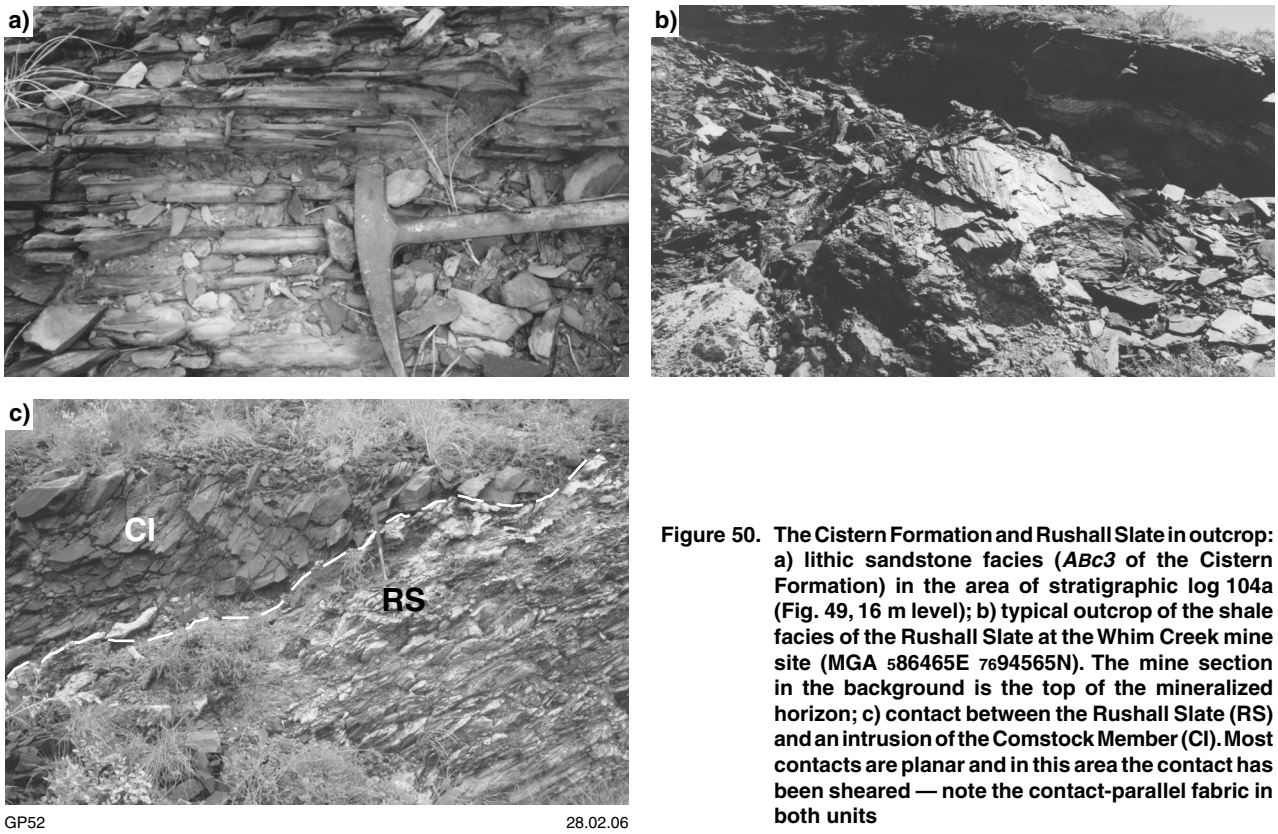

Figure 50. The Cistern Formation and Rushall Slate in outcrop: a) lithic sandstone facies (*ABc3* of the Cistern Formation) in the area of stratigraphic log 104a (Fig. 49, 16 m level); b) typical outcrop of the shale facies of the Rushall Slate at the Whim Creek mine site (MGA $_{5}$86465E $_{76}$94565N). The mine section in the background is the top of the mineralized horizon; c) contact between the Rushall Slate (RS) and an intrusion of the Comstock Member (CI). Most contacts are planar and in this area the contact has been sheared — note the contact-parallel fabric in both units

Interpretation

Nelson (2000; GSWA 142949) recognized equal amounts of quartz and feldspar, and the facies thus contains arkose that is similar to the matrix of the sheared conglomerate facies. The diffuse planar lamination and upward-fining character are suggestive of turbidity current deposition, but exposure is too poor to confirm this interpretation.

Sandstone turbidite facies

Granule- to fine-grained sand-sized sedimentary rocks of the sandstone turbidite facies (*ABc1*) are interbedded with the upper sections of the conglomerate facies. The facies is dominated by planar-laminated lithic arenite that typically fines upwards to lithic greywacke. Basal units may be rich in matrix-supported granule to pebble breccia, typically with very angular clasts (Fig. 48b). The breccia is mostly derived from a felsic volcanic source similar to the Mons Cupri Dacite Member. Bed sets vary between metre and decimetre scale, but are typically less than 1 m in thickness. The base may be planar or irregular, and erosive into the underlying unit (Fig. 48c). Granule and pebble breccia is restricted to the base of each bed set, and typically fines upward over about 40 cm into fine-grained sandstone and mudstone. These upper units have well-developed planar lamination. The facies is dominated by quartz and chert clasts with lesser amounts of volcaniclastic (basement) material. Individual depositional packages are the T_b and T_d units of the Bouma Sequence (Fig. 48c).

Interpretation

As noted above, the conformable relationship between the conglomerate facies and the sandstone turbidite facies suggests a subaqueous fan setting.

Shale facies

The shale facies (*ABr1*) is a diverse grouping that includes a range of medium- to fine-grained sedimentary rocks. This facies dominates the Rushall Slate, and has a maximum stratigraphic thickness of 300 m around the settlement of Whim Creek. The base of the shale facies is here considered as the transition from the sandstone turbidite facies, quartz-rich sandstone facies, or lithic sandstone facies to wacke, shale, and chert (Fig. 50b). Black (1998) noted the following rock types:

- slate dominated by quartz, sericite, chlorite, opaque minerals, and biotite (= shale facies);
- siliceous slate comprising silt, slate, and chert beds to 3 mm in 5 cm bed-sets (= blue chert facies);
- sandstone with medium to large grains, 25–45% quartz, feldspar, and feldspathic, quartzose, and cherty lithics (= lithic sandstone facies).

Medium- to coarse-grained sandstone and rare pebble beds are also in the shale facies. Sandstone shows variable composition, but is dominated by quartz, feldspar and mafic, lithic grains. A mudstone (Fig. 49; 15.5 m) includes interbedded, thin (0.5 – 1 cm) tabular sandstone beds with thicker (1 – 1.5 cm) shale horizons. Individual beds may

be traced for many metres without any obvious thinning, basal erosion or fining. Coarser grained examples form a regularly bedded package of fine- and medium-grained sandstone. The basal 15 m of the facies contain numerous coarse-grained sandstone beds, with a tabular or, rarely, a ribbon-like geometry. These beds are typically 20 cm to 2 m in thickness, massive to laminated, and contain very well sorted subangular grains. Rarely, subrounded clasts of aphanitic, sericite-altered felsic volcanic rocks may be included in the basal portion of the coarse-grained sandstone. Above 15 m from the base, the shale facies becomes dominated by mudstone with only rare laminae of fine-grained sandstone. Typical examples are light blue-grey to light purple, with a dull silky sheen along cleavage (Fig. 49). The dominant components are clay minerals, and the more deformed examples are characterized by the growth of white mica. Several horizons contain ovoid, iron-rich nodules that are flattened parallel to the dominant cleavage. These are interpreted to represent primary pyrite nodules, and suggest anoxic conditions at the time of deposition.

Interpretation

The environment of deposition for the shale facies was of low energy, with influxes of moderate energy, but generally non-erosive currents. The regular tabular geometry of most beds, coupled with well-sorted grains, suggests that deposition occurred from settling within a water column. The finer material shows equally spaced siltstone and fine-grained sandstone laminae that suggest a regular variation in depositional conditions. These are probably distal turbidity current deposits (T_d–T_e subdivisions).

Blue chert facies

Foliated shale facies rocks are typically associated with small amounts (generally <1 m stratigraphic thickness) of the blue chert facies. The blue chert facies rocks typically form very low exposures, and although the facies may be more widespread under alluvial cover its outcrops are too restricted to be mapped at 1:10 000 scale. The facies is commonly massive or millimetre-scale laminated, and no other sedimentary structures are noted. The facies is at the base of the Rushall Slate, and forms thin interbeds within the Louden Volcanics.

Interpretation

The facies is clearly sedimentary, and represents deposition in a stagnant or very low energy water body with little clay or organic input. Such environments may have existed between pulses of shale-facies deposition because the two facies are commonly interbedded.

Mount Negri Volcanics and Louden Volcanics

The Mount Negri Volcanics and Louden Volcanics are basalt-dominated units that were originally described as a single unit (Negri Volcanics) by Fitton et al. (1975). Hickman's (1983) widely accepted subdivision into two units (e.g. Smithies, 1998; Pike, 2001) is based on field, petrographic, and geochemical differences. A summary of the field observations is given in Table 6.

Both Hickman (1983) and Smithies (1998) placed the Mount Negri Volcanics stratigraphically above the Louden Volcanics. Hickman (1983) also placed an unconformity between the two units. However, the Mount Negri Volcanics commonly overlies the Rushall Slate conformably, and overlies the Whim Creek Group unconformably or disconformably.

Lithofacies characteristics

The lithofacies of the Mount Negri Volcanics and Louden Volcanics have been discussed in detail by Hickman (1983) and Smithies (1998), and the following discussion is summarized mainly from these two authors. Hickman (1983) described variolitic mafic to intermediate lava flows from the Mount Negri Volcanics that are dominated by a pyroxene-phyric lithofacies with a matrix of fibrous amphibole. Hickman (1983) also described pillow basalt, mafic–intermediate lava, spinifex-textured harzburgite, dolerite, and gabbro from the Louden Volcanics. The Louden Volcanics lavas contain a skeletal olivine-phyric (now serpentine) lithofacies within a groundmass of pyroxene (now amphibole), as well as pyroxene-phyric lithofacies (Hickman, 1983).

Table 6. Field observations and basic petrographic subdivisions of the Mount Negri Volcanics and the Louden Volcanics

Feature	*Mount Negri Volcanics*	*Louden Volcanics*
Phenocrysts	Pyroxene (lesser olivine)	Euhedral clinopyroxene
Matrix colour	Light–medium blue-grey	Bottle green
Texture	Porphyritic to aphanitic with rare pyroxene spinifex (thin section)	Porphyritic with abundant, coarse-grained pyroxene spinifex, finer grained pyroxene spinifex, and lesser olivine spinifex
Lava morphology	Tabular, about 5 m-thick flows	Tabular, about 2 m-thick flows with abundant pillow lava
Pillows – pillow breccia	Very rare (<1%)	Common (<50%)
Primary breccia	Rare pillow breccia and spatter breccia	No significant primary breccia
Outcrop	Two main areas north and west of Whim Creek and Mons Cupri	Widespread from Government Well to west of Red Hill

Table 7. Facies and facies associations of the Bookingarra Group (volcanic component)

Facies association	*Facies*	*Area*	*Code on Plates*
~ ~ ~ ~ ~ ~ ~ ~ ~ ~ ~ ~ ~ ~ ~ ~ *Unconformably overlying Mount Roe Basalt (c. 2770 Ma) of the Fortescue Group* ~ ~ ~ ~ ~ ~ ~ ~ ~ ~ ~ ~ ~ ~ ~ ~			
Quartz-rich sedimentary rock (Louden Volcanics)	Grey sandstone[a]	–	–
	Basalt conglomerate[a]	–	–
	Cross-laminated sandstone[a]	–	–
	Quartzite and black chert breccia[a]	–	–
Sheet and pillow basalt lava (Louden Volcanics)	Basalt sheet lava	Mons Cupri	ABe1
	Basalt pillow lava[a]	–	–
Siliciclastic and felsic volcanic (Mount Negri Volcanics)	Quartz-phyric rhyolite	Salt Creek	ABtfr
Basalt volcaniclastic[b] (Mount Negri Volcanics)	Cleaved siliciclastic and volcanic breccia[b]	Salt Creek	–
	Angular basalt breccia[b]	Salt Creek	–
Basalt lava (Mount Negri Volcanics)	Basalt pebble breccia[a]	–	–
	Massive basalt lava	Good Luck Well	ABt1
	Basalt breccia and cobble beds (Louden Volcanics)	Salt Creek	ABt2
Dolerite and basalt (Mount Negri Volcanics)	Fine-grained intrusive facies (Comstock Member)	Mons Cupri	ABtc
	Fine- to coarse-grained intrusive facies (Comstock Member)[b]	Mons Cupri	–
	Dolerite intrusion (Opaline Well Intrusion)	Good Luck Well	AaO
	Dispersed basalt (Opaline Well Intrusion)[b]	Good Luck Well	AaO
~ ~ ~ ~ ~ ~ ~ ~ ~ ~ ~ ~ ~ ~ ~ ~ *Conformably underlying Rushall Slate or Cistern Formation of the Bookingarra Group* ~ ~ ~ ~ ~ ~ ~ ~ ~ ~ ~ ~ ~ ~ ~ ~			

NOTES: (a) Facies outside the area of Plates 1 and 2
(b) Facies too restricted to be shown on Plates 1 and 2

Smithies (1998) described the following lithofacies:

- The Mount Negri Volcanics contains variolitic basalt with varioles of acicular clinopyroxene and interstitial plagioclase and glass within a groundmass of clinopyroxene, plagioclase, and glass. Euhedral clinopyroxene phenocrysts up to 2 mm are distributed throughout the varioles and glass.
- The Louden Volcanics consists dominantly of acicular pyroxene or olivine-phyric basalt (or both) within a groundmass of glass, pyroxene, and plagioclase, with some olivine cumulates and rare plagioclase-phyric types. Dominant field-defined lithofacies are pyroxene-spinifex basalt, clinopyroxene-phyric basalt, and olivine-spinifex basalt.

The facies are listed in Table 7, and described in more detail below.

Dolerite and basalt association

The dolerite and basalt association comprises units previously assigned to the Opaline Well Intrusion (*AaO*; e.g. Smithies, 1998). The four facies recognized are associated with all facies of the Rushall Slate and Cistern Formation. Figure 51 is a log through the contact between the Rushall Slate (*ABr1*) and the Mount Negri Volcanics (*ABt1*), and shows the spatial distribution of these facies.

Dispersed basalt facies

The contact between the blue chert facies of the Bookingarra Group and dolerite or basalt in the Good Luck Well area is typically planar. However, in one area (Figs 51 and 52) the dispersed basalt facies is exposed over about 0.5 m stratigraphic thickness and indicates a different contact relationship. The chert forms irregular apophyses into the basalt in a complex association of chert and basalt (Fig. 52b). The chert apophyses show irregular, weakly brecciated margins that may be a later tectonic feature. However, small, equant, irregular clasts of chert form inclusions in basalt, suggesting that the chert was incorporated into the basalt during its emplacement. Clasts of basalt are also noted within chert close to the contact. The basalt ranges from coherent material to brecciated, angular, and irregular clasts that are dispersed within a structureless chert matrix. The basalt is light blue and fine grained with up to 20%, 3–8 mm amygdales, and contains stubby to elongate, 1 mm pyroxene crystals and rare, blocky, 1 mm plagioclase. The basalt clasts are typically strongly altered to a limonite-rich assemblage.

Interpretation

The recognition of basalt (Fig. 51), basalt breccia (Fig. 52a), and isolated basalt clasts (Fig. 52b,c) suggests a transition from coherent basalt facies to mixed basalt–chert breccia facies. This contact provides evidence of interaction between the basalt magma and the chert (blue chert facies of Rushall Slate) when it was still soft sediment (cf. Kokelaar, 1982), indicating that it is a peperite. Such a relationship is important because it suggests that the basalt illustrated in Figure 51 was emplaced before burial and lithification, and is therefore a component of the Bookingarra Group. The basalt is part of a large sill mapped by Smithies (1998) as the Opaline Well Intrusion.

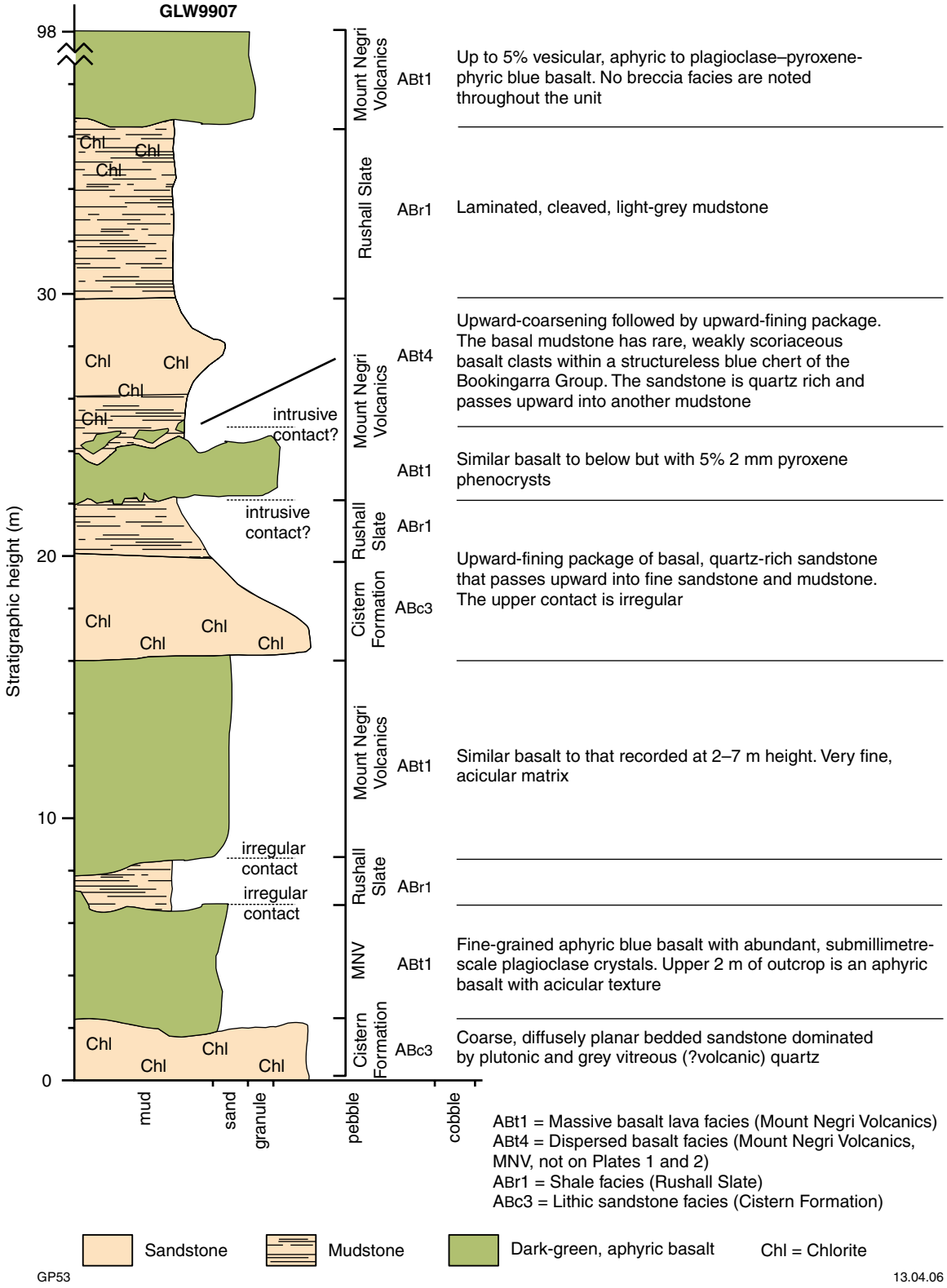

Figure 51. Stratigraphic log GLW9907 (MGA 572224E 7680437N), through the contact between the Rushall Slate and Mount Negri Volcanics, Bookingarra Group, 4 km south of Good Luck Well

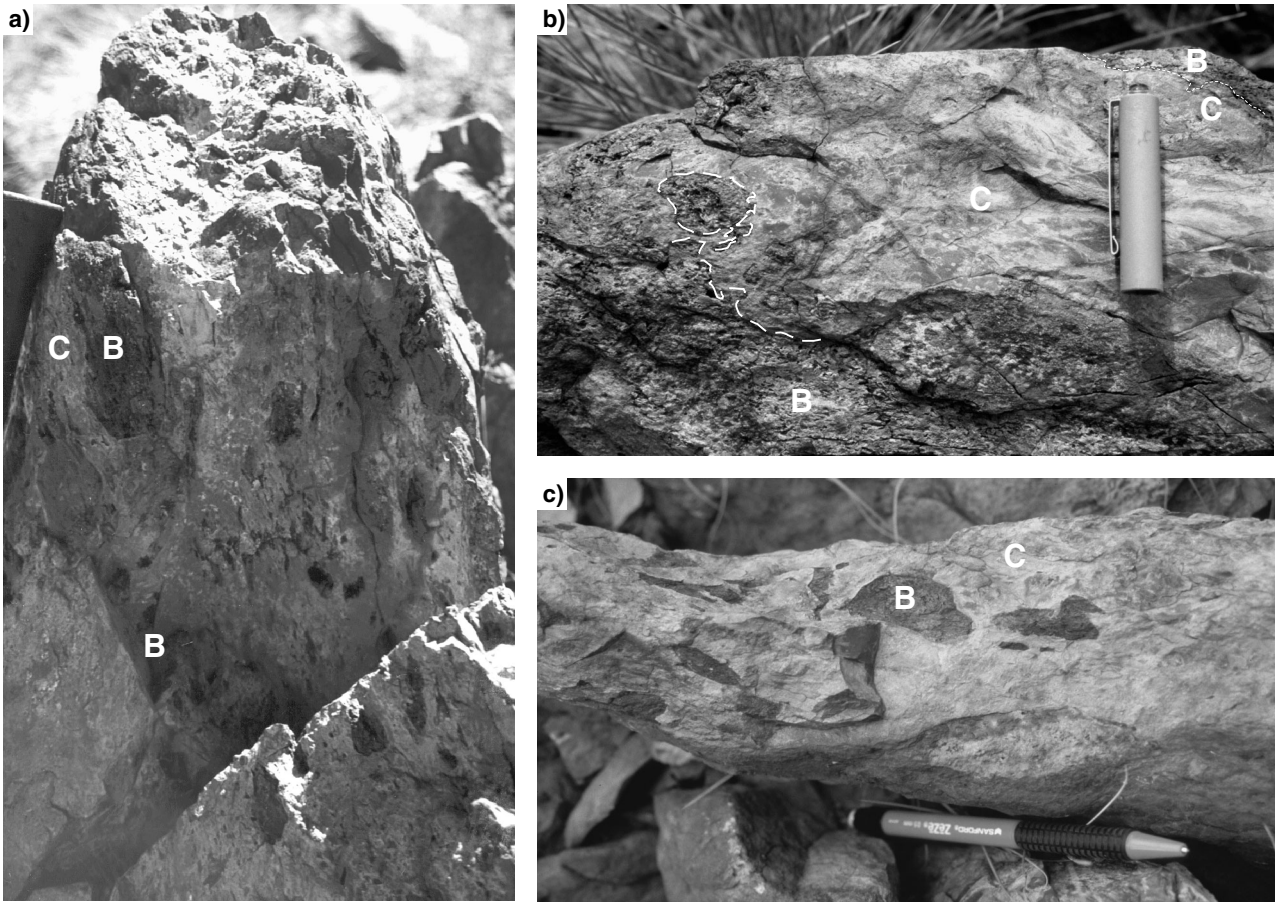

Figure 52. The dispersed basalt facies (*ABt4*), Mount Negri Volcanics (log in Fig. 51, 24 m): a) typical, weakly scoriaceous basalt clasts (B) within chert matrix (C); b) chert apophysis (C) within poorly preserved basalt (B); c) dispersed basalt clasts (B) within chert (C)

Dolerite intrusion facies

The dolerite intrusion facies has been studied from a unit mapped as the Opaline Well Intrusion by Smithies (1998). The intrusion forms dykes along major faults in the Whim Creek Group. These dykes are up to 400 m in width, and typically trend north–south or (less commonly) east–west. However, the same intrusion forms sills up to 200 m thick that intrude immediately above the Cistern Formation – Rushall Slate contact. They are characterized by blue, vesicular, synsedimentary basalt margins (dispersed basalt facies) and a coarser grained dolerite interior. The different geometries of the sills and dykes may have been caused by the orientation of the component units; the dykes were intruded as subvertical bodies into Whim Creek Group basement, whereas the sills were intruded as horizontal sheets.

Interpretation

Smithies (1998) described gabbro with acicular clinopyroxene and plagioclase, and a finer grained groundmass of interstitial plagioclase, clinopyroxene, quartz, and clay minerals. This texture is interpreted as the result of high-level intrusion, and is consistent with the interpretations given here. Additional lithofacies include dolerite, fine-grained gabbro, and basalt with up to 60% glass that Smithies (1998) described as being petrographically similar to vesicular basalt of the Louden Volcanics. Vesicular basalt is described above from the succession hosting the dispersed basalt facies.

Fine-grained intrusive facies

The fine-grained intrusive facies (*ABtc*) is typically less than 10 m above the transition from the lithic sandstone facies into the shale facies (i.e. stratigraphically above the Cistern Formation – Rushall Slate contact). The fine-grained intrusive facies was mapped as the Comstock Andesite by Miller and Gair (1975). The term Comstock Member is preferred, and the unit is up to 70 m thick (Hickman, 1983), and has a single facies.

The fine-grained intrusive facies is strongly chlorite altered throughout, and also contains a weak schistosity. The facies is entirely coherent, and dominated by chlorite and limonite. The contact with the enclosing sedimentary rocks is very poorly exposed, but is commonly tectonic and planar, with no brecciated facies.

Interpretation

An intrusive origin is inferred based on the complete lack of any primary breccia within the body of the unit, the identical shale-facies rocks both above and below the chloritic basalt facies, and from a comparison with the dolerite intrusion facies sills that also intrude about 10 m above the Cistern Formation – Rushall Slate contact.

Fine- to coarse-grained intrusive facies

The fine- to coarse-grained intrusive facies (too small to be mapped at 1:10 000 scale) comprises fine- to coarse-grained mafic intrusive rock and minor extrusive rocks, with or without olivine. This facies typically forms vertical or subvertival dykes in rocks below the Bookingarra Group, and sills within the Bookingarra Group. Peperite is locally developed where the facies intrudes the Rushall Slate (Fig. 50c).

Interpretation

The fine- to coarse-grained intrusive facies is interpreted to be an intrusive component of the Comstock Member.

Basalt lava association

Basalt breccia and cobble bed facies

The basalt breccia and cobble bed facies (*ABt2*) is characterized by fragments of basalt (similar to basalt in the overlying coherent basalt facies) that form a clast-supported breccia. Individual clasts are dominantly cobble sized, but may be up to 0.5 m long. They are typically elongate and weakly rounded. Plagioclase phenocrysts form up to 10% of each clast and are 2–5 mm in length. Quartz amygdales form a minor component of the basalt (<5%). The matrix material has a fine-grained sand to silt grain size, and is light grey-brown in colour.

In the Salt Creek area (Plate 2c) the basalt breccia and cobble beds facies is mapped as three subfacies: pumiceous, nonpumiceous, and intraclast rich. All three subfacies are characterized by cleaved siliciclastic and mafic volcaniclastic breccia. The pumiceous subfacies contains rare clasts of aphanitic tube pumice, whereas the nonpumiceous subfacies is devoid of pumice. The intraclast-rich subfacies contains coarse-grained, resedimented, angular, shard-rich basalt breccia (hyaloclastic) with up to 10% sandstone clasts.

Coarse-grained, monomictic breccia of the basalt breccia and cobble bed facies is exposed above the contact with the shale facies (MGA 587896E 7700976N) southeast of Salt Creek. The contact with underlying shale and overlying basalt lava is concealed.

Interpretation

The basalt breccia and cobble bed facies is dominated by autobreccia (angular pebble- to boulder-sized clasts) with rare pillow lavas and associated hyaloclastite breccia (angular pebble-sized clasts). Rare pillows with abundant autobreccia and hyaloclastite suggest a subaqueous environment with a relatively low supply rate of lava to the flow front. The similarity between autobreccia clasts and clasts from the basalt breccia and cobble bed facies suggests that basalt clastic material was locally reworked with mud from the underlying shale facies. The facies is dominated by large subrounded basalt clasts within a much finer matrix. The conformably underlying shale facies was formed in deep water, and the coarse-grained component of the basalt breccia and cobble bed facies may have been transported into deep water. Transport may have involved slumping or debris flow, but poor exposure precludes a definitive interpretation.

Massive basalt lava facies

The massive basalt lava facies (*ABt1*) includes dominantly tabular sheets with minor breccia. Smithies (1998) suggested that the entire Mount Negri Volcanics lacks pillow structures, but small amounts of pillow lava and associated breccia are noted from the base of the Mount Negri Volcanics north of Mount Negri, and between Hill Well and Stones Well. A subfacies (the brecciated subfacies) consisting of basaltic breccia, is mapped in the Red Hill area. Pillow breccia generally comprises only a few cubic metres of outcrop, but is exposed in areas of flat topography and may thus be more voluminous than is recognized. Pillows and coarse-grained breccia are illustrated in Figure 53. Pillow lava and breccia are dominated by pebble- to cobble-sized clasts of poorly vesicular basalt with rare boulders. These clasts are similar in size to those of the basalt breccia and cobble bed facies. However, there is no mud matrix, and a finer grained angular basalt breccia (Fig. 53c,d) is common. This clast-rotated breccia is monomict and derived from the same basalt parent as the clasts. Poorly developed pillows grade outwards into the angular breccia.

Interpretation

The massive basalt lava facies is dominated by gently dipping tabular sheets of several metres thickness. Rare breccia and pillow lava throughout the succession suggest an extrusive origin, but the presence of subvolcanic sills is not discounted. Exposure is poor and little internal structure is noted. The facies dominates, but is not restricted to, two areas between Sams Ridge and south of Mount Negri, and between Mons Cupri and Hill Well.

Basalt pebble breccia facies

Basalt rocks of the basalt pebble breccia facies (e.g. around MGA 589153E 7703284N, outside the areas of Plate 1) form poorly exposed subcrop with metre-scale rocky bluffs protruding above the surrounding spinifex. The facies is typified by granule- to cobble-sized, well-rounded clasts on weathered surfaces and coherent lava on fresh surfaces. Two clast sizes are recognized: 4–15 mm, well-sorted, subrounded vesicular or scoriaceous basalt; and large (up to 200 mm) clasts of similar composition. Smithies (R. H., 2000, written comm.) mapped an apparent bomb sag with the original bomb (Fig. 54) in place. Typical clasts are moderately well rounded, and some show increasing vesicularity towards the margin. The recognition of a coherent core to individual blocks

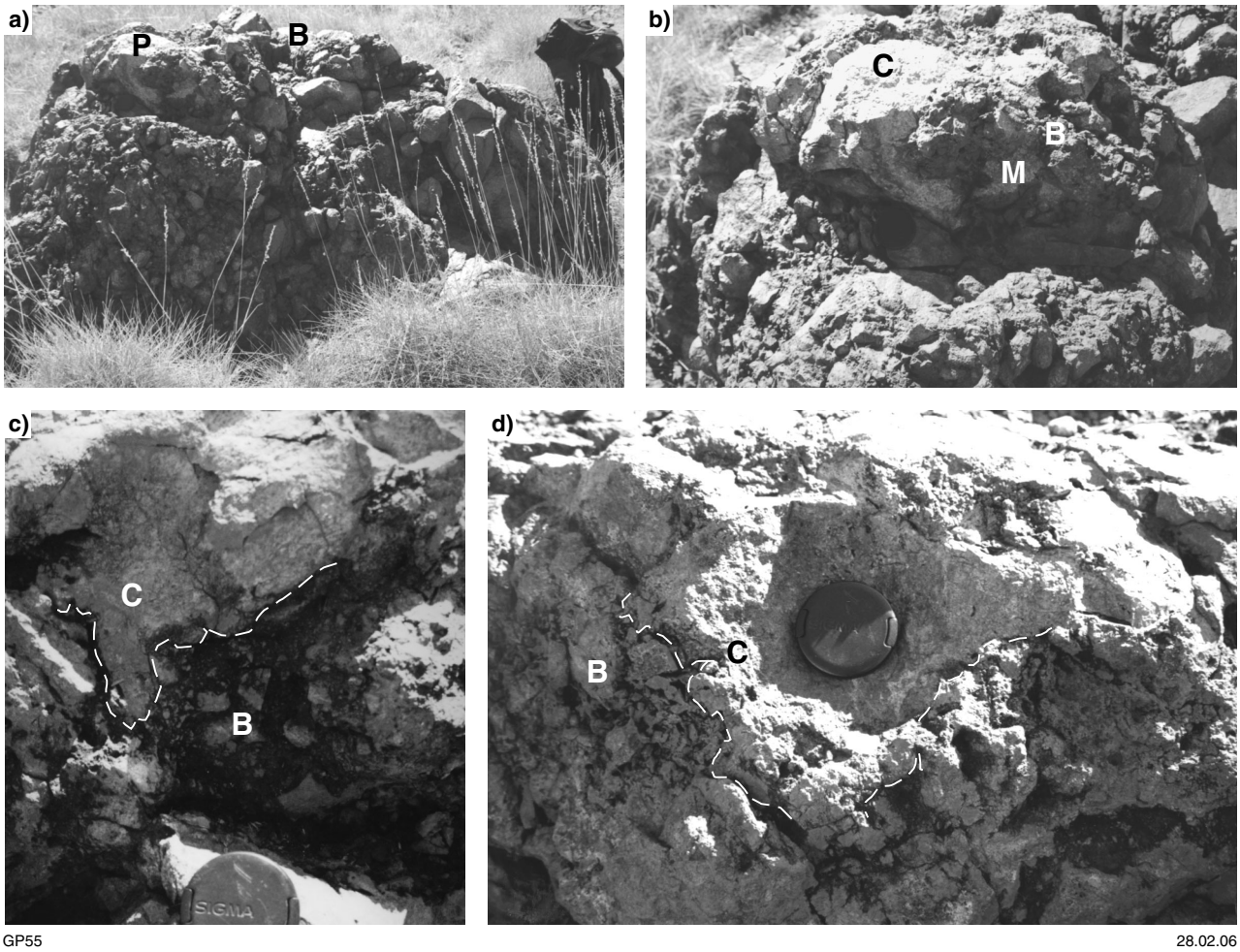

GP55 28.02.06

Figure 53. The massive basalt lava facies (*ABt1*), Mount Negri Volcanics: a) blocky exposure dominated by angular, monomictic basalt breccia (B) and rare pillows (P; MGA 587343E 7702418N); b) close-up of (a) showing a large blocky clast within a finer grained, angular pebble breccia matrix. The large clast (C) has rare brecciated margins (M) that pass outwards into the angular basalt breccia (B). This suggests that the block was hot and continued brecciating in contact with water after dissociation from the parent flow; c) coherent (C) and brecciated (B) basalt apophysis into breccia (interpreted as a pinch structure at the base of a pillow; MGA 578539E 7685655N); d) poorly developed pillow with coherent (C) and brecciated (B) basalt

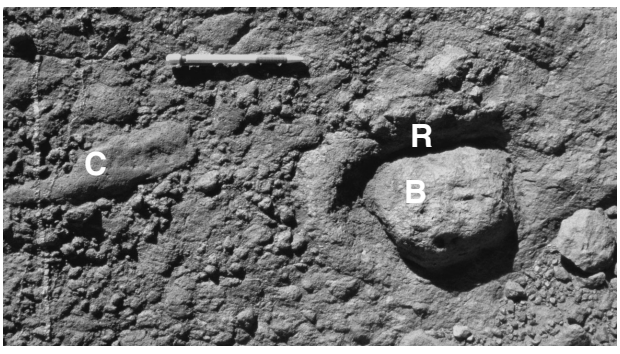

GP56 08.08.05

Figure 54. The basalt pebble breccia facies (MGA 589153E 7703284N), Mount Negri Volcanics, showing a basaltic breccia with irregular clasts (C) of basalt. A single clast interpreted as a bomb (B), due to the raised rim (R), is suggestive of a small impact crater

suggests that weathering preferentially removes the matrix material revealing the larger clasts.

Interpretation

The facies is interpreted as a spatter breccia produced from a fire fountain or more explosive eruption. The facies may represent proximity to a vent, although no other evidence of this vent is noted in the area.

Sheet and pillow basalt lava association

Basalt pillow lava facies

The northern area of the Whim Creek greenstone belt (outside the areas of Plates 1 and 2) contains large areas of Louden Volcanics basalt and associated sedimentary rocks. These rocks are dominated by the basalt pillow lava facies. Some cliff sections display an excellent

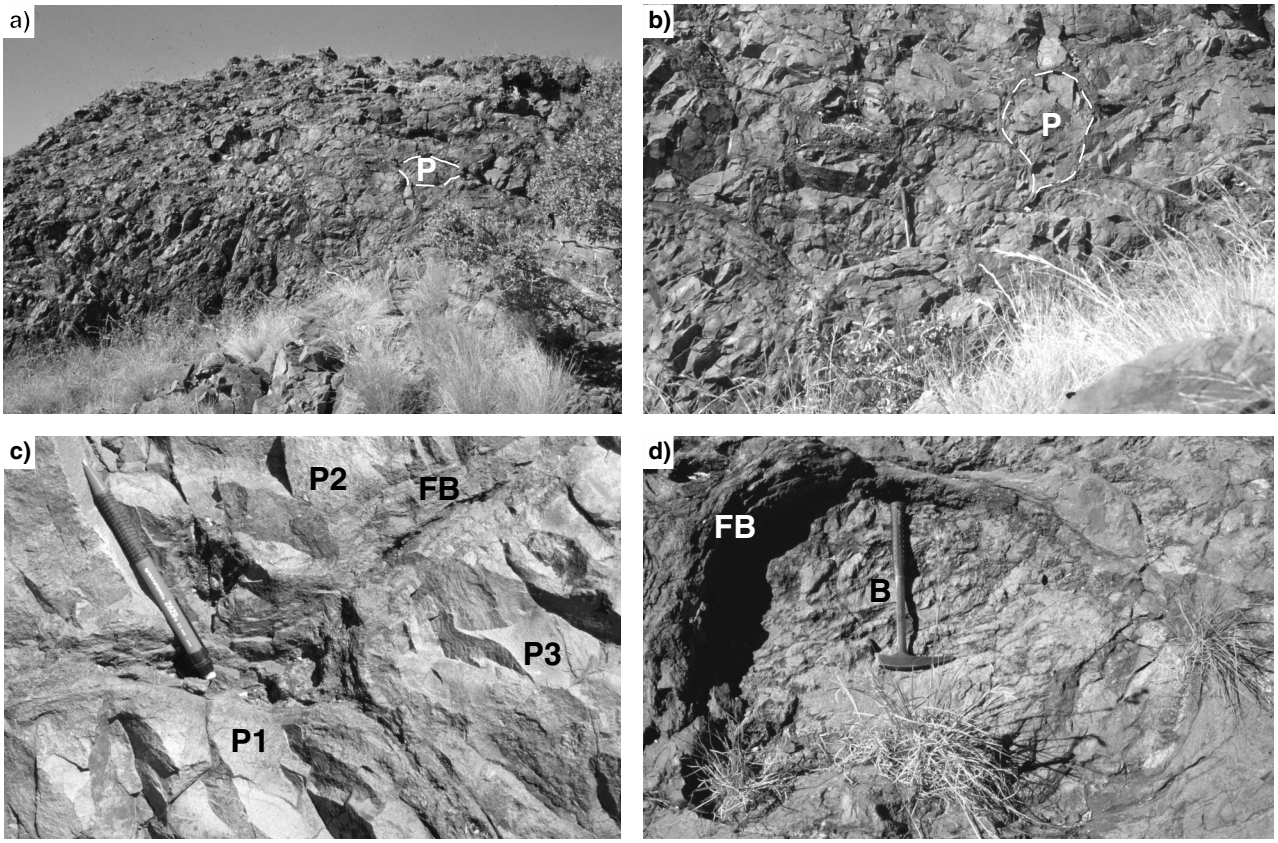

Figure 55. The basalt pillow lava facies, Louden Volcanics. In contrast to the Mount Negri Volcanics, pillow lavas form thick units of more than 10 m thickness, are associated with little or no breccia, and consist of well-formed, large (up to 1.5 m) pillows: a) a thick pile of right-way-up pillows (a single pillow is outlined, P), illustrating the thickness of pillowed basalt (MGA 595245E 7712548N); b) close-up view of (a) illustrating the morphology of individual pillows; c) extreme close-up view of (b) illustrating breccia-free contacts between pillows. P1, P2 and P3 are individual pillows and the margin contains a foliated basalt (FB). This is interpreted as a flow banding caused by the shear at the cooling plastic margins of individual pillows (P); d) close-up view of a weathered pillow (MGA 595469E 7712690N), in which the foliated pillow margin (FB) is less weathered than the centre of the pillow (B)

cross section through pillow lava sets (Fig. 55) that are generally subhorizontal and the correct way up. Pillow basalt units are at least 10 m thick in some sections, but incomplete exposure suggests much greater thicknesses. Pillow basalt units are laterally extensive over hundreds of metres. Pillows are interlocking and elongate, and characteristically have no interpillow breccia. Abundant vein quartz is noted between some pillows, and represents pore spaces (1–10 cm diameter) that were present after emplacement. This suggests that very little primary breccia was associated with pillow formation. The largest pillows are up to 1.5 m in diameter and variable in shape, but generally ovoid. Pillow margins are concentric rims 1–10 cm thick that show weakly scoriaceous textures or an abundance of about 10 mm lithophysae around spherical quartz amygdales. Pillows may partially merge, suggesting that the hot margins annealed immediately after emplacement.

Interpretation

The abundance of pillow lava in the north of the Whim Creek greenstone belt suggests that the area was entirely subaqueous at the time of deposition. Pillow formation was not associated with significant autobrecciation or quench fragmentation, and this suggests that the pillows were isolated from the water body by a stable vapour film (Mills, 1984).

Basalt sheet lava facies

The basalt sheet lava facies (*ABe1*) dominates the entire southern limb of the Whim Creek greenstone belt. Sheet-like, tabular basalt units of between 1 and 5 m thickness dominate the facies, and are associated with subordinate primary breccia. Figure 56a illustrates the tabular, gently dipping nature of the facies. In this locality abundant primary breccia overlies tabular coherent basalt. The breccia is angular and comprises granule- to pebble-sized, monomictic, jigsaw-fit clasts (Fig. 56b,c). The matrix to these breccias is white and more strongly altered than the clasts. Many examples are spinifex textured, with randomly oriented blades of 1–5 cm pyroxene-spinifex crystals.

Interpretation

The jigsaw-fit primary breccia is basalt hyaloclastite and indicates an extrusive subaqueous origin for much of the

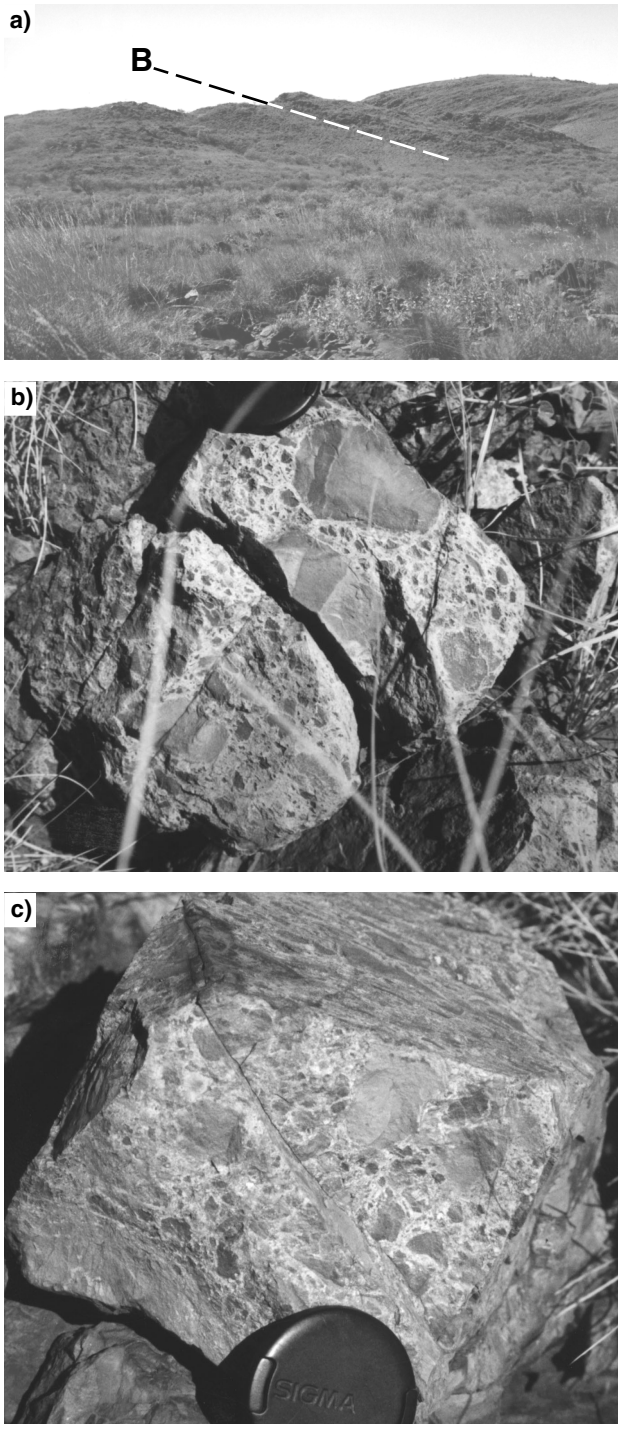

Figure 56. The basalt sheet lava facies (*ABe1*), Louden Volcanics, near Stones Well: a) outcrop of the basalt sheet lava facies illustrating gently south-dipping, tabular lava sheets (from MGA 5 83065E 7 6 65538N, looking west). The layering of the lava is parallel to regional south-dipping bedding (B); b and c) boulders of basalt hyaloclastite, Louden Volcanics (both from MGA 5 82028E 7 6 86224N)

basalt sheet lava facies. It probably represents an extrusive equivalent of the basalt pillow lava facies, perhaps related to the rate of magma emplacement.

Quartz-rich sedimentary rock association

Coarse- to fine-grained sandstone and granulestone are associated with subcrop of shale-facies rocks in the north of the Whim Creek greenstone belt, and entirely outside the areas of Plates 1 and 2. Fine-grained sandstone, siltstone, and shale typically form extensive subcrop or calcretized outcrop, and may be more extensive than mapped by Smithies (1998).

Quartzite and black chert breccia facies

The quartzite and black chert breccia facies typically forms lensoidal outcrop of 10–50 m strike length and 1–5 m thickness, although mappable units of several tens of metres thickness are also recognized. The characteristic rock type of the quartzite and black chert breccia facies is a coarse-grained sandstone-pebble breccia dominated by two main clast types: quartz and black chert. Plutonic quartz is dominant and forms grains 1–5 mm in size that make up more than 90% of the rock. Quartz grains are typically subangular and 1–5 mm in diameter (Fig. 57a). The original grains were probably subrounded and well sorted. Black chert clasts in the coarse-grained sandstone are similar in quantity, size, and shape to the quartz grains. However, the granule- to pebble-sized fraction of the rock is dominated by black chert. Typical clasts are subrounded and up to 20 mm. A few have a fine internal lamination that suggests a sedimentary origin. Bedding-discordant quartz veins within chert clasts show that the chert was lithified and subject to at least one deformation before uplift and erosion. The quartzite is compositionally a quartz arenite and displays crude, diffuse planar lamination defined by the elongation of black chert clasts. No imbrication is noted, but Smithies (R. H., 2000, written comm.) recorded trough cross-bedding within the facies. In thin section (Fig. 57a), grains are dominated by quartz with lesser chert and subordinate vein quartz. Most quartz grains show straight extinction and some show undulose extinction in distinct bands, suggestive of a single compressional event. Quartz grains typically show sutured contacts without any evidence of a finer grained matrix material.

Interpretation

The quartzite and black chert breccia facies is interbedded with the basalt pillow lava facies, and was deposited within a subaqueous environment. The lack of any debris finer than coarse-grained sand indicates high-energy transportation conditions. Diffuse planar bedding suggests that aggradation rather than mass freezing of debris flows was the dominant depositional mechanism. Some exposures display lensoidal geometry suggestive of topographic control, perhaps within subaqueous channels. The recognition of trough cross-beds suggests rapid input of large volumes of sediment under high-energy conditions, and is entirely consistent with the lack of fine-grained matrix. Hence, the best model involves localized, subaqueous channel-controlled flows of sediment that must have been derived from outside the depositional basin, because they contain no basaltic debris.

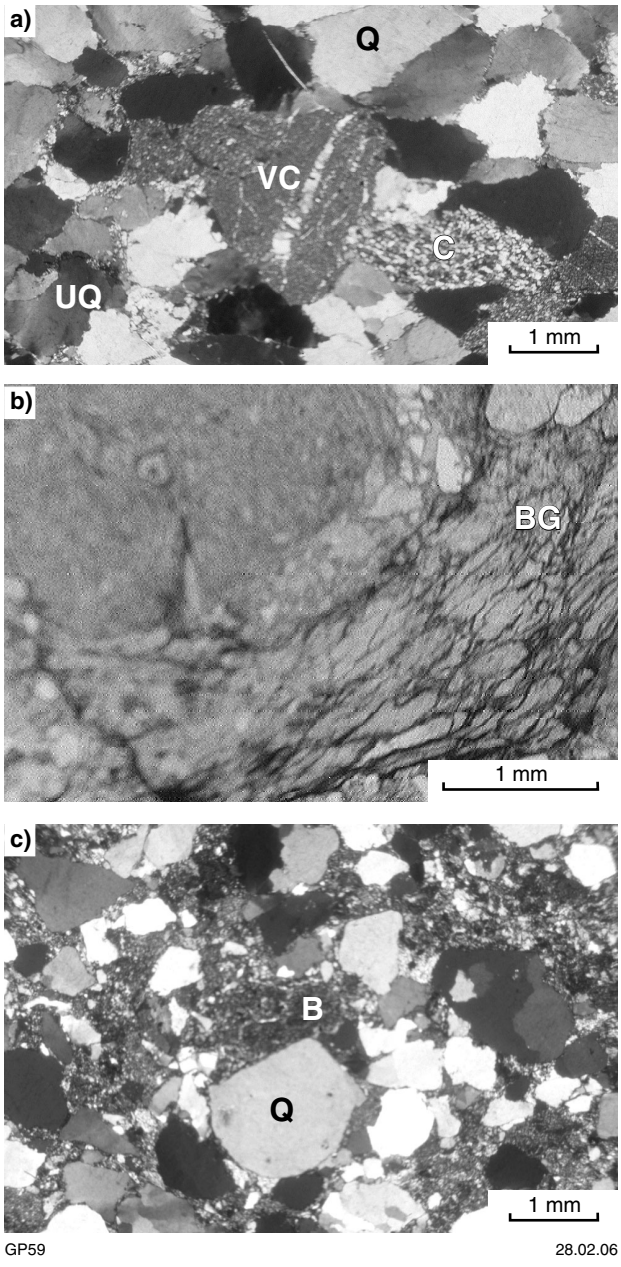

Figure 57. Photomicrographs of sedimentary facies of the Louden Volcanics (cross-polarized light): a) the quartzite and black chert breccia facies (outcrop northwest of MGA 595839E 7709056N). A single clast of quartz-veined chert (VC) is in the centre and other chert clasts (C) are also present. Quartz grains are the most abundant component and include those with undulose extinction (UQ) and straight extinction (Q). Overall, the facies is dominated by quartz and siliceous components with no fine-grained matrix. The grains show typically sutured contacts; b) the matrix of the basalt conglomerate facies (MGA 593281E 7712603N). The clast labelled BG in the bottom right is chloritic and very fine grained, and is interpreted as a clast of basalt glass; c) the dominant basalt (B) and quartz components of the matrix of the basalt conglomerate facies (MGA 593281E 7712603N)

Cross-laminated sandstone facies

Poorly exposed, calcretized fine-grained sandstone is commonly associated with the quartzite and black chert breccia facies, and forms extensive subcrop. The characteristic features of the cross-laminated sandstone facies include tabular, 1–10 mm laminae of considerable (metre-scale) lateral extent. A variety of cross-laminae are seen. High-angle, concave-up cross-laminae are relatively common, but low-angle foresets of less than 5° are more common. The association of the cross-laminated sandstone facies with the quartzite and black chert breccia facies suggests that the two formed in a similar depositional environment.

Interpretation

The finer grain size of the cross-laminated sandstone facies compared to the quartzite and black chert breccia facies suggests that differences between the two may be related simply to the energy of depositional currents. No compositional estimate of the facies is given due to the very poor subcrop, but the facies contains abundant quartz with carbonate cement and is typically well sorted.

Basalt conglomerate facies

Rare exposure of the basalt conglomerate facies (Fig. 58), adjacent to the Sholl Shear Zone and east of Government Well, is dominated by massive pebble to cobble conglomerate with some more angular clasts. The total thickness of the single unit is unknown, but of the order of tens of metres. The following clast types are recognized:

- aphanitic basalt, subrounded, pebble to cobble size (50%);
- vesicular basalt, typically subrounded, pebble to cobble size (25%);
- spinifex-textured basalt, very irregular angular clasts (5%);
- subrounded grey chert (5%);
- hematitic, weakly scoriaceous basalt (5%);
- vein quartz (5%);
- elongate, diffuse, planar-bedded, dark-grey sandstone (grey sandstone facies, 5%).

Rare clasts of aphanitic or spinifex-textured basalt are elongate and irregular in shape. Their angular margins show little or no evidence of significant transport. The facies is clast supported, with about 80% clasts in a matrix of subangular, fine- to medium-grained, quartz-rich sandstone. It is interbedded with thin, laterally discontinuous quartz-rich sandstone of the grey sandstone facies. Dark-grey quartz grains may also be present in the matrix. In thin section (Fig. 57b,c) the matrix grains include abundant quartz that is similar to that of the quartzite and black chert breccia facies, as well as finer grained equivalents of the basaltic clasts noted above.

Interpretation

The basalt conglomerate facies has a mixed provenance with allochthonous quartz-rich debris and large basalt clasts (both juvenile and epiclastic) derived from the Louden Volcanics. Much of the basaltic material was

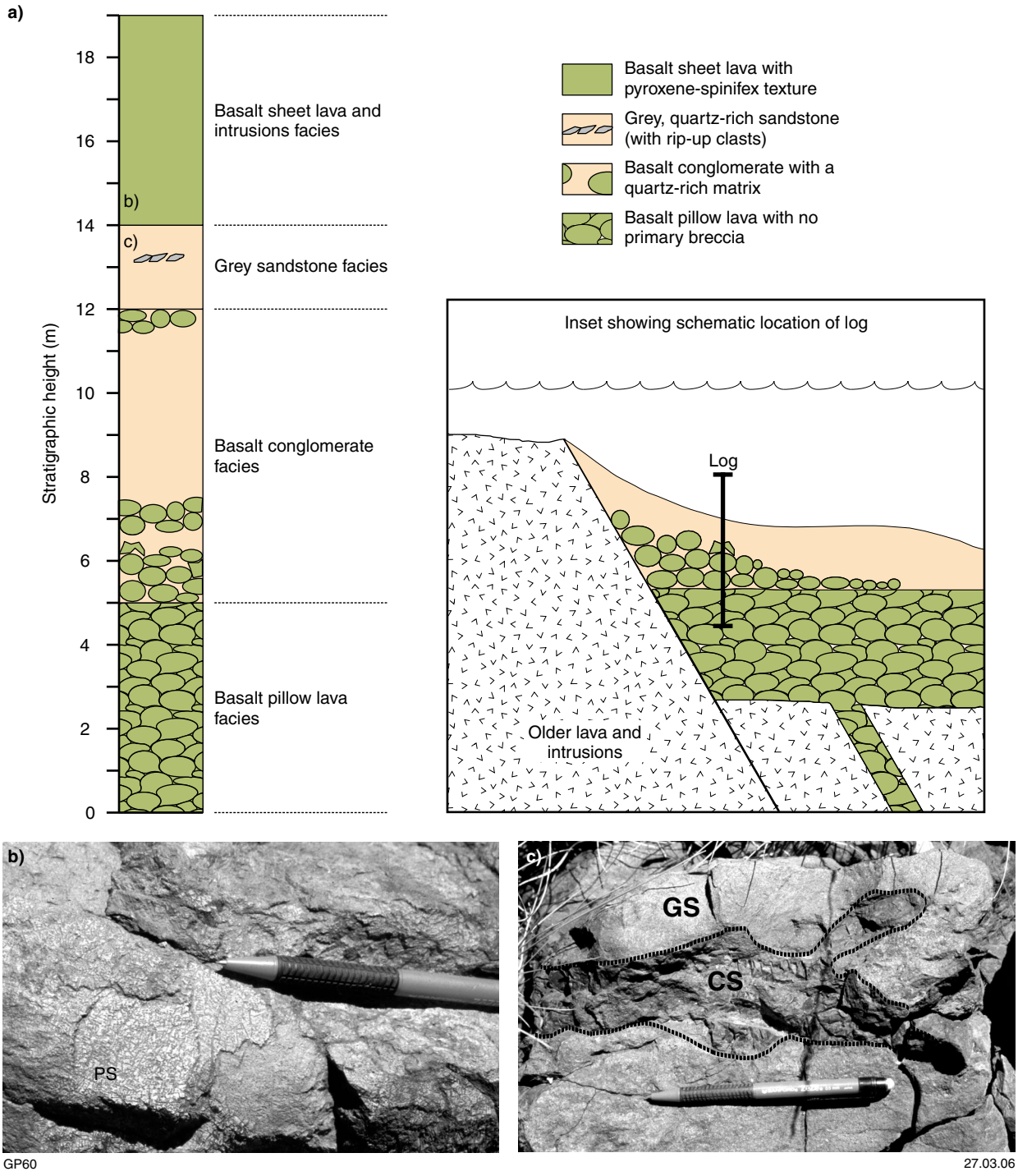

Figure 58. Features of the Louden Volcanics north of Mount Negri: a) schematic log compiled from outcrops of sedimentary rocks of the Louden Volcanics; b) outcrop of pyroxene-spinifex-textured basalt; c) outcrop of coarse-grained sandstone from the grey sandstone facies (GS), showing a siltstone rip-up clast (CS)

rounded in a subaerial or shallow subaqueous environment before redeposition, suggesting the presence of an elevated block or topographic high. The facies is restricted to a linear band along the Shear Sholl Zone, which indicates that this feature controlled deposition. The simplest model is that the Shear Sholl Zone underwent a phase of south-block-down movement (± strike-slip movement) with basalt clasts derived from the north and/or laterally from the east or west. The lack of basement lithics (Whundo Group, Whim Creek Group, granite) within the basalt conglomerate facies is more consistent with an extensional or transtensional fault movement with basalt clasts of intrabasinal origin. Angular irregular basalt clasts also indicate that volcanic activity and sedimentation were approximately coeval. The facies is interpreted as a subaqueous fanglomerate that developed on the

hangingwall block of the Shear Sholl Zone adjacent to a shallow-water or subaerial (or both) footwall block to the north.

Grey sandstone facies

The grey sandstone facies is poorly exposed and typically interbedded with the basalt conglomerate facies. It is of limited thickness (up to a few metres) and lateral extent, but may be of use as a marker horizon due to its distinctive clast composition. The facies is a sublitharenite, and is dominated by volcanic quartz with a very distinctive dark-grey or black colour giving the whole rock a dark-grey colour. These grains are typically well sorted and subangular, and clast size fines upward in some localities. Hematitic siltstone with silica-replaced pyrite cubes forms large (~5 cm) intraclasts (Fig. 58c). The tapered irregular ends of these clasts suggest that they may be rip-up clasts, indicating an upstream, anoxic, low-energy environment with intermittent erosive currents.

Interpretation

The grey sandstone facies is associated with the upper margin of basalt conglomerate facies, but represents a much lower energy deposit. Rip-up clasts suggest that depositional currents were erosive upstream, and capable of transporting large (centimetre-scale) fragments. The source was rich in an unusually dark, crystalline quartz. Upward-fining packages suggest aggradation of the grey sandstone facies from turbidity currents.

Kialrah Rhyolite

The Kialrah Rhyolite (exposed outside the areas of Plates 1 and 2), described by Hickman (1997, 2000) and Hickman and Smithies (2001), is a flow-banded, porphyritic rhyolite that Hickman (2000) placed stratigraphically above the Louden Volcanics. Hickman and Smithies (2001) suggested that the contact between the two units is not observed, but that the Kialrah Rhyolite either intrudes or overlies the Louden Volcanics, and is thus younger. The recognition of spherulitic texture, caused by devitrification of glass (Hickman and Smithies, 2001) suggests that the Kialrah Rhyolite is an extrusive or high-level intrusive unit. The Kialrah Rhyolite outcrops west of the Red Hill area over a strike length of about 5 km. The thickness of the unit is unknown.

Probable Bookingarra Group facies at Salt Creek

In the Salt Creek area Smithies (1998) mapped metamorphosed tuffaceous felsic volcanic rock, fine- to coarse-grained felsic volcaniclastic rock, and andesite to dacite with thin metabasaltic flows and sills (Fig. 59). These rocks are very similar in composition and facies to rocks of the Bookingarra Group, and are correlated. An additional facies, the quartz-phyric rhyolite, is tentatively assigned to the siliciclastic and felsic volcanic association (Table 7).

Siliciclastic and felsic volcanic association

Quartz-rich sandstone facies

Coarse-grained sandstone and granule beds of the quartz-rich sandstone facies (*ABc2*) are interbedded with and underlie the lithic sandstone facies (*ABc3*), but are also assigned to the Cistern Formation (Table 5). In the Salt Creek area the facies is divided into five subfacies: volcaniclastic, arkosic, interbedded, fine-grained, and granulestone. The volcaniclastic subfacies consists of massive quartz-rich granulestone containing larger shards of basalt in a mudstone matrix, whereas the granulestone subfacies consists of subrounded quartz grains and lithic grains. The arkosic subfacies includes variable amounts of feldspathic grains, whereas the fine-grained subfacies, although also locally arkosic, is distinguished by its generally finer grain size, and a silty and chloritic composition. The interbedded subfacies is composed of alternating beds of quartz-rich sandstone and clay-rich mudstone, at about 10 cm intervals.

The quartz-rich sandstone facies may contain up to 10%, up to 3 mm, spherical, subangular quartz grains within a quartz-dominated, poorly sorted matrix. Feldspar and chloritic (?originally mafic lithic) grains form a minor component of the facies, and the rock is essentially a sub-arkose to sublitharenite. The quartz is dull and light grey in colour, suggesting a plutonic source. Bedding is absent except in the interbedded subfacies.

Interpretation

The quartz-rich sandstone facies indicates a chemically mature sedimentary component, and abundant subangular grains suggest that the sediment was chemically mature, but physically submature. In this aspect the facies is similar to the quartzite and black chert breccia facies, and may indicate the presence of a chemically corrosive atmosphere. The facies is commonly altered to quartz–sericite(–chlorite), and this alteration is particularly intense around the quartz-phyric rhyolite facies.

Lithic sandstone facies

The lithic sandstone facies (*ABc3*) comprises medium- to coarse-grained sandstone of the Cistern Formation (Table 5). Sedimentary structures are not known to have been preserved; they may have been destroyed by the development of the structural fabric. Grains are dominantly (70%) dark-green to grey chlorite that appears to replace mafic lithic grains, and the facies thus contains (mafic) lithic arenite. Feldspathic grains (20%) are white and typically have diffuse margins. Quartz is a minor component and forms less than 10% of the facies. The lithic sandstone facies is spatially associated with the quartz-rich sandstone facies (granulestone subfacies) and appears to become more quartz rich and less chloritic upwards. The source was most probably a region dominated by mafic rocks, although lesser felsic material was also present. The facies is interbedded with the base of the cleaved mudstone facies, and also forms isolated outcrops.

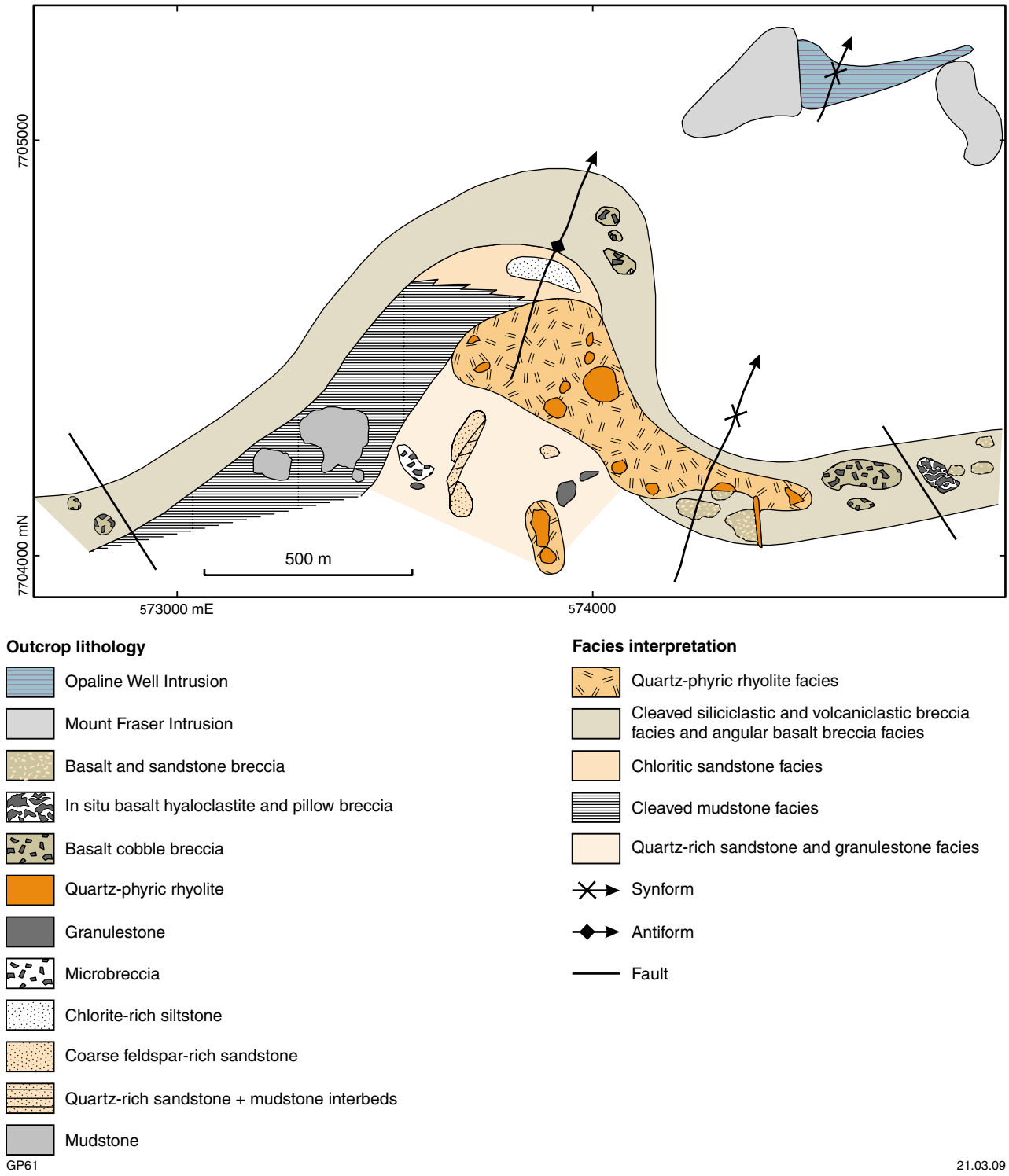

Figure 59. Simplified geological map of the Salt Creek area. Arrows indicate gently northeast-plunging synforms and antiforms. The succession is right-way-up based on a subvolcanic dyke in the quartz-phyric rhyolite facies, as well as the upward fining of the succession and similarity to the Mons Cupri and Good Luck Well successions. Krapez and Eisenlohr (1998) suggested that the succession is exposed in an antiformal syncline, but the present study found no evidence to support that interpretation

Interpretation

Mafic sandstone grading upwards into a clay-rich facies is analogous to the contact between the lithic sandstone facies and the shale facies south of the Whim Creek mine site (see **Siliciclastic-dominated sedimentary rock association, Shale facies**).

Cleaved mudstone facies

Fine-grained units such as the cleaved mudstone facies (not separately mapped at 1:10 000 scale; Table 5) are highly deformed, and preserve two strong cleavages that result in a strong rodded fabric (Fig. 60). Outcrop may be subdivided into 5–20 mm siliceous zones that are lensoidal in shape, and more abundant (70%) clay- or mica-rich foliated material. The siliceous lenses are light blue to dark green-blue, depending on the abundance of chlorite. The clay-rich foliated material is brown when weathered, but purple along cleavages, again due to chlorite alteration. Rare examples show a granular texture indicating that they originally contained some fine-grained sand- or silt-sized material.

Interpretation

The facies represents a deformed mudstone with interbeds of silt or fine-grained sand. No other structures are preserved within the facies. The clay-rich composition and stratigraphic position above mafic and quartz-rich sandstone suggest that these rocks may be lateral equivalents of the shale facies (Rushall Slate; Table 5).

GP62 28.02.06

Figure 60. Typical exposure of the cleaved mudstone facies from the Salt Creek area (MGA 573589E 7704573N). The facies typically contains two intersecting cleavages that result in a strong rodded fabric. Strong deformation and alteration typically mask sedimentary structures

Quartz-phyric rhyolite facies

The quartz-phyric rhyolite facies (*ABtrf*; Table 7) is typically strongly sericite altered with minor chlorite along cleavages. The facies preserves abundant 5–10 mm spherulites and lithophysae cored by quartz phenocrysts (volcanic, bipyramidal) or 3–4 mm quartz amygdales. Amygdales are ubiquitous and form up to 25% of the facies. One outcrop shows a thin (centimetre-scale) unit that appears to crosscut stratigraphy at 90° to inferred bedding.

Interpretation

The quartz-phyric rhyolite facies is clearly either volcanic or a high-level intrusion, but the preserved outcrop does not favour either interpretation. Crosscutting relationships suggest the presence of a small dyke, and the abundance of amygdales throughout the facies suggest that this could be a synsedimentary dyke feeding effusive felsic volcanism.

Basalt volcaniclastic association

Cleaved siliciclastic and volcanic breccia facies

Commonly, the cleaved mudstone facies (Table 5) passes upwards into a breccia with abundant dark clasts, which is called the cleaved siliciclastic and volcanic breccia facies (Table 7; Fig. 61), and assigned to the Mount Negri Volcanics, but not mapped separately on Plate 2c (Salt Creek). The matrix is similar to the cleaved mudstone facies, and clasts are typically flattened and strongly elongate in one direction to around 10 cm length. However, the clasts are rarely greater than 5 mm in thickness, suggesting that either they were originally elongate or, more likely, that they have been subsequently subjected to high strain. The clasts are dark brown, and may contain abundant hematite. No internal structure is noted except for the development of a strong cleavage and rare feldspathic zones, both of which are attributed to deformation. The clasts were originally suspended within the matrix and formed 10–40% of the total volume. Clast-poor examples at the gradational contact with the cleaved mudstone facies reflect the upward increase in the proportion of clasts that were supplied to the basin. Rare examples contain a light-coloured, strongly cleaved clast type that may be tube pumice. In thin section, clasts are chlorite-altered and angular, with wispy apophyses and terminations. All clasts are vesicle poor, but a single clast (Fig. 61e) contains a relic plagioclase phenocryst.

Pebble to cobble breccia containing abundant (40–95%) clasts east of the area contains a matrix of coarse-grained, quartz-rich sands similar to the quartz-rich sandstone facies. However, within these coarser grained rocks the deformation is considerably lower and the clasts appear to be moderately vesicular in places with 1–3 mm rounded amygdales. The clasts are very angular and show no signs of significant transport. They are interpreted to represent quench breccia from basalt volcanism.

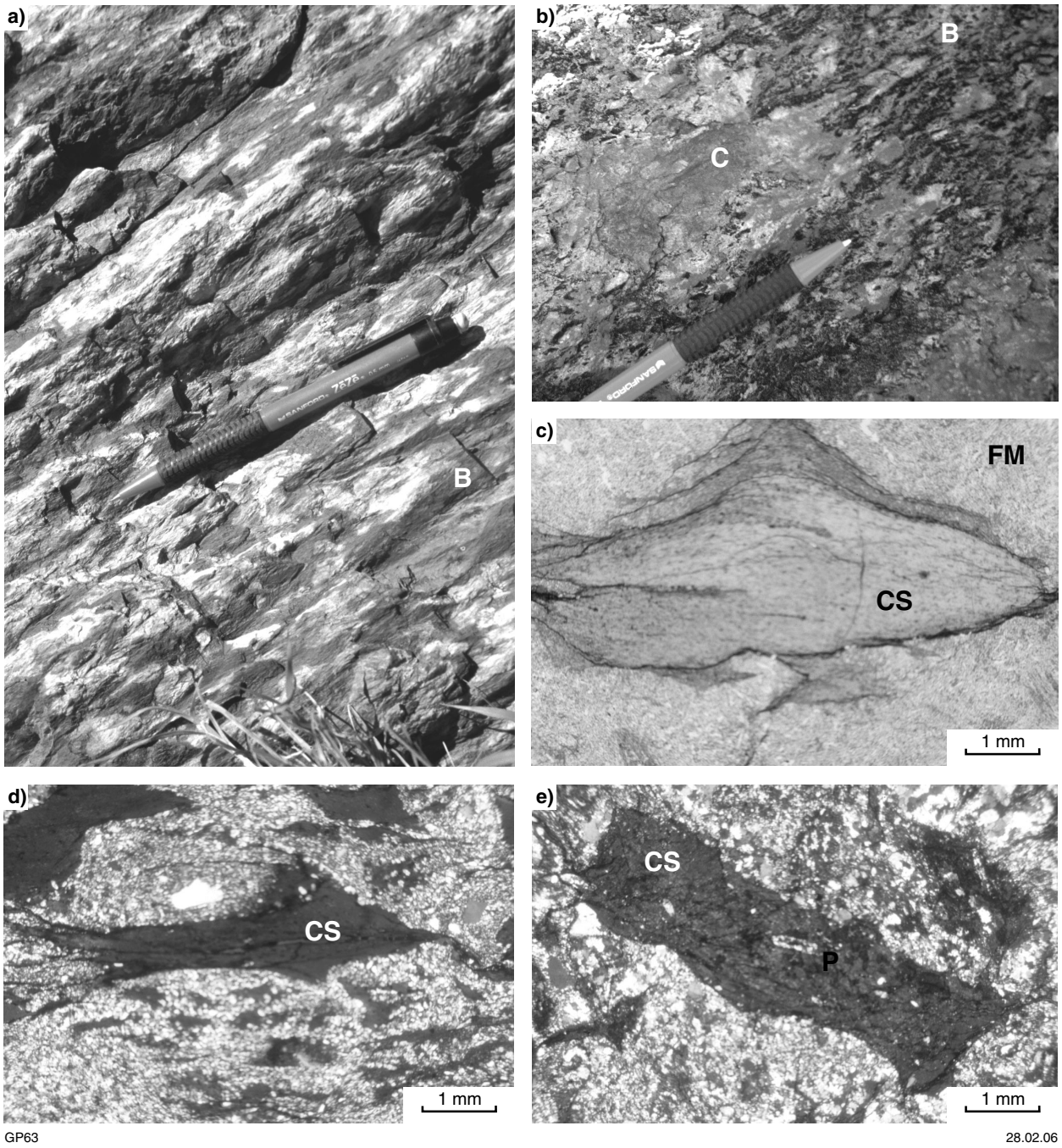

Figure 61. Facies of the Bookingarra Group, Salt Creek area (see Table 7): a) the cleaved siliciclastic and volcanic breccia facies with angular, dark-grey basalt clasts (B) apparently floating within a fine-grained, quartz-replaced matrix material (originally siltstone; MGA 572063E 7704343N); b) angular basalt (B) breccia facies, showing coherent (C) wispy material within a dominantly angular, brecciated, hyaloclastite matrix; c to e) very angular, dominantly aphanitic, chlorite-altered shards (CS) within a fine-grained, quartz-rich matrix (FM). A single shard (e) contains a relic plagioclase phenocryst

Interpretation

The association of basalt breccia with sedimentary rocks shows that deposition of coarse-grained and fine-grained sediments was coeval, with the coarser grained material being deposited to the east. The basalt clasts were probably produced by quench fragmentation of a basaltic lava because they are extremely angular and very fine grained (originally glassy) with few vesicles or amygdales. The association of basalt clasts and clay-rich matrix is analogous to the basalt breccia and cobble bed facies from the area south of Mount Negri. An important difference, however, is that the clasts from the cleaved siliciclastic and volcanic breccia facies were not significantly reworked before redeposition. The abundance of matrix and presence of 'floating clasts' suggest a debris-flow origin, perhaps generated by oversteepening of a clastic pile during basalt volcanism.

GP64 28.02.06

Figure 62. Basalt clast-rich breccia from the angular basalt breccia facies, Bookingarra Group, Salt Creek area (MGA 574825E 7704387N)

Angular basalt breccia facies

Abundant basaltic breccia (Fig. 62) of the angular basalt breccia facies is exposed east of the cleaved siliciclastic and volcanic breccia facies, and not mapped separately on Plate 2c. The facies contains pebble- to cobble-sized clasts that are very angular and show little evidence of transport. They are very similar to clasts in the cleaved siliciclastic and volcanic breccia facies. The angular basalt breccia facies contains rare examples of irregular, apparently intrusive basalt into the breccia (Fig. 61b). Much of the breccia is clast rotated, but the intrusive coherent basalt suggests that in situ basalt is probably nearby, but unexposed.

Interpretation

The facies is interpreted as both in situ and clast-rotated hyaloclastite. It may be a component of the Mount Negri Volcanics because the Louden Volcanics is characteristically free of hyaloclastite.

Geochemistry

A geochemical investigation of selected lithofacies from the Whim Creek greenstone belt was undertaken to assist in constraining the tectonic environments during deposition of the Whim Creek and Bookingarra Groups. Summary interpretations of the resulting data are outlined below, and further discussed later in this Report (see **Basin evolution**).

Geochemical sampling — methodology and data

Geochemical analysis of coherent, relatively unaltered volcanic lithofacies undertaken on samples collected during April–June 1999 comprised 36 analyses of volcanic rocks from the Whim Creek Group and a single analysis of granite. Additional data from GSWA are incorporated into many plots. The new samples were analysed for 11 major element oxides and 42 trace elements (<0.1 wt%), and data are presented in the Appendix.

Samples from the Whim Creek Group include aphanitic and plagioclase-phyric basalt of the Warambie Basalt, the rhyodacite pumice breccia facies of the Red Hill Volcanics, and three lithofacies of the Mons Cupri Dacite Member: spherulitic dacite, feldspar-phyric dacite, and grey dacite. The granite sample is from granite that intruded the basal unconformity.

Element mobility in the Whim Creek greenstone belt may be attributed to interaction of magma or hot volcanic rock with lake water or seawater, greenschist-facies metamorphism, late alteration by silica- or carbonate-rich fluids (or both) or weathering. Alteration assemblages of sericite, chlorite, carbonate, and quartz locally overprint primary mineralogy, but MgO, $FeO_{(total)}$, TiO_2, and Al_2O_3 show consistent trends against silica suggesting relative immobility (Fig. 63). Mobile elements include alkalis (K_2O and Na_2O), and normalized multi-element diagrams (Fig. 64) show likely mobility of Rb, Ba, and Th. In this study, relatively immobile elements include TiO_2, MgO, $FeO_{(total)}$, Al_2O_3, and the rare earth elements (REE), including Ta, Nb, Ce, Zr, Y, and Sc.

Classification plots for ancient rocks use elements that may be considered immobile under a range of crustal or surface conditions. Winchester and Floyd (1977) showed that a plot of Zr/TiO_2 versus Nb/Y (Fig. 65) is useful in the classification of ancient rocks. The Mons Cupri Dacite Member samples plot as rhyodacite–dacite, as do the Red Hill Volcanics pumice breccias. The Warambie Basalt shows two distinct groups that are classified as 'andesite basalt' (basaltic andesite) and subalkaline basalt. SiO_2 values for sampled lithofacies are generally higher than would be expected from the classification of Winchester and Floyd (1977). The interpretation is that the silica content of all sampled lithofacies has increased after deposition due to replacement by silica-rich fluids or depletion of other major elements (e.g. Na_2O, K_2O) or both.

Tectonic discrimination from the Whim Creek Group

Warambie Basalt

Barley (1987) classified the Warambie Basalt rocks from the Red Hill area as tholeiitic basalt. The plagioclase-phyric lithofacies suggests that the parent magma was silica saturated, and that a tholeiitic interpretation is valid. The basalt samples show enrichment of K_2O, Rb, Ba, Th, and Ce with respect to MORB (mid-ocean ridge basalt; Fig. 64), and these elements may suggest either derivation from primitive mantle (i.e. mantle that was not depleted in alkali, alkali earth, and high field-strength elements — HFSE), or assimilation of continental crust or melt. Winchester and Floyd (1977) suggested subdivision into

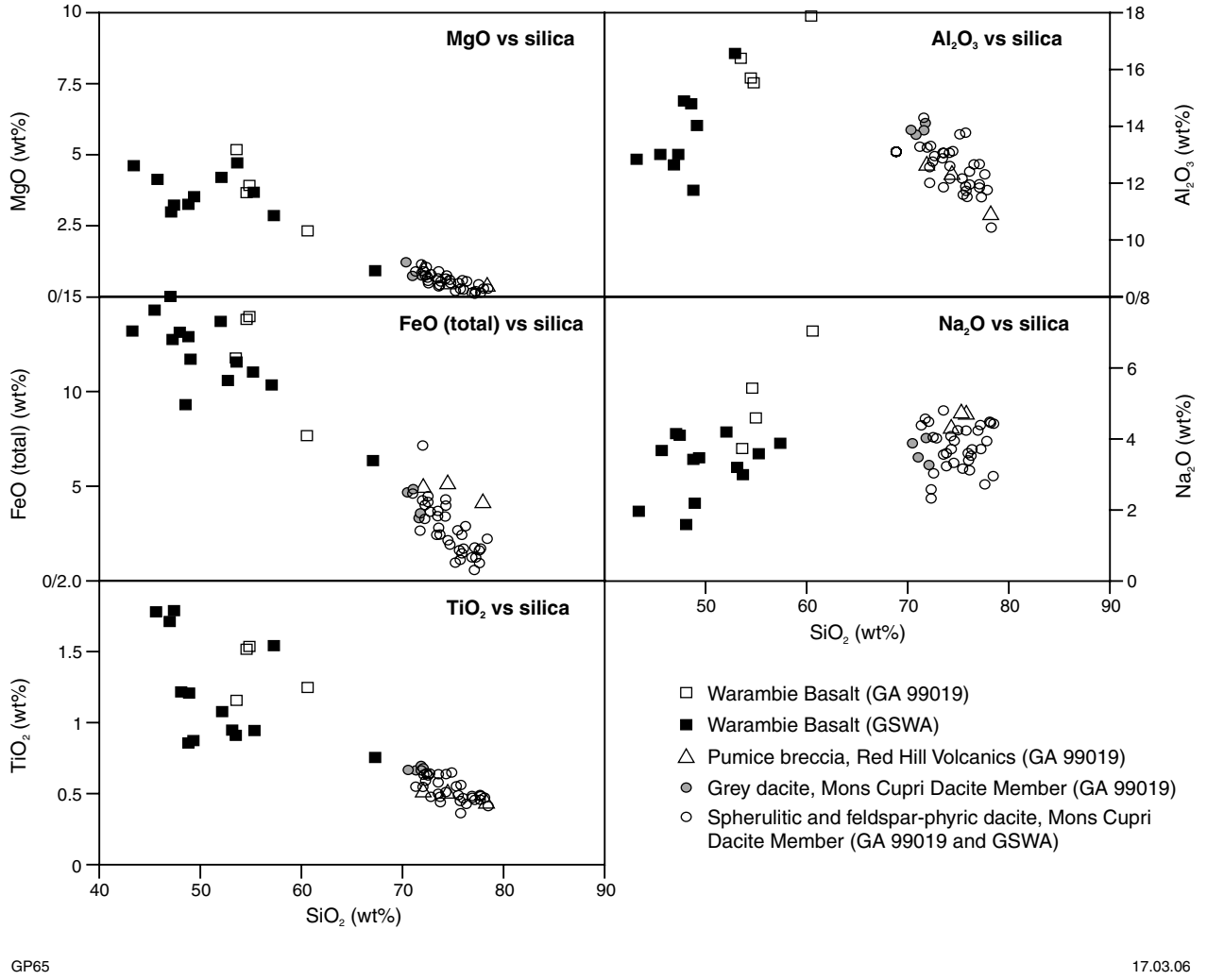

Figure 63. Summary of major element geochemistry of the Whim Creek Group (Geoscience Australia and GSWA data are fully referenced in Pike, 2001)

high P_2O_5/low Zr (alkalic) and low P_2O_5/high Zr (tholeiite) basalt. The Warambie Basalt samples are relatively low in both P_2O_5 (wt%) and Zr (ppm), but are clearly classified as tholeiitic.

Tectonic discrimination diagrams for basaltic rocks from Cabanis and Lecolle (1989), Meschede (1986) and Mullen (1983) are presented as Figure 66. These plots classify the Warambie Basalt samples as follows: volcanic-arc calc-alkali basalt (Cabanis and Lecolle, 1989), within-plate tholeiite – volcanic-arc basalt (Meschede, 1986), and island-arc tholeiite (Mullen, 1983). Consequently, the Warambie Basalt samples appear to have a tholeiitic arc signature, but are more enriched in elements such as the light rare earth elements (LREE, La) suggesting some transitional calc-alkaline character. In order to characterize the trace element anomalies, the samples are plotted on a multi-element diagram (Fig. 67) normalized to a tholeiitic arc basalt (from Kamenetsky et al., 2001). The components K_2O, Rb, Ba, Th, Nb, Ce, P_2O_5, Zr, Sm, TiO_2, Y, and Yb all show enrichment relative to tholeiitic arc basalts. In some cases this may be due to alteration effects (e.g. Rb, K_2O), but most elements show consistently high values that indicate an enriched melt. In particular, Rb, Th, Nb, Zr, and Ce show strong enrichment and are elements concentrated in continental crust. The Warambie Basalt is thus described as enriched tholeiitic basalt lava.

Mons Cupri Dacite Member

The Mons Cupri Dacite Member comprises lithofacies with distinctive silica contents (spherulitic dacite 78 wt% SiO_2, feldspar-phyric dacite 75 wt% SiO_2, and grey dacite 72 wt% SiO_2), although these values have probably been enhanced by alteration and metamorphism. Trace element data (Fig. 65) suggest that all samples were originally rhyodacite or dacite, with the grey dacite having the more mafic composition. Barley (1987) described felsic rocks of the Mons Cupri Dacite Member as 'calc-alkaline'. The trivariant plot of Al_2O_3 versus $Fe_{(total)}$ + TiO_2 versus MgO of Jensen and Pyke (1982) is shown as Figure 68a, and the total alkali versus $FeO_{(total)}$ versus MgO plot (Fig. 68b) is illustrated with the fields of Kuno (1968) and Irvine and Baragar (1971). The geochemical trends observed on MORB-normalized multi-element diagrams (Fig. 64)

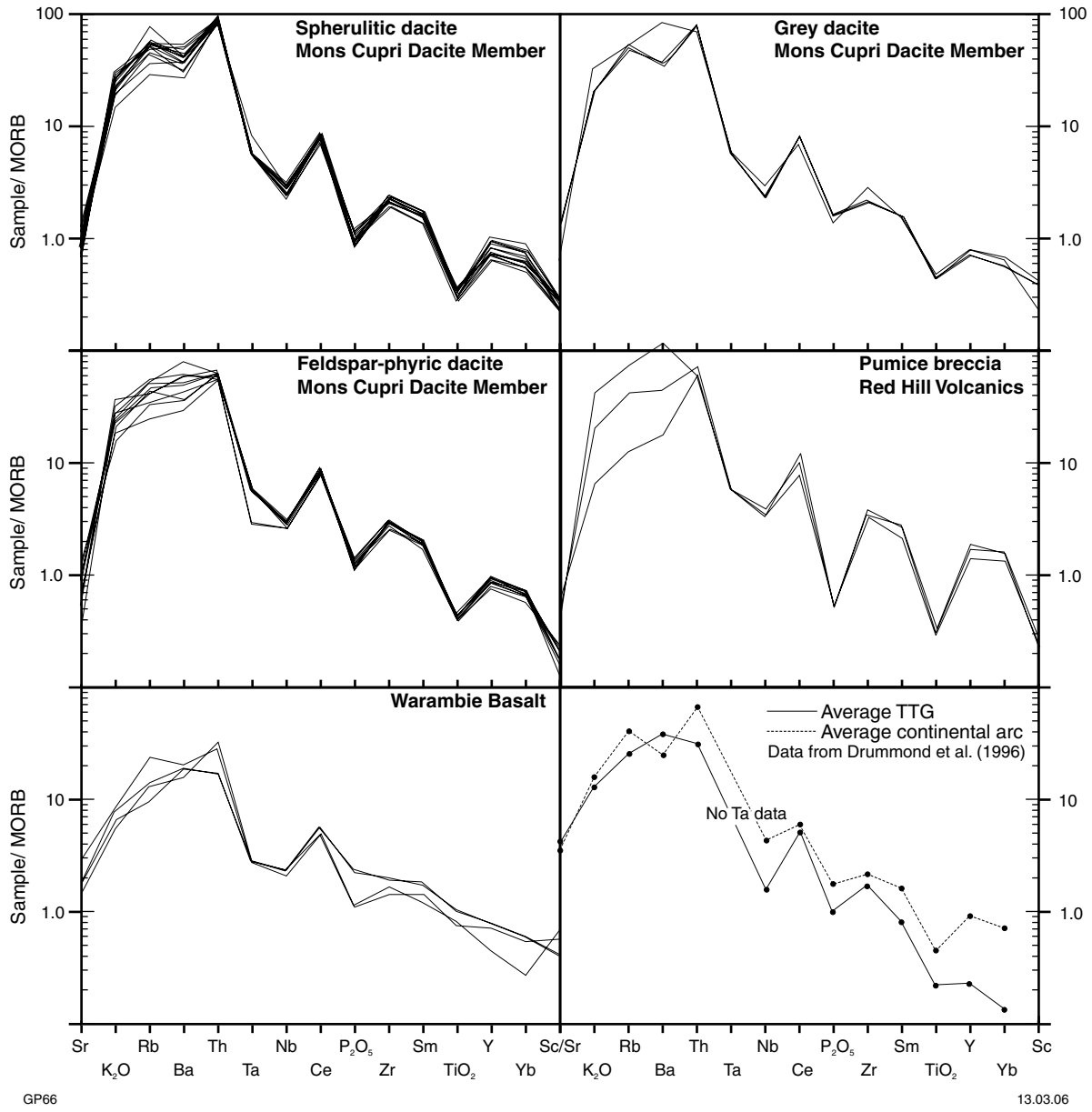

Figure 64. MORB-normalized multi-element diagrams for major lithofacies of the Whim Creek Group. Normalizing values are from Pearce (1982, 1983). Also included are average compositions for Archean tonalite–trondhjemite–granodiorite (TTG) and average continental arc. All felsic samples show similar trends to the average continental arc data of Drummond et al. (1996) rather than TTG

are consistent with those of modern calc-alkaline felsic rocks. These features include relative depletion of Ta, Nb, P_2O_5, and TiO_2 and relative enrichment of Th and Ce and, to a lesser extent, Zr and Sm (i.e. enrichment of high field-strength elements). The Ta and Nb depletion suggests fractionation or retention of sphene, whereas TiO_2 depletion indicates residual magnetite or Ti-augite, and P_2O_5 depletion suggests that apatite was retained. However, these geochemical features are not diagnostic of arc-related calc-alkaline rocks and may form in other tectonic settings (e.g. plume-related settings; Condie, 2000). In addition, the geochemistry of the dacites may reflect both or one of the tectonic setting or the chemistry of the material being melted rather than the tectonic setting in which they were emplaced, and further analysis of tectonic setting is required. Like the Warambie Basalt the Mons Cupri Dacite Member appears to be transitional between tholeiitic and calc-alkaline geochemistry.

Bivariant plots using Nb, Y, and Rb from Pearce et al. (1984) are shown in Figure 69. Förster et al. (1997) recently evaluated the Rb versus (Y+Nb) discrimination diagram and found a reasonable correlation between geochemistry and tectonic setting of silicic igneous rocks. Figure 69 shows that the Mons Cupri Dacite Member samples plot as volcanic arc granites, and the single granite sample is transitional between volcanic arc and syncollisional granites.

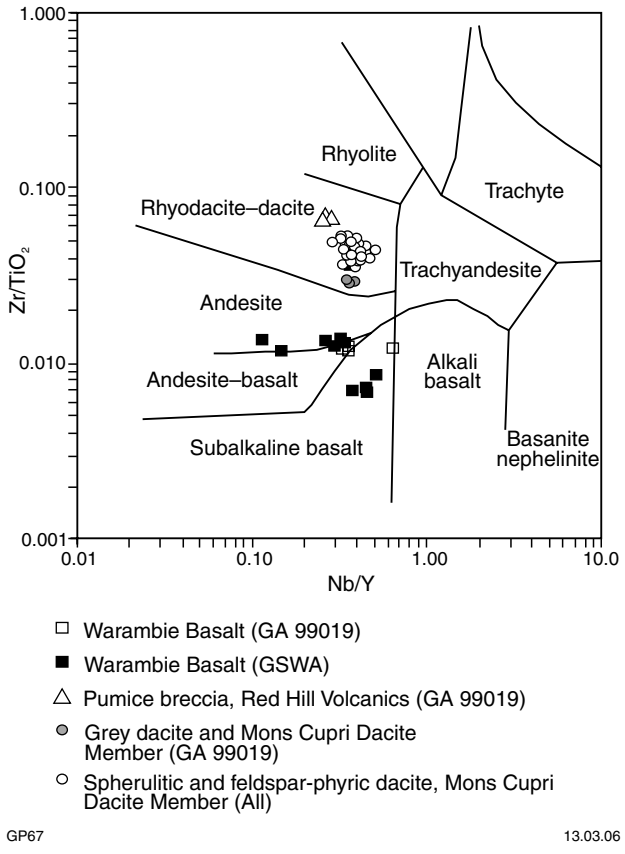

Figure 65. Zr/TiO_2 vs Nb/Y classification plot (from Winchester and Floyd, 1977) applied to the Whim Creek Group

Sedimentary rocks of the Red Hill Volcanics

Although the sampled pumice breccias are part of the same formation (Red Hill Volcanics) as the Mons Cupri Dacite Member, the former are allochthonous volcano-sedimentary rocks derived away from the site of deposition, and hence may have distinct geochemistry. Samples were taken only from the rhyodacite pumice breccia facies because they are interpreted as essentially monomictic breccias derived from a single eruption or eruption phase. The dacite–rhyodacites (Fig. 65) are more felsic than the Mons Cupri Dacite Member samples, and are more enriched in nearly all trace elements (Fig. 64), with lower amounts of P_2O_5 and TiO_2. LREE values are similar to the Mons Cupri Dacite Member, but HREE values are much higher. Tectonic discrimination diagrams give an indication of source, but many more samples are required in order to be statistically significant. Figure 69 suggests transitional within-plate – volcanic-arc signatures that Förster et al. (1997) showed to be characteristic of systems displaying arc accretion onto a continental margin.

Basin evolution

Information from the present study provides a working model for the evolution of the Whim Creek greenstone belt. The following discussion integrates this model with published work to constrain paleotectonic conditions for the northern Pilbara Craton and Archean Earth. The Whim Creek greenstone belt overlies significantly older terranes formed under plate-tectonic conditions (e.g. West Pilbara Granite–Greenstone Terrane; Van Kranendonk et al., 2002), and hence the preserved basin fragments are discussed with reference to plate-tectonic analogues.

The Pilbara Craton before the Whim Creek Group

The Whim Creek Group was deposited over continental crust comprising amalgamated East and West Pilbara Granite–Greenstone Terranes. The West Pilbara Granite–Greenstone Terrane (Fig. 2) comprises the 3270–3250 Ma Roebourne Group, the Regal Formation (a possible obducted MORB slice), the 3130–3115 Ma Whundo Group, and the 3020 Ma Cleaverville Formation (Hickman, 1997; Sun and Hickman, 1998; Van Kranendonk et al., 2002; Hickman, 2004). There are no preserved stratigraphic relations between the Roebourne Group and the Whundo Group because they are restricted to opposite sides of the Sholl Shear Zone. The Cleaverville Formation disconformably overlies the Regal Formation and the Whundo Group, and was deformed and eroded before deposition of the Whim Creek Group (Hickman, 2004).

The Whundo Group, which consists of a 10 km-thick pile of calc-alkaline volcanic rocks south of the Sholl Shear Zone, is poorly exposed as basement to the Whim Creek Group in the Red Hill and Good Luck Well areas. The Whundo Group was deposited in a northeast-striking rift between the Roebourne Group (WPGGT) and the EPGGT (Hickman, 2001, 2004; Van Kranendonk et al., 2002; Beintema 2003). Thick chert in the Cleaverville Formation suggests that part of the formation was deposited below wave base away from significant terriginous input. However, Sugitani et al. (1998) provided evidence of shallow-water sedimentation for part of the formation near Roebourne, and Hickman (2004) noted that the formation contains local basal sandstone and widespread intercalated clastic rocks including siltstone and shale. Detrital zircons from these clastic units include c. 3460, 3290–3250, 3180–3170, c. 3110, and 3070–3050 Ma grains (Nelson, 1998). Most of these ages coincide with the ages of exposed components of the WPGGT, providing strong evidence of derivation of detritus through c. 3020 Ma erosion of the terrane (Hickman and Smithies, in prep.).

Blewett (2000) recorded folds trending north-northwest – south-southeast in the Cleaverville Formation that formed during deformation at c. 3015 Ma, and he also suggested that a northwest-trending greenschist to amphibolite schistosity and crenulation cleavage in the Whundo Group formed at this time. Hence, uplift of the basement rocks may have resulted from compression oriented east-northeast–west-southwest, and may have been related to the same tectonic regime that later resulted in extension and opening of the Whim Creek Group depositional basin. The recognition of basalt lava and coarse-grained clastic rocks at the base of the Warambie Basalt that are transitional into thick hyaloclastite suggest that the original depositional setting was in subaerial to

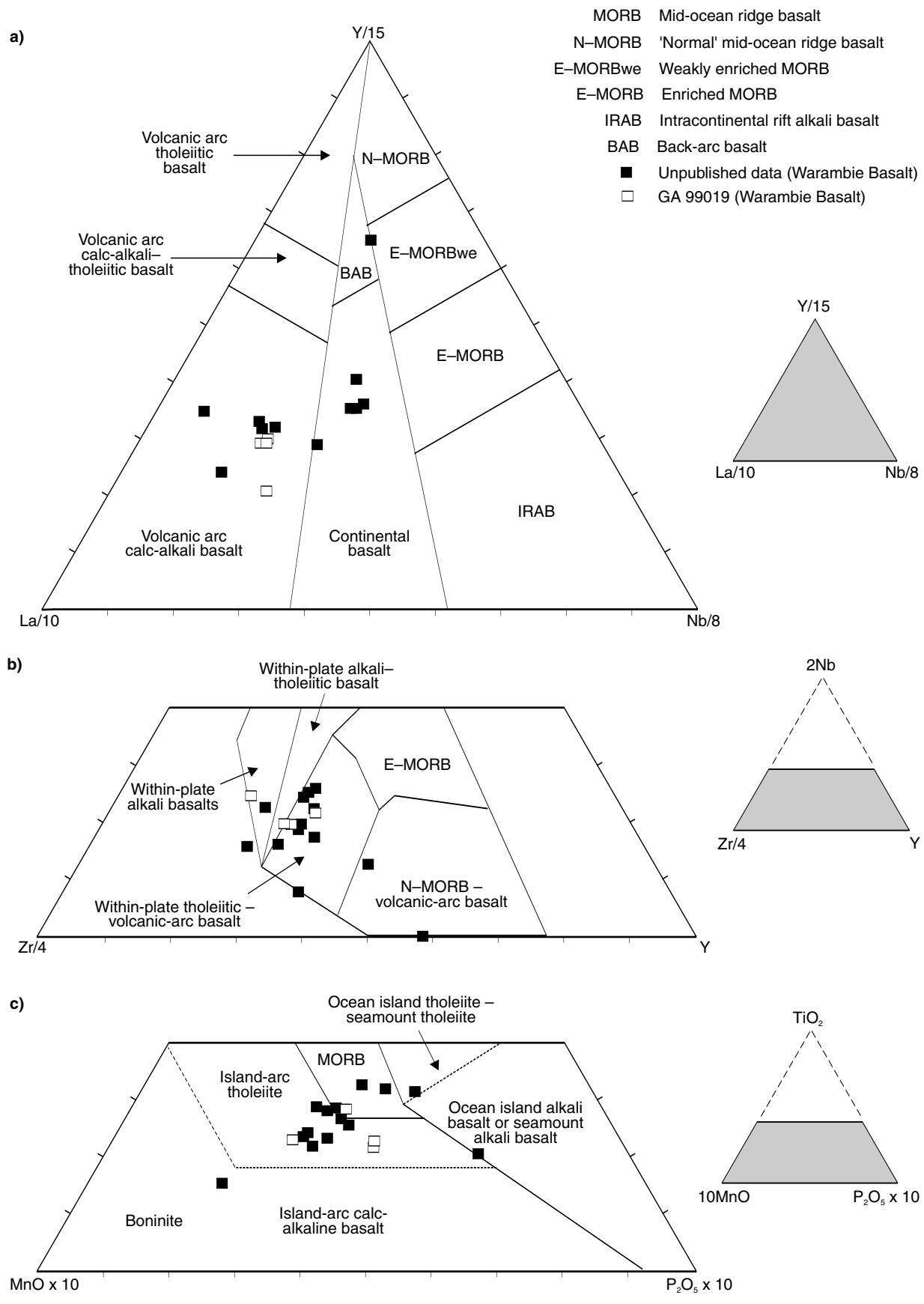

Figure 66. Basalt tectonic discrimination diagrams applied to the Warambie Basalt. Diagrams are from: a) Cabanis and Lecolle (1989); b) Meschede (1986); c) Mullen (1983)

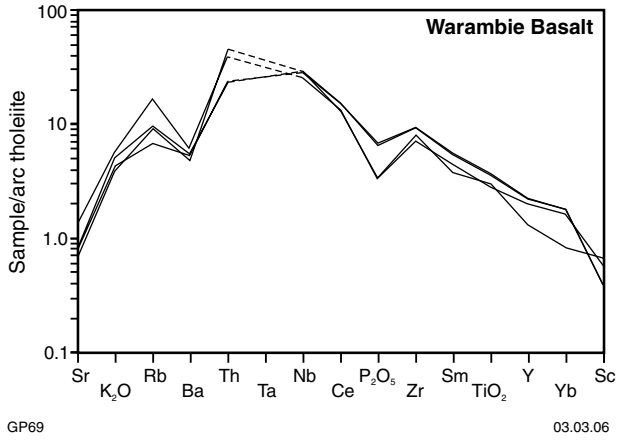

Figure 67. Geochemical data from the Warambie Basalt normalized against a tholeiitic arc basalt. The normalizing sample is MD38 from Kamenetsky et al. (2001) from the eastern Manus Basin

very shallow water conditions, and that the basement rapidly subsided during extension.

Basin models use an event stratigraphic approach (see Pike and Cas, 2002 for a discussion of the limitations of a sequence stratigraphic interpretation). Uranium–Pb SHRIMP zircon geochronology is then used to give absolute ages to specific events where applicable. The collection, sampling, and analysis of detrital zircon ages was discussed in detail by Nelson (2001), and the majority of samples discussed here have been collected and analysed by D. R. Nelson since 1996. The first event directly studied here is recorded by the basal unconformity to the Whim Creek Group, and is a major erosional event termed event WC-1. Subsequent events are attributed a hierarchical numbering system and events are subdivided into smaller events of local significance (e.g. event WC-2i, WC-2ii, etc.).

Event stratigraphy

Introduction and event overview

Event WC-1 includes uplift and tilting of the basement rocks resulting in regression and subaerial exposure. The widespread large volume dacite facies is a regional marker assigned to event WC-3. Before intrusion, sedimentation was restricted to the Good Luck Well area during event WC-2, whereas after intrusion, sedimentation occurred in the Red Hill area (event WC-4). Event WC-5 is post-Whim Creek Group, and includes anorogenic granite magmatism at 2990 Ma (Figs 70 and 71). Following this, events WC-6 to 9 record the early phases of Mallina Basin opening.

Event WC-2

Most of the Warambie Basalt and Red Hill Volcanics mapped on the Good Luck Well sheet (Plate 2a) pre-date the large volume dacite facies intrusion and are assigned to

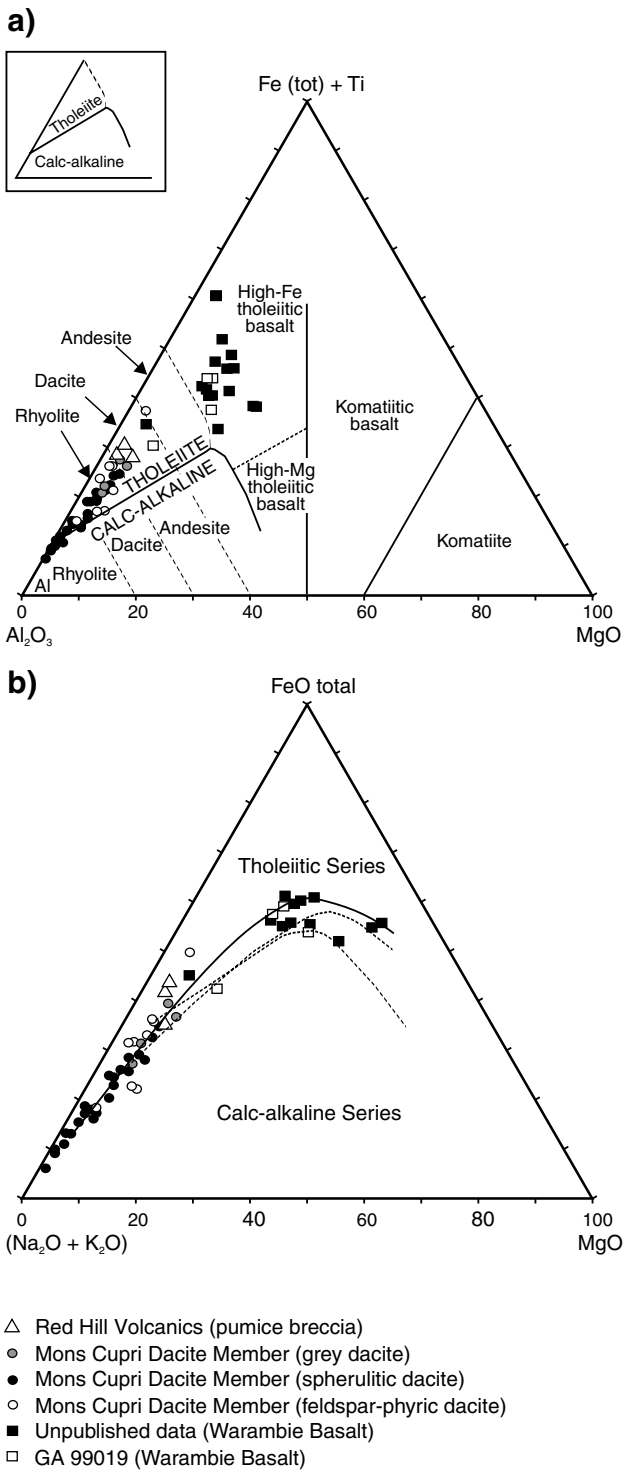

Figure 68. Classification diagrams for all samples of volcanic rocks from the Whim Creek greenstone belt: plotted on classification diagram of Jensen and Pyke (1982); b) AFM classification diagram, showing calc-alkaline–tholeiitic boundary fields (Kuno, 1968: fine dashed line; Irvine and Baragar, 1971: coarse dashed line). The best-fit line for the Whim Creek Group samples is shown as a solid line

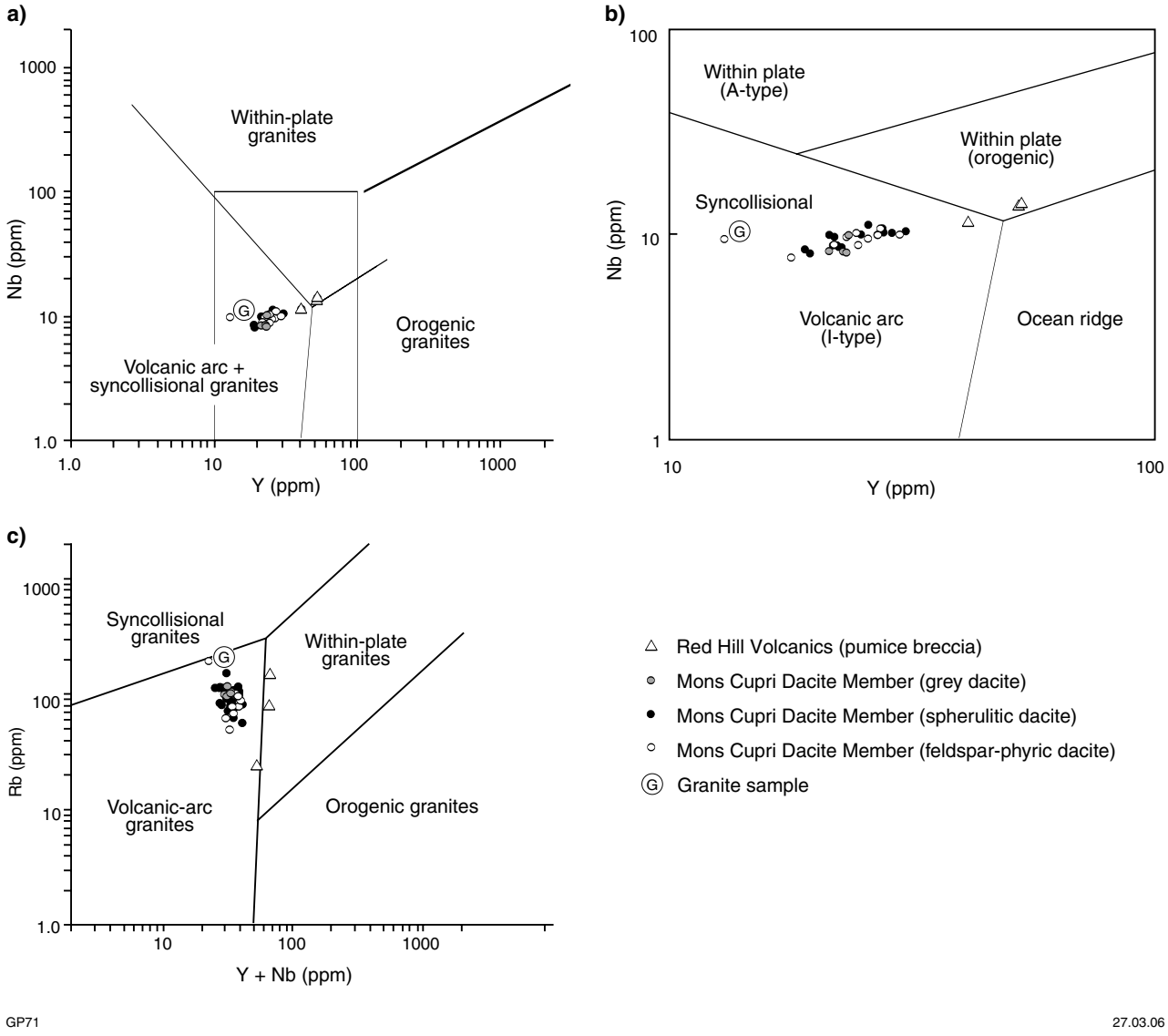

Figure 69. Tectonic discrimination diagrams (from Pearce et al., 1984) for granitic rocks: a) Nb vs Y classification plot, Red Hill Volcanics and Mons Cupri Dacite Member; b) expanded section of the Nb vs Y classification plot from (a); c) Rb vs (Y+Nb) classification plot, Red Hill Volcanics and Mons Cupri Dacite Member

event WC-2. The oldest sedimentary rocks of the tabular-bedded sandstone facies and massive volcaniclastic breccia facies form the base of the package (Fig. 70) and represent very early, reworked volcaniclastic material that was transported by subaqueous mass flow into topographic lows over exposed Whundo Group basement (Fig. 71e). These early sedimentary rocks were then overlain and intruded by both the Warambie Basalt (grey dolerite and basalt facies) and small volume dacite facies before lithification. Thus event WC-2 can be subdivided into distinct but time-conformable events (Fig. 71f) — sedimentation (WC-2i) and bimodal volcanism – soft sediment intrusion (WC-2ii). Epiclastic volcanic sedimentary rocks such as the coarse-grained dacite-rich breccia facies overlie the small volume dacite facies, suggesting that WC-2ii resulted in localized regression forced by emplacement of domes and lava. Erosion and deposition of reworked products is assigned to WC-2iii and was followed by explosive volcanism and transport of small amounts of pumice and crystal-rich breccia facies into the basin (WC-2iv; Fig. 70). The final phase of deposition resulted in fine-grained facies such as the siltstone facies (WC-2v) as the basin deepened or the volcanic influence waned or both.

Overall, WC-2 represents volcaniclastic sedimentation within a distinct sub-basin. The event was generally transgressive (basin deepening), but was interrupted by localized regressions as basin faults tapped bimodal magmas that were emplaced as isolated Warambie Basalt and Mons Cupri Dacite Member bodies.

Event WC-3

The large volume dacite facies contains at least 250 km^3 of dacite magma (and probably much more) that was emplaced rapidly over a very large area during event

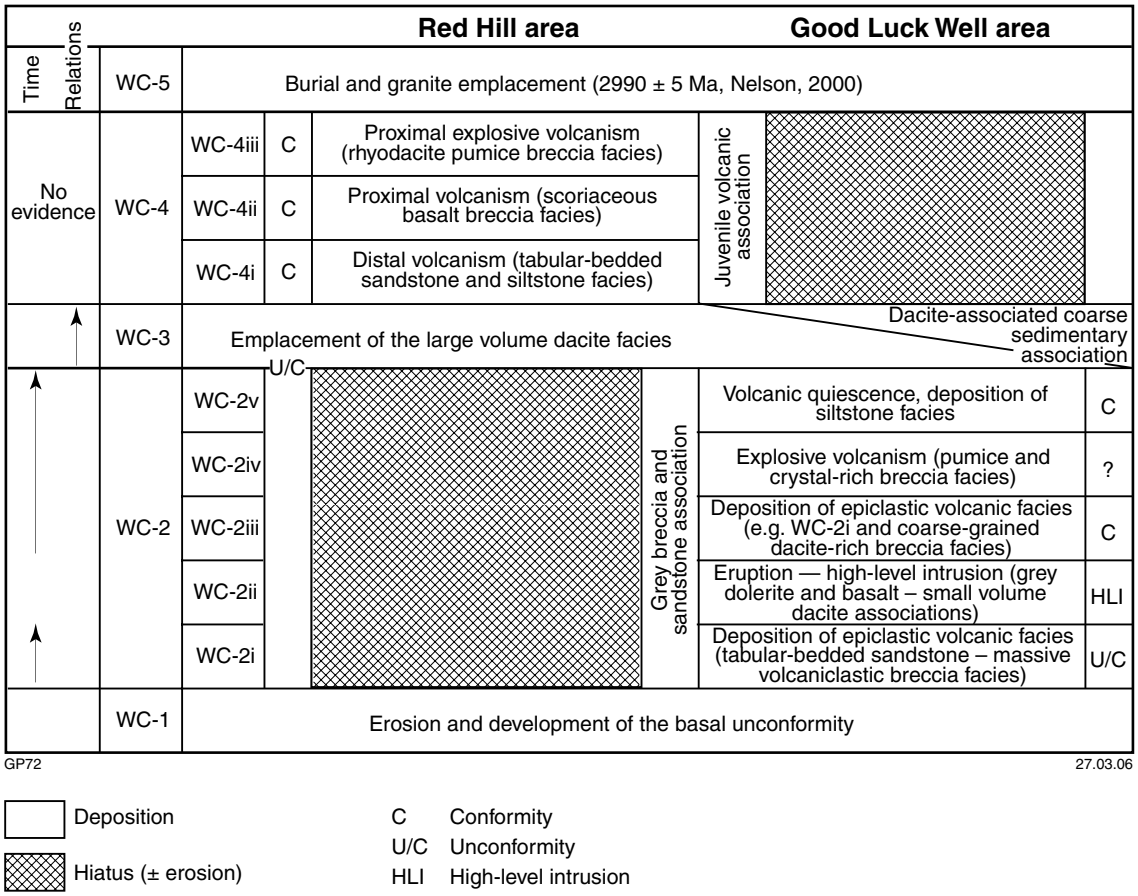

Figure 70. Summary diagram illustrating the subdivision of events WC-2 to WC-4 from the Red Hill and Good Luck Well areas

WC-3. High-level intrusion of dacite was approximately coeval with Warambie Basalt volcanism in the Red Hill area (Figs 70 and 71g,h), although lava and hyaloclastite deposition preceded intrusion. Emplacement of the dacite and basalt package probably either initiated or accelerated subsidence of the Whim Creek Basin. Earlier depocentres such as that mapped in the Good Luck Well area were buried by up to 1100 m of the Mons Cupri Dacite Member, and the Red Hill area subsided several hundred metres allowing space for deposition of deepwater facies during event WC-4.

Event WC-3 also incorporated those products formed from erosion and reworking of the large volume dacite facies. These are restricted to the Good Luck Well area and include coarse-grained clastic rocks of the dacite-associated coarse-grained sedimentary association that suggest either shallow subaqueous or subaerial erosion (i.e. a major, magmatically forced regressive event).

Event WC-4

The thickness of the large volume dacite facies (up to 1.1 km) appears to have effectively ended sedimentation during event WC-2 (in the Good Luck Well area), but conversely preceded (and perhaps initiated) subsidence and deposition of event WC-4 (in the Red Hill area). Event WC-4 comprises three sub-events (Fig. 70). WC-4i resulted in deposition of the tabular-bedded sandstone and siltstone facies in apparent conformity over the Warambie Basalt. These mixed juvenile and reworked volcaniclastic rocks represent relatively distal products of explosive volcanic eruptions, and required an active volcanic centre in the basin hinterland (likewise for the more restricted pumice and crystal-rich breccia facies that formed during event WC-2iv). A relatively minor pulse of Warambie Basalt magmatism resulted in formation of the scoriaceous basalt breccia facies (event WC-4ii), which probably represents weakly effusive (?fire fountain) eruption and quenching in a subaqueous setting. This minor event preceded deposition of the rhyodacite pumice breccia facies and flattened tube-pumice breccia facies during event WC-4iii. Event WC-4iii clearly represents major explosive volcanism near t3he depositional basin, and supplied large amounts of juvenile volcaniclastic material, either directly from pyroclastic flows or from their rapidly resedimented equivalents.

The best available constraint on the age of WC-4iii is a 3009 ± 4 Ma SHRIMP U–Pb age on a zircon population within the rhyodacite pumice breccia facies (Nelson, 1998). However, Barley et al. (1994) used the same method to date the large volume dacite facies (event WC-3) at 2991 ± 12 Ma. Clearly these dates are not

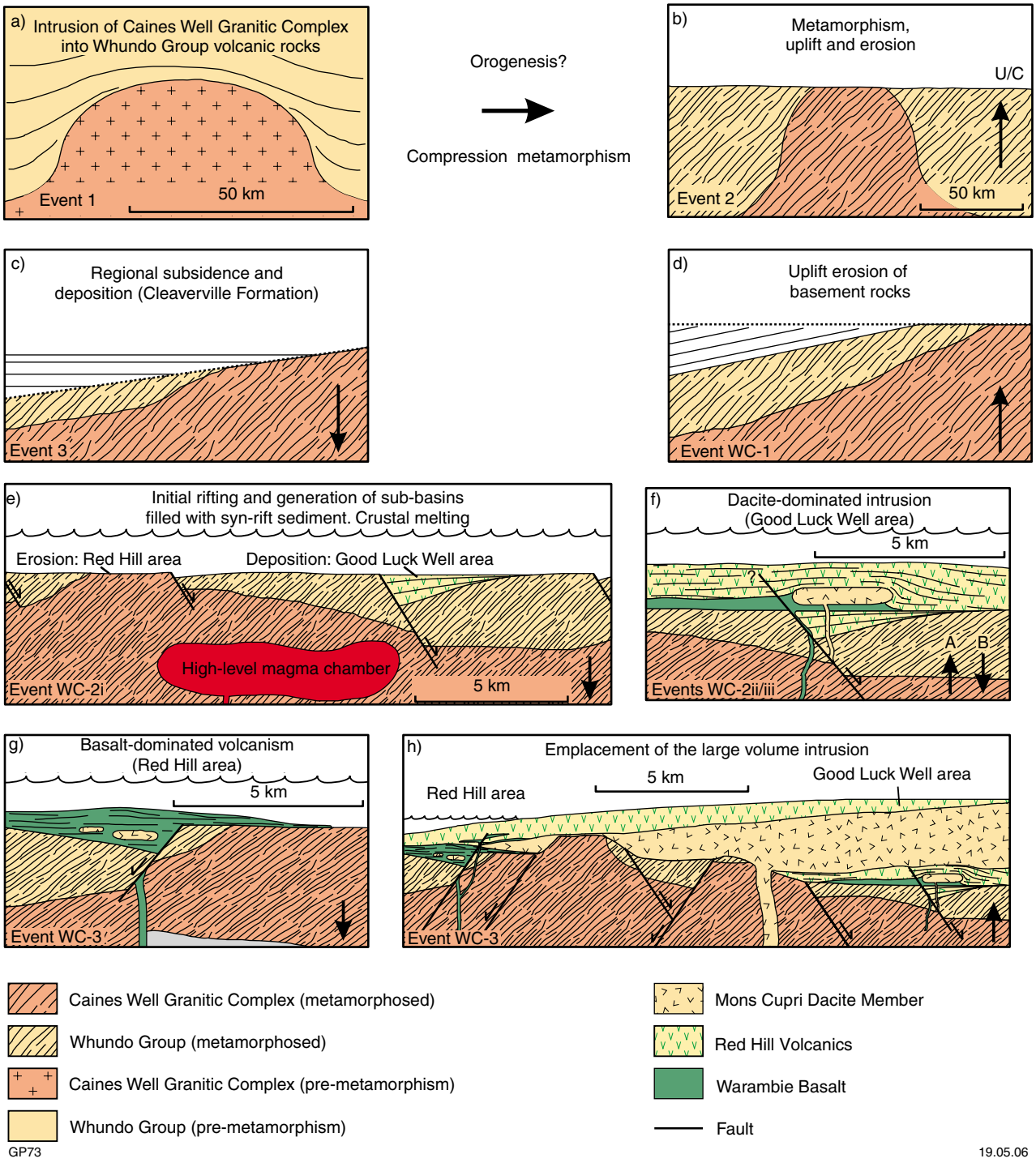

Figure 71. Summary diagrams illustrating the evolution of the depositional basin to the Whim Creek Group: a to c) early evolution of the West Pilbara Granite–Greenstone Terrane; d) Event WC-1 is the first event of importance to the Whim Creek greenstone belt, which resulted in erosion of the West Pilbara Granite–Greenstone Terrane between 3020 and 3010 Ma; e) the beginning of event WC-2 is marked by continued erosion in the Red Hill area, but deposition of the grey breccia and sandstone association in the Good Luck Well area; f) Warambie Basalt and Mons Cupri Dacite Member volcanism occurred during event WC-2ii (Good Luck Well area); g) Warambie Basalt and Mons Cupri Dacite Member volcanism also occurred during event WC-3 (Red Hill area), suggesting that there is very little time recorded by event WC-2; h) flooding of the basin during Event WC-3 resulted in subaerial conditions (Good Luck Well area) and subaqueous conditions (Red Hill area)

consistent if the model of synchronous volcanism and sedimentation presented here is correct. There is no stratigraphic break recognized in the Whim Creek Group that could represent a 2–34 million-year time break. It is possible that the age determined by Barley et al. (1994) was reset by a later thermal event associated with WC-5 granite magmatism (see below). Nelson's (1998) data are considered to contain zircons that represent the age of volcanism that produced the rhyodacite pumice breccia facies because the facies is not anomalously enriched in Zr (if all zircons were xenocrysts, the facies would contain virtually no Zr; Pike, 2002).

Event WC-5

Pike (2002) discussed widespread granite magmatism that occurred at c. 2990 Ma and suggested that the lack of equivalent extrusive rocks suggested an end to extension in the region by c. 2990 Ma followed by an anorogenic granitic event. Hickman (2004) has since discussed a major east-northeasterly trending belt of 3006–2970 Ma granites that together comprise the most voluminous granites in the WPGGT. These comprise most of the Caines Well Granitic Complex and most of three other granitic complexes southwest towards Cape Preston. These are assigned to the Maitland River Supersuite using the new Pilbara supersuite stratigraphy (Van Kranendonk et al., 2004). Consequently, Hickman (2004) demonstrated an important event in the evolution of the North Pilbara Terrain and demonstrated regional granitic magmatism that overlaps in age with younger portions of the Whim Creek Basin as well as the younger Mallina Basin. There is no significant deformation in the Whim Creek greenstone belt between the Whim Creek and Bookingarra Groups, and the regional granitic event is probably anorogenic.

The relationship between events WC-4 and WC-5 is not fully understood and relies greatly on the 3009 ± 4 Ma age provided by Nelson (1998) for the WC-4iii rhyodacite pumice breccia facies. Zircons selected by Nelson (1998) to arrive at that age spanned dates of 3043 to 2995 Ma. Older zircons to 3154 Ma are certainly xenocrysts. If some of the older zircons (specifically six zircons aged 3013–3019 Ma) are xenocrysts then the youngest concordant zircons may provide the best estimate of depositional age, that is 3007–2995 Ma (11 zircons), which coincides with the older part of the age range of the Maitland River Supersuite. On balance, it is likely that felsic volcanism of event WC-4 was related to the same overall tectonic setting as later Maitland River Supersuite granitic magmatism.

Event WC-6

The Cistern Formation and Rushall Slate were deposited as a broadly upward-fining (basin-deepening) package during event WC-6. This is the earliest phase of the opening of the complex Mallina Basin (Fig. 72a–d). Figure 73 illustrates two condensed sections from the Mons Cupri and Good Luck Well areas that show a significant extensional fault control on deposition. Initial faulting, shallow subaqueous to subaerial erosion, and reworking of Whim Creek Group basement is assigned to event WC-6i (Fig. 72a). It was followed by deposition of conglomerate facies (subaqueous fanglomerate) during event WC-6ii in isolated sub-basins adjacent to fault scarps (Fig. 72b). The dominance of rounded clasts suggests that debris was derived from significantly reworked sediments. While this may suggest a significant hinterland, the dominance of Mons Cupri Dacite Member clasts suggests a very local source with high-energy reworking (e.g. beach or barrier bar type environment). The minor pumice breccia throughout the matrix of the conglomerate facies and sheared conglomerate facies suggests explosive volcanism adjacent to the Mallina Basin.

The transition from conglomerate facies upward through sandstone turbidite facies to quartz-rich sandstone facies or lithic sandstone facies marks the onset of event WC-6iii (Fig. 72c). Syndepositional faults were still active because variations in facies thickness were strongly controlled by these features. Fragments of basal Whim Creek Group rocks are much less abundant than previously described, suggesting both burial of the Whim Creek Group and a much broader source region (including abundant granite and chert) that was tapped as the basin grew and deepened. In the Good Luck Well area the oldest Cistern Formation facies (black chert breccia, volcanic breccia, and overlying planar-laminated sandstone facies) probably correlate to event WC-6iii, based on their similar grain size and the presence of allochthonous basement lithic clasts.

The thick shale facies and lesser blue chert facies of the Rushall Slate formed during event WC-6iv (Fig. 72d). Syndepositional faults were still active, but sedimentation was more widespread and dominated by mud, with lesser quartz and mafic material (i.e. sourced from distal uplifted basement with typical granite–greenstone characteristics).

Event WC-7

Mount Negri Volcanics basaltic volcanism occurred during event WC-7 (Fig. 72e,f). The dispersed basalt facies is a peperite at the northern margin of the Opaline Well Intrusion on Plate 2a, and is evidence that the Opaline Well Intrusion intruded the Rushall Slate during or immediately after deposition. At Mount Negri (MGA 588027E 7701349N) the basalt breccia and cobble bed facies separate the shale facies (Rushall Slate) from the massive basalt lava facies (Mount Negri Volcanics), and indicates a transitional conformable contact between the two. Hence basaltic volcanism probably flooded a developing basin system. The outcrop patterns of the Mount Negri Volcanics and Rushall Slate are similar, suggesting that both were deposited in local sub-basins.

Event WC-8

The Louden Volcanics were deposited during event WC-8 (Fig. 72g). No good contacts between the Mount Negri Volcanics and Louden Volcanics have been recognized. The Louden Volcanics are noted from the westernmost exposure of the Whim Creek greenstone belt from the ROEBOURNE 1:100 000 sheet (Hickman, 2000) to the

northernmost exposure near Government Well (MGA 591700E 7712000N). This indicates that they essentially flooded the entire basin, which is consistent with the concept that the Mount Negri Volcanics filled in earlier, fault-controlled depocentres.

Event WC-9

Event WC-9 has not been extensively studied in this Report. The emplacement of the Kialrah Rhyolite probably occurred conformably over the Louden Volcanics, although Hickman and Smithies (2001) noted the steeper dip of flow bands in the Kialrah Rhyolite compared to the regional dip of the Louden Volcanics, perhaps indicating a low-angle unconformity.

Dating events WC-6 to WC-9

Dating of samples from the quartz-rich sandstone and sheared conglomerate facies of the Cistern Formation by Nelson (2000) gives constraints on the age of the Mallina Basin and provenance of sediment (Table 8). The quartz-rich sandstone facies has more populations, consistent with a wider source region and includes a c. 3150 Ma group that may relate to rocks formed in a subduction setting (cf. Beintema, 2003). Both samples contain a Cleaverville Formation age population (3016 and 3020 Ma), in addition to a c. 2990 Ma population that may be derived from event WC-5 granites. The 2980–2960 Ma population thus gives the maximum depositional age of the Bookingarra Group.

The minimum age of the Bookingarra Group is given by the age of the Kialrah Rhyolite (event WC-9). Nelson (1997) used the SHRIMP U–Pb zircon method to calculate a maximum depositional age of 2975 ± 4 Ma for this formation, but an alternative depositional age of 2943 ± 7 Ma (same data) was noted by Huston et al. (2000). Hence, the entire Bookingarra Group was probably deposited between 2980 and 2943 Ma.

The tectonic setting of the Whim Creek Group

Stratigraphic considerations suggest that the Whim Creek Group developed in a volcanically active, extensional basin over continental crust. This early Pilbara continent was probably a shallow-water or emergent block with little topographic expression, based on the scarcity of allochthonous clasts in the Whim Creek Group. Geochemically, the felsic rocks plot as either volcanic arc granites (Mons Cupri Dacite Member) or transitional within-plate – volcanic arc granites (Red Hill Volcanics pumice breccia) on the Förster et al. (1997) Rb vs (Y+Nb) discrimination diagram (Fig. 69). An arc-like setting is thus favoured on both stratigraphic and geochemical grounds.

The Mons Cupri Dacite Member magma contained aggregates of polycrystalline plagioclase, quartz, and minor K-feldspar (including the crystalline inclusions facies), suggesting that the chamber was in the process of crystallizing a plutonic rock but was ruptured, allowing access of the magma to the surface. Voluminous extrusive felsic lava flows are typically associated with intracontinental rift systems. An ancient example is the Proterozoic (~9000 km^3) Eucano Dacite in the Gawler Craton of South Australia (Morrow and McPhie, 2000). In this example, large volume flows (100 to 1000 km^3) are recognized. Cas (1992) documented subaqueous felsic lavas and also recognized a division between small, dome-like (e.g. small volume dacite facies) and large volume felsic bodies (e.g. large volume dacite facies). Similar conditions of crustal thinning, heating, and melting may be expected in an intra-arc setting. The 'enriched tholeiite' chemistry of the Warambie Basalt may be explained by an arc tholeiite contaminated by one or both of melt and continental crust from a thick slab of arc-derived continental crust. An independent line of evidence for the presence of an arc before 2970 Ma is the suggestion of a depleted mantle source (Smithies and Champion, 2000) beneath the Mallina Basin, indicating depletion of this mantle by earlier arc volcanism.

Busby et al. (1998) proposed a three-stage model of modern arc evolution containing an initial highly extensional intra-oceanic arc, followed by a mildly extensional fringing arc, and finally a compressional continental-arc system. Interestingly, the c. 3020 Ma Cleaverville Formation was characterized by oceanic-like sedimentation (chert dominated), arc volcanism, granite intrusion, (Beintema, 2003) and finally a c. 3015 Ma deformation and metamorphism (Blewett, 2000). Hence the three-stage model of Busby et al. (1998) may be recorded immediately pre-Whim Creek Group, with the Whim Creek Group representing arc rifting and collapse. The volcano-sedimentary rocks of the Whim Creek Group fulfil the criteria of Smith and Landis (1995) for intra-arc basins. The association of autochthonous arc-related volcanic rocks (Warambie Basalt and Mons Cupri Dacite Member) with allochthonous volcaniclastic facies (Red Hill Volcanics) is very strong evidence that the Whim Creek Group formed within an intra-arc basin (e.g. Carey, 2000). The small size of the preserved basin (~40 km strike) is also consistent with an intra-arc basin, although it is recognized that the basin may have been considerably more extensive than the exposed Whim Creek Group.

Intra-arc basins gained popular acceptance after the work of Smith and Landis (1995). Many examples of subaerial intra-arc basin formation, uplift, and dissection are documented (e.g. Riggs and Busby-Spera, 1991; Wilson et al., 1995; Sowerbutts and Underhill, 1998). However, subaqueous intra-arc basins are far less well documented due to their relative inaccessibility.

Smith and Landis (1995) recognized two end-member basin styles for intra-arc basins: fault bound and volcano bound. Although these authors suggest a continuum between the two types, a basic consideration is that extensional fault-bound intra-arc basins must form in a setting characterized by upper crust extension, whereas the latter may be expected over a range of extensional, neutral or compressive regimes. The fault-bound style is considered to be most applicable to the Whim Creek greenstone belt, based on the abundant evidence for extension during its evolution.

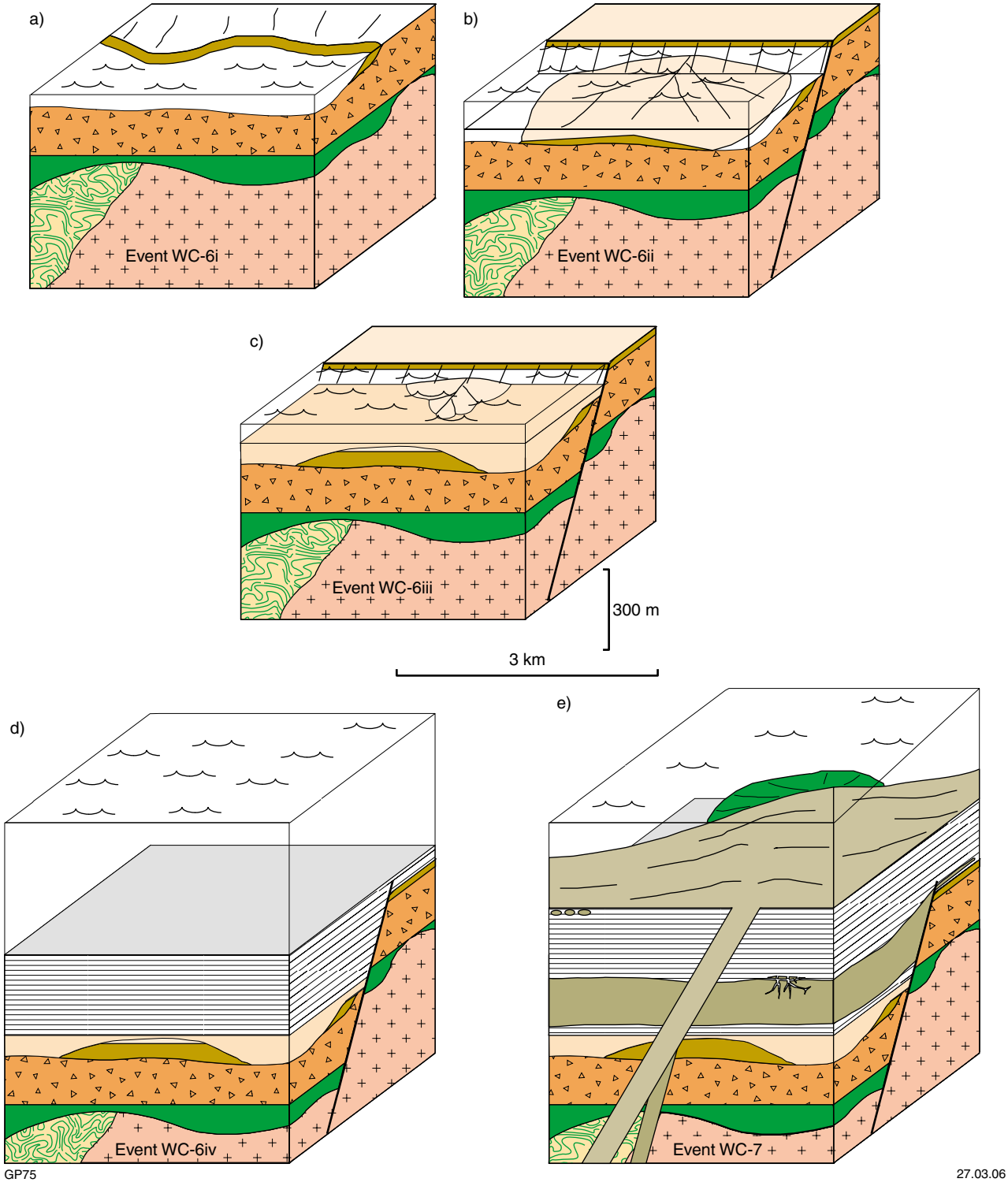

Figure 72. Block models illustrating the event stratigraphy of the Bookingarra Group, based primarily on observations from the Mons Cupri and Mount Negri areas: a to d) event WC-6 records the opening of isolated, half graben sub-basins controlled by east-trending syndepositional faults. The entire event records a major (tectonically controlled) transgression; e and f) event WC-7 resulted in the emplacement of the partly subaerial Mount Negri Volcanics and suggests a volcanic-forced regression; g) event WC-8 deposited the subaqueous Louden Volcanics and indicates a further transgression (perhaps linked to the regional sag of the depositional basin)

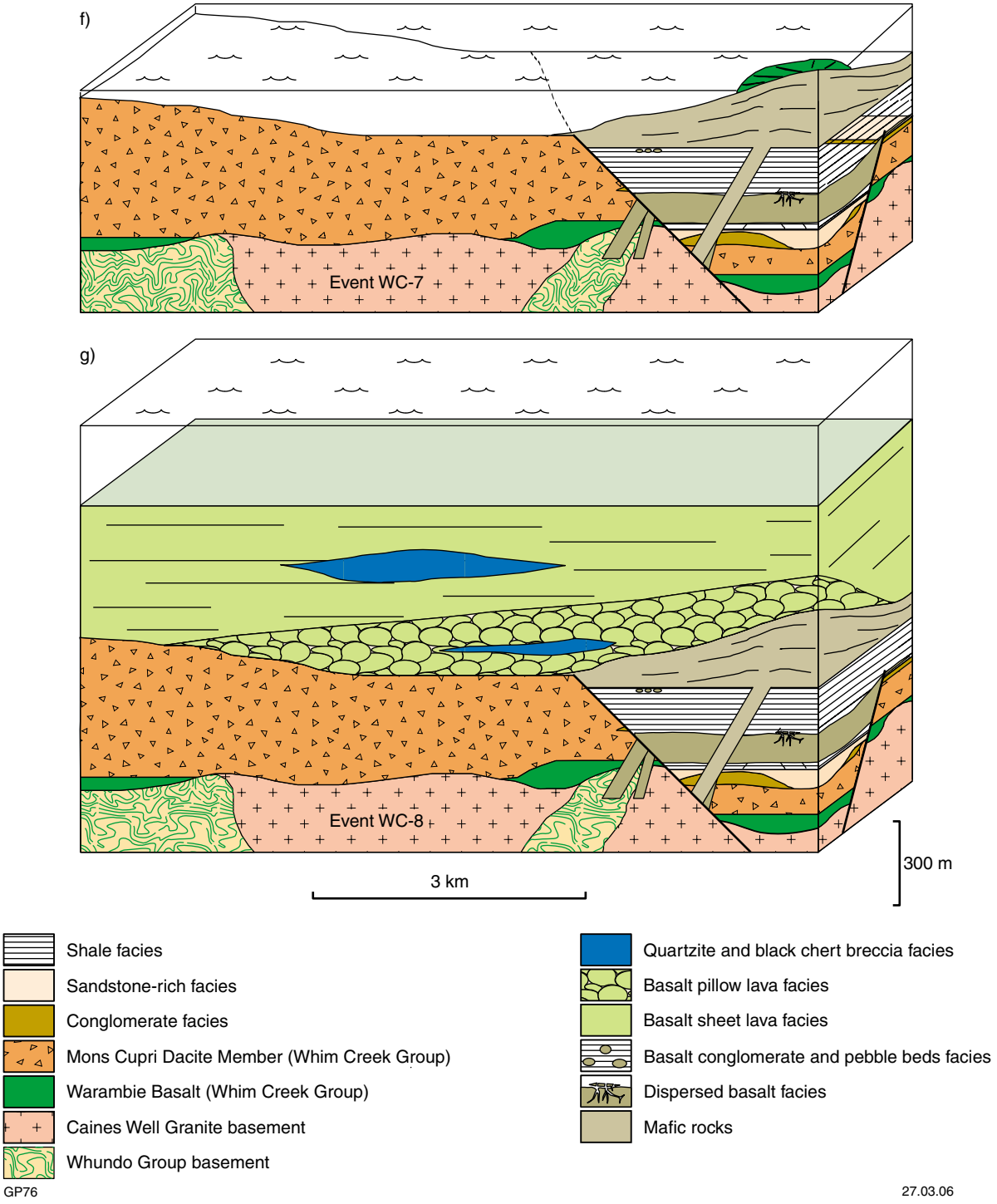

Figure 72. (continued)

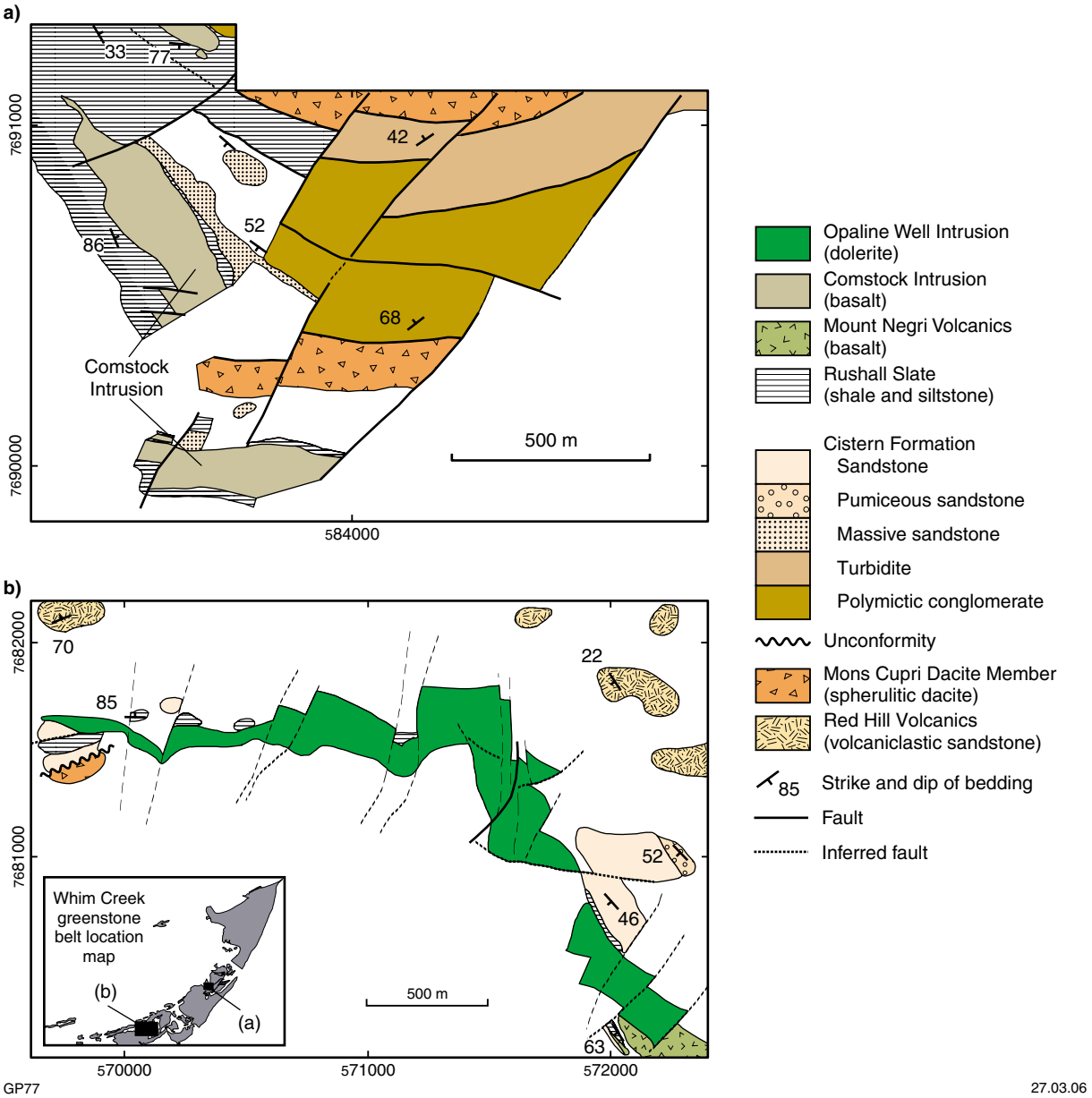

Figure 73. Sketch maps of condensed sequences from the Bookingarra Group: a) from the Mons Cupri deposit area; b) from the Good Luck Well area

Table 8. Comparison of U–Pb SHRIMP detrital zircon geochronology from the Cistern Formation (data from Nelson, 2000)

Equivalent age event	*Quartz-rich sandstone*	*Sheared conglomerate*
?Event WC-5	2980–2960 Ma (11 analyses)	–
Event WC-5	2990–2980 Ma (12 analyses)	2990 Ma (2 analyses)
Cleaverville Formation	3020 Ma (2 analyses)	3016 Ma (20 analyses)
WPGGT subduction event	3150 Ma (2 analyses)	–

Figure 74 outlines the principal components of intra-arc basins derived from facies observations from the Whim Creek Group, theoretical considerations, and exposed examples (e.g. Smith and Landis, 1995 and references therein). These components include:

- juvenile volcanic debris (pyroclastic flows or their water-transformed equivalents), resedimented autobrecciated clasts, and hyaloclasts;
- epiclastic debris from reworked volcanic, metamorphic, sedimentary, and plutonic rocks and autochthonous biogenic and chemically precipitated rocks;
- water-settled debris — clay and ash (planktonic debris in Phanerozoic examples).

In situ volcanic rocks in intra-arc basins can include lava flows from adjacent arcs in proximal settings. However, the two main components defined from the Whim Creek Group are large volumes (100 to 1000 km^3 units) of one or both of felsic lava or shallow intrusions (Mons Cupri Dacite Member) and a lesser volume (<1 to 10 km^3) of one or both of basalt lava or shallow intrusions (Warambie Basalt). These suggest that the preserved part of the basin developed over an active zone of extension that included large felsic magma chambers. The recognition of the effusive and locally high-level intrusive Mons Cupri Dacite Member suggests that large felsic volcanic systems need not be explosive (such as those of the subaerial to subaqueous Taupo Volcanic Zone, e.g. Wilson et al., 1995). Factors such as deep water, low initial volatile contents or early degassing may favour effusive flows over voluminous ignimbrites.

Evolution of the 3020–2990 Ma arc system

After at least 100 million years of little tectonic activity, the c. 3020 Ma Cleaverville Formation is here interpreted to represent the preserved portion of an arc system. The basal unconformity could have resulted from uplift due to volcanism, deformation, and metamorphism at c. 3015 Ma. The first phase of extension may have resulted from a change in subduction magnitude (slab rollback) or direction, and the 3009 ± 4 Ma (Nelson, 1998) age of event WC-4iii suggests that extension occurred within 10 million years of peak metamorphism.

Sedimentation during events WC-2 and WC-4 included allochthonous hyaloclasts and pyroclasts from nearby volcanism. Hence, volcanic activity continued in the arc through compression, metamorphism, and intrusion (i.e. the compressional continental-arc system of Busby et al., 1998). The rhyodacite pumice breccia facies (event WC-4iii) indicates development of a nearby volcanic centre which was in shallow water or possibly subaerial. This facies is the youngest recorded in the Whim Creek Group, and may represent a cataclysmic eruptive event or series of events that essentially emptied remaining magma chambers.

Granite magmatism of event WC-5 occurred after the Whim Creek Group was deposited and may be related to a later phase of the same tectonic setting.

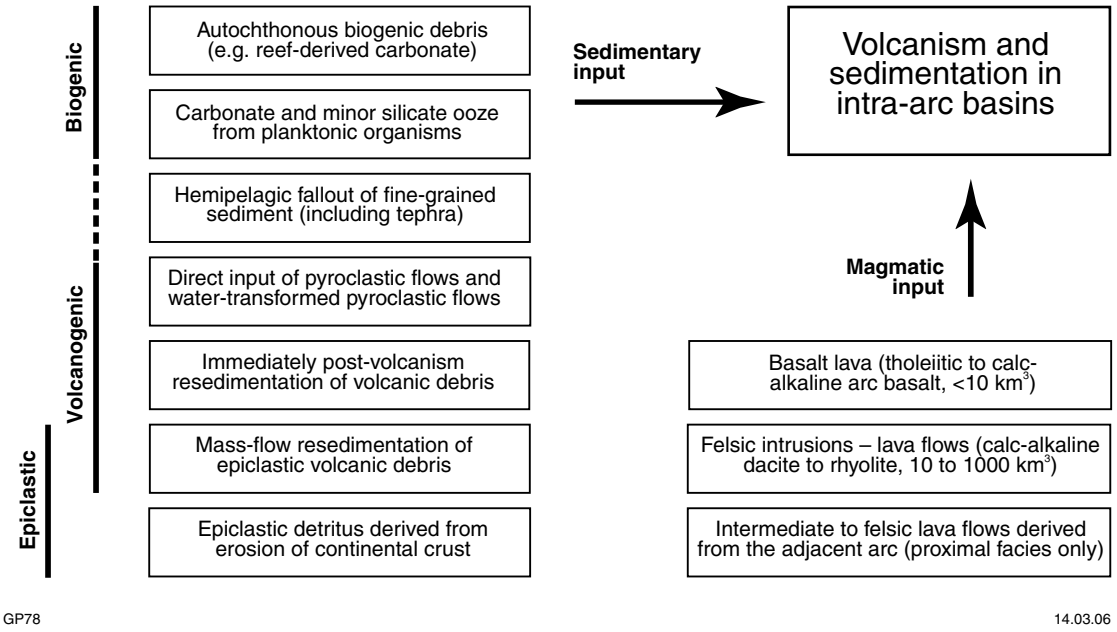

Figure 74. Proposed sedimentary and magmatic inputs for subaqueous intra-arc basins based on the facies architecture of the Whim Creek group and studies of modern intra-arc basins (e.g. Smith and Landis, 1995)

The tectonic setting of the Bookingarra Group

Correlation across the Loudens Fault and Mallina Shear Zone

Stratigraphic correlation of the Rushall Slate (Bookingarra Group) and Mallina Formation (De Grey Group) across the Loudens Fault was suggested by Fitton et al. (1975), but criticized by Hickman (1983, p. 106–107) because of differences in lithology, thickness, and stratigraphic relations. The correlation was subsequently followed by Smithies et al. (1999, 2001), Huston et al. (2000), and Van Kranendonk et al. (2002), but stratigraphic evidence presented here shows that the Cistern Formation, Rushall Slate, and Mount Negri Volcanics were deposited in isolated sub-basins, and the Louden Volcanics are restricted to west of the Loudens Fault. Similar basaltic rocks in the Mallina Basin separate the underlying Constantine Sandstone from the overlying Mallina Formation. Consequently, the Constantine Sandstone was most probably deposited during event WC-6. The maximum total thickness of the Mallina Basin in the Whim Creek greenstone belt is about 2 km. Fitton et al. (1975) estimated the maximum thicknesses of the Constantine Sandstone and Mallina Formation as 5 and 2.5 km respectively.

Structural features of the early Mallina Basin

Unequivocal syndepositional faults trended east–west in both the Whim Creek greenstone belt and the Mallina Basin, parallel to the Mallina Shear Zone and western portion of the Sholl Shear Zone. The early Mallina Basin was an extensional basin developed over continental crust that included 3020–2990 Ma arc rocks, and was sourced from a relatively large, granite-dominated hinterland. Siliceous komatiitic basalt suggests a strong mantle influence on basin evolution. Coarser grained sediments in the southern part of the basin suggest that the basin boundary fault was also to the south, and the same interpretation explains the increasing abundance of Louden Volcanics pillow lava northwards as the product of decreased flow rate due to distance from eruptive source. A basin boundary fault to the Bookingarra Group could be the Mallina Shear Zone because it trends east–west, is of crustal scale, and no Bookingarra Group is exposed to the south. Alternatively, the basin boundary fault could be farther south, beneath cover rocks.

Figure 75a illustrates the main structural features of the Mallina Basin, and Figure 75b simplifies the orientation of those features that show stratigraphic or facies evidence of activity during deposition. The Bookingarra Group can be explained by simple north–south extension, but the growth of the Mallina Basin requires at least two extensional pulses at different orientations. Figure 75c is a cross section through the inferred east-trending basin system that produced the Bookingarra Group in the Mallina Basin. This east–west component (Fig. 75d) is then interpreted to have been extended obliquely to produce a second set of faults (including the Loudens Fault) during a later phase of basin evolution (Fig. 75e).

Continental rift-basin characteristics

Rift basins are characterized by four distinct stages (rift initiation, rift climax, late-stage rifting, and early post-rift), each with a distinct stratigraphic fill (Prosser, 1993, Ravnås and Steel, 1998). Events WC-6 and WC-7 occurred within the rift initiation stage and the basin was then flooded during event WC-8 by the voluminous Louden Volcanics. The Bookingarra Group displays an excellent two-fold conglomerate–sandstone–mudstone motif suggesting that it was sediment-underfilled (Ravnås and Steel, 1998) in the initiation stage. This, in turn, implies a limited source region (i.e. low topography or small area of provenance or both). Events WC-8 and WC-9 require rapid subsidence because they resulted in the emplacement of more than 2 km thickness of basalt and lesser rhyolite within a wholly subaqueous environment, despite the presence of the underlying, partly subaerial Mount Negri Volcanic facies. Consequently, these events probably occurred during the rift climax stage, characterized by increase in fault zone efficiency, hard linkage of faults (Walsh and Watterson, 1991), and rapid subsidence–generation of accommodation space. The size of the basin is unclear. Using the terminology established by Olsen and Morgan (1995), events WC-6 and WC-7 probably occurred in small (kilometre-scale width) simple grabens, with probable evolution into a continental rift with a width in the order of tens of kilometres. In many examples the rift boundary fault system can be estimated from stratigraphic thickening or the facies. In Figure 75c the Mallina Shear Zone is interpreted as a basin boundary fault, although the true basin boundary fault may be farther south. The Sholl Shear Zone existed before basin opening, and thus complicates the interpretation of the basin. This fault has a south-side-down component of movement illustrated by the basalt conglomerate facies at Government Well. Because the Loudens Fault separates the approximately 2 km of Bookingarra Group from about 7.5 km of De Grey Group, it was almost certainly active during Mallina Basin growth, but probably after event WC-9.

Tectonic discrimination from the Bookingarra Group basalts

The Mount Negri Volcanics and Louden Volcanics are composed of high TiO_2 (0.8 – 1.3 wt% TiO_2, 1.7 – 3.7 FeO*/MgO) and low TiO_2 (0.3 – 1.6 wt% TiO_2, 0.1 – 0.6 FeO*/MgO) basalt lavas and subordinate intrusive rocks (Smithies, 1998). Both units show some features, noted by Arndt et al. (1993), of Phanerozoic flood basalts. These features include relatively thick flows (~1–10 m thickness) of uniform, phenocryst-poor basalt with high SiO_2 (wt%) content. The high- and low-TiO_2 Mount Negri Volcanics and Loudens Volcanics are similar to lavas from the Siberian Traps that comprise a lower third of high-Ti basalt overlain by low-Ti basalt (Ardnt et al., 1993). Although the preserved volume of the Mount Negri – Loudens

* FeO* = total Fe as FeO.

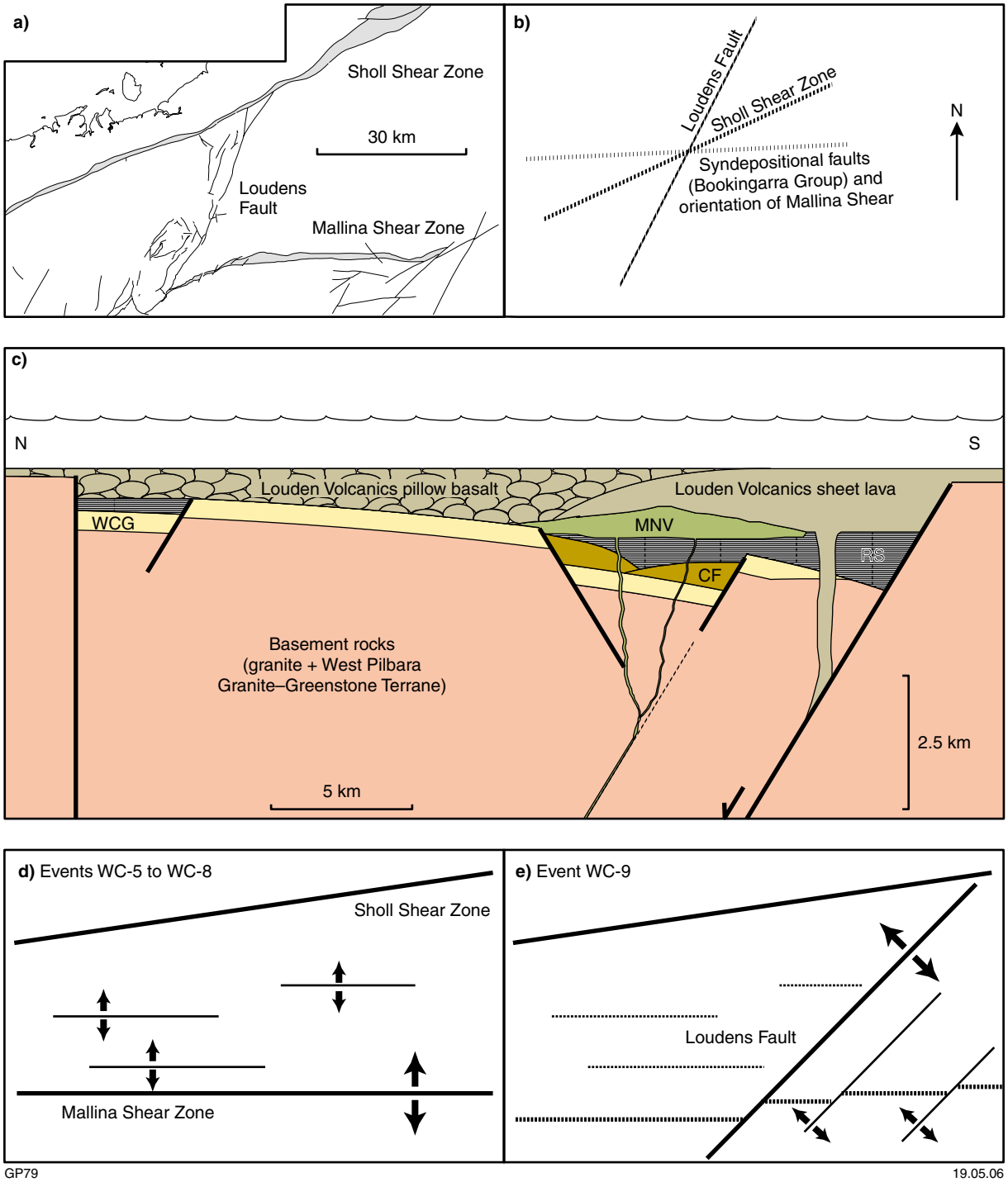

Figure 75. Illustration of problems and potential solutions to the opening of the Mallina Basin: a) the main structural features of the Mallina Basin are the Sholl Shear Zone, Loudens Fault, and Mallina Shear Zone. The Sholl Shear Zone and Loudens Fault appear to have been active during the formation of the Mallina Basin, and the Mallina Shear Zone is parallel to syndepositional faults in the Whim Creek greenstone belt; b) the three principal extensional, syndepositional fault sets; c) cross section showing how the Mallina Shear Zone may have been part of an early, east-trending fault system that deposited the entire Bookingarra Group (WCG = Whim Creek Group, MNV = Mount Negri Volcanics, CF = Cistern Formation, RS = Rushall Slate); d and e) the two inferred extensional fault sets trending east–west (d) and northeast–southwest (e)

Volcanics (~100 km^3) is insufficient to classify them as flood basalts, they may originally have been significantly more extensive because the Whim Creek greenstone belt is only a fragment of the original basin system. Komatiitic basalts are noted from the Mallina Basin (Smithies, 1999), and are of similar age to the Mount Negri Volcanics and Louden Volcanics. Sun et al. (1991) described the Mount Negri Volcanics and Louden Volcanics as siliceous high-magnesian basalt and suggested that they were derived from crustally contaminated mantle plumes. Arndt et al. (1993) suggested that continental flood basalts are generated by plume-related partial melts that interact with continental crust, and suggested two controls on the geochemistry of erupted products. The first is the depth of partial melting and the second is the buffering effect of country rocks surrounding crustal magma chambers. Depleted concentrations of Ta and Nb are thought by Arndt et al. (1993) to be related to the latter process, and the negative Nb anomalies noted from Figure 64 may reflect the low concentration of Nb in continental crust (i.e. in the assimilated component).

Geochemical trends suggest that the Mount Negri Volcanics and Comstock Intrusion (Fig. 73a) are related units based on very similar normalized multi-element plots and gently sloping rare earth elements. These two units are geochemically distinct from the Louden Volcanics. In all samples the large-ion lithophile elements (Cs to K) show large variability attributed mainly to mobility during metamorphism, alteration, and weathering. In the case of the strongly chlorite-altered Comstock Intrusion, Rb and K have been considerably depleted, and this is due to the intense alteration associated with the Mons Cupri copper–zinc–lead deposit (Collins and Marshall, 1999, Pike et al., 2002). Niobium is depleted in all samples, but especially in the Louden Volcanics. This trend may indicate a considerable degree of continental crust assimilation, consistent with the development of crustal magma chambers. The tight grouping of Nb data from within all four groups may be evidence of the buffering process of this element by crustal material.

Sedimentation in the Mallina Basin

Smithies et al. (1999, 2001) recognized sedimentary rocks previously mapped as Mallina Formation (Smithies, 1999) that have a maximum depositional age of 2941 ± 9 Ma. These sedimentary rocks are younger than the Mallina Formation because the latter must be older than intrusive granitic rocks dated at 2948 ± 5 and 2946 ± 6 Ma. These data suggest that sedimentation in the Mallina Basin occurred in at least two cycles separated by deformation and intrusion. Hence, the Mallina Basin is a complex multiphase basin with Bookingarra Group – Constantine Sandstone at its base.

Summary model

A summary model from the above discussion is as follows (see Fig. 76):

1. Arc construction in a subduction setting (Cleaverville Formation) at c. 3020 Ma.
2. Compressional arc deformation and metamorphism at c. 3015 Ma.
3. Arc extension and collapse (Whim Creek Group) before 3009 (?3007–2995 Ma).
4. Anorogenic granite magmatism, heating, and uplift at 3006–2970 Ma.
5. Continental rifting (Bookingarra Group – Constantine Sandstone) at 2980–2975 Ma.
6. Continued De Grey Group sedimentation east of the Loudens Fault from 2970 to 2955 Ma.
7. Deformation at 2955–2945 Ma.
8. Granitic magmatism in the Mallina Basin at c. 2945 Ma.
9. Deposition of siliciclastic rocks during a second depositional cycle after 2945 Ma.

The Earth at 3000 Ma

Rocks between c. 3020 to 2950 Ma in age dominate the central part of the northern Pilbara Craton. In this section analogous successions, in terms of both age and lithology, are briefly introduced, and compared and contrasted with the Whim Creek greenstone belt.

The Archean era (c. 4000–2500 Ma) records a transition from a likely hot, undifferentiated Earth to a Proterozoic Earth with many geological similarities to the modern day. The concept of a fundamental change in the rock record towards the end of the Archean (c. 3000 Ma) is not new. Lowe (1994) suggested that sedimentary rocks older than 3000 Ma record mainly oceanic spreading and hot spot volcanism, whereas those that formed after 3000 Ma typically record magmatism, deformation, and accretion along convergent plate margins.

Growth and evolution of continental crust

Models for the growth and evolution of the continental crust can be divided into those suggesting that most continental crust formed early in Earth's history (e.g. Armstrong, 1968; Bowring and Housh, 1995; Sylvester et al., 1997) and those proposing constant or episodic growth throughout geological time (Hurley and Rand, 1969; Veizer and Jansen, 1979; McLennan and Taylor, 1982; Nelson and DePaolo, 1985). Much of the early continental crust has been efficiently recycled or buried, leaving scattered inliers of Archean (>2500 Ma) material. A review by Eriksson (1995) of isotopic continental crust growth models shows a broad agreement, from different isotopic systems, for a model involving slow rates of growth to 3000 Ma, rapid growth between 3000–2500 Ma, and slower growth post-2500 Ma (Fig. 77). The study of Collerson and Kamber (1999) on depleted mantle Th–U–Nb systematics favours a similar crustal growth model.

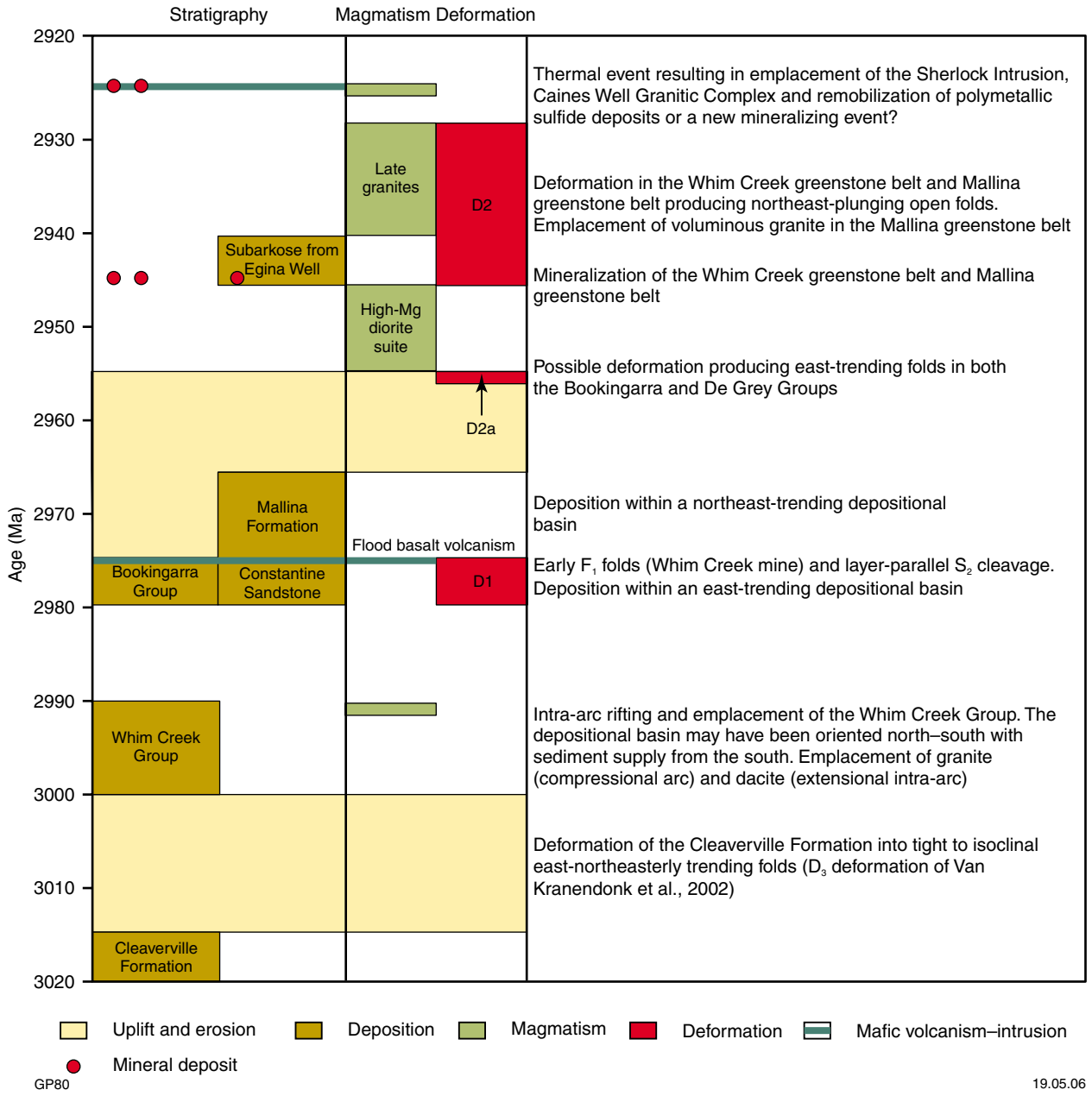

Figure 76. Summary diagram illustrating the evolution of the central portion of the northern Pilbara Craton (from Pike, 2001). The diagram is modified from Smithies et al. (2001), and includes additional work from Van Kranendonk et al. (2002)

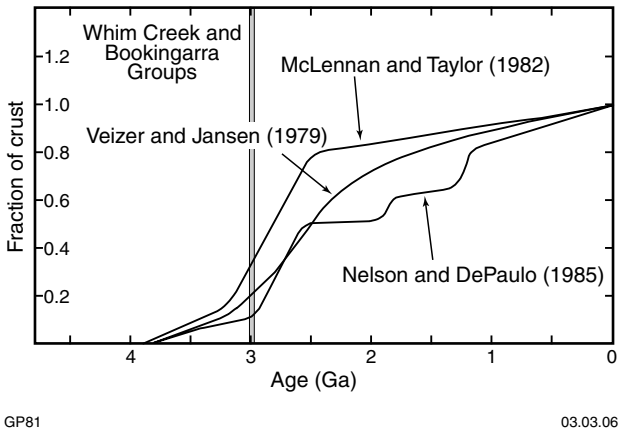

Figure 77. Graph of fractionation of continental crust versus time (from Eriksson, 1995). Eriksson (1995) summarized the work of Veizer and Jansen (1979), McLennan and Taylor (1982), and Nelson and DePaulo (1985). These authors agreed that the present volume of continental crust is the maximum volume yet attained, and that a large change in the volume of continental crust occurred between 3000 and 2500 Ma. The depositional time frame of the Whim Creek and Bookingarra Groups is shown in grey

Global analogues for the Whim Creek Group – Mallina Basin succession

The following section briefly reviews some of the best studied potential analogues for the Whim Creek greenstone belt.

Ravensthorpe greenstone belt, Yilgarn Craton (Witt, 1999)

The Ravensthorpe greenstone belt of the Yilgarn Craton in Western Australia comprises three tectonic components: the Ravensthorpe Terrane, Carlingup Terrane, and Cocanarup greenstones. The Ravensthorpe Terrane contains a 3000–2950 Ma, calc-alkaline intrusive–extrusive association that is interpreted to be the product of continental island-arc magmatism in which continental crust played only a minor role in magma petrogenesis. The adjacent Carlingup Terrane is interpreted to have developed close to the Ravensthorpe Terrane based on similar ages. The Ravensthorpe Terrane appears to be geochemically, temporally, and stratigraphically analogous to the Whim Creek greenstone belt, but does not contain an unconformably overlying analogue of the Bookingarra Group. However, the Carlingup Terrane comprises an association of mafic to ultramafic rocks including aluminium-depleted komatiite, psammitic to pelitic sedimentary rocks, chert, and banded iron-formation, and is dated at 2958 ± 4 Ma. The Carlingup Terrane also contains polymictic conglomerates derived from the Ravensthorpe Terrane that imply a close association between the two terranes, and these are considered analogous to subaqueous fanglomerates of the Cistern Formation (Bookingarra Group) derived from reworking of the underlying Whim Creek Group.

Steep Rock and Lumby Lake greenstone belts, Superior Province, Canada (Tomlinson et al., 1999)

The Steep Rock and Lumby Lake greenstone belts are examples of 3000–2900 Ma crust in the western Superior Province of Canada. The Steep Rock greenstone belt overlies 3005 ± 5 Ma tonalite and comprises platformal sedimentary facies (150 m of quartzofeldspathic conglomerate, 500 m of stromatolitic limestone, 400 m of iron formation and Mn–Fe mudstone, 50–400 m of pyroclastic komatiite, and 5 km of mafic and subordinate felsic subaqueous volcanic rocks). The volcano-sedimentary succession contains abundant 2990–3000 Ma zircons, and felsic volcanic rocks dated at 2932 ± 2 Ma. The Lumby Lake greenstone belt contains dominantly volcanic rocks, including thick mafic pillow lavas, komatiite flows, pyroclastic rocks, felsic volcanic units, and chemical and clastic sediments. A felsic tuff contains zircons aged 2999 to 2903 Ma. Mafic rocks are subdivided into enriched komatiitic basalt, unfractionated komatiitic basalt, spinifex-textured komatiitic basalt, and basaltic to andesitic lava. Enriched komatiitic basalt is interpreted as the product of a deep plume source, whereas the unfractionated komatiitic basalt and other basalts are interpreted as the products of the plume head and depleted upper mantle respectively. The mafic and ultramafic association was emplaced in a continental setting preceded by rifting of the continental crust.

North Caribou greenstone belt, Superior Province, Canada (Hollings and Kerrich, 1999)

The c. 3000 Ma North Caribou greenstone belt, Superior Province comprises four supracrustal assemblages. These are the 2980 Ma Aguta Arm assemblage of arc-related volcanic rocks, Keeyask assemblage of quartz-rich sedimentary rocks, McGruer volcanic assemblage, and the Eyapamikama assemblage containing rocks of a submarine turbidite fan. The McGruer volcanic assemblage includes massive and pillowed mafic flows with felsic and intermediate volcanic units and subordinate ultramafic flows. An age of c. 2932 Ma is obtained from the assemblage and the mafic–volcanic assemblage has depositional contacts with the underlying Keeyask assemblage. The North Caribou greenstone belt thus represents quartz-rich sedimentary rocks overlain by mafic and ultramafic volcanic rocks that are probably younger than arc-related volcanic rocks. Trace element systematics are used to suggest the presence of both tonalite–trondhjemite–granodiorite-contaminated komatiite that was erupted through continental crust and uncontaminated tholeiites. The former is considered to have had an important role in the assembly of terranes of the North Caribou belt from 2980 and 2871 Ma, and plume magmatism is considered to have been a major contributor to the growth of the proto-continental Superior Province.

Other analogous terranes and basins

The Keeyask Lake sedimentary assemblage in the North Caribou greenstone belt of the Superior Province of Canada is considered one of many examples of regional c. 3000 Ma quartz arenite-rich sedimentary successions (Donaldson and de Kemp, 1998). Similar quartz-rich sedimentary successions from the Superior Province have maximum ages of older than 3004 to 2959 Ma, and are interpreted as fluvial to shallow-water successions deposited over relatively stable continental crust (Donaldson and de Kemp, 1998). The relationship between quartz-rich sandstones and ultramafic rocks has been considered uncharacteristic of younger terranes, and is interpreted to represent emplacement of ultramafic sills and flows in regions of thin but stable crust (Donaldson and de Kemp, 1998). Wyche et al. (2004) discussed a quartzite–metabasalt succession that they suggested may have covered much of the central and western Yilgarn Craton in Western Australia. The succession comprises a lowermost quartzite that passes upward through muscovite-bearing quartzite into mafic and ultramafic schist (with lesser banded iron-formation), and finally tholeiitic basalt lava. There is no obvious unconformity in the succession, and a population of detrital zircons gives a maximum age of c. 3060 Ma (Nelson, 2001).

An assessment of Archean synrift and stable-shelf sedimentary successions (Eriksson and Fedo, 1994) documents other potential analogue systems. Rocks from the Limpopo Province (southern Africa) and Dharwar Craton (India) appear to be of similar age and original lithology as those of the Mallina Basin (Eriksson and Fedo, 1994), but have not yet been studied in detail. The Nsuze Group (Pongola Supergroup) of the Kaapvaal Craton (southern Africa) comprises quartz wacke and feldspathic arenite with lesser conglomerate. These sedimentary rocks are associated with basalt and basaltic andesite of several kilometres thickness, but at c. 3100 Ma may be older than the other successions documented so far. The succession is interpreted as an intracratonic rift and stratigraphically overlying successions (e.g. Witwatersrand Supergroup and Mozaan Group) deposited between 2940 and 2870 Ma contain similar, quartz-dominated sedimentary facies, but do not show a significant mafic component.

A 4 km-thick quartzite – shale – mafic volcanic association from the 3100–2900 Ma Buhwa greenstone belt in the Zimbabwe Craton in southern Africa (Fedo and Eriksson, 1996) comprises a shelf association and 4.4 km-thick basinal association. The basinal association includes greenstones, metachert, and iron formation. The shelf association includes 1 km of quartz arenite and shale, 1 km of shale (with quartz arenite, conglomerate, and limestone), 500 m of iron formation, and 500 m of hematite-rich and quartz-rich silty shale and greenstone. A shelf and deep-water passive-margin origin is favoured, and suggests that a phase of rifting of the passive margin succession was responsible for the mafic component. The quartzite–shale – mafic volcanic association from the Buhwa greenstone belt is interpreted as one of several quartzite–shale – iron formation successions in southern Africa that represent widespread shelf sedimentation at c. 3000 Ma.

Quartz arenite – shale – basalt association

The examples presented above suggest that a distinctive lithological association may be common in 3000–2900 Ma successions. The association comprises a sedimentary component of quartz-rich conglomerate, quartz arenite or wacke with fine-grained detrital and chemical sedimentary rocks including chert, shale, iron formation, banded iron-formation, and carbonate. A volcanic component includes komatiite, komatiitic basalt, and high- and low-Ti basalt that typically form extensive lava flows with abundant volcaniclastic breccia and subvolcanic intrusions. This association is termed the quartz arenite – shale – basalt association. Eriksson et al. (1994) recognized six lithological associations within Archean successions and suggested that, despite compositional differences, there is considerable overlap of stratigraphic style with Phanerozoic depositional systems. The quartz arenite – shale – basalt association groups together some of the units from the mafic–ultramafic volcanic and conglomerate–arenite associations of Eriksson et al. (1994), and suggests an intimate relationship between the processes that resulted in the development of thick, siliciclastic sedimentary basins and those that produced large amounts of mafic magma.

Evidence for crustal growth between 3000 and 2900 Ma

A review of U–Pb SHRIMP zircon geochronological data by Condie (1998) identified two abundance peaks of Archean age. By far the largest peak is at c. 2700 Ma, but a smaller peak is evident at c. 2950 Ma. Condie (1998) related these peaks to major geological events and, in turn, to continental growth. The small size of the c. 2950 Ma age abundance peak may not accurately reflect the true significance or scale of geological events at that time because of bias inherent in restricting the analyses to SHRIMP zircon data. Older rocks are typically buried by younger material, and therefore the area exposed for sampling is reduced. Successive events (e.g. at 2700 Ma) may also act to remove older components by crustal recycling and resetting of U–Pb ages during crustal melting. In addition, earlier events would have affected an Earth with smaller volumes of continental crust. Interaction of mantle melts with oceanic-like crust would not be expected to form melts capable of crystallization of abundant zircon. Conversely, later events would have resulted in heating and crustal anatexis of much larger volumes of continental crust.

Neodymium-isotope studies of the western Superior Province in Canada by Henry et al. (2000) supported the suggestion of a major tectonic event at c. 3000 Ma, and provided further evidence for significant crustal growth at that time. This study indicates that the western Superior Province formed in three main events at 3400 ± 100, 3020–2920, and 2760–2690 Ma, and that about 45% of the total crust formed in the 3020–2920 Ma event.

There is an obvious overlap in ages between the major crust-forming event in Canada (Henry et al., 2000) and the evolution of the Whim Creek Group – Mallina Basin system. Recent mapping of the nothern Pilbara Craton suggests that sedimentary packages of similar age to rocks of the Mallina Basin outcrop in other areas of the craton. An implication could be that the present extent of the Mallina Basin records only the preserved root of a basin that once extended over a much wider area, and the 3010–2950 Ma rocks of the Mallina Basin (and equivalents) may once have formed a significant portion of the Archean Pilbara crust. New work by Wyche et al. (2004) could be interpreted as consistent with a similarly large basin that covered the developing Yilgarn Craton at a similar age.

The evidence presented by Condie (1998) and Henry et al. (2000) is consistent with a significant global Archean tectonic event at c. 3000 Ma, whereas the work of Eriksson (1995) suggests a change in the rate of crustal growth. Thus, the smooth crustal extraction curves of Eriksson (1995) may be 'stepped' in reality, with two major steps at c. 3000 and c. 2700 Ma. The evolution of the Mallina Basin at this time reflects a major regional tectonic process or event. The recognition of similar supracrustal packages on other continents suggests a globally significant phenomenon. This was partly suggested by

Lowe (1994) with the recognition that sedimentation styles changed from chemical to dominantly siliciclastic at about that time. It is possible, therefore, that the quartz arenite – shale–basalt association marks a significant transition from submerged basins largely free of detrital siliciclastic sediment to siliciclastic-rich basins. This transition resulted in subaerial erosion and the earliest formation of thick intra-continental rift basins.

Possible changes in crustal evolution during the Archean

The following events are important in the present model:

- subaerial erosion or rift-basin formation over continental basement at 2950 ± 30 Ma;
- widespread and ?voluminous mafic–ultramafic volcanism at 2950 ± 30 Ma;
- change from dominantly chemical to siliciclastic sedimentation (e.g. Lowe, 1994);
- the first peak in U–Pb SHRIMP zircon analyses at 2950 Ma (Condie, 1998);
- isotopic evidence for a rate increase in continental crust growth (Eriksson, 1995);
- Nd-isotope evidence for significant 3020–2920 Ma crustal growth (Henry et al., 2000);
- igneous rocks showing strong evidence for derivation from a subduction-enriched mantle wedge first appeared at 3000 ± 20 Ma (Smithies et al., 2003).

The timing of crustal growth is relatively well constrained. Condie's (1998) 2950 Ma peak in zircon ages may reflect crustal extraction or recycling and gives a minimum age. The 2950 ± 30 Ma rocks of the sandstone–shale–basalt association were deposited in continental rift or passive margin basins that clearly show the presence of older eroding continents. The Nd-isotope work of Henry et al. (2000) gives an age of 3020–2920 Ma that represents extraction of material from the mantle. This work agrees with the recognition of the first clear evidence for subduction-modified mantle source regions at c. 3000 Ma (Smithies et al., 2003). The model of c. 3000 Ma continental crust evolution presented here thus involves the initiation of subduction and arc formation – crustal extraction at 3020–2980 Ma. This is followed by arc accretion and recycling of crust (<3010 Ma), and then by widespread subaerial erosion and formation of a first-order unconformity (<3010 Ma). Finally, continental rifting led to basin formation and mafic–ultramafic magmatism (2980–2920 Ma).

Two sources of continental crust are considered important: material extracted from an enriched mantle wedge above a subducting slab, and material derived during partial melting of upwelled nonenriched mantle. The relative contribution of these components is unknown. However, both appear to have contributed to the evolution of the Mallina Basin (Smithies and Champion, 2000; Van Kranendonk et al., 2002).

Conclusions

Lithologically and chronologically similar successions to the Whim Creek and Bookingarra Groups are described from Australia, Africa, Asia, Europe, and North and South America. A typical succession comprises a 3000 ± 20 Ma arc-related succession overlain unconformably by 2950 ± 50 Ma sandstone–shale–basalt association rocks. This succession suggests a general model of arc accretion, resulting in continent construction, followed by rifting of these continental blocks with significant contribution from mantle melt. The relative contribution to new crust of material from either a sub-arc mantle wedge or a plume (and adiabatic upper mantle melts) is unclear, but the former was probably dominant.

A major global event of crust generation at c. 2700 Ma is indicated by the vast areas of rocks of this age, and also by the abundance of U–Pb SHRIMP zircon analyses of this age. The global extent of older crust-forming events is more difficult to assess due to greater fragmentation and reworking. However, the present study supports a 3020–2920 Ma global event that formed crust with a distinctive lithological character. This interpretation is consistent with episodic crustal growth dominated by plate-tectonic processes, and suggests a nonlinear crustal extraction curve. Proof of a 3020–2920 Ma global event will require considerably more study of ancient rocks.

Acknowledgements

The authors are indebted to the School of Earth Sciences, Monash University, for support of this project throughout G. Pike's PhD candidature. Straits Resources Ltd, and in particular Bruce Hooper, is acknowledged for generous field and logistical support. R. Hugh Smithies (GSWA) and Dave Huston (GA) are thanked for considerable scientific input into the study, and Arthur Hickman, Alan Thorne, Bruce Groenewald, and Caroline Strong (all from GSWA) are thanked for reviewing and editing this report and the accompanying maps. Steve Beresford, Mark Tait, Jessica Trofimovs, and the Monash University volcanologists are thanked for their scientific input, friendship, and support. The Bicentennial Gold '88 Endowment and Society of Economic Geology, who have proven generous supporters of field-based research, also gave financial support. Finally, G. Pike thanks the governments and people of Australia for providing the opportunity to work in the beautiful northwest of Western Australia.

References

ALLEN, S. R., and McPHIE, J., 2000, Water-settling and resedimentation of submarine rhyolitic pumice at Yali, eastern Aegean, Greece: Journal of Volcanology and Geothermal Research, v. 95, p. 285–307.

ARMSTRONG, R. L., 1968, A model for the evolution of strontium and lead isotopes in a dynamic Earth: Reviews of Geophysics, v. 6, p. 175–199.

ARNDT, N., CZAMANSKE, G. K., WOODEN, J. L., and FEDORENKO, V. A., 1993, Mantle and crustal contributions to continental flood volcanism: Tectonophysics, v. 223, p. 30–52.

BARLEY, M. E., 1987, The Archaean Whim Creek Belt, an ensialic fault-bounded basin in the Pilbara Block, Australia: Precambrian Research, v. 37, p. 199–215.

BARLEY, M. E., McNAUGHTON, N. J., WILLIAMS, I. S., and COMPSTON, W., 1994, Geological Note: Age of Archaean volcanism and sulphide mineralization in the Whim Creek Belt, west Pilbara: Australian Journal of Earth Sciences, v. 41, p. 175–177.

BEINTEMA, K. A., 2003, Geodynamic evolution of the West and Central Pilbara Craton in Western Australia: a mid-Archaean active continental margin: The Netherlands, Utrecht University, Faculty of Earth Sciences, Geologica Ultraiectina, PhD thesis (unpublished).

BLACK, S. J., 1998, Genesis of the Whim Creek sediment-hosted volcanogenic massive sulphide deposit, Western Australia: Perth, Western Australia, Curtin University of Technology, BSc (Honours) thesis (unpublished).

BLEWETT, R. S., 2000, A 'virtual' structural field trip of the North Pilbara Craton: Australian Geological Survey Organisation, Record 2000/45, <http://www.ga.gov.au/rural/projects/pilbara/html_web2/frame3.htm>.

BOWRING, S. A., and HOUSH, T., 1995, The Earth's early evolution: Science, v. 269, p. 1535–1540.

BUSBY, C. J., SMITH, D., MORRIS, W., and FACKLER-ADAMS, B. N., 1998, Evolutionary model for convergent margins facing large ocean basins; Mesozoic Baja California, Mexico: Geology (Boulder), v. 26, p. 227–230.

CABANIS, B., and LECOLLE, M., 1989, Le diagramme La/10–Y/15–Nb/8; un outil pour la discrimination des series volcaniques et la mise en evidence des processus de melange et/ou de contamination crustale; The La/10-Y/15-Nb/8 diagram; a tool for distinguishing volcanic series and discovering crustal mixing and/or contamination: Comptes Rendus de l'Academie des Sciences, Serie 2, Mecanique, Physique, Chimie, Sciences de l'Univers, Sciences de la Terre, v. 309, p. 2023–2029.

CAREY, S. N., 2000, Volcaniclastic sedimentation around island arcs, *in* Encyclopedia of volcanoes *edited by* H. SIGURDSSON, B. F. HOUGHTON, S. R. McNUTT, H. RYMER, and J. STIX: London, United Kingdom, Academic Press, p. 627–642.

CAS, R. A. F., 1992, Submarine volcanism; eruption styles, products, and relevance to understanding the host-rock successions to volcanic-hosted massive sulfide deposits. A special issue devoted to Australian volcanic-hosted massive sulfide (VHMS) deposits and their volcanic environment: Economic Geology and the Bulletin of the Society of Economic Geologists, v. 87, p. 511–541.

COLLERSON, K. D., and KAMBER, B. S., 1999, Evolution of the continents and the atmosphere inferred from Th–U–Nb systematics of the depleted mantle: Science, v. 283, p. 1519–1522.

COLLINS, P. L. F., and MARSHALL, A. E., 1999, Volcanogenic base metal deposits of the Whim Creek Belt, *in* Lead, zinc and silver deposits of Western Australia *by* K. M. FERGUSON: Western Australia Geological Survey, Mineral Resources Bulletin, v. 15, p. 44–73.

CONDIE, K. C., 1998, Episodic continental growth and supercontinents; a mantle avalanche connection?: Earth and Planetary Science Letters, v. 163, p. 97–108.

CONDIE, K. C., 2000, Episodic continental growth models: afterthoughts and extensions: Tectonophysics, v. 322, p. 153–162.

DONALDSON, J. A., and de KEMP, E. A., 1998, Archaean quartz arenites in the Canadian Shield; examples from the Superior and Churchill provinces: Precambrian clastic sedimentation systems: Sedimentary Geology, v. 120, p. 153–176.

DRUMMOND, M. S., DEFANT, M. J., and KEPEZHINSKAS, P. K., 1996, Petrogenesis of slab-derived trondhjemite–tonalite–dacite/adakite magmas: Transactions of the Royal Society of Edinburgh, Earth Science, v. 87, p. 205–215.

ERIKSSON, K. A., 1995, Crustal growth, surface processes, and atmospheric evolution of the early Earth, *in* Early Precambrian processes *edited by* M. P. COWARD and A. C. RIES: London, United Kingdom, The Geological Society, Special Publication, no. 95, p. 11–25.

ERIKSSON, K. A., and FEDO, C. M., 1994, Archean synrift and stable-shelf sedimentary successions, *in* Archean crustal evolution *edited by* K. C. CONDIE: Amsterdam, The Netherlands, Elsevier, Developments in Precambrian Geology, no. 11, p. 171–204.

ERIKSSON, K. A., KRAPEZ, B., and FRALICK, P. W., 1994, Sedimentology of Archean greenstone belts; signatures of tectonic evolution: Earth-Science Reviews, v. 37, p. 1–88.

FEDO, C. M., and ERIKSSON, K. A., 1996, Stratigraphic framework of the approximately 3.0 Ga Buhwa greenstone belt; a unique stable-shelf succession in the Zimbabwe Archean craton: Precambrian Research, v. 77, p. 161–178.

FISHER, R. V., and SCHMINCKE, H.-U., 1984, Pyroclastic rocks: New York, U.S.A., Springer-Verlag, 472p.

FITTON, M. J., HORWITZ, R. C., and SYLVESTER, G. C., 1975, Stratigraphy of the early Precambrian of the west Pilbara, Western Australia: Australia CSIRO, Mineral Research Laboratories, Report FP11, 41p.

FÖRSTER, H.-J., TISCHENDORF, G., and TRUMBULL, R. B., 1997, An evaluation of the Rb vs. (Y + Nb) discrimination diagram to infer tectonic setting of silicic igneous rocks: Lithos, v. 40, p. 261–293.

HENRY, P., STEVENSON, R. K., LARBI, Y., and GARIEPY. C., 2000, Nd isotopic evidence for early to late Archean (3.4–2.7 Ga) crustal growth in the western Superior Province (Ontario, Canada): Tectonophysics, v. 322, p. 135–151.

HICKMAN, A. H., 1983, Geology of the Pilbara Block and its environs: Western Australia Geological Survey, Bulletin 127, 268p.

HICKMAN, A. H., 1997, A revision of the stratigraphy of Archaean greenstone successions in the Roebourne–Whundo area, west Pilbara: Western Australia Geological Survey, Annual Review 1996–97, p. 76–81.

HICKMAN, A. H., 2000, Roebourne, W.A. Sheet 2356: Western Australia Geological Survey, 1:100 000 Geological Series.

HICKMAN, A. H., 2001, Geology of the Dampier 1:100 000 sheet: Western Australia Geological Survey, 1:100 000 Geological Series Explanatory Notes, 39p.

HICKMAN, A. H., 2004, Two contrasting granite–greenstones terranes in the Pilbara Craton, Australia: evidence for vertical and horizontal tectonic regimes before 2900 Ma: Precambrian Research, v. 131, p. 153–172.

HICKMAN, A. H., and SMITHIES, R. H., 2001, Roebourne, W.A. (2nd edition): Western Australia Geological Survey, 1:250 000 Geological Series Explanatory Notes, 52p.

HICKMAN, A. H., and SMITHIES, R. H., in prep., Geology and mineral potential of the northwestern Pilbara Craton, Western Australia: Western Australia Geological Survey Report 92.

HOLLINGS, P., and KERRICH, R., 1999, Trace element systematics of ultramafic and mafic volcanic rocks from the 3 Ga North Caribou greenstone belt, northwestern Superior Province: Precambrian Research, v. 93, p. 257–279.

HORWITZ, R. C., 1990, Palaeogeographic and tectonic evolution of the Pilbara Craton, northwestern Australia: Precambrian Research, v. 48, p. 327–340.

HURLEY, P. M., and RAND, J. R., 1969, Pre-drift continental nuclei: Science, v. 164, p. 1229–1242.

HUSTON, D. L., SMITHIES, R. H., and SUN, S-S., 2000, Correlation of the Mallina–Whim Creek Basin: implications for base metal potential of the central part of the Pilbara granite–greenstone terrane: Australian Journal of Earth Sciences, v. 47, p. 217–230.

IRVINE, T. N., and BARAGAR, W. R. A., 1971, A guide to the chemical classification of the common volcanic rocks: Canadian Journal of Earth Sciences, v. 8, p. 523–548.

JENSEN, L. S., and PYKE, D. R., 1982, Komatiites in the Ontario portion of the Abitibi Belt, *in* Komatiites *edited by* N. T. ARNDT and E. G. NISBET: London, United Kingdom, George Allen and Unwin, p. 147–157.

KAMENETSKY, V. S., BINNS, R. A., GEMMELL, J. B., CRAWFORD, A. J., MERNAGH, T. P., MAAS, R., and STEELE, D., 2001, Parental basaltic melts and fluids in eastern Manus backarc basin; implications for hydrothermal mineralisation: Earth and Planetary Science Letters, v. 184, p. 685–702.

KOKELAAR, B. P., 1982, Fluidisation of wet sediments during the emplacement and cooling of various igneous bodies: Journal of the Geological Society of London, v. 139, p. 21–33.

KRAPEZ, B., and EISENLOHR, B., 1998, Tectonic settings of Archaean (3325–2775 Ma) crustal–supracrustal belts in the West Pilbara Block: Precambrian Research, v. 88, p. 173–205.

KUNO, H., 1968, Differentiation of basalt magmas, *in* Basalts — The Poldervaart treatise on rocks of basaltic composition *edited by* H. H. HESS and A. POLDERVAART: New York, U.S.A., Interscience, v. 2, p. 623–688.

LOFGREN, G., 1971, Experimentally produced devitrification textures in natural rhyolitic glass: Geological Society of America, Bulletin, v. 82, p. 111–123.

LOWE, D. R., 1994, Archean greenstone-related sedimentary rocks, *in* Archean crustal evolution *edited by* K. C. CONDIE: Amsterdam, The Netherlands, Elsevier, Developments in Precambrian Geology, no. 11, p. 121–169.

McARTHUR, A. N., CAS, R. A. F., and ORTON, G. J., 1998, Distribution and significance of crystalline, perlitic and vesicular textures in the Ordovician Garth Tuff (Wales): Bulletin of Volcanology, v. 60, p. 260–285.

McLENNAN, S. M., and TAYLOR, S. R., 1982, Geochemical constraints on the growth of the continental crust: Journal of Geology, v. 90, p. 347–361.

McPHIE, J., DOYLE, M., and ALLEN, R. L., 1993, Volcanic Textures: a guide to the interpretation of textures in volcanic rocks: Hobart, Tasmania, University of Tasmania, Centre for Ore Deposit and Exploration Studies, 198p.

MESCHEDE, M., 1986, A method of discriminating between different types of mid-ocean ridge basalts and continental tholeiites with the Nb–Zr–Y diagram: Chemical Geology, v. 56, p. 207–218.

MILLER, L. J., and GAIR, H. S., 1975, Mons Cupri copper–lead–zinc–silver deposit, *in* Economic Geology of Australia and Papua New Guinea — 1. Metals *edited by* C. L. KNIGHT: The Australasian Institute of Mining and Metallurgy, Monograph 5, p. 195–202.

MILLS, A. A., 1984, Pillow lavas and the Leidenfrost effect: Journal of the Geological Society of London, v. 141, p. 183–186.

MORROW, N., and McPHIE, J., 2000, Mingled silicic lavas in the Mesoproterozoic Gawler Range Volcanics, South Australia: Journal of Volcanology and Geothermal Research, v. 96, p. 1–13.

MULLEN, E. D., 1983, $MnO/TiO_2/P_2O_5$; a minor element discriminant for basaltic rocks of oceanic environments and its implications for petrogenesis: Earth and Planetary Science Letters, v. 62, p. 53–62.

NELSON, D. R., 1997, Compilation of SHRIMP U–Pb zircon geochronology data, 1996: Western Australia Geological Survey, Record 1997/2, 187p.

NELSON, D. R., 1998, Compilation of SHRIMP U–Pb zircon geochronology data, 1997: Western Australia Geological Survey, Record 1998/2, 242p.

NELSON, D. R., 2000, Compilation of SHRIMP U–Pb zircon geochronology data, 1999: Western Australia Geological Survey, Record 2000/2, 251p.

NELSON, D. R., 2001, An assessment of the determination of depositional ages for Precambrian clastic sedimentary rocks by U–Pb dating of detrital zircons: Sedimentary Geology, v. 141–142, p. 37–60.

NELSON, B. K., and DePAOLO, D. J., 1985, Rapid production of continental crust 1.7 to 1.9 b.y. ago: Nd isotopic evidence from the basement of the North American-midcontinent: Geological Society of America, Bulletin, v. 96, p. 746–754.

OLSEN, K. H., and MORGAN, P., 1995, Progress in understanding continental rifts, *in* Continental rifts; evolution, structure, tectonics *edited by* K. H. OLSEN: Amsterdam, The Netherlands, Elsevier, Developments in Geotectonics 25, p. 3–26.

PEARCE, J. A., 1982, Trace element characteristics of lavas from destructive plate boundaries, *in* Andesites; orogenic andesites and related rocks *edited by* R. S. THORPE: Berlin, Germany, Springer-Verlag, 390p.

PEARCE, J. A., 1983, Role of the sub-continental lithosphere in magma genesis at active continental margins, *in* Continental basalts and mantle xenoliths *edited by* C. J. HAWKESWORTH and M. J. NORRY: Nantwitch, United Kingdom, Shiva Geology Series, 272p.

PEARCE, J. A., HARRIS, N. B. W., and TINDLE, A. G., 1984, Trace element discrimination diagrams for the tectonic interpretation of granitic rocks: Journal of Petrology, v. 25, p. 956–983.

PICHLER, H., 1965, Acid hyaloclastites: Bulletin of Volcanology, v. 28, p. 293–310.

PIKE, G., 2001, Facies architecture of two contrasting volcano-sedimentary basin successions from the Archaean Whim Creek Belt, North Pilbara Terrain, Western Australia: the intra-continental arc-related Whim Creek Group and plume-related, continental rift-hosted Bookingarra Group: Victoria, Monash University, Department of Earth Sciences, PhD thesis (unpublished).

PIKE, G., and CAS, R. A. F., 2002, Stratigraphic evolution of Archaean volcanic rock-dominated rift basins from the Whim Creek Belt, west Pilbara Craton, Western Australia: International Association of Sedimentologists, Special Publication 33, p. 213–234.

PIKE, G., CAS, R., and SMITHIES, R. H., 2002, Geological constraints on base metal mineralization of the Whim Creek greenstone belt, Pilbara Craton, Western Australia: Economic Geology, v. 97, p. 827–845.

PROSSER, S., 1993, Rift-related linked depositional systems and their seismic expression, *in* Tectonics and seismic sequence stratigraphy *edited by* G. D. WILLIAMS and A. DOBB: London, United Kingdom, The Geological Society, Special Publication, no. 71, p. 35–66.

RAVNÅS, R., and STEEL, R. J., 1998, Architecture of marine rift-basin successions: American Association of Petroleum Geologists, Bulletin, v. 82, p 110–146.

RIGGS, N. R., and BUSBY-SPERA, C. J., 1991, Facies analysis of an ancient, dismembered, large caldera complex and implications for intra-arc subsidence; Middle Jurassic strata of Cobre Ridge, southern Arizona, USA: Sedimentary Geology, v. 74, p. 39–68.

RUDDOCK, I., 1999, Mineral occurrences and exploration potential of the west Pilbara: Western Australia Geological Survey, Report 70, 63p.

SHANMUGAM, G., 1997, The Bouma Sequence and the turbidite mind set: Earth-Science Reviews, v. 42, p. 201–229.

SMITH, G. A., and LANDIS, C. A., 1995, Intra-arc basins, *in* Tectonics of sedimentary basins *edited by* C. J. BUSBY and R. V. INGERSOLL: London, United Kingdom, Blackwell Science, p. 263–298.

SMITH, J. B., BARLEY, M. E., GROVES, D. I., KRAPEZ, B., McNAUGHTON, N. J., BICKLE, M. J., and CHAPMAN, H. J., 1998, The Sholl Shear Zone, West Pilbara: evidence for a domain boundary structure from integrated tectonic analyses, SHRIMP U–Pb dating and isotopic and geochemical data of granitoids: Precambrian Research, v. 88, p. 143–171.

SMITHIES, R. H., 1998, Geology of the Sherlock 1:100 000 sheet: Western Australia Geological Survey, 1:100 000 Geological Series Explanatory Notes, 29p.

SMITHIES, R. H., 1999, Geology of the Yule 1:100 000 sheet: Western Australia Geological Survey, 1:100 000 Geological Series Explanatory Notes, 15p.

SMITHIES, R. H., and CHAMPION, D. C., 2000, The Archaean high-Mg diorite suite: links to tonalite–trondhjemite–granodiorite magmatism and implications for early Archaean crustal growth: Journal of Petrology, v. 41, p. 1653–1671.

SMITHIES, R. H., CHAMPION, D. C., and CASSIDY, K. F., 2003, Formation of Earth's early Archaean continental crust: Precambrian Research, v. 127, p. 89–101.

SMITHIES, R. H., HICKMAN, A. H., and NELSON, D. R., 1999, New constraints on the evolution of the Mallina Basin, and their bearing on relationships between the contrasting eastern and western granite–greenstone terrains of the Archaean Pilbara Craton, Western Australia: Precambrian Research, v. 94, p. 11–28.

SMITHIES, R. H., NELSON, D. R., and PIKE, G., 2001, Detrital and inherited zircon age distributions — implications for the evolution of the Archaean Mallina Basin, Pilbara Craton, northwestern Australia: Sedimentary Geology, v. 141–142, p. 79–94.

SOWERBUTTS, A. A., and UNDERHILL, J. R., 1998, Sedimentary response to intra-arc extension; controls on Oligo-Miocene deposition, Sarcidano Sub-basin, Sardinia: Journal of the Geological Society of London, v. 155, p. 491–508.

SUGITANI, K., YAMAMOTO, K., ADACHI, M., KAWABE, I., and SUGISAKI, R., 1998, Archean cherts derived from chemical, biogenic, and clastic sedimentation in a shallow restricted basin: examples from the Gorge Creek Group in the Pilbara Block: Sedimentology, v. 45, p. 1045–1062.

SUN, S-S., and HICKMAN, A. H., 1998, New Nd-isotopic and geochemical data from the west Pilbara: implications for Archaean crustal accretion and shear zone development: Canberra, Australian Geological Survey Organisation, Research Newsletter, no. 28, p. 25–29.

SUN, S.-S., WALLACE, D. A., HOATSON, D. M., GLIKSON, A. Y., and KEAYS, R. R., 1991, Use of geochemistry as a guide to platinum group element potential of mafic–ultramafic rocks: examples from the west Pilbara Block and Halls Creek Mobile Zone, Western Australia: Precambrian Research, v. 50, p. 1–35.

SYLVESTER, P. J., CAMPBELL, I. H., and BOWYER, D. A., 1997, Niobium/uranium evidence for early formation of the continental crust: Science, v. 275, p. 521–523.

TOMLINSON, K.Y., HUGHES, D. J., THURSTON, P. C., and HALL, R. P., 1999, Plume magmatism and crustal growth at 2.9 to 3.0 Ga in the Steep Rock and Lumby Lake area, western Superior Province: Lithos, v. 46, p. 103–136.

TYLER, I. M., and HOCKING, R. M., 2001, Tectonic units of Western Australia (scale 1: 2 500 000): Western Australia Geological Survey.

VAN KRANENDONK, M. J., HICKMAN, A. H., SMITHIES, R. H., and PIKE, G., 2002, Geology and tectonic evolution of the Archaean North Pilbara Terrain, Pilbara Craton, Western Australia: Economic Geology, v. 97, p. 695–732.

VAN KRANENDONK, M. J., SMITHIES, R. H., HICKMAN, A. H., BAGAS, L., WILLIAMS, I. R., and FARRELL, T. R., 2004, Event stratigraphy applied to 700 million years of Archaean crustal evolution, Pilbara Craton, Western Australia: Western Australia Geological Survey, Annual Review 2003–04, p. 49–61.

VEIZER, J., and JANSEN, S. L., 1979, Basement and sedimentary recycling and continental evolution: Journal of Geology, v. 87, p. 341–370.

WALKER, R. G., 1975, Generalized facies models for resedimented conglomerates of turbidite association: Geological Society of America, Bulletin, v. 86, p. 737–748.

WALSH, J. J., and WATTERSON, J., 1991, Geometric and kinematic coherence and scale effects in normal fault systems, *in* The geometry of normal faults *edited by* A. M. ROBERTS, G. YIELDING, and B. FREEMAN: London, United Kingdom, The Geological Society, Special Publication no. 56, p. 193–203.

WILSON, C. J. N., HOUGHTON, B. F., McWILLIAMS, M. O., LANPHERE, M. A., WEAVER, S. D., and BRIGGS, R. M., 1995, Volcanic and structural evolution of Taupo volcanic zone, New Zealand; a review: Journal of Volcanology and Geothermal Research, v. 68, p. 1–28.

WINCHESTER, J. A., and FLOYD, P. A., 1977, Geochemical discrimination of different magma series and their differentiation products using immobile elements: Chemical Geology, v. 20, p. 325–343.

WITT, W. K., 1999, The Archaean Ravensthorpe Terrane, Western Australia; synvolcanic Cu–Au mineralization in a deformed island arc complex: Precambrian Research, v. 96, p. 143–181.

WYCHE, S., NELSON, D. R., and RIGANTI, A., 2004, 4350–3130 detrital zircons in the Southern Cross Granite–Greenstone Terrane, Western Australia: implications for the early evolution of the Yilgarn Craton: Australian Journal of Earth Sciences, v. 51, p. 31–56.

Appendix 1

Geochemistry of the Whim Creek Group and a granite

Sample no.	*99-0938*	*99-0989*	*99-1003*	*99-1123*	*99-1124*	*99-1125*	*99-1132*	*99-1136*
Unit and rock type	*SD*	*SD*	*SD*	*SD*	*SD*	*SD*	*SD*	*SD*
Rock type	*Rhyodacite/*	*Rhyodacite/*	*Rhyodacite/*	*Rhyodacite/*	*Rhyodacite/*	*Rhyodacite/*	*Rhyodacite/*	*Rhyodacite*
(Winchester and Floyd, 1977)	*dacite*	*dacite*	*dacite*	*dacite*	*dacite*	*dacite*	*dacite*	*dacite*
MGA coordinate (Northing)	*7682734*	*7682011*	*7683048*	*7683017*	*7683090*	*7681718*	*7682907*	*7682637*
MGA coordinate (Easting)	*570899*	*573476*	*570847*	*571477*	*572334*	*573516*	*555528*	*554835*
Rock type (SiO_2 classification)	*Rhyolite*	*Rhyolite*	*Rhyolite*	*Rhyolite*	*Rhyolite*	*Rhyolite*	*Dacite*	*Rhyolite*
				Percentage				
SiO_2	73.47	72.19	70.68	71.08	74.50	75.55	69.15	70.87
TiO_2	0.46	0.49	0.41	0.47	0.41	0.43	0.52	0.45
Al_2O_3	11.79	12.69	12.49	12.40	12.08	11.19	12.85	12.57
Fe_2O_3 (tot)	2.69	2.19	2.40	3.51	2.93	1.65	4.69	3.69
MnO	0.10	0.11	0.13	0.12	0.09	0.13	0.12	0.11
MgO	0.41	0.51	0.46	0.55	0.48	0.38	0.81	0.70
CaO	1.18	1.40	2.24	1.48	0.82	1.02	1.76	1.25
Na_3O	3.07	3.84	3.08	3.42	3.60	2.65	4.27	3.89
K_3O	4.17	3.49	3.89	3.57	2.72	4.37	3.07	3.83
P_3O_5	0.10	0.12	0.11	0.11	0.11	0.10	0.14	0.11
MLOI	2.33	2.80	3.94	3.13	2.06	2.32	2.46	2.36
Rest	0.18	0.17	0.17	0.18	0.14	0.20	0.16	0.17
Total	**99.95**	**100.00**	**100.00**	**100.02**	**99.94**	**99.99**	**100.00**	**100.00**
				Parts per million				
Ag	-0.50	-0.50	-0.50	-0.50	-0.50	-0.50	-0.50	-0.50
As	2.90	2.20	1.40	0.50	3.30	1.30	2.10	1.60
Ba	881.00	749.00	841.00	796.00	625.00	975.00	599.00	750.00
Be	1.60	1.50	1.20	1.80	1.30	1.10	1.80	1.70
Bi	0.20	0.20	-0.10	-0.10	-0.10	-0.10	0.20	-0.10
Cr	-1.00	-1.00	-1.00	-1.00	-1.00	-1.00	2.00	-1.00
Cs	1.00	0.60	1.30	1.20	0.90	1.00	0.70	0.80
Cu	11.00	8.00	18.00	19.00	21.00	8.00	32.00	16.00
F	359.00	395.00	329.00	407.00	431.00	227.00	420.00	313.00
Ga	16.10	17.90	15.90	18.10	16.10	14.50	18.50	17.30
Ge	1.00	0.90	0.80	0.90	0.90	0.80	1.10	0.80
Li	6.00	6.00	8.00	8.50	8.00	4.00	7.50	8.50
Mo	0.80	1.10	0.40	0.80	0.80	1.10	1.10	0.90
Nb	10.10	10.50	8.40	9.90	8.10	10.00	8.60	8.70
Ni	7.00	3.00	3.00	2.00	3.00	3.00	6.00	4.00
Pb	9.00	14.50	7.50	9.00	8.00	48.50	32.00	16.50
Rb	105.00	115.00	116.00	112.00	85.00	109.00	101.00	105.00
S	290.00	160.00	140.00	120.00	350.00	190.00	200.00	120.00
Sb	1.00	0.80	1.20	1.00	1.60	1.40	0.40	1.40
Sc	11.00	12.00	9.00	11.00	11.00	9.00	12.00	11.00
Sn	2.00	2.00	1.00	2.00	1.00	2.00	1.00	1.00
Sr	85.00	110.00	103.00	126.00	104.00	83.00	151.00	119.00
Ta	1.00	1.00	1.00	1.00	1.00	1.00	1.00	1.00
Th	18.10	18.80	16.80	18.30	16.60	17.60	16.70	17.20
U	5.90	6.30	4.30	4.60	4.60	4.00	4.60	5.90
V	21.00	27.00	37.00	31.00	44.00	19.00	65.00	43.00
Zn	41.00	41.00	36.00	45.00	46.00	73.00	63.00	45.00
Zr	213.00	215.00	172.00	207.00	172.00	208.00	189.00	187.00
La	44.60	46.30	37.90	44.80	38.60	44.00	42.50	41.20
Ce	84.60	88.00	71.30	83.60	71.80	82.90	79.30	77.70
Pr	8.90	9.30	7.40	8.80	7.50	8.80	8.40	8.20
Nd	31.60	32.30	25.40	31.00	25.90	30.50	29.60	28.40
Sm	5.70	5.70	4.50	5.60	4.50	5.50	5.20	5.00
Eu	1.10	1.10	0.90	1.10	0.90	1.00	1.10	1.00
Gd	5.30	5.30	4.10	5.20	3.90	4.90	4.60	4.40
Tb	0.90	0.80	0.60	0.80	0.60	0.80	0.70	0.70
Dy	4.50	4.40	3.20	4.40	3.10	4.00	3.70	3.50
Ho	0.90	0.90	0.60	0.90	0.60	0.80	0.70	0.70
Er	2.80	2.60	1.80	2.60	1.90	2.50	2.20	2.20
Yb	2.70	2.50	1.70	2.60	1.90	2.40	2.10	2.10
Lu	0.40	0.40	0.30	0.40	0.30	0.40	0.30	0.30
Y	28.60	27.60	19.10	26.80	19.40	24.90	22.60	22.00

NOTES: MLOI=measured loss
Trace results in ppm. Negative result means less than detection limit, i.e. -0.5 means less than detection limit of 0.5 ppm
Mons Cupri Dacite Member: SD = spherulitic dacite, FPD = feldspar-phyric dacite, GD = grey dacite, sSD = sericitic spherulitic dacite
Bookingarra Group: KR = Kialrah Rhyolite
Warambie Basalt: WB = Warambie Basalt
Red Hill Volcanics: PB = Pumice breccia
Caines Well Granitic Complex: G = granite

Appendix 1 (continued)

Sample no.	*99-1134*	*99-0901*	*99-0902*	*99-0988*	*99-0964*	*99-0967*	*99-0972*	*99-1072*
Unit and rock type	*SD*	*SD*	*SD*	*SD*	*FPD*	*FPD*	*FPD*	*FPD*
Rock type	*Rhyodacite/*	*Rhyodacite/*	*Rhyodacite/*	*Rhyodacite/*	*Rhyodacite/*	*Rhyodacite/*	*Rhyodacite/*	*Rhyodacite/*
(Winchester and Floyd, 1977)	*dacite*	*dacite*	*dacite*	*dacite*	*dacite*	*dacite*	*dacite*	*dacite*
MGA coordinate (Northing)	*7682768*	*7683244*	*7683470*	*7682161*	*7682243*	*7681451*	*7680923*	*7683119*
MGA coordinate (Easting)	*555217*	*557859*	*557785*	*573464*	*574352*	*573563*	*574173*	*577343*
Rock type (SiO_2 classification)	*Rhyolite*	*Rhyolite*	*Rhyolite*	*Rhyolite*	*Dacite*	*Dacite*	*Rhyolite*	*Dacite*
				Percentage				
SiO_2	70.14	76.05	72.86	74.00	67.91	69.06	70.17	69.10
TiO_2	0.52	0.44	0.50	0.43	0.58	0.63	0.54	0.55
Al_2O_3	12.89	11.47	12.80	11.61	12.49	13.71	12.45	11.98
Fe_2O_3 (tot)	4.34	1.66	3.47	1.70	3.28	2.70	2.39	4.07
MnO	0.12	0.08	0.10	0.10	0.12	0.13	0.12	0.15
MgO	0.79	0.20	0.60	0.43	0.94	1.02	0.79	0.64
CaO	1.12	0.35	0.35	1.18	3.06	1.11	2.12	2.21
Na_3O	4.35	4.36	3.62	3.40	2.17	4.37	4.58	2.42
K_3O	3.23	2.87	3.71	4.24	3.38	3.19	2.17	4.56
P_3O_5	0.14	0.10	0.13	0.10	0.13	0.15	0.14	0.14
MLOI	2.21	2.26	1.65	2.61	5.72	3.50	4.35	3.75
Rest	0.17	0.17	0.19	0.20	0.20	0.33	0.16	0.19
Total	**100.02**	**100.01**	**99.98**	**100.00**	**99.98**	**99.90**	**99.98**	**99.76**
				Parts per million				
Ag	-0.50	-0.50	-0.50	-0.50	-0.50	-0.50	-0.50	-0.50
As	1.50	0.60	1.60	1.70	3.30	3.50	2.80	8.20
Ba	724.00	747.00	828.00	1 034.00	1 009.00	1 149.00	694.00	1 211.00
Be	1.80	1.10	2.00	1.10	2.20	1.90	1.90	1.40
Bi	-0.10	0.20	0.10	0.80	0.60	0.20	-0.10	0.10
Cr	2.00	-1.00	-1.00	-1.00	-1.00	-1.00	-1.00	-1.00
Cs	0.90	0.70	1.40	0.50	0.60	0.80	0.50	0.60
Cu	12.00	14.00	18.00	9.00	65.00	94.00	2.00	7.00
F	335.00	167.00	389.00	172.00	447.00	427.00	342.00	367.00
Ga	17.10	15.30	18.50	13.70	19.70	19.40	18.30	16.90
Ge	0.80	0.70	0.90	0.80	0.90	0.70	0.70	0.80
Li	9.50	4.50	11.00	5.50	9.50	7.50	4.00	6.00
Mo	0.80	0.70	0.70	1.00	1.80	0.80	0.40	1.40
Nb	8.60	9.70	8.80	10.10	9.80	10.30	8.80	8.80
Ni	5.00	8.00	5.00	1.00	9.00	6.00	4.00	3.00
Pb	12.50	26.50	33.50	41.00	19.50	158.00	8.00	11.50
Rb	93.00	71.00	153.00	95.00	100.00	79.00	63.00	105.00
S	110.00	140.00	200.00	100.00	210.00	640.00	220.00	1 030.00
Sb	1.20	0.40	0.80	0.60	0.40	1.00	1.40	1.20
Sc	12.00	9.00	11.00	9.00	7.00	9.00	9.00	7.00
Sn	1.00	2.00	2.00	-1.00	1.00	3.00	2.00	1.00
Sr	140.00	87.00	112.00	84.00	104.00	107.00	155.00	69.00
Ta	1.00	1.50	1.00	1.00	1.00	1.00	1.00	0.50
Th	17.00	17.40	17.10	17.90	12.20	13.10	11.60	11.00
U	4.60	4.30	4.60	4.10	3.00	3.60	2.60	2.90
V	67.00	20.00	57.00	17.00	15.00	20.00	19.00	15.00
Zn	55.00	43.00	53.00	19.00	29.00	880.00	30.00	48.00
Zr	188.00	204.00	188.00	209.00	264.00	265.00	240.00	228.00
La	42.30	42.50	43.90	44.00	46.50	46.60	39.70	40.40
Ce	78.90	79.20	82.60	82.60	88.40	88.80	76.40	77.40
Pr	8.40	8.40	8.70	8.80	9.60	9.70	8.30	8.40
Nd	29.20	29.10	29.60	30.60	34.50	35.40	29.90	30.30
Sm	5.10	5.10	5.10	5.70	6.50	6.60	5.50	5.70
Eu	1.10	1.00	0.90	1.20	1.40	1.50	1.20	1.30
Gd	4.70	4.40	4.50	5.50	6.00	6.10	5.10	5.40
Tb	0.70	0.70	0.70	0.90	0.90	1.00	0.80	0.80
Dy	3.60	3.60	3.60	4.60	4.70	5.00	3.80	4.30
Ho	0.70	0.70	0.70	0.90	0.90	1.00	0.70	0.80
Er	2.20	2.10	2.10	2.70	2.70	2.70	2.10	2.40
Yb	2.10	1.90	2.00	2.60	2.40	2.20	1.90	2.10
Lu	0.30	0.30	0.30	0.40	0.30	0.30	0.30	0.30
Y	22.20	21.70	22.10	27.50	26.70	28.10	21.70	24.40

Appendix 1 (continued)

Sample no.	*99-1122*	*99-1126*	*99-1137*	*99-0910*	*99-1216*	*99-1073*	*99-1127*
Unit and rock type	*FPD*	*FPD*	*FPD*	*FPD*	*KR*	*GD*	*GD*
Rock type	*Rhyodacite/*	*Rhyodacite/*	*Rhyodacite/*	*Rhyodacite/*	*Rhyodacite/*	*Low Si-*	*Low Si-*
(Winchester and Floyd, 1977)	*dacite*	*dacite*	*dacite*	*dacite*	*dacite*	*dacite*	*dacite*
MGA coordinate (Northing)	*7683297*	*7685512*	*7682536*	*7679036*	*1 m from*	*7683219*	*7685291*
MGA coordinate (Easting)	*571241*	*574574*	*554091*	*558837*	*GSWA 144261**	*577743*	*574672*
Rock type (SiO_2 classification)	*Rhyolite*	*Rhyolite*	*Rhyolite*	*Rhyolite*	*Rhyolite*	*Dacite*	*Dacite*
				Percentage			
SiO_2	71.94	70.06	70.51	70.56	71.44	69.87	67.39
TiO_2	0.61	0.61	0.60	0.61	0.61	0.65	0.63
Al_2O_3	11.77	11.66	12.37	13.12	12.97	13.67	13.20
Fe_2O_3 (tot)	4.50	7.49	4.24	4.68	3.82	3.40	4.76
MnO	0.20	0.14	0.11	0.11	0.09	0.09	0.11
MgO	0.58	0.64	0.48	0.56	0.34	0.67	1.07
CaO	0.82	0.61	0.89	0.82	0.57	1.08	1.91
Na_3O	3.95	2.48	2.94	3.92	3.49	3.17	3.68
K_3O	2.77	3.82	5.13	3.05	3.80	4.53	2.86
P_3O_5	0.13	0.15	0.14	0.14	0.16	0.16	0.18
MLOI	2.52	2.06	2.42	2.23	2.45	2.46	3.97
Rest	0.13	0.15	0.21	0.17	0.26	0.25	0.17
Total	**99.92**	**99.87**	**100.04**	**99.97**	**100.00**	**100.00**	**99.93**
				Parts per million			
Ag	-0.50	-0.50	-0.50	-0.50	-0.50	-0.50	-0.50
As	0.80	0.90	1.00	0.70	1.40	1.00	1.60
Ba	584.00	837.00	1 152.00	733.00	1 552.00	1 625.00	750.00
Be	1.60	1.10	1.00	2.00	1.40	2.20	1.60
Bi	-0.10	-0.10	-0.10	-0.10	-0.10	-0.10	-0.10
Cr	-1.00	-1.00	-1.00	-1.00	-1.00	-1.00	-1.00
Cs	0.30	0.70	0.60	0.60	1.10	0.60	1.10
Cu	14.00	22.00	10.00	24.00	16.00	3.00	23.00
F	385.00	597.00	312.00	439.00	385.00	571.00	528.00
Ga	17.10	22.90	17.20	20.90	20.30	18.30	18.60
Ge	0.70	1.10	0.80	1.00	0.80	0.80	0.90
Li	9.00	8.00	4.50	5.00	4.50	9.00	15.50
Mo	0.60	0.80	0.70	2.10	0.30	0.30	0.90
Nb	9.60	9.50	10.10	10.00	10.40	9.80	8.10
Ni	4.00	8.00	8.00	5.00	6.00	4.00	5.00
Pb	13.00	4.50	12.00	7.50	16.00	6.50	9.00
Rb	49.00	68.00	79.00	89.00	101.00	101.00	95.00
S	340.00	520.00	100.00	180.00	160.00	60.00	350.00
Sb	1.00	-0.20	0.40	0.20	1.40	1.00	1.20
Sc	5.00	8.00	6.00	9.00	7.00	9.00	16.00
Sn	-1.00	1.00	1.00	2.00	2.00	2.00	1.00
Sr	92.00	41.00	61.00	70.00	106.00	73.00	151.00
Ta	1.00	1.00	1.00	1.00	1.00	1.00	1.00
Th	10.40	10.60	11.10	11.70	12.10	13.20	15.60
U	1.80	2.40	2.40	3.00	3.10	3.40	4.00
V	13.00	15.00	13.00	13.00	17.00	22.00	103.00
Zn	37.00	79.00	53.00	70.00	75.00	30.00	64.00
Zr	241.00	248.00	248.00	271.00	264.00	255.00	186.00
La	43.10	42.20	44.20	44.70	39.90	34.40	41.40
Ce	84.50	81.60	86.00	86.40	78.20	65.80	77.70
Pr	9.40	9.10	9.60	9.40	8.50	7.10	8.30
Nd	34.50	33.20	35.30	34.10	31.10	26.00	28.90
Sm	6.30	6.20	6.40	6.50	6.00	4.80	5.10
Eu	1.40	1.40	1.40	1.40	1.30	1.00	1.20
Gd	5.90	5.50	5.60	6.20	5.90	4.60	4.70
Tb	0.90	0.90	0.90	1.00	1.00	0.80	0.70
Dy	4.30	4.30	4.20	5.20	4.90	3.90	3.80
Ho	0.80	0.90	0.80	1.00	0.90	0.80	0.80
Er	2.30	2.50	2.30	2.90	2.70	2.30	2.30
Yb	2.10	2.30	2.10	2.50	2.40	2.10	2.20
Lu	0.30	0.30	0.30	0.40	0.30	0.30	0.30
Y	23.10	25.50	24.10	29.80	27.8NOT0	23.40	23.10

NOTE: * GSWA 144261 was sampled by A. H. Hickman from MGA 536754E 7681956N

Appendix 1 (continued)

Sample no.	*99-1128*	*99-1129*	*99-0966*	*99-1133*	*99-1135*	*99-1138*	*99-1139*
Unit and rock type	*GD*	*GD*	*FPD*	*WB*	*WB*	*WB*	*WB*
Rock type	*Low Si-*	*Low Si-*	*Rhyodacite/*	*Sub-alkaline*	*Andesite/*	*Andesite/*	*Andesite/*
(Winchester and Floyd, 1977)	*dacite*	*dacite*	*dacite*	*basalt*	*basalt*	*basalt*	*basalt*
MGA coordinate (Northing)	*7685382*	*7685395*	*7682305*	*7682959*	*7682978*	*7682525*	*7682551*
MGA coordinate (Easting)	*574613*	*574349*	*574529*	*555512*	*555255*	*553982*	*554008*
Rock type (SiO_2 classification)	*Dacite*	*Dacite*	*Rhyolite*	*Andesite*	*Basalt*	*Basalt*	*Basalt*
				Percentage			
SiO_2	69.33	68.92	72.90	57.28	48.12	49.17	49.90
TiO_2	0.66	0.64	0.62	1.17	1.03	1.37	1.38
Al_2O_3	13.36	13.27	13.35	16.93	14.76	13.92	14.35
Fe_2O_3 (tot)	3.57	4.90	1.90	7.88	11.62	13.64	13.70
MnO	0.10	0.11	0.09	0.16	0.22	0.23	0.24
MgO	0.59	0.66	0.40	2.18	4.60	3.48	3.31
CaO	2.01	2.12	0.72	2.09	5.98	3.55	3.49
Na_3O	3.90	3.36	4.13	6.66	3.34	4.11	4.98
K_3O	2.93	3.08	3.33	0.80	1.13	1.03	0.89
P_3O_5	0.19	0.19	0.13	0.13	0.12	0.24	0.25
MLOI	3.15	2.57	2.24	4.55	8.94	9.04	7.29
Rest	0.17	0.18	0.21	0.18	0.18	0.17	0.15
Total	**99.96**	**100.00**	**100.02**	**100.01**	**100.04**	**99.95**	**99.93**
				Parts per million			
Ag	-0.50	-0.50	-0.50	-0.50	-0.50	-0.50	-0.50
As	1.50	2.80	1.90	42.80	2.10	1.50	1.20
Ba	688.00	733.00	998.00	316.00	412.00	374.00	363.00
Be	1.70	2.10	1.90	1.70	1.30	1.50	1.50
Bi	-0.10	-0.10	-0.10	-0.10	-0.10	-0.10	-0.10
Cr	-1.00	-1.00	-1.00	25.00	27.00	23.00	19.00
Cs	1.10	1.30	0.80	0.70	1.10	1.90	1.10
Cu	17.00	17.00	13.00	127.00	76.00	254.00	248.00
F	548.00	608.00	311.00	854.00	859.00	957.00	1 005.00
Ga	18.40	18.60	20.70	21.10	18.40	19.10	19.70
Ge	0.90	1.10	0.90	0.70	1.10	1.10	0.90
Li	9.50	9.00	3.50	28.00	37.50	22.00	19.00
Mo	0.80	1.30	0.50	0.10	1.20	0.80	0.50
Nb	8.20	8.30	10.50	8.20	7.10	8.10	8.00
Ni	7.00	5.00	3.00	232.00	94.00	71.00	61.00
Pb	14.50	17.50	39.00	37.50	6.00	7.00	6.50
Rb	98.00	115.00	95.00	26.00	47.00	28.00	19.00
S	300.00	190.00	180.00	260.00	200.00	430.00	480.00
Sb	1.00	1.20	0.80	0.20	0.40	0.60	0.20
Sc	15.00	15.00	8.00	27.00	23.00	16.00	16.00
Sn	1.00	1.00	2.00	1.00	-1.00	1.00	1.00
Sr	165.00	162.00	147.00	172.00	340.00	214.00	203.00
Ta	1.00	1.00	1.00	0.50	0.50	0.50	0.50
Th	15.50	15.80	12.50	6.60	5.60	3.40	3.40
U	3.90	3.80	2.50	2.00	0.90	0.70	0.60
V	104.00	103.00	16.00	224.00	188.00	159.00	158.00
Zn	63.00	59.00	25.00	112.00	116.00	144.00	143.00
Zr	191.00	188.00	279.00	148.00	127.00	176.00	169.00
La	42.90	43.30	45.90	23.60	24.60	26.50	26.50
Ce	80.30	81.90	88.50	48.10	49.10	56.10	56.70
Pr	8.50	8.70	9.70	5.60	5.80	6.90	7.00
Nd	30.10	30.90	35.00	21.40	22.90	28.40	29.10
Sm	5.20	5.40	6.60	4.00	4.70	5.80	6.00
Eu	1.10	1.20	1.50	1.40	1.40	1.70	1.70
Gd	4.60	4.80	6.30	3.70	4.90	5.50	5.70
Tb	0.70	0.70	1.00	0.60	0.80	0.80	0.90
Dy	3.60	3.80	5.00	2.60	3.90	4.20	4.20
Ho	0.70	0.80	1.00	0.50	0.70	0.80	0.80
Er	2.10	2.20	2.70	1.30	2.10	2.30	2.30
Yb	1.90	2.20	2.30	0.90	1.80	2.00	2.00
Lu	0.30	0.30	0.30	0.10	0.30	0.30	0.30
Y	21.30	22.80	27.20	13.30	21.00	23.10	23.30

Appendix 1 (continued)

Sample no.	*99-1143*	*99-1144*	*99-1146*	*99-1140*	*99-1141*	*99-1142*	*99-1131*
Unit and rock type	*sSD*	*sSD*	*sSD*	*PB*	*PB*	*PB*	*G*
Rock type	*Rhyodacite/*	*Rhyodacite/*	*Rhyodacite/*	*Rhyodacite/*	*Rhyodacite/*	*Rhyodacite/*	*Granite*
(Winchester and Floyd, 1977)	*dacite*	*dacite*	*dacite*	*dacite*	*dacite*	*dacite*	
MGA coordinate (Northing)	*7692733*	*7691359*	*7691367*	*7681365*	*7681355*	*7681604*	*7682906*
MGA coordinate (Easting)	*586347*	*584801*	*585055*	*554763*	*554842*	*555200*	*555370*
Rock type (SiO_2 classification)	*Rhyolite*	*Rhyolite*	*Rhyolite*	*Rhyolite*	*Rhyolite*	*Rhyolite*	*Granite*
				Percentage			
SiO_2	71.99	73.31	73.97	72.04	76.20	70.42	72.31
TiO_2	0.48	0.52	0.53	0.48	0.41	0.49	0.20
Al_2O_3	12.20	13.31	13.41	11.92	10.59	12.37	14.01
Fe_2O_3 (tot)	4.08	0.93	1.07	5.37	4.37	5.21	1.51
MnO	0.14	0.09	0.08	0.14	0.14	0.13	0.09
MgO	0.67	0.10	0.16	0.42	0.36	0.94	0.51
CaO	1.30	0.63	0.34	0.55	0.48	0.57	1.05
Na_3O	4.17	4.61	4.58	3.20	4.33	1.55	3.55
K_3O	2.08	3.65	3.30	2.82	0.90	6.18	4.76
P_3O_5	0.11	0.13	0.13	0.06	0.06	0.06	0.06
MLOI	2.64	2.44	2.15	2.61	2.02	1.71	1.80
Rest	0.13	0.18	0.20	0.17	0.12	0.38	0.17
Total	**99.99**	**99.90**	**99.92**	**99.78**	**99.98**	**100.01**	**100.02**
				Parts per million			
Ag	-0.50	-0.50	-0.50	-0.50	-0.50	-0.50	-0.50
As	2.20	16.40	4.20	2.30	3.90	0.40	-0.20
Ba	532.00	840.00	1077.00	862.00	333.00	2 392.00	822.00
Be	1.90	2.00	1.60	2.10	1.90	1.80	2.20
Bi	0.10	-0.10	-0.10	0.10	-0.10	-0.10	0.10
Cr	-1.00	-1.00	-1.00	11.00	6.00	10.00	1.00
Cs	1.30	0.70	0.80	0.60	0.20	0.70	4.00
Cu	15.00	14.00	10.00	13.00	14.00	20.00	6.00
F	544.00	167.00	289.00	486.00	346.00	385.00	447.00
Ga	17.00	18.50	19.30	18.60	13.70	16.80	19.20
Ge	0.80	0.80	0.80	1.40	1.00	1.00	0.90
Li	10.50	2.00	5.00	7.00	6.00	9.50	7.50
Mo	1.00	0.60	0.80	2.00	0.30	-0.10	0.10
Nb	10.30	9.80	11.10	13.20	11.10	13.50	9.40
Ni	4.00	8.00	7.00	10.00	5.00	11.00	4.00
Pb	23.00	30.50	25.50	7.50	13.50	4.50	24.50
Rb	56.00	106.00	104.00	81.00	24.00	151.00	194.00
S	230.00	500.00	420.00	990.00	180.00	120.00	80.00
Sb	2.00	4.60	4.40	0.40	-0.20	0.20	-0.20
Sc	12.00	10.00	11.00	11.00	9.00	10.00	5.00
Sn	2.00	2.00	2.00	2.00	2.00	3.00	2.00
Sr	101.00	98.00	95.00	61.00	69.00	49.00	117.00
Ta	1.00	1.00	1.00	1.00	1.00	1.00	1.00
Th	17.40	19.10	19.80	13.80	11.90	13.90	19.40
U	5.10	5.20	5.80	3.40	2.90	3.50	4.90
V	23.00	44.00	28.00	8.00	5.00	6.00	13.00
Zn	62.00	38.00	36.00	78.00	90.00	80.00	34.00
Zr	219.00	208.00	230.00	331.00	291.00	335.00	164.00
La	43.00	43.40	47.80	47.70	39.60	67.20	40.10
Ce	81.50	81.80	89.20	96.00	75.80	121.50	74.20
Pr	8.70	8.80	9.40	11.10	8.70	13.30	7.50
Nd	31.00	30.60	32.80	41.50	33.00	49.30	24.70
Sm	5.70	5.40	5.80	8.30	6.60	9.10	4.00
Eu	1.10	1.10	1.10	1.80	1.40	2.20	0.60
Gd	5.40	4.70	5.10	8.60	6.70	8.90	3.10
Tb	0.90	0.70	0.80	1.50	1.20	1.50	0.50
Dy	4.70	3.60	4.20	8.30	6.50	8.10	2.10
Ho	1.00	0.70	0.80	1.80	1.40	1.70	0.40
Er	3.00	2.10	2.40	5.30	4.30	5.40	1.20
Yb	3.00	1.90	2.30	5.10	4.30	5.20	1.10
Lu	0.40	0.30	0.30	0.80	0.70	0.80	0.20
Y	30.40	21.20	25.70	52.50	41.30	53.00	13.00

PLATE 1

MONS CUPRI For location see Inset 1

SYMBOLS

Geological boundary
- exposed
Fault
- exposed
- concealed
Small-scale fold axis, showing trend and plunge
- unspecified
Bedding, showing strike and dip
- inclined
Way-up indicator
- sedimentary structure
Cleavage, showing strike and dip
- inclined
Crenulation cleavage, showing strike and dip
- inclined
Lineation, unspecified, showing trend and plunge
- inclined

Highway with national route marker
Track
Fence, generally with track
Locality — Mons Cupri
Contour line, 20 metre interval

Watercourse
Well
Windpump

DATA DIRECTORY

Theme	Data Source	Data Currency	Agency
Geology	GSWA	1998 — 2001	Dept of Industry and Resources
Cadastre	TENGRAPH*	FEB 2003	Dept of Industry and Resources
Horizontal control	GESMAR	FEB 2003	Dept of Land Information
Topographic nomenclature	GEONOMA	2003	Dept of Land Information
Topography	Base maps from Straits Exploration (Australia)	2002	Straits Exploration (Australia)

*GSWA and DoIR databases can be viewed online (www.doir.wa.gov.au/aboutus/geoview_launch.asp) or can be downloaded from the GSWA Data and Software Centre (www.doir.wa.gov.au/GSWA/downloadcentre)

Facies mapping by G. Pike (Shell Deepwater, USA) 1998–2001 and regional geology by R. H. Smithies (GSWA) 1997

Edited by C. Strong, G. Hall, and G. Loan

Cartography by G. Wright and P. Taylor

Published by the Geological Survey of Western Australia. Digital and hard copies of this map are available from the Information Centre, Department of Industry and Resources, 100 Plain Street, East Perth, WA, 6004. Phone (08) 9222 3459, Fax (08) 9222 3444
Web www.doir.wa.gov.au Email geological.survey@doir.wa.gov.au

The recommended reference for Plate 1 is:
PIKE, G., and SMITHIES, R. H., 2005, Geology of areas within the Whim Creek greenstone belt, Pilbara Craton, Western Australia: Mons Cupri (scale 1:10 000), *in* Archean volcanic and sedimentary rocks of the Whim Creek greenstone belt, Pilbara Craton, Western Australia *by* G. PIKE., R. A. F. CAS., and A. H. HICKMAN. : Western Australia Geological Survey, Report 101, Plate 1.

The recommended reference for Plate 2 is:
PIKE, G., and SMITHIES, R. H., 2005, Geology of areas within the Whim Creek greenstone belt, Pilbara Craton, Western Australia: Good Luck Well, Red Hill, and Salt Creek (scale 1:10 000), *in* Archean volcanic and sedimentary rocks of the Whim Creek greenstone belt, Pilbara Craton, Western Australia *by* G. PIKE., R. A. F. CAS., and A. H. HICKMAN. : Western Australia Geological Survey, Report 101, Plate 2.

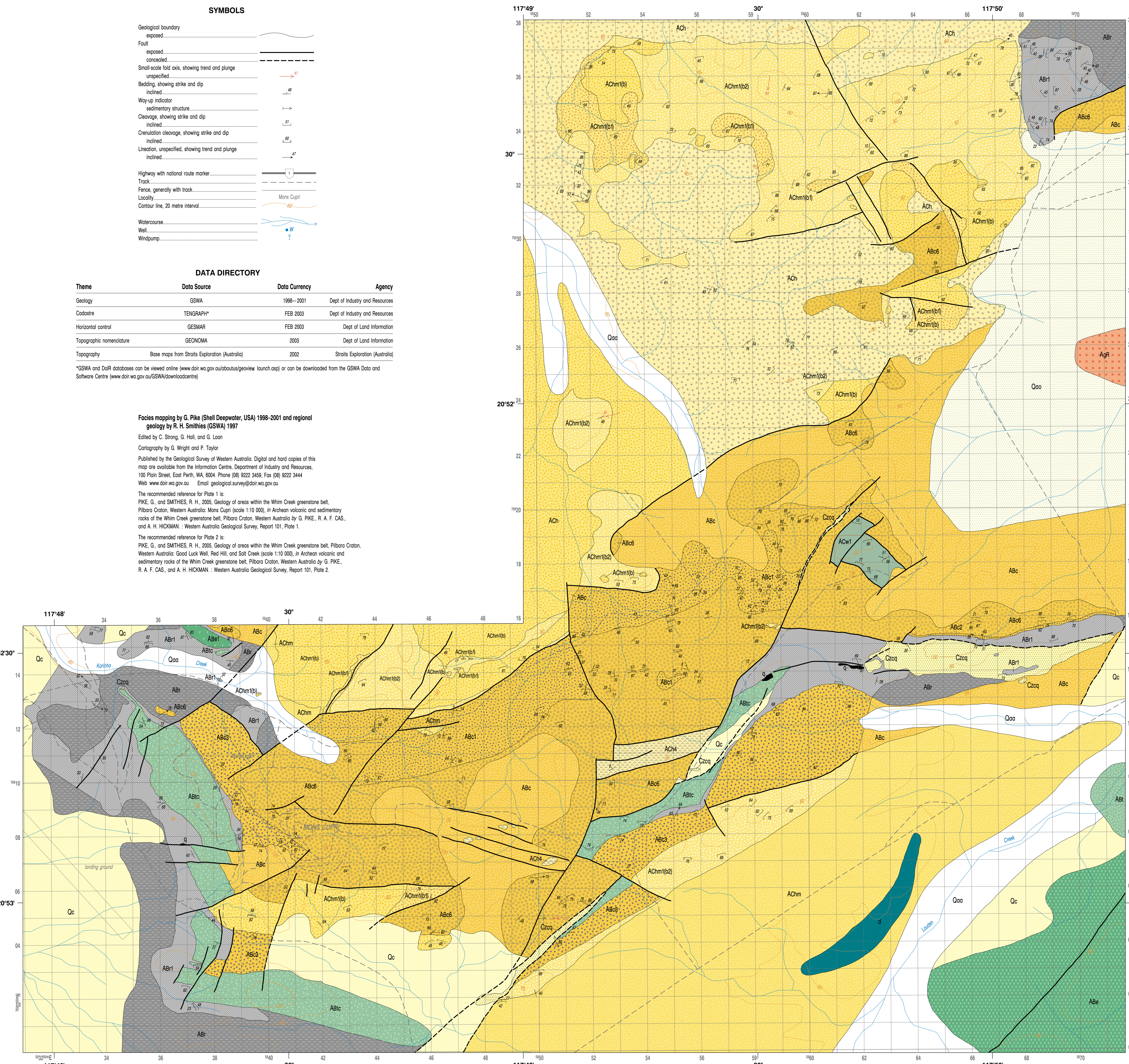

TECTONIC UNITS

REGIONAL SETTING OF WHIM CREEK AREA (tectonic units modified after Tyler and Hocking, 2001)

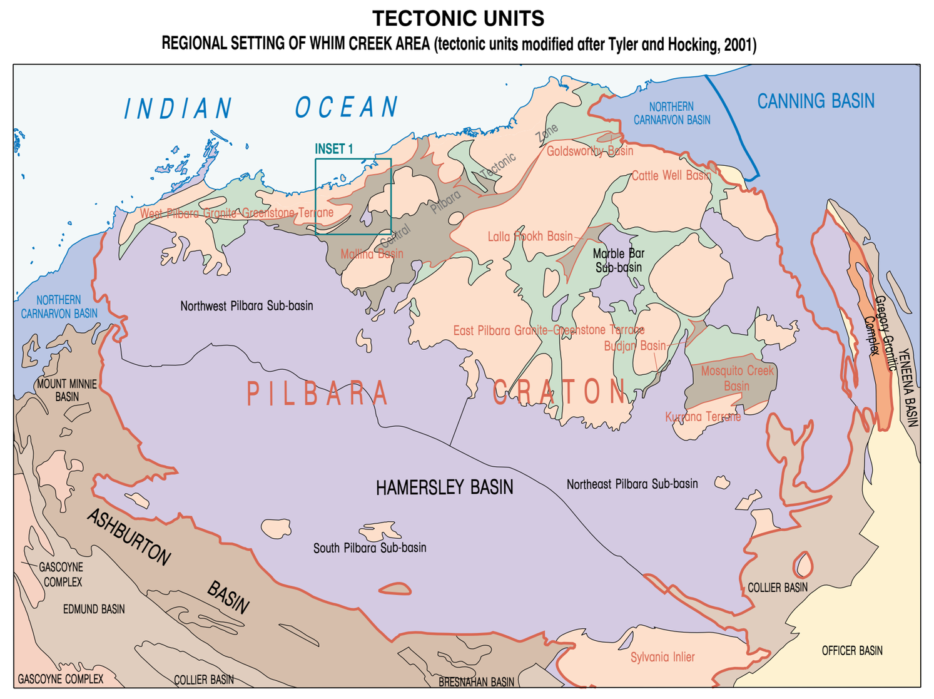

REFERENCE: TYLER, I. M., and HOCKING, R. M., 2001, Tectonic units of Western Australia (scale 1:2 500 000): Western Australia Geological Survey.

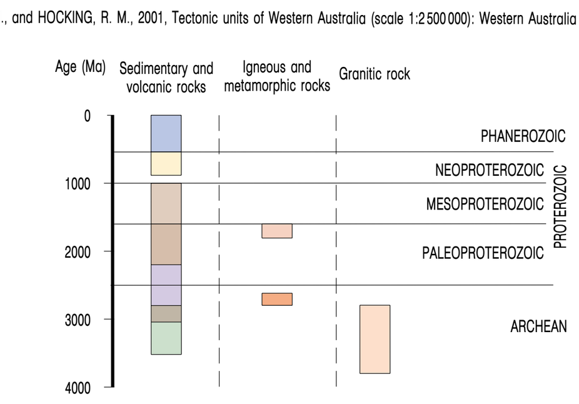

SCALE 1:5 000 000
50 0 50 100
Kilometres

INSET 1 **INTERPRETED BEDROCK GEOLOGY OF WHIM CREEK AREA**

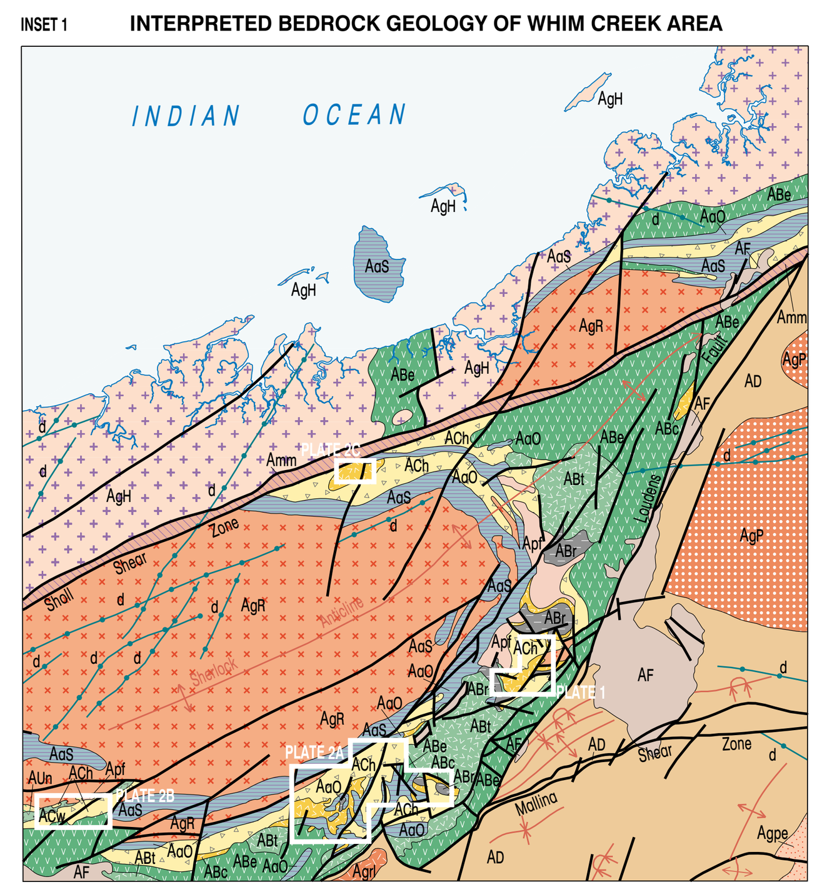

SCALE 1:500 000
0 5 10 15 20
Kilometres

AF Fortescue Group

Bookingarra Group
- ABe Louden Volcanics
- ABt Mount Negri Volcanics
- ABr Rushall Slate
- ABc Cistern Formation

AD De Grey Group

Whim Creek Group
- ACh Red Hill Volcanics
- ACw Warambie Basalt

Whundo Group
- AUn Nallana Formation

Intrusive rocks
- d Dolerite dyke
- Agrl Nerrely Leucogranite
- Amm Mylonite, sheared intrusive rocks
- AaS Sherlock Intrusion
- AgP Portree Granitic Complex
- Agpe Peawah Granodiorite
- Apf Felsic porphyritic rock
- AaO Opaline Well Intrusion
- AgH Harding Granitic Complex
- AgR Caines Well Granitic Complex

HAMERSLEY BASIN — West Pilbara Granite–Greenstone Terrane — Mallina Basin — Whim Creek Basin — West Pilbara Granite–Greenstone Terrane — PILBARA CRATON

Fault — Fold axes

For further details, refer to main reference

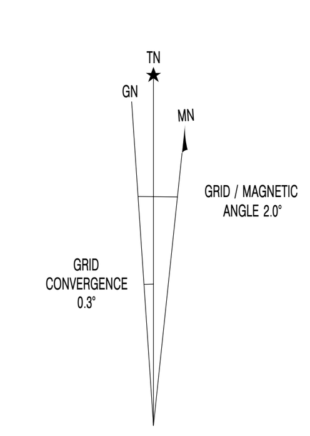

True north, grid north and magnetic north are shown diagrammatically for the centre of the map. Magnetic north is correct for 2005 and moves easterly by about 0.1° in 5 years.

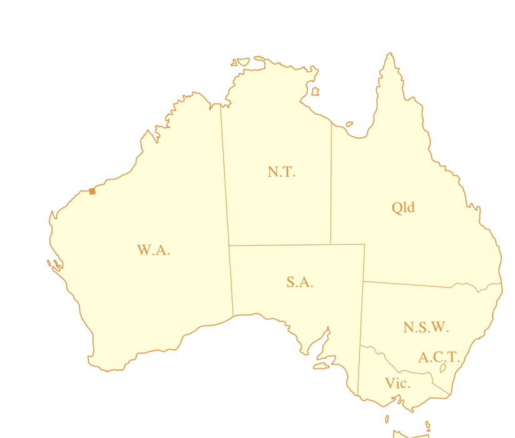

SHEET INDEX

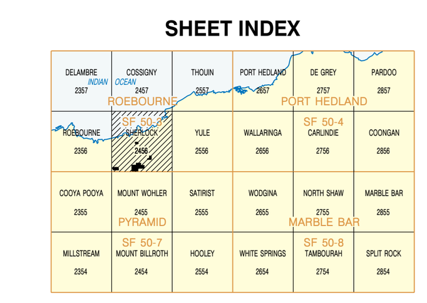

1:100 000 maps shown in black
Published 1:100 000 Geological Series map used in compilation
1:250 000 maps shown in brown
Search for current GSWA map products online (www.doir.wa.gov.au/ebookshop)

REFERENCE FOR PLATES 1, 2A, 2B, and 2C

PHANEROZOIC — CENOZOIC — QUATERNARY

Qaa | Qao | Qc

- Qaa Alluvial sand and gravel in rivers and creeks; clay, silt, and sand in channels on floodplains
- Qao Alluvial sand, silt, and clay in floodplains adjacent to main drainage channels; includes local areas of gilgai surface in areas of expansive clay
- Qc Colluvium — sand, silt, and gravel in outwash fans; scree and talus

Czak | Czcq

- Czak Alluvial calcrete; massive, nodular, and cavernous limestone, variably silicified
- Czcq Consolidated quartz-rich colluvium derived from vein quartz; includes local outcrops of vein quartz

ARCHEAN

d | q

- d Dolerite dyke
- q Quartz vein, or extensive quartz veining of Archean rocks

AaS **Sherlock Intrusion:** fine- to coarse-grained mafic intrusive rock; includes gabbro, olivine gabbro, leucogabbro, and granophyric gabbro; metamorphosed

Apf Quartz–feldspar porphyry; granophyric textures, sericite altered; numerous aplite dykes; includes Mount Fraser intrusion

AaO **Opaline Well Intrusion:** fine- to coarse-grained mafic intrusive rock; minor extrusive mafic rock; metamorphosed

De Grey Supergroup — Bookingarra Group

ABe | ABe1

- ABe **LOUDEN VOLCANICS:** undivided basalt and komatiitic basalt; tabular basalt lava flows; pyroxene-spinifex textures and lava-top breccia; abundant pillow breccia; interbedded clastic units and chert; metamorphosed
- ABe1 *Basalt sheet lava facies:* tabular basalt units; subordinate primary basalt breccia

ABt | ABtfr | ABt1 | ABt1(a) | ABt1(b) | ABt1(c) | ABt2(a) | ABt2(b) | ABt2(c) | ABtc

- ABt **MOUNT NEGRI VOLCANICS:** undivided variolitic and vesicular basalt; tabular basalt lava; rare pillow basalt, autobreccia, and splatter clasts; metamorphosed
- ABtfr *Quartz-phyric rhyolite facies:* spherulite-rich matrix; sericite altered
- ABt1 *Massive basalt lava facies:* basalt, typically forming tabular sheets, rare primary breccia and pillow basalt
- ABt1(a) *Brecciated subfacies:* basalt breccia
- ABt1(b) *Coherent subfacies:* coherent basalt
- ABt1(c) *Variolitic subfacies:* variolitic basalt
- ABt2 *Basalt breccia and cobble bed facies**
- ABt2(a) *Pumiceous subfacies:* cleaved siliciclastic and mafic volcaniclastic breccia; basalt cobble breccia with rare clasts of aphanitic tube pumice
- ABt2(b) *Non-pumiceous subfacies:* cleaved siliciclastic and mafic volcaniclastic breccia; basalt cobble breccia with no pumice
- ABt2(c) *Intraclast-rich subfacies:* cleaved siliciclastic and mafic volcaniclastic breccia; coarse, resedimented, angular, shard-rich basalt breccia (hyaloclasts) with up to 10% of lithic clasts comprising quartz- and feldspar-rich sandstone
- **Comstock Member**
- ABtc *Fine-grained intrusive facies:* massive, strongly chloritic, mafic intrusive rock with rare pyroxene-spinifex texture; intrudes **RUSHALL SLATE**

ABr | ABr1

- ABr **RUSHALL SLATE:** undivided well-laminated shale and siltstone; mud-rich sedimentary rock; lesser sandstone, chert and graphitic shale; metamorphosed
- ABr1 *Shale facies:* clay-rich laminated mudstone; minor laminae of quartz-rich and mafic lithic-rich sandstone, decreasing in abundance upwards; minor pyrite and rare cm-thick ironstone beds; weakly to strongly cleaved

ABc | ABc1 | ABc2 | ABc2(a) | ABc2(b) | ABc2(c) | ABc2(d) | ABc2(e) | ABc3 | ABc4 | ABc5 | ABc6

- ABc **CISTERN FORMATION:** undivided clastic and felsic volcaniclastic rocks; fine- to coarse-grained wacke, siltstone, and volcaniclastic sandstone; includes polymictic cobble and breccia deposits; metamorphosed
- ABc1 *Sandstone turbidite facies:* upward-fining, decimetre-scale tabular beds of volcaniclastic and quartz-rich sandstone; abundant pebble-sized breccia clasts overlying erosional bases and fining upward to fine sandstone caps
- ABc2 *Quartz-rich sandstone facies:* coarse, subrounded quartz- and lithic-rich sandstone
- ABc2(a) *Volcaniclastic subfacies:* 1–3 mm quartz-rich granulestone with coarser clasts of dark-grey, aphanitic basalt shards; mudstone matrix; basalt shards are resedimented (juvenile hyaloclasts)
- ABc2(b) *Arkosic subfacies:* coarse-grained sandstone with variable amounts of feldspathic grains
- ABc2(c) *Interbedded subfacies:* angular, decimetre-scale bedded quartz-rich sandstone with cm-scale interbeds of clay-rich mudstone
- ABc2(d) *Fine-grained subfacies:* fine-grained, typically silt-rich, chloritic and locally arkosic sandstone
- ABc2(e) *Granulestone subfacies:* quartz- and lithic-rich granulestone
- ABc3 *Lithic sandstone facies:* massive and cm-scale bedded sandstone with light-coloured volcaniclastic grains, quartz grains, and subordinate grains of mafic minerals; typically poorly exposed
- ABc4 *Rippled sandstone facies:* mixed volcaniclastic and quartz-rich sandstone with subordinate, finer grained, lithic fragments of black and grey chert
- ABc5 *Black chert breccia facies:* volcaniclastic breccia and sandstone with abundant reworked volcaniclastic debris and subordinate quartz; contains up to 10% elongate black and grey sedimentary chert fragments and rip-up clasts; massive to graded beds
- ABc6 *Conglomerate facies:* pebble- to cobble-conglomerate and subordinate breccia with clast- and matrix-supported subfacies; clasts dominantly derived from uplifted **Mons Cupri Dacite Member** with lesser clasts derived from **WARAMBIE BASALT** and **CAINES WELL GRANITIC COMPLEX;** quartz-poor matrix with rare granule pumice

AgR | AgRmc

CAINES WELL GRANITIC COMPLEX
- AgR Granitoid gneiss and foliated granitoid rock, undivided
- AgRmc Medium- to coarse-grained, K-feldspar-porphyritic biotite monzogranite; weakly to moderately foliated; metamorphosed

Whim Creek Group

ACh | ACh1 | ACh2 | AChm | AChm1 | AChm1(a) | AChm1(b) | AChm1(b1) | AChm1(b2) | AChm1(c) | AChm1(d) | AChm2(a) | AChm2(b) | AChm3 | AChm3(a) | ACh3 | ACh4 | ACh5 | ACh6 | ACh7 | ACh8 | ACh9 | ACh10 | ACh11(a) | ACh11(b) | ACh11(c) | ACh11(d) | ACh12

- ACh **RED HILL VOLCANICS:** undivided volcaniclastic conglomerate, breccia, sandstone, and siltstone with abundant juvenile and reworked, dominantly aphanitic, volcanic clasts; typically debris flows and turbidites with subordinate fluvial facies; metamorphosed
- ACh1 *Polymictic conglomerate and breccia facies:* coarse, typically clast-supported breccia and conglomerate, dominated by clasts derived from the **Mons Cupri Dacite Member**; massive units with little internal structure
- ACh2 *Imbricate conglomerate facies:* interbedded, fluvial conglomerate and sandstone with low-angle dune cross-bedding and lenses of imbricate conglomerate
- AChm **Mons Cupri Dacite Member:** undivided plagioclase-phyric dacite; typically coherent and with a cryptocrystalline groundmass; metamorphosed
- AChm1 *Large volume dacite facies:* massive, composite dacite unit up to 1.1 km thick
- AChm1(a) *Feldspar-phyric dacite subfacies:* massive dacite with blocky plagioclase phenocrysts and a cryptocrystalline, steel-blue to dark-grey groundmass
- AChm1(b) *Spherulitic dacite subfacies:* massive dacite with 2 mm plagioclase phenocrysts and variable amounts of cognate quartz- and plagioclase-rich xenoliths; abundant matrix spherulites
- AChm1(b1) Limonite-altered spherulitic dacite; typically located adjacent to faults
- AChm1(b2) Sericite-altered dacite with lesser chlorite and limonite alteration; abundant matrix spherulites
- AChm1(c) *Grey dacite subfacies:* dark-grey aphyric to plagioclase-phyric dacite; moderately vesicular
- AChm1(d) *Silicified dacite subfacies:* light-grey, strongly silicified plagioclase-phyric dacite
- AChm2 *Small volume dacite facies**
- AChm2(a) *Feldspar-phyric dacite subfacies:* feldspar-phyric dacite; weakly flow-banded at margins
- AChm2(b) *Spherulitic dacite subfacies:* spherulitic dacite forming elongate units with brecciated, peperite contacts with other rocks of **RED HILL VOLCANICS;** strongly flow-banded at margins
- AChm3 *Dacite pods facies:* dacite, forming small (1–10 m) ovoid units within **WARAMBIE BASALT** or within breccia units of the **RED HILL VOLCANICS**
- AChm3(a) *Feldspar-phyric dacite subfacies:* coherent, plagioclase-phyric dacite with or without flow-banded margins
- ACh3 *Siltstone facies:* fine-grained, strongly cleaved siltstone and mudstone
- ACh4 *Pumice and crystal-rich breccia facies:* granule- to pebble-sized oligomictic tube-pumice breccia, forming massive debris-flow or grain-flow units
- ACh5 *Massive sandstone facies:* medium- to coarse-grained sandstone; chlorite-altered matrix
- ACh6 *Coarse-grained dacite-rich breccia facies:* tabular massive beds of matrix-supported debris-flow breccia; clasts dominantly of quenched, vesicular, weakly plagioclase-phyric dacite; matrix typically comprising quartz-poor volcaniclastic sandstone
- ACh7 *Sandstone and breccia facies:* poorly exposed, massive, tabular, bedded and laminated sandstone with lesser breccia; may be altered (calcretized) equivalents of tabular-bedded sandstone facies
- ACh8 *Massive volcaniclastic breccia facies:* coarse-grained, poorly sorted breccia and minor conglomerate; typically massive debris flows with a quartz-poor matrix of volcaniclastic sandstone
- ACh9 *Tabular-bedded sandstone facies:* typically tabular bedsets of decimetre- to cm-scale, coarse-grained sandstone and cm-scale, laminated, fine-grained sandstone and siltstone caprock; normal grading with rare asymmetric ripples, flame structures, and low-angle cross-beds; grains are juvenile glass shards with minor pumice and reworked volcaniclastic debris
- ACh10 *Flattened tube-pumice breccia facies:* variably flattened tube-pumice breccia with clasts up to 5 cm in length
- ACh11 *Rhyodacite pumice breccia facies**
- ACh11(a) *Vesicle-poor subfacies:* granule- to pebble-breccia comprising non-vesicular and vesicle(tube)-poor angular (juvenile) volcanic clasts
- ACh11(b) *Granule subfacies:* granule-sized, oligomictic tube-pumice breccia with a fine-grained (?ash), recrystallized matrix
- ACh11(c) *Pebble subfacies:* pebble-sized, oligomictic tube-pumice breccia with a fine-grained (?ash), recrystallized matrix; massive units up to 20 m thick
- ACh11(d) *Sandstone subfacies:* sand-sized, oligomictic tube-pumice breccia with a fine-grained (?ash), recrystallized matrix; locally thinly bedded to laminated
- ACh12 *Tabular-bedded sandstone and siltstone facies:* thin (typically 10–30 cm) bedsets comprising a base of coarse- to medium-grained, massive, diffuse planar-bedded, or graded, sandstone and a laminated siltstone top; interpreted as sandy debris flows and turbidites (base) overlain by water-settled tops

ACw | ACw1 | ACw2 | ACw3(a) | ACw3(b) | ACw4(a) | ACw4(b)

- ACw **WARAMBIE BASALT:** undivided basalt and basaltic andesite lava; locally abundant hyaloclastite and lesser autobreccia; metamorphosed
- ACw1 *Schistose basalt facies:* coherent basalt; strongly limonite altered and schistose
- ACw2 *Grey dolerite and basalt facies:* plagioclase- and clinopyroxene-phyric dolerite and basalt; tabular units with rare vesicles
- *Aphanitic basalt breccia facies*
- ACw3(a) *Aphanitic basalt subfacies:* angular, granule- to pebble-sized breccia comprised of aphanitic basalt clasts; includes jigsaw-fit and clast-rotated examples with wispy, coherent basalt apophyses; autobreccia with hyaloclastite matrix
- ACw3(b) *Glomeroporphyritic basalt subfacies:* angular, granule- to pebble-sized plagioclase-glomeroporphyritic basalt breccia; includes jigsaw-fit and clast-rotated examples with wispy, coherent basalt apophyses; autobreccia with hyaloclastite matrix
- *Thick- and thin- sheet basalt facies*
- ACw4(a) *Aphanitic basalt subfacies:* irregular, 0.5–2.0 m thick basalt units with either reworked conglomerate tops (lower in stratigraphy) or hyaloclastite caps (higher in stratigraphy); common separation layers; plagioclase phenocrysts rare or absent
- ACw4(b) *Plagioclase-glomeroporphyritic basalt subfacies:* irregular, 0.5–2.0 m thick basalt units; blocky and lath-shaped plagioclase phenocrysts, typically in clusters

Unassigned
- Aba Amphibolite

Whundo Group
- AUn **NALLANA FORMATION:** metabasalt, with minor metamorphosed ultramafic, felsic, and sedimentary units

* The undivided facies is not shown on the plates

West Pilbara Granite–Greenstone Terrane — Mallina Basin — PILBARA CRATON — Whim Creek Basin — West Pilbara Granite–Greenstone Terrane

Department of Industry and Resources
ALAN CARPENTER, M.L.A. MINISTER FOR STATE DEVELOPMENT
JIM LIMERICK DIRECTOR GENERAL

Geological Survey of Western Australia
TIM GRIFFIN DIRECTOR

SCALE 1:10 000
100 0 100 200 300 400 500 600 700 800 900 1000
Metres

UNIVERSAL TRANSVERSE MERCATOR PROJECTION
HORIZONTAL DATUM: GEOCENTRIC DATUM OF AUSTRALIA 1994
VERTICAL DATUM: AUSTRALIAN HEIGHT DATUM

Grid lines indicate 100 metre interval of the Map Grid Australia Zone 50

The Map Grid Australia (MGA) is based on the Geocentric Datum of Australia 1994 (GDA94)
GDA94 positions are compatible within one metre of the datum WGS84 positions

GEOLOGICAL SURVEY OF WESTERN AUSTRALIA

REPORT 101 PLATE 1

GEOLOGY OF AREAS WITHIN THE WHIM CREEK GREENSTONE BELT, PILBARA CRATON, WESTERN AUSTRALIA: MONS CUPRI

Version 1.1 — November 2005

Department of Industry and Resources
ALAN CARPENTER, M.L.A
MINISTER FOR STATE DEVELOPMENT

Geological Survey of Western Australia
JIM LIMERICK
DIRECTOR GENERAL

TIM GRIFFIN
DIRECTOR

SCALE 1:10 000

100 0 100 200 300 400 500 600 700 800 900 1000
Metres Metres

UNIVERSAL TRANSVERSE MERCATOR PROJECTION
HORIZONTAL DATUM: GEOCENTRIC DATUM OF AUSTRALIA 1994
VERTICAL DATUM: AUSTRALIAN HEIGHT DATUM
Grid lines indicate 100 metre interval of the Map Grid Australia Zone 50

GDA

The Map Grid Australia (MGA) is based on the Geocentric Datum of Australia 1994 (GDA94).
GDA94 shiftfiles are compatible within one metre of the datum WGS84 positions.

GEOLOGICAL SURVEY OF WESTERN AUSTRALIA

REPORT 101 PLATE 2

GEOLOGY OF AREAS WITHIN THE WHIM CREEK GREENSTONE BELT, PILBARA CRATON, WESTERN AUSTRALIA: GOOD LUCK WELL, RED HILL, AND SALT CREEK

Version 1.1 - November 2005

FOR REFERENCE SEE PLATE 1

PLATE 2A

GOOD LUCK WELL For location see Inset 1 on PLATE 1

PLATE 2C

SALT CREEK For location see Inset 1 on PLATE 1

RED HILL For location see Inset 1 on PLATE 1

PLATE 2B

The Whim Creek greenstone belt, in the northwestern part of the Pilbara Craton, contains parts of two Mesoarchean volcano-sedimentary basins. The older, c. 3010 Ma, Whim Creek Basin contains basalt, dacite, and andesitic volcaniclastic rocks (Whim Creek Group). The unconformably overlying, c. 2950 Ma Mallina Basin contains a succession of conglomerate, quartzite, shale, basalt, and komatiite (Bookingarra Group).
This Report describes and interprets the lithofacies within both basins, and discusses their stratigraphic relationships.
This information, combined with new geochemical and geochronological data from the greenstone belt, is used to present a tectonic model involving a history of subduction, accretion, volcanism, igneous intrusion, deformation, and sedimentation.

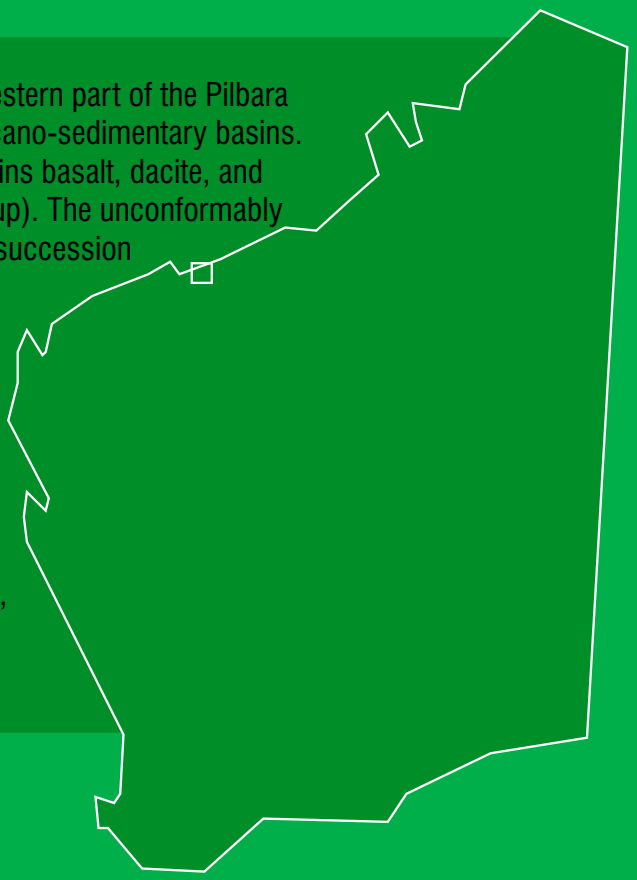

This Report is published in digital format (PDF) and is available online at: www.doir.wa.gov.au/gswa/onlinepublications. Laser-printed copies can be ordered from the Information Centre for the cost of printing and binding.

Further details of geological publications and maps produced by the Geological Survey of Western Australia are available from:

Information Centre
Department of Industry and Resources
100 Plain Street
East Perth, WA 6004
Phone: (08) 9222 3459 Fax: (08) 9222 3444

www.doir.wa.gov.au/gswa/onlinepublications

PIKE et al.

Archean volcanic and sedimentary rocks of the Whim Creek greenstone belt, Pilbara Craton, Western Australia

REPORT 101